Die Expedition ANTARKTIS X/3 mit FS „Polarstern" 1992

The Expedition ANTARKTIS X/3 of RV "Polarstern" in 1992

Herausgegeben von / Edited by

Michael Spindler, Gerhard Dieckmann and David Thomas

unter Mitarbeit der Fahrtteilnehmer /
with contributions of the participants

Ber. Polarforsch. 121 (1993)
ISSN 0176 - 5027

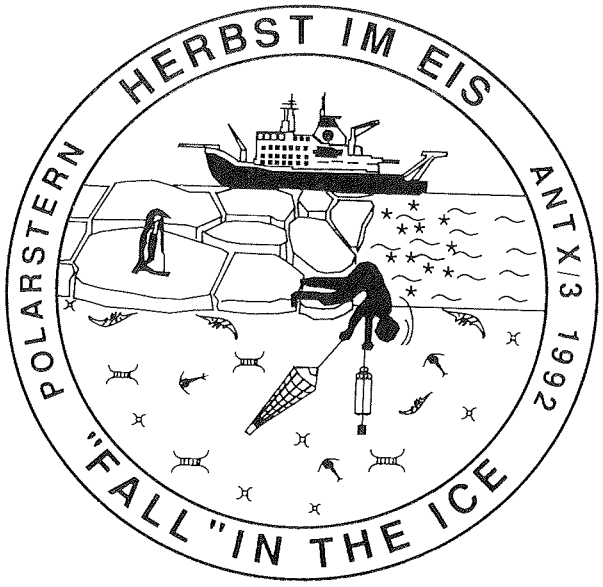

Michael Spindler
Institut für Polarökologie der Universität Kiel
Wischhofstraße 1-3
D-2300 Kiel 14

Gerhard Dieckmann, David Thomas
Alfred-Wegener-Institut für Polar- und Meeresforschung
Columbusstraße
D-2850 Bremerhaven 1

INHALT / CONTENTS

EINLEITUNG

Die zehnte Antarktis-Expedition des FS "Polarstern" begann am 14. November 1991 und wird bis zum 20. Februar 1993 dauern. Die Reise teilt sich in acht Fahrtabschnitte mit multidisziplinären Forschungsarbeiten, wobei der regionale Schwerpunkt im Gebiet des Weddellmeeres liegt.

Zum dritten Fahrtabschnitt (ANT X/3) lief "Polarstern" am 27. März 1992 von Kapstadt (Südafrika) aus und endete im gleichen Hafen am 19. Mai 1992. Dieser dritte Fahrtabschnitt firmierte unter dem Motto "Herbst im Eis". Unser Interesse galt den saisonalen Veränderungen von physikalischen, chemischen und biologischen Prozessen im sich bildenden antarktischen Packeisgürtel. Schwerpunkte während dieser Expedition waren Untersuchungen zur Meereisbiologie und des Planktons im oberflächennahen Wasser sowie zur Ozeanographie. Unser Hauptuntersuchungsziel war es, die Vorgänge vor, während und nach der Eisbildung sowohl in der Wassersäule als auch im Eis zu erfassen. Dazu wurden mehrere Schnitte vom freien Wasser durch das sich bildende Eis in den schon vorhandenen Packeisgürtel und zurück gefahren (Fig. 1). Gleichzeitig konnten dabei die Ozeanographen die Ausbildung verschiedener Wassermassengrenzen im kontinentalen Bereich des Weddellmeeres mit Hilfe eines engen Probennetzes studieren. Weitere Arbeitsgruppen, die an Bord vertreten waren, beschäftigten sich mit Tiefseebenthos und -mikrobiologie sowie Fischphysiologie. Außerdem wurden mehrere Langzeitverankerungen im Untersuchungsgebiet geborgen und zum Teil auch wieder eingesetzt.

Ein kurzer Besuch bei der deutschen Überwinterungsstation "Georg von Neumayer" diente der Versorgung mit noch fehlenden Ersatzteilen.

FS "Polarstern" wurde auf dem Abschnitt ANT X/3 von Kapitän H. Jonas geführt. Ihm, den Offizieren und der Mannschaft schulden wir großen Dank für ihre hervorragende, engagierte Arbeit und ihre verständnisvolle Hilfe, die zum Erfolg der wissenschaftlichen Arbeit maßgeblich beigetragen haben.

Unser herzlicher Dank gilt auch der Logistik des Alfred-Wegener-Instituts für die Vorbereitung der Expedition, Ingrid Lukait für ihre bereitwillige Hilfe vor und während der Expedition sowie Herrn Dr Zipan Wang bei der Zusammenstellung des Berichtes.

FOREWORD

The tenth Antarctic expedition of the RV "Polarstern" began on 14th November 1991 and ended on 20th February 1993. The cruise consisted of eight legs of multidisciplinary research in the Weddell Sea area.

The third leg (ANT X/3) began on 27 March 1992 in Cape Town and ended there on 19th May 1992. The motto of the third leg was "Fall in the ice". Our interests focussed on seasonal changes in physical, chemical and biological processes in the region of pack ice formation. Investigations concentrated on sea ice biology, plankton in upper water layers as well as oceanography. The major goal was to obtain a comprehensive picture of processes prior to, during and after the onset of sea ice formation. To achieve this, "Polarstern" sailed on several transects from open water into the ice and out again (Fig. 1). This cruise track also provided the oceanographers with a detailed station grid to study water mass boundaries in the continental area of the Weddell Sea.
Additional research was undertaken on deep-sea benthos, microbiology, and fish physiology. During the cruise several long-term moorings were recovered and redeployed.

A short visit to the German overwintering station "Georg von Neumayer" was made in order to provide the station with supplies.

Captain H. Jonas was the master of RV "Polarstern". We are grateful to him, the officers and crew for excellent, committed work and their willing assistance which contributed considerably to the scientific success of the cruise. We would like to extend our thanks to the logistics personnel of the Alfred Wegener Institute for their assistance in the preparation of the expedition and to Ingrid Lukait for her help prior to and during the cruise as well as Dr. Zipan Wang for his help in compiling this report.

ANT X/3, CAPE TOWN - CAPE TOWN

27.3.92 - 19.05.92

1. ZUSAMMENFASSUNG UND FAHRTVERLAUF

M. SPINDLER

Nach reibungsloser Anreise aller Fahrtteilnehmer legte "Polarstern" am 27. März um 14.00 Uhr mit 51 wissenschaftlichen Fahrtteilnehmern und 41 Besatzungsmitgliedern in Kapstadt ab (Fig.1). Nach dem Aussetzen von zwei verankerten Pegelmessern noch in der Nähe von Kapstadt in 1000 m Wassertiefe, begannen regelmäßige ozeanographische Messungen mit XBT´s auf dem Weg zur ersten Station bei 50° S und 5° O. Dort wurde erfolglos versucht, die erste Sedimentfallenverankerung aus 3800 m Wassertiefe aufzunehmen. Danach wurden zwei weitere Pegelmesser in der Nähe von Bouvet in jeweils 1000 m Tiefe abgesetzt, bevor wir mit fast südlichem Kurs auf den antarktischen Kontinent zuliefen.

Am 6. April wurde auf einer Probestation die noch eisfreie Wassersäule bis 4000 m beprobt. Gegen 20.00 Uhr trafen wir auf das erste Meereis (Pfannkucheneis). Die Wassertemperaturen fielen unter -1° C, während die Lufttemperaturen von -6° allmählich auf -22° C sanken. Wir durchquerten in der Nacht einen über 140 km breiten Pfannkucheneisgürtel, bis wir am 7. 4. in dichtem Packeis etwa 20 km vor der Schelfeisküste zum ersten Mal rammen mußten, um unsere erste Fischereistation anzulaufen. Am 8.4. erreichten wir die Atkabucht, mit der deutschen Überwinterungsstation Georg von Neumayer (GvN). Die schwierige Eislage erlaubte kein Anlegen von "Polarstern" an der Schelfeiskante. Die Versorgungsgüter für GvN konnten jedoch mit Hubschraubern eingeflogen werden. Als Begleitung konnte bei diesen Flügen der Großteil von Besatzung und Wissenschaft GvN einen Besuch abstatten. Parallel zu diesem Besuch liefen in der Atkabucht eine Reihe von Untersuchungen. Verschiedenen Netze, Sonden und ein mit Videokamera bestückter Mehrfachgreifer gingen in das eisige Wasser und die Meereisforscher durchlöcherten das Festeis der Bucht. Am 10.4. begann "Polarstern" den ersten Ozeanographen/Biologenschnitt abzuarbeiten, der vom Eis bis ins freie Wasser reichte und am 14.4. im eisfreien Wasser bei 67°58´ S beendet wurde. Auf diesem und den folgenden Nord/Süd- und Süd/Nord-Schnitten kamen Sonden, verschiedene Wasserschöpfer und Netze zum Einsatz, die z.T. bis auf den Tiefseeboden ausgebracht wurden.

Dabei wurden die verschiedenen Wasserkörper jeweils nördlich und südlich der beiden Frontensysteme beprobt, und zwar der Schelffront (etwa 20 km vor der Schelfeisküste) und der Kontinentalgrenzenfront (etwa 240 km von der Küste entfernt). Parallel zu den meisten Stationen hatten die Eisforscher immer wieder Gelegenheit, interessante Stadien der Eisbildung zu beproben. Trotz der Osterfeiertage wurde das Programm unvermindert weitergeführt. Die Feiertagsstimmung kam dann jedoch am Ostersonntag auf. Der Kapitän veranstaltete für alle einen Empfang im Blauen Salon, und ein Blick auf die Essenskarte des Tages ließ die Herzen höher schlagen.

Am 21.4. gelangten wir nach Beendigung unseres 4. Schnittes bis auf 3 km an die Schelfeiskante. Die Eisforscher nutzten dies für eine Festeisstation. Gleichzeitig konnte Eisgang für Besatzung und Wissenschaft freigegeben werden. Strahlender Sonnenschein bei Temperaturen um -22° C lockte die meisten, zumindest kurzfristig, auf das Eis.
Der 25. und 26. April waren dann Arbeiten an der Meereiskante gewidmet. Um sie anzutreffen, mußten wir inzwischen schon nördlich bis auf 67° 45´ S dampfen. Hier wurden dann aber auch alle Stadien der Meereisbildung in geringer Entfernung voneinander angetroffen und konnten beprobt werden.

Am Abend des 28.4. begannen wir unseren letzten Schnitt nach Süden. In der Nacht briste der Wind auf und erreichte am Tage Windstärken von 8-9. Der Schiffsführung bereitete es Mühe, "Polarstern" so in den Wind zu legen und zu halten, daß die eingesetzten Geräte noch gefahrlos zu bedienen waren. Gegen Abend hatte sich der Sturm voll entwickelt und blies mit guten 12 Windstärken. Alle Arbeiten mußten abgebrochen werden und mußten auch den nächsten Tag noch ruhen. Gegen Mitternacht flaute der Wind auf Stärke 7 ab, so daß am nächsten Morgen die Stationsarbeiten wieder fortgesetzt werden konnten, worunter auch die erfolgreiche Bergung einer Langzeit-Tiefseeverankerung fiel. Am 2.5. waren unsere regelmäßigen Arbeiten auf den Schnitten von Nord nach Süd und umgekehrt beendet. Für die nächsten Tage liefen wir ausgewählte Positionen an, an denen Fischerei- und Festeisarbeiten sowie Planktonfänge durchgeführt wurden. In der Nacht vom 6. auf den 7. Mai verließen wir das Eis endgültig, bei Windstärken um 7-8 und Wellen bis 3m Höhe war die ruhige Zeit vorbei. Am 10. 5. erreichten wir die südliche Sedimentfallenverankerungsposition und konnten die Falle nach eineinhalbstündigem Aufstieg aus 4000 m Wassertiefe eingeholen, neu bestücken und wieder in der Tiefe für ein weiteres Jahr verankern. Auch die nächste Bergung und Neuverankerung am 12. 5. auf Position 54°20´ S und 03°22´ W wurde erfolgreich abgeschlossen, so daß wir noch einmal versuchten, die am Beginn der Reise nicht eingebrachte Verankerung erneut zu bergen. Auch diesmal blieben unsere Bemühungen ohne Erfolg. Obwohl Wind (Stärke 8-9) und Wellen das Unternehmen nicht begünstigten, wurde unter großem Einsatz der Mannschaft dennoch eine neue Verankerung ausgesetzt.

Am Abend des 15. Mai und den ganzen nächsten Tag gerieten wir noch einmal in ein gewaltiges Sturmtief, das die Wellen bis auf 8 m Höhe ansteigen ließ. Mit verminderter Fahrt und ausgefahrenen Stabilisatoren kamen wir einigermaßen glimpflich davon, so daß dem Einlaufen in Kapstadt am Morgen des 19.5.1992 nichts mehr im Wege stand.

2. SUMMARY AND ITINERARY

M. SPINDLER

After the safe arrival of all cruise participants "Polarstern" left Cape Town on 27 March at 14.00 h, with 51 scientists and 41 crew members on board (Fig.1). While still in the vicinity of Cape Town two pressure gauges were deployed, at 1000 m water depth, and these will be recovered after two years. Thereafter, on our way towards 50° S and 5°E to recover and redeploy a sediment trap mooring, regular oceanographical data were collected using XBT´s. We reached the trap position on 31 March but failed to recover the instruments from 3800 m water depth. In the vicinity of Bouvet Island we deployed two pressure gauges at 1000 m depth and headed towards the Antarctic continent.

During a test station on 6 April water samples were collected down to a depth of 4000 m from a still ice-free ocean. That evening we encountered the first traces of sea ice, small pancake floes a few cm in diameter. At the same time water temperatures dropped below minus 1°C, while the air temperature gradually decreased from -6 to -22°C. During the night we passed a 140 km wide field of pancakes until we reached heavy pack-ice about 20 km off the shelf-ice coast the next day. Our first fisheries station could only be reached breaking the ice by ramming.

On 8 April we reached Atka Bay. The German overwintering station, Georg von Neumayer (GvN), was situated 16 km inland of our position. A difficult ice situation prevented the ship from landing at the shelf ice edge. Since visibility was reasonable we could start helicopter flights to GvN to pass over supplies. Most of the crew and scientists joined the flights. Simultaneously, research went on in Atka Bay: Different types of nets, sondes and a multicorer equipped with a video system were successfully deployed and the sea-ice crew drilled holes in the ice of the bay.

During noon on 10 April ice workers finished their station and "Polarstern" sailed north again to work on an oceanography/biology grid extending into the ice free waters. This grid lasted till 14 April and ended at 67°58´ S. On this and the following north/south and south/north transects a variety of samples were collected sometimes down to the deep sea floor. Different water masses were sampled north and south of two frontal systems. These systems are the continental shelf front, about 20 km off the shelf ice, and the continental break front, about 240 km offshore. The scientists interested in ice biology used the time when instruments were lowered to the deep water to work on ice floes.

Work continued despite Easter holidays. However, some "Feiertagsstimmung" developed on Sunday morning during an Easter reception hosted by the captain and as a result of viewing the days menu.

On 21 April "Polarstern" moved as close as 3 km from the coast after finishing the fourth transect. The scientists interested in the sea ice, capitalised on the proximity to the shelf ice to investigate land-fast ice. There, the gangway was deployed, and ship´s crew and scientists were free to leave the ship for a walk on the ice. People enjoyed the bright sunshine with temperatures around -22°C and took photos of the ship. On 25 and 26 April work was devoted to ice work close to the sea ice edge. We had to move north to a position of 67°45´S to find all developmental stages of ice formation.

On the evening of 28th April, we started our last transect to the south. During the night wind speeds increased and reached force 8-9 during the following day. The ships officers had problems keeping "Polarstern" into the wind to guarantee safe handling of collecting gear. The storm continued, with wind strengths reaching force 12, resulting in all station work being stopped and nobody was allowed on the outside decks. The next day conditions were still poor and no station work was possible. About midnight the wind decreased to strength 7 and we were able to start station work the next morning with the successful recovery of a deep sea mooring.

On 2 May we finished our regular work on the north-south transect pattern. The next days were allocated to investigations on selected positions for fishery, fast-ice stations as well as plankton catches. During the night from 6 to 7 May we left the ice covered region, however, strong winds and wave heights of more than 3 m were an experience most people did not like. On 10th May we reached the southern sediment trap position and were able to recover the trap after 1.5 h ascent from a depth of 4000 m. After recovery some new instruments were deployed and anchored for another year. Also the next mooring positioned further to the West at 54°20´ S and 03°22´ W was successfully recovered and redeployed. This success encouraged us to give our first failed mooring recovery another try. Unfortunately, the repeated acoustic signals failed to release the trap from the sea floor. In spite of strong winds and high waves which created difficult working conditions, new traps were successfully moored.

On the evening of 15 May and also the next day we encountered another storm area, where waves built up to more than 8 m height. We had to slow the ship´s speed and extend the stabilizers. However, weather conditions improved and we made up lost time, arriving in Cape Town on schedule during the morning of 19 May 1992.

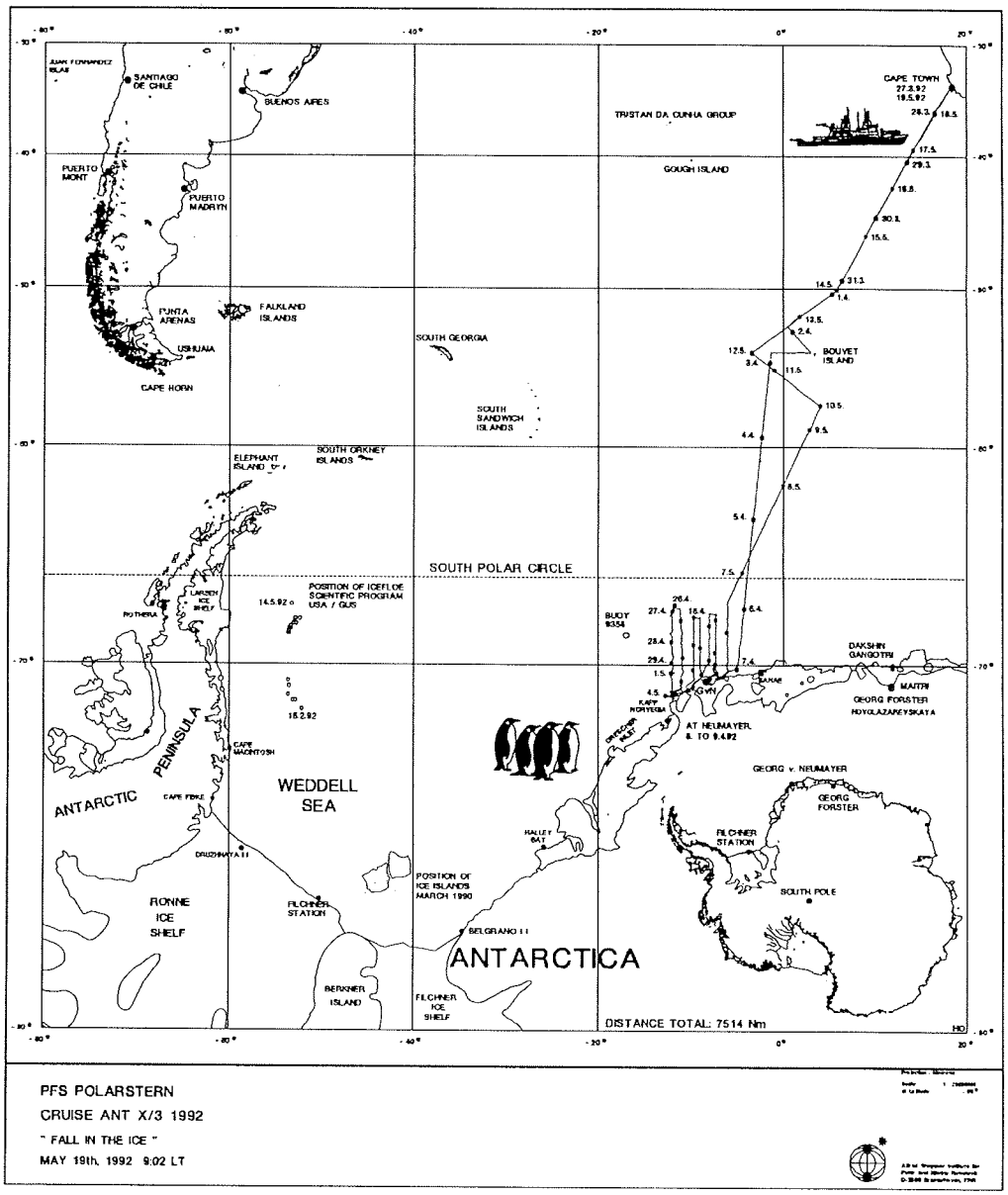

Fig. 1: Cruise track of RV Polarstern during ANT X/3

3. SCIENTIFIC REPORTS

3.1. Physical Oceanography

G. KRAUSE, A. MAUL, K. OHM, R. PLUGGE, J. LÜTJEHARMS, R. PHILLIPS, G. RIGG, H.VALENTINE

On the occasion of "Polarstern's" first autumn cruise into the Weddell Sea, physical oceanographers of AWI and Cape Town University joined forces to investigate:

- the Antarctic Slope Front
- the onset of winter convection

while

- an XBT-section was carried out along the WOCE repeat line from Cape Town to Antarctica
- pressure gauges were deployed and recovered

and

- underway measurements of temperature, salinity and optical properties were performed.

After a short description of the instruments used, reports on the above topics will follow.

3.1.1. INSTRUMENTATION

3.1.1.1. The COMED system for underway measurements.

COMED (Continuously measuring device) is a data acquisition system the sensors of which are mounted in the hydrographic well flush with the ship's hull at about 10 m depth. It measures temperature and conductivity by an instrument of the ME company (ME OTS 1500) as well as light backscattering, chlorophyll, Gelbstoff fluorescence together with navigational data. The optical sensors are products of Dr. Haardt (Mikroelektronik) while a beam attenuance sensor with an optical path length of 300 mm was designed at AWI.

The registration of 10 s averages and standard deviations covers the ship's course from near Cape Town to the first encounter with ice, and the same way back.
Part of the COMED system is a back-up PC which is also used for processing of the recorded data with the commercial software package DADISP.

3.1.1.2. The Bio-Rosette

This instrument consists of a CTD-unit (ME 98) with additional sensors for chlorophyll fluorescence and Mie backscattering (Dr. Haardt) together with a rosette sampler with 12 Niskin bottles. Calibrated by the manufacturer to an accuracy in temperature of 0.02 K, conductivity of 0.025 $mScm^{-1}$ and pressure of 0.25%, the instrument meets all requirements of biologists, and no post-processing is necessary for these variables.

The conversion of chlorophyll fluorescence into concentrations, however, requires further study and calibration. On-board comparisons with filtered samples showed that a stable linear relationship exists between the two quantities for a large number of profiles, but sometimes deviations by a factor of 2 occur, possibly as a result of a different quantum efficiency of changing plankton communities.

3.1.1.3. The CTD

The CTD is a Bathysonde LS200 of Salzgitter Elektronik. The instrument and its backup were recently calibrated at Wormley with the highest available accuracy.

During the cruise this calibration was checked by other instruments and water sampling.

It turned out that the depth calibration of both Bathysondes showed a difference of about 1% compared to 4 electronic pressure sensors of the SIS company, cable length and bottom depth by echo sounder. The temperatures seem to have an offset of 0.02 K against very carefully performed readings of reversing thermometers of Gohla with polar range.

The sources of these deviation are not yet known. Thus it is clear that post-processing and recalibration is necessary before the data can enter into a final report.

3.1.1.4. Inverted CTD

This is a small CTD (ADM Company) equipped with additional sensors for Mie backscattering, chlorophyll fluorescence and light attenuation. It is designed for obtaining vertical profiles close to the sea-surface. Therefore the sensors point in the upward direction, and measurements are performed on the up-trace only.

3.1.1.5. XBT - Expendable Bathythermograph

The accuracy of the XBT system of 0.1 K can normally be improved by adjusting the measured temperature profile to a known temperature at one point. Therefore separate temperature readings were obtained by using a Crawford bucket at the sea surface. The COMED data are also convenient for this purpose. Simultaneous profile measurements of Bio-Rosette and XBTs revealed a considerable thermal lag of the XBTs in the surface layer down to 30 to 80 m, apparently caused by the large temperature contrast between water and probes prior to launching (Fig. 2).

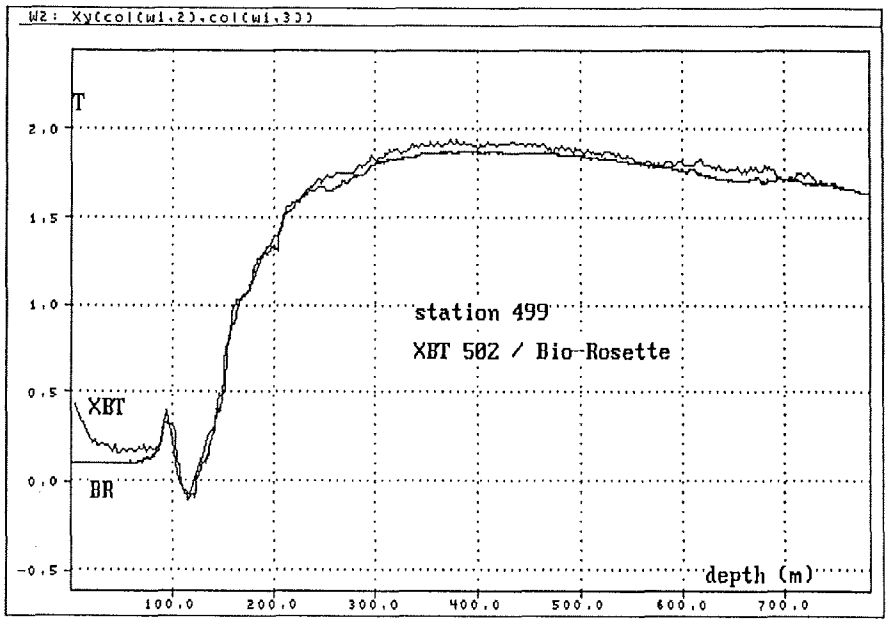

Fig. 2: Temperature profiles of XBT and Bio-Rosette measured simultaneously showing thermal lag of the XBT down to 80 m.

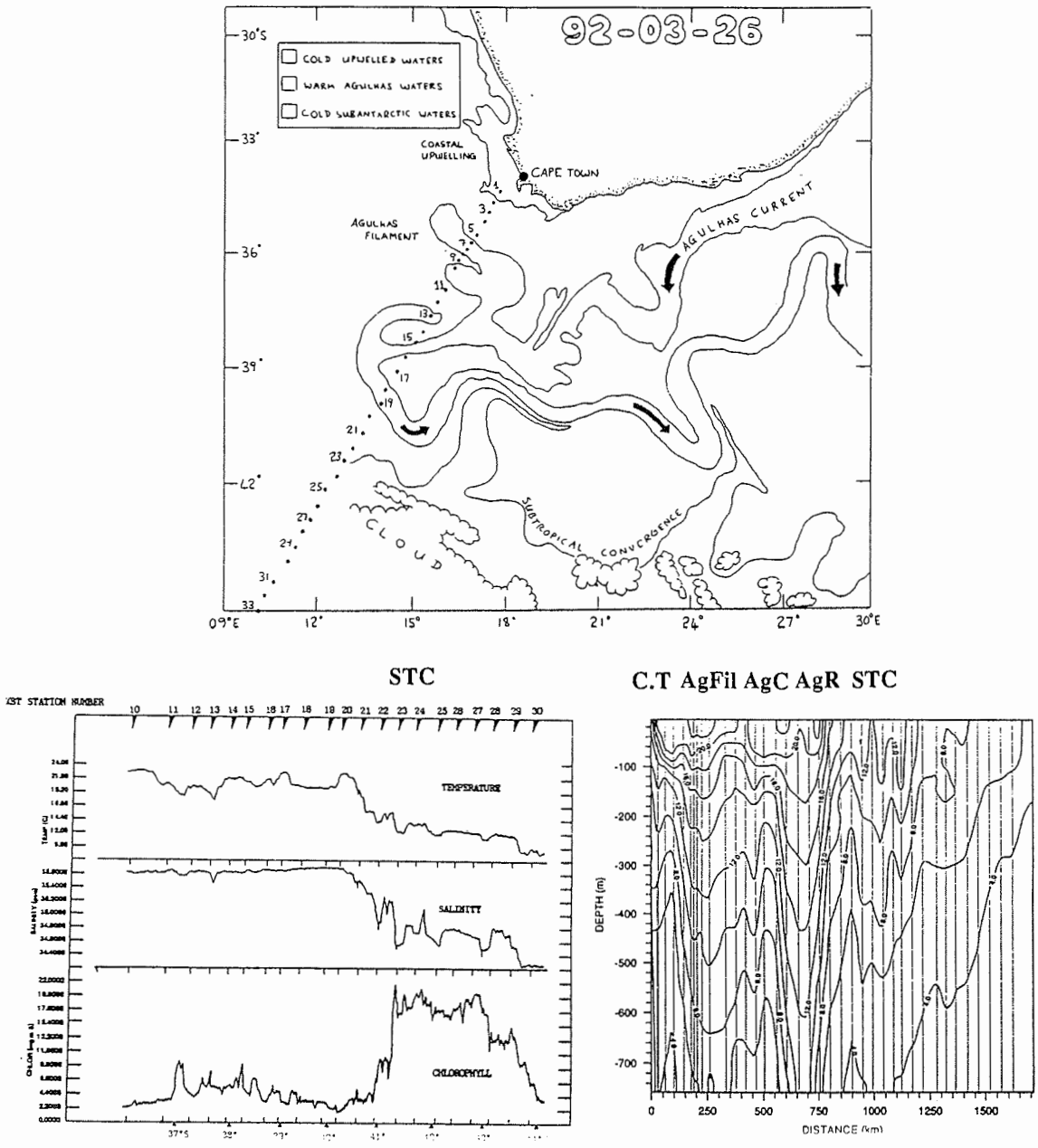

Fig. 3: Results of underway measurements between Cape Town and the Subtropical Convergence. The upper panel shows a line drawing interpretation of the disposition of circulation elements as seen on a thermal infrared satellite image for 26 March 1992. The first diagram in the lower panel shows surface values for temperature, salinity and chlorophyll whilst the second diagram in the lower panel shows the thermal structure of the upper water column over the same length of cruise line, as revealed by XBT measurements. Notable features indicated are: the Agulhas Current (AgC); the Agulhas Return Current (AgR); an Agulhas Filament (AgFil) and the Subtropical Convergence (STC).

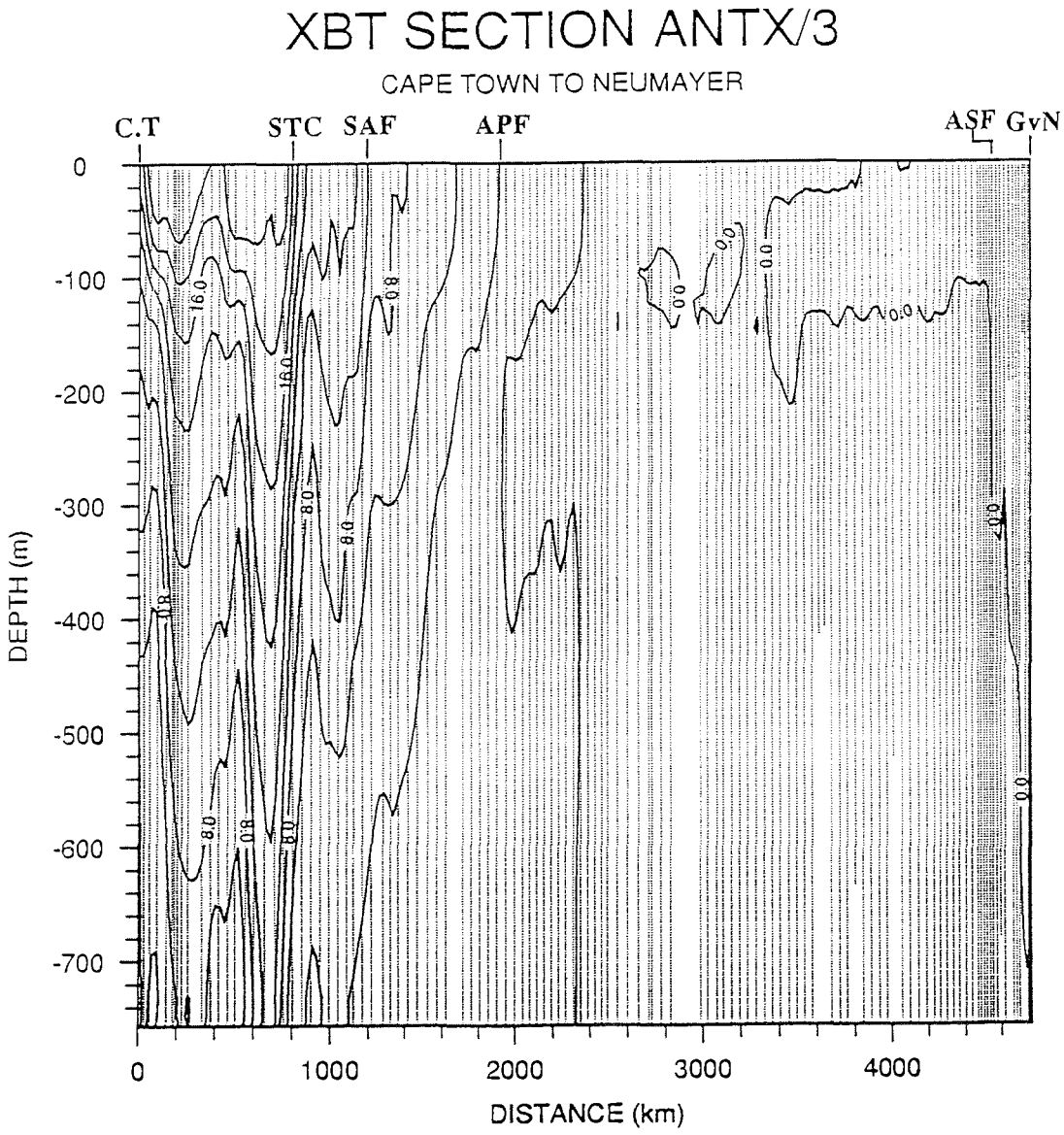

Fig. 4: The thermal characteristics of the upper water column from Cape Town to Antarctica during ANT X/3. Notable features are: the Subtropical Convergence (STC); the Subantarctic Front (SAF), the Antarctic Polar Front (APF) and the Antarctic Slope Front (ASF).

3.1.2. THE ANTARCTIC SLOPE FRONT IN AUTUMN

If a vertical section of closely-spaced hydrographic stations is carried out between Africa and Antarctica a few notable oceanographic features stand out. These include the Agulhas Current, the Subtropical Convergence, the Antarctic Polar Front and the Antarctic Slope Front (ASF). Of these, the ASF emerges as the feature with by far the most striking vertical extent, reaching to depths that exceed 5000 m.

It therefore comes as a surprise that so little research work has specifically been directed to a better understanding of this front and that so little is known about it. This may be due both to it's relative inaccessibility and due to the fact that it is covered by ice for a large part of the year. In a recent review of what is known about the ASF) has pointed out the importance of this front both from a biological point of view, from the view of bottom water formation and from dynamics of the Antarctic continental shelf.

The aims of this component of cruise ANT X/3 were therefore first, to study the detail of the ASF in a multidisciplinary way and over an extensive stretch of coast-line. This has not been done before. Second, this investigation would describe the general hydrography of the coastal and shelf environment off Georg von Neumayer station over a geographic area much greater than achieved before. Third, all this would be done during the autumn while the first ice was being formed. This also, either from a global or a site specific view, has not been done before and would therefore contribute new and potentially valuable knowledge on the ocean in general and on the ASF in particular.

The observational part of these aims were all amply achieved. Eight station lines at right angles to the coast were carried out, four to the east of GvN, four to the west (Figure 5). The two most easterly lines both consisted of XBT stations only, being the first and the last lines of the survey. In this way changes that had occurred over a period of 6 weeks in the hydrography of the upper layers could be established. The other lines consisted mostly of alternate XBT and CTD stations with an average station spacing of 15 km, with closer spacing of CTD stations at the shelf and the slope. The total area covered is $86*10^3$ km^2 which compares with the $92*10^3$ km^2 of Portugal.

Measurements of temperature with depth were made with Sippican *Deep Blue* XBT probes, via a Toshiba laptop. Compared to CTD measurements, these showed a temperature discrepancy that was not entirely persistent but varied with depth (or temperature). A number of combined stations of CTD and XBT measurements on the return leg were therefore carried out for inter-comparison purposes. The manner and accuracy with which the CTD, nutrients and oxygen measurements were carried out are described elsewhere in this cruise report.

Two hydrographic sections for this cruise are shown in Figure 6. They are for transect 5 along 11°W. Three features are of greatest importance. One, the increasing downward slope of both isotherms and isohalines on approaching the coastline defining the ASF, two: the absence of a clear surface expression of the ASF. In the surface salinities, there is a gradual increase in salinities seaward, but this is very gradual and does not form a front in any of the cruise lines. Third, in Figure 6 there is evidence of a tongue of warm Circumpolar Deep Water approaching the coast. This general portrayal is reflected also in the dissolved oxygen and in the nutrients taken along this section.

A preliminary analysis of the location of the greatest downward slope in the isolines shows that this corresponds to the upper continental slope, as is to be expected, but not closely. On certain transects the front was found further offshore than on others. An intriguing inverse relationship was found between the depth of the 0°C isotherm and deep bottom topography. Where the topography is shallower than 3000 m, the 0°C isotherm remained deeper than 300 m.

The vertical structure of the water column in summer exhibits a very strong, but shallow thermocline, below the warmed summer surface layer. With the onset of autumn this seasonal thermocline should be eroded away resulting in a uniformly cold surface layer above the warm Circumpolar Deep Water. This erosion will theoretically result in a number of possible temperature inversion configurations. On this cruise these were all found and a number of examples are given in Figure 7. The distribution of stations where remnant summer water was evident in the water column showed no geographically significant pattern but a gradual decrease in these type of temperature profiles with time occurred until on the last transect no remains of summer water was found. This clearly shows that autumn had by this time passed and that full winter conditions pertained. This also suggests that as far as the seasonal changes in the water column are concerned, ANT X/3 took place during the latter part of autumn.

Measurements were conducted by three teams consisting of Klaus Ohm, Henry Valentine, Dieter Gerdes, Rainer Plugge, Gordon Rigg and Richard Phillips. Data processing was done by Andreas Maul and Gunther Krause. Underway observational strategy, planning and data interpretation was carried out by Gunther Krause and Johann Lütjeharms. We are indebted to David Thomas for oxygen determinations and to Marthie Stürcken-Rodewald and Ursula Klauke for nutrient analyses.

Conclusion: This hydrographic study was primarily intended as a pilot investigation for a possible subsequent investigation of the detail of the front. In all respects the aims of the project were amply met. A large and complex data set on the ASF was gathered and put together that awaits further analysis. Preliminary results show that the ASF is found along this whole coastline, is well developed at depth but that it´s surface expression rapidly erodes with the onset of autumn.

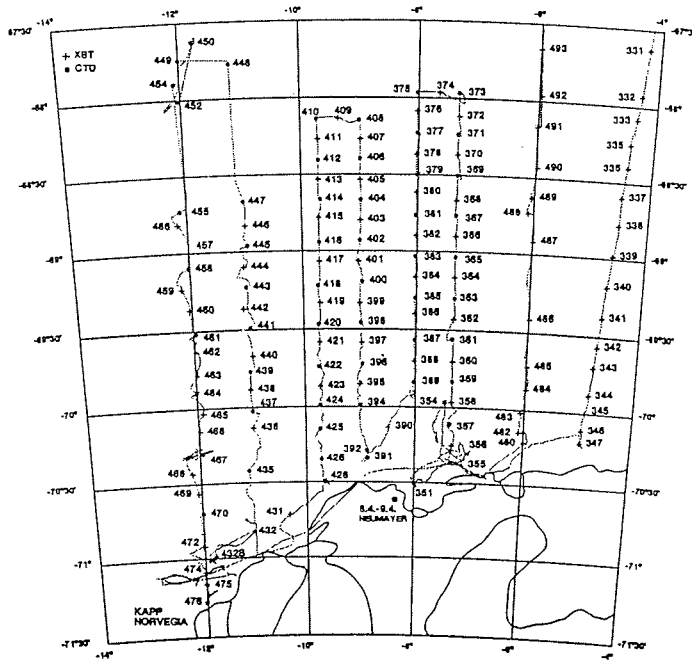

Fig. 5: Hydrographic stations during ANT X/3. Dots indicate CTD stations; crosses XBT stations.

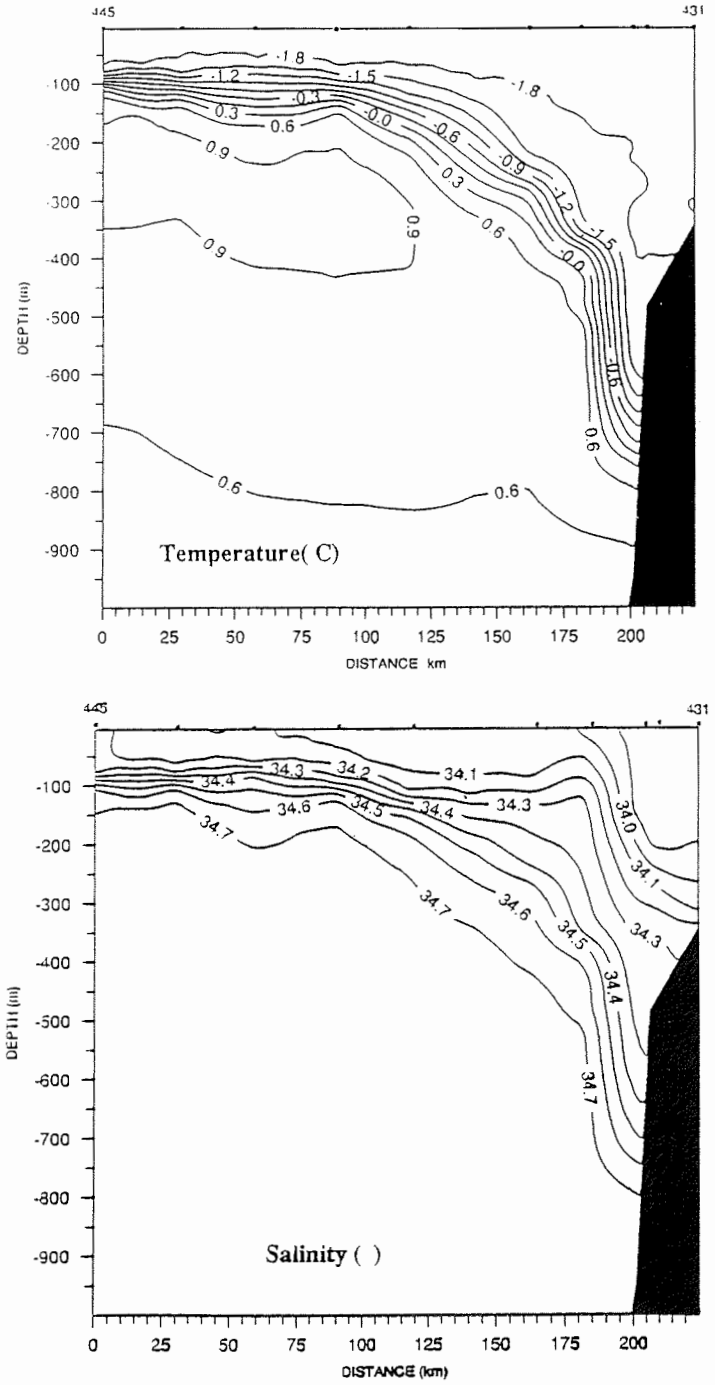

Fig. 6: The distribution of temperature (upper panel) and salinity along transect 5 of the ANT X/3 cruise.

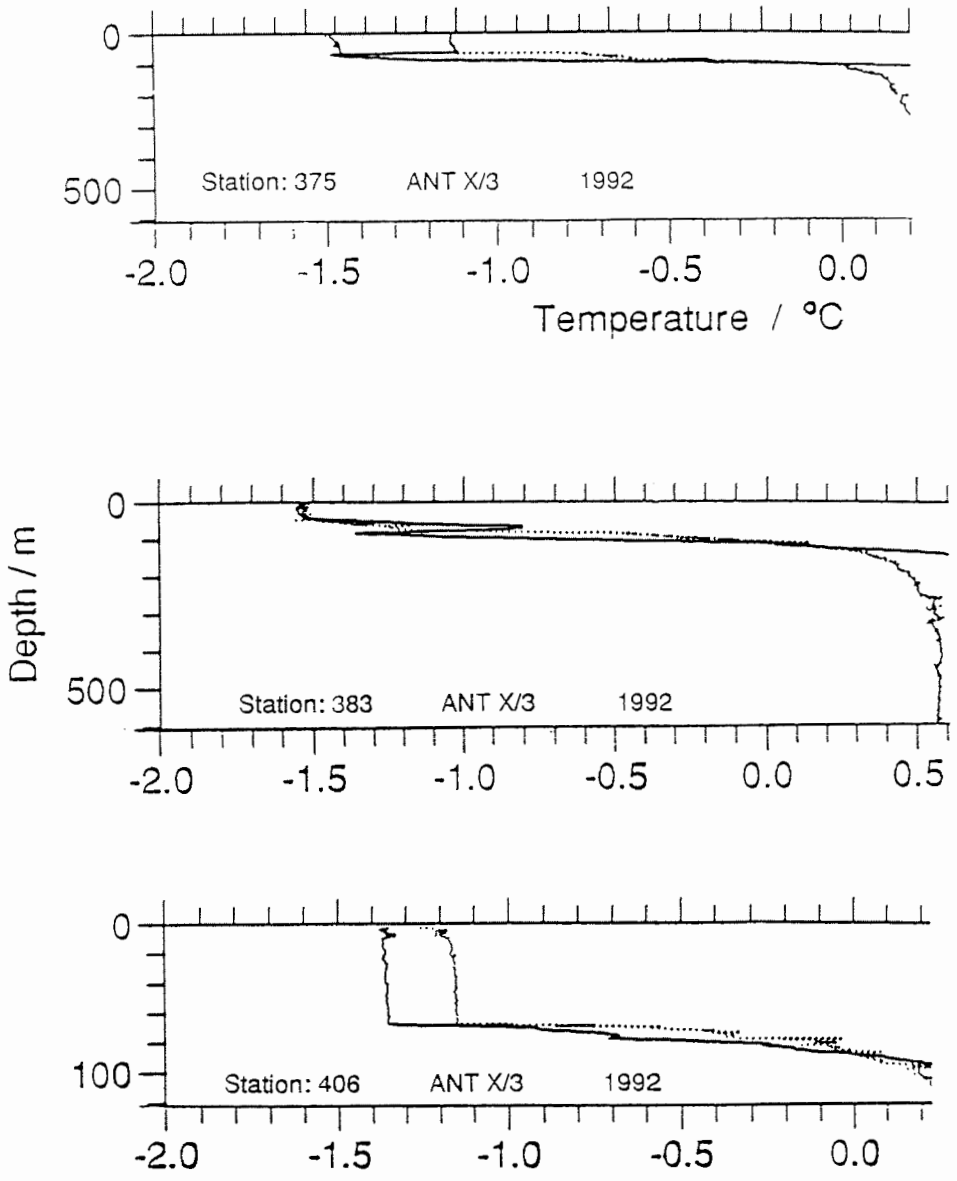

Fig. 7: Vertical traces of temperature and salinity at the stations indicated. The upper two show erosion of the summer water with small remnants while in the trace for station 40b all vestiges of summer water have been removed.

3.1.3. PRESSURE GAUGE DEPLOYMENT AND RECOVERY

Judged by its geographic extent, mass and volume flux, the major ocean current on the globe is the Antarctic Circumpolar which lies as an annulus around the Antarctic continent where it connects all the world's ocean basins. The volume, heat and salt flux of this current has been studied in the Drake Passage during the International Southern Oceans Studies (ISOS) of the 1970's. In order properly to understand global climate and the influence of the ocean on it, the nature and variability of the fluxes of the Antarctic Circumpolar Current (ACC) need to be understood circumpolarly and over a longer period than the ISOS measurements.

During this cruise two aspects of these general goals were touched.

3.1.4. LONG-TERM WATER LEVEL AND CURRENT MEASUREMENTS OFF KAP NORVEGIA

Since 1987 a mooring with one pressure gauge and two current meters has been maintained on the Continental Shelf off Kap Norvegia. This project of G. Krause aims at:

- improving tidal constants for the area.
- monitoring long-term water level fluctuations.
- measuring seasonal and inter-annual variations of the Antarctic Coastal Current.

The location of the mooring is not far away from the Georg von Neumayer Station where air pressure is recorded. Therefore it is possible to convert bottom pressure data into water levels with good accuracy.

The mooring is regularly exchanged during the yearly supply voyages of "Polarstern". In the austral summer 1991/92 it was only possible to deploy the new mooring but not to recover the previous one because of a heavy ice cover.

During this expedition the overdue mooring could be recovered. This success will not only add one more valuable time series to the long-term data set. The overlap period with the 1992 mooring was 5 months. This is very useful for maintaining the datum for the water level measurements and for instrument comparisons.

3.1.5. INITIATION OF MONITORING OF THE ANTARCTIC CIRCUMPOLAR CURRENT

The second monitoring endeavor involves the full ACC between Africa and Antarctica. To this end a research project has been designed by Dr. D. Pillsbury of Oregon State University and Dr. T. Whitworth of Texas A&M University in the USA as part of which pressure recorders are to be placed across the so-called choke points of the ACC south of Africa, south of New Zealand and in the Drake Passage. South of Africa four sets of moorings consisting of two gauges each were to be placed at a depth of about 1000 m in co-operation with Prof. G. Brundrit of the University of Cape Town. These specific gauges are intended to remain on the sea floor for two years and will be replaced biannually to carry out the monitoring for an intended period of ten years. They will monitor the barotropic flux variability over this period.
Of these four sets of moorings the southernmost one; on the continental slope of Antarctica off SANAE was deployed during ANT X/2. During ANT X/3 two sets of moorings were deployed: one on the African continental slope off Cape Town at position: 34° 35.32' S 17° 48.69' E on 27 March 1992; and the other off Bouvet Island at position: 54° 20.61' S 03° 01.43' E on 2 April 1992. The last set of gauges was to be placed at Discovery Seamount at about 42° 00' S 00° 00' E, but due to lack of time was handed

over to the Chief Scientist of ANT X/4 to be deployed on Shannon Seamount instead. All deployments were carried without complications.

Apart from the helpful ship's crew, the responsibility for these deployments during ANT X/3 rested with Henry Valentine and Johann Lütjeharms.

Conclusions: Two pressure gauges were successfully deployed with the minimum of trouble or delay. Due to favourable ice conditions in the coastal polynya it was possible to recover one more pressure gauge and current meter mooring for the long-term recording programme started in 1987. In this way valuable contributions were made to furthering the aims of the World Ocean Circulation Experiment (WOCE).

3.1.6. THE UPPER WATER COLUMN BETWEEN SOUTH AFRICA AND ANTARCTICA

The stretch of water from the southern tip of Africa to the Antarctic continent has, rather illogically, been designated a "choke point" for the Antarctic Circumpolar Current; other so-called choke points being the Drake Passage and the passage between New Zealand and Antarctica. In its attempt to gather a high-quality, consistent oceanographic data set in the next decade, the World Ocean Circulation Experiment (WOCE) observational plan includes the regular monitoring of these choke points.

The area between the southern tip of Africa and the Subtropical Convergence has furthermore been recognized by WOCE as an ocean region of special interest since vigorous exchange of water between ocean basins takes place here. This includes exchanges between the Indian and the Atlantic Oceans mostly via Agulhas rings, and between the subtropical basins and the Southern Ocean.

In order to study these processes en route and thus simultaneously to make a contribution to the aims of WOCE, underway measurements were made between Cape Town and Georg von Neumayer as well as on the return cruise leg. These included continuous temperature and salinity measurements as well as continuous chlorophyll (fluorescence measurements) and mixing observations in the hydrographic well of the ship. These measurements were started on 28 March 1992 at 36° 20'S; 16° 40'E. Data acquisition was at a sampling rate of 1 measurement per second. Means and standard deviations for every 10 s were recorded. At an average ship speed of 10 knots, or 5 ms^{-1}, this gave a nominal sampling resolution of 50 m. In view of the very long distance traversed, these data were decimated to give a resolution of 1 km.

When the ice-edge was crossed a protective plate was placed over the well, but measurements continued. The flushing rate in the well was, however, so reduced that continuous measurements in the well were terminated and only restarted when the ice-edge was again crossed on the return leg at about 67°S on May 7,1992. The geographic detail afforded by these high resolution measurements was very valuable, particularly in support of the subsurface measurements. An example is shown in Figure 3.

In addition, a line of T-7 XBT measurements to a nominal depth of 760 m was made for the full distance from Cape Town to Antarctica. These stations started when still within sight of Table Mountain and continued up to the shelf ice edge. Samples of surface water for salinity measurements were taken at the same time as were measurements of the sea surface temperatures by Crawford bucket to calibrate the XBT measurements.

The failure rate of XBT probes in the ice was high. A number of attempts were made to overcome this problem, including launching probes in the ice-free wake of the ship with a hand-held launcher from the stern, occasionally stopping the vessel as well as creating an ice-free area with the side-thrusters and launching into this region. These attempts were met with varying degrees of success, however, the failure rate remained high.

Results from these underway measurements were nevertheless exceptionally good. An excellent declouded, geometrical manipulated and atmospherically corrected satellite image for the cruise line from Cape Town to 45°S was produced in advance for this purpose by Dr O. Malan of the Ocean Climatology Research Group at the University of Cape Town. A line drawing interpretation of this thermal infrared image is given in Figure 3. XBT as well as continuous well-measurements confirmed all the circulation elements in this portrayal and to define their nature more closely.

The thermal characteristics of the upper water column as portrayed by the XBTs for the full cruise leg to Antarctica is shown in Figure 4, locating the Subtropical Convergence (STC), the Subantarctic Front (SAF), the Antarctic Polar Front (APF) and the Antarctic Slope Front (ASF).

The station spacing was halved over the last part of the transect. The purpose of increasing the spatial resolution for this section was to locate and circumscribe both the surface and subsurface expression of the Antarctic Slope Front with appropriate geographical detail even before the proper grid of hydrographic stations to study this front commenced. In this way the efficiency of the subsequent measuring programme could be maximized. This supposition proved to be correct. Only a feint surface expression of the Antarctic Slope Front was found, coincident with the ice-edge. It was considerably further north than usually found here in summer. Remnants of the subsurface temperature minimum characteristic of summer conditions were found at all these preliminary XBT stations bar two. This result indicated that although ice formation was far advanced, the water column was still characterised by the transition from a summer to winter situation.

On the return leg of the cruise an XBT section was carried out only from 45°S to Cape Town to minimise expense. A repeat of the full 5000 km section so shortly after the first traverse was believed probably not to be going to contribute substantially more information.

The scientific well measurements were run by Klaus Ohm, Rainer Plugge and Gunther Krause. The underway XBT measurements were carried out by Henry Valentine, Gordon Rigg, Richard Phillips, and Johann Lütjeharms.

Conclusion: The underway measurements between Cape Town and Antarctica successfully delineated the various frontal features. In the region of prime interest they were very useful in presenting an advance indication of the hydrographic structure to be expected.

3.2. Biology of sea ice and upper water column

3.2.1. MICROBIOLOGY OF SEA ICE

S. GROSSMANN

3.2.1.1. Objectives

Microbiological investigations focussed upon the effect of sea ice formation on natural bacterial populations. During the formation and growth of sea ice, biologically important parameters can be changed significantly. Temperature, salinity and nutrients will be shifted to extreme values. In many cases, the exchange of organic and inorganic material is reduced. For this study, characteristic, successive stages of ice formation were distinguished. Firstly, the transition from an open water situation to the beginning of new ice formation. Dependent on wind conditions and water movements, a thin layer of grease or nilas ice will be formed. After the growth of this first layer of new ice, small pancakes form which will be consolidate to form individual ice floes. At the final stage of

ice growth individual floes consolidate forming pack ice sheets and ridges. Alternatively, at longer periods of calm conditions, thin nilas ice grows into bigger floes without forming pancakes.

To obtain information about the fate of bacteria having been incorporated within sea ice, subsequent investigations of different, successive stages of ice formation were carried out. Bacterial response to incorporation into newly formed ice and the behavior of microbial populations during sea-ice growth were compared with those of associated water samples.

In addition to the determination of distribution patterns of bacterial cells and biomass, this study focussed mainly on changes in bacterial growth and activity between successive stages of sea ice and associated water samples.

3.2.1.2. Work at sea

During the cruise, samples of various stages of sea ice formation were obtained. Grease ice was sampled directly by zodiac or by a winch operated grease ice sampler (see 3.2.9). Small pancakes up to about one meter in diameter were sampled by hand or by a ship operated 'ice basket' which was designed to keep the sample undisturbed. Larger pancakes above one meter in diameter and consolidated ice sheets were sampled using 3" and 4"-ice corer.

All measurements of bacterial parameters were carried out on the brine. Depending on their consistence, samples of different ice stages were either sieved or centrifuged (450 g, 10 min) to separate the brine from ice crystals. Alternatively to the centrifuging-technique, brine of larger pancakes or consolidated ice floes was obtained by sack holes. Comparative surface water samples were obtained from the water rosette or by bucket.

On brine and water samples the following microbiological parameters were determined:

Bacterial cell numbers and biomass by direct epifluorescence microscopy. For this purpose, subsamples were fixed with 0.4 % formaldehyde (final conc.) for further microscopic analysis in the laboratory.

^{3}H-thymidine incorporation into DNA as a measure for multiplication rate. Triplicate samples of 20 ml were incubated with 10 nM of methyl-[^{3}H]-thymidine (diluted to 42 Ci mmol^{-1}) for 90-100 min. Incubations were stopped with formaldehyde (0.4 % final conc.). Three killed samples were used as blank. The samples were filtered onto 0.2 µm Nuclepore filters, extracted 5 min with 5% ice-cold trichloroacetic acid (TCA) and radioassayed in a liquid scintillation counter. For dependence of thymidine incorporation on incubation time and ^{3}H-thymidine concentration, time and concentration series were performed.

^{3}H-leucine incorporation into proteins as a measure for biomass production. Triplicate samples of 20 ml were incubated with 10 nM of L-[4,5-^{3}H]-leucine (diluted to 47 Ci mmol^{-1}) for 90-100 min. Extraction was performed for 30 min with 5% hot TCA. Otherwise, samples were processed parallel to the procedure described above for determining thimidine incorporation.

Percentage of actively metabolising cells using the micro-autoradiography-technique with ^{3}H-leucine as substrate. Samples of 10 ml were incubated with 10 µCi ml^{-1} of L-[4,5-^{3}H]-leucine (141 Ci mmol^{-1}). After 3 and 6 hrs, incubations were fixed with 0.4 % formaldehyde for further processing in the laboratory. A killed sample was used as blank.

Uptake of dissolved organic compounds using ^{3}H-leucine as substrate. For calculation of leucine turnover rates, triplicate samples of 20 ml were incubated with 50 µCi l^{-1} of L-[4,5-^{3}H]-leucine (141 Ci $mmol^{-1}$) for 90-100 min. Incubations were stopped with formaldehyde (0.4 % final conc.). Three killed samples were used as blanks. Samples were filtered onto 0.2 µm Nuclepore filters and radioassayed in a liquid scintillation counter.

Activities of extracellular enzymes using 4-methyl-7-coumarinylamide-L-leucine (MCA-leucine) as fluorescent model substrate. Triplicate samples of 20 ml were incubated with various concentrations of MCA-leucine of 2.5 to 50 µM . At t=0 and after 3 and 6 hrs., fluorescent response was measured at 445 nm under 365 nm excitation in a Kontron-fluorometer. Substrate saturation curves and Lineweaver-Burk plots were established in order to calculate hydrolyzation times, hydrolyzation rates and maximum velocities of hydrolysis.

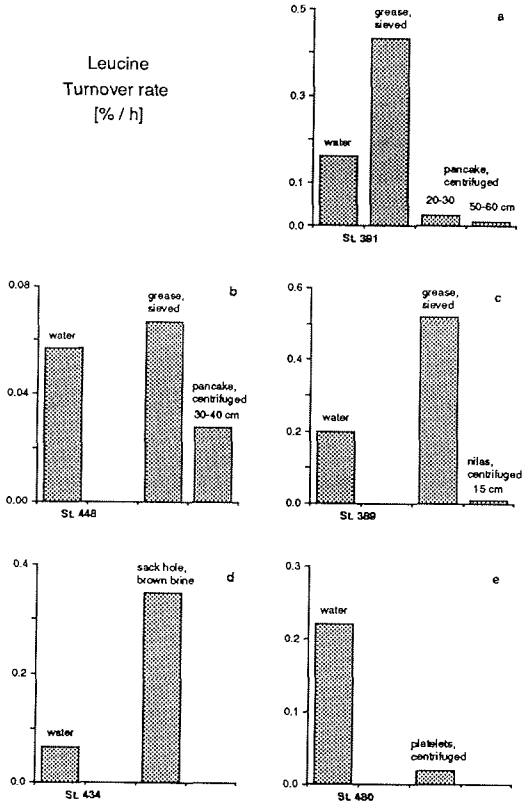

Fig. 8: Leucine turnover rates of ice samples at 5 stations. Different, successive stages of ice formation were compared with associated water samples obtained at the same station. Ice samples were sieved or centrifuged to separate ice and brine. Brine and associated water samples were incubated with ^{3}H-leucine. a) Sieved grease ice and centrifuged pancakes of 20-30 and 50-60 cm in diameter compared with associated water. b) Sieved grease ice and centrifuged pancakes of 30-40 cm in diameter compared with associated water. c) Sieved grease ice and centrifuged nilas ice of 15 cm thickness compared with associated water. d) Coloured brine of an 40 cm-sack hole (thickness of the sampled floe = 50 cm) compared with associated water sampled next to the floe. e) Platelets under a 45-60 cm-ice floe near the shelf ice cost - obtained through a 3"-hole - compared with associated water sampled next to the floe.

3.2.1.3. Preliminary results

The leucine turnover rates of different stages of new ice and associated water samples at 5 characteristic stations are shown in Figure 8 a-e. Comparing turnover rates of grease ice with those of open water samples, the uptake capacity for leucine in this first stage of new ice was enhanced (Fig. 8 a, c) or nearly equal to that of surface water (Fig. 8b). By contrast, turnover rates of pancakes were decreased compared to the open water (Fig. 8 a,b), with minimal activity in 50-60 cm sized pancakes (Fig. 8a). In the brown brine of consolidated floes the turnover rate increased again, exceeding the uptake capacity of associated water samples (Fig. 8d). From these results it could be concluded that bacterial activity was subjected to clear changes during the formation of sea ice. In contrast to brownish layers of older ice floes, abiotic and biotic conditions of the investigated pancake ice samples seem to be unfavorable for the development of bacterial populations.

Comparisons of leucine uptake rates of nilas ice with grease ice and related water samples (Fig. 8c) showed almost negligible activity in this type of ice. A similar scenario was observed for a sample of platelet ice (Fig. 8e). In contrast to grease ice, these two types of newly formed ice showed no physical or biological enrichments of bacterial activity.

As these first results of leucine turnover rates were calculated using the samples as a whole, no conclusions could be made about the relative activity per cell. Further information about changes of bacterial activity during the succession of ice types will be obtained by comparisons of turnover rates with bacterial cell numbers and biomass.

3.2.2. ECOPHYSIOLOGY OF POLAR MARINE MICROALGAE

M.GLEITZ, D. N. THOMAS

3.2.2.1. Objectives

The aim of this investigation was to determine physiological and biochemical changes that take place within phytoplankton communities during the transition from open water through various stages of new sea-ice formation. It is clear that during this process organisms will encounter profound changes in the prevailing physico-chemical environment. Therefore, measurements of *in situ* temperature, salinity, oxygen, nutrient levels together with measurements of carbonate system components (pH, alkalinity, concentrations of the different carbonate species) were made in different types of newly formed sea ice. Variations in such abiotic parameters will have an influence on the physiology and biochemistry of incorporated organisms. In order to gain an insight into these sorts of change, ATP, pigment and biogenic silicate concentrations were routinely measured. Samples were also taken for analysis of total carbon, nitrogen, carbohydrate, lipid and protein content. In order to determine the physiological status of the phototrophic component, we studied the ways in which primary production, carbon metabolism, and species composition vary due to the transition from turbulent low-light conditions in the open water to the stabilized light environment in the ice matrix.

3.2.2.2. Sampling strategies:

Several water and ice-types were sampled during the cruise using a variety of sampling techniques:

Open surface water was sampled using niskin bottles attached to the Biorosi at 2 or 10 m depth. At several stations, surface water was also collected next to the ship or from a zodiac with a bucket. Grease ice was sampled using a sampler that allowed the few centimeters of ice lying on the surface to be collected with little dilution by surrounding seawater. This material was immediately drained over a coarse sieve to avoid salinity changes due to later melting of ice. In order to collect indisturbed grease ice layers, the ship´s zodiac was employed. Small, fragile pancakes (up to 30 cm in diameter) were sampled in the same fashion. Larger pancake ice floes (up to 1 m in diameter) were collected using an ice basket operated from the ship using a winch.

Pancake ice consisting of several smaller pancakes frozen together with a diameter of > 10 m or consolidated pack ice sheet was sampled by means of coring. In these cases, sackholes of a depth ranging from approx. 30-50 cm were drilled, covered and allowed to fill. After time spans of several minutes up to approx. one hour, enough brine had accumulated to start sampling. Immediately, a 100 ml oxygen bottle was slowly filled and fixed for subsequent determination of oxygen concentration using a Winkler method. A 60 ml Nalgene bottle was then imersed in the liquid and tightly covered for pH and alkalinity determinations. The temperature of the sackhole brine was measured, and the remaining brine was collected for biochemical and/or activity determinations. Only sackhole data collected in this fashion were used for the evaluation of *in situ* physico-chemical features of newly formed sea ice. At several stations floes were unsuitable for sackhole sampling, and ice-cores were drilled, these were later cut in sections (approx. 5 cm) and centrifuged at -2°C and 1400 rpm in the laboratory. The collected brine was used for biochemical and primary production measurements.

3.2.2.3. Analytical methods:
In situ temperatures were measured using a digital temperature meter (Testoterm 7000) equipped with an oscillating quartz sensor.

Salinity was measured using a microprocessor conductivity meter (WTW LF 2000). Oxygen concentrations were determined by means of a computer based, automatic photometric Winkler titration system. Sample handling was done according to standard procedures. Carbonate species were calculated after determination of the total alkalinity using a potentiometric titration method. The sample was allowed to warm up to room temperature (about 20°C) in the dark. In case of the sackhole samples, the initial pH of the brine was measured using a microelectrode (Ingold U402-M6-S7/100) connected to a microprocessor pH meter (WTW pH 3000). In order to achieve an immediate pH determination, the electrode was allowed to acclimate to about the same salinity of the sample for approx. one hour using 0,2 µm filtered brine samples of known salinity. A pH reading that was stable for at least 60 s. was obtained after approx. 2 to 3 min., and this value used to calculate the corresponding *in situ* pH value. This was clearly not possible for drained or centrifuged samples. Subsequently, all samples were titrated to a pH of about 3 using 0,035 N HCl, the normality of which had been calibrated using potassium iodate. Approx. 20 pH readings ranging between 4 and 3 were used to calculate the amount of acid required to neutralize all weak bases in the solution.

Concentrations of nitrate, phosphate, silicate and ammonia were measured by means of an autoanalyzer (Technicon ASM 2). Immediately after the ice work, samples were stored at 4°C for a few hours before analysis. Only in a very few cases were samples frozen at -20°C prior measurent.

Aliquots between 100 and 2000 ml were filtered onto GF/C filters (Whatman) for the determination of Chl a, phaeopigment, total carbohydrate, lipid and protein concentrations. Precombusted GF/C filters were used for filtering samples for CHN analyses. Samples for determination of biogenic silicate were filtered onto cellulose acetate filters (0,4 µm, Sartorius GmbH), and ATP samples were filtered onto membrane filters (0,4 µm; Millipore). With the exception of pigment analyses, all other determinations will be carried out in the AWI, Bremerhaven.

The photosynthetic performance of microalgae was measured at three standard irradiances of 30, 90 and 160 µmoles PAR m^{-2} s^{-1} at a constant temperature of -1,5°C in a temperature-controlled incubator. Irradiances were adjusted using neutral density foil and measured with a quantum meter (LICOR 185 B) using a spherical light sensor (LICOR 193 SB). Production incubations were conducted in 50 or 100 ml glass bottles and started by adding $NaH^{14}CO_3$ (Ammersham Buchler GmbH) at specific activities of approx. 4 - 12 KBq ml^{-1}. After 5 h, incubations were terminated by filtering the samples

onto cellulose nitrate filters (0,45 µm; Sartorius GmbH). The filters were subsequently dried, placed for 30 s over fuming HCl, disolved in Quickszint 361 scintillation cocktail (Zinsser GmbH) and counted in a liquid scintillation counter (Packard TriCarb 1900). Quench correction was performed automatically using an external standard. Dark uptake rates determined in triplicate and were subtracted from light uptake measurements in all cases. In addition, triplicate light bottles inoculated with approx. 8 - 24 KBq ml^{-1} of $NaH^{14}CO_3$ were incubated for 10 h at 90 µmol PAR m^{-2} s^{-1}. These samples were then filtered onto GF/C filters for later determination of incorporation of newly assimilated carbon into major metabolic pools: carbohydrates, lipids, proteins and low molecular weight metabolites.

3.2.2.4. Preliminary Results and Discussion

The temperatures of sackhole samples ranged from about -1,8° to almost -7°C with corresponding salinities of 34 to nearly 110 psu Clearly the organisms incorporated into newly formed sea ice are exposed to severe temperature and salinity changes on a time scale of days to weeks. The capability to withstand such conditions will be a governing factor in dertermining primary production and species composition of sea ice microalgae.

Total alkalinity (TA) and the total disolved inorganic carbon concentration (Ct) of sackhole brine samples both appear to be linear functions of salinity up to about 100 psu (Fig. 9). Larger deviations in the Ct vs Sal plot are related to larger variations in the observed *in situ* pH values, which are primarily related to *in situ* partial pressure of disolved CO_2 gas. *In situ* pH values ranged from about 7,8 to 9,0 with corresponding pCO_2 values from about 900 to 50 ppm. As a decrease of pCO_2 and an increase in pH below and above surface seawater values would be expected due to physico-chemical processes associated with a decrease in temperature, the very high pCO_2 values recorded clearly do not follow this trend and might be indicative of biological activity in the brine (respiration activity).

No obvious relation was observed for the oxygen concentrations (ranging from about 350 to 600 µM) with respect to *in situ* temperatures (and salinities). It is evident, however, that essentially all values recorded were above surface seawater conditions, which can only partly be explained by increased oxygen concentrations due to an increased solubility at lower temperatures. Again, biological activity in the brine (photosynthetic oxygen production) might explain oxygen concentrations of almost twice the surface seawater value.

From nutrient concentration determinations it is obvious that nitrate, phosphate and silicate are generally lower than levels expected from extrapolating sea water values to the increased salinities of the brine (Fig. 10). Indeed, up to a salinity of about 70 psu, the opposite trend is observed: nutrient concentrations decrease with increasing salinities, and only above 70 psu there is an increase in nutrient concentrations, although these levels are still below predicted concentrations. Biological uptake and *in situ* activity of incorporated microalgae are suggested to be main causes for the observed trends. This is supported by enhanced ammonia concentrations, indicative of an active heterotrophic component of young sea ice microbial assemblages.

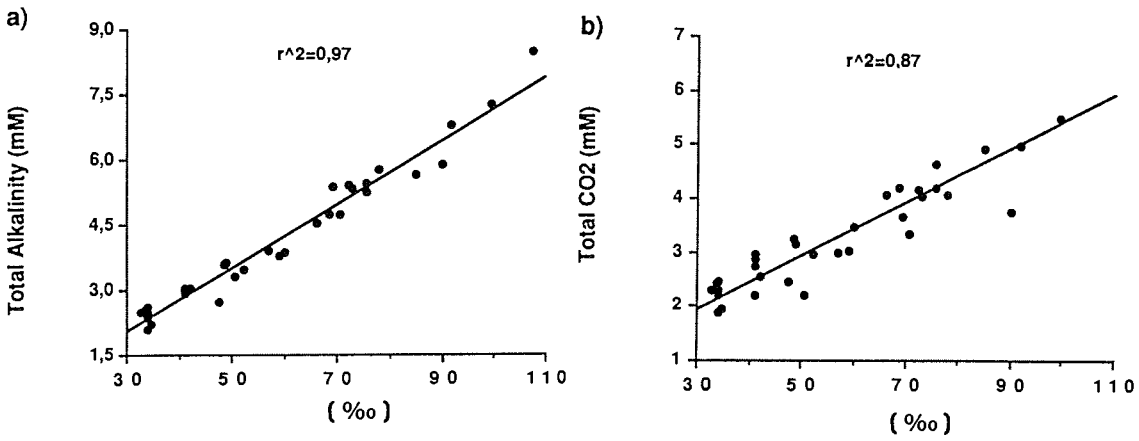

Fig. 9: Total alkalinity (a) and total concentration of inorganic carbon (b) of all sackhole samples (n=35) as a function of salinity. Linear regression coefficients and regression lines (solid) are also shown.

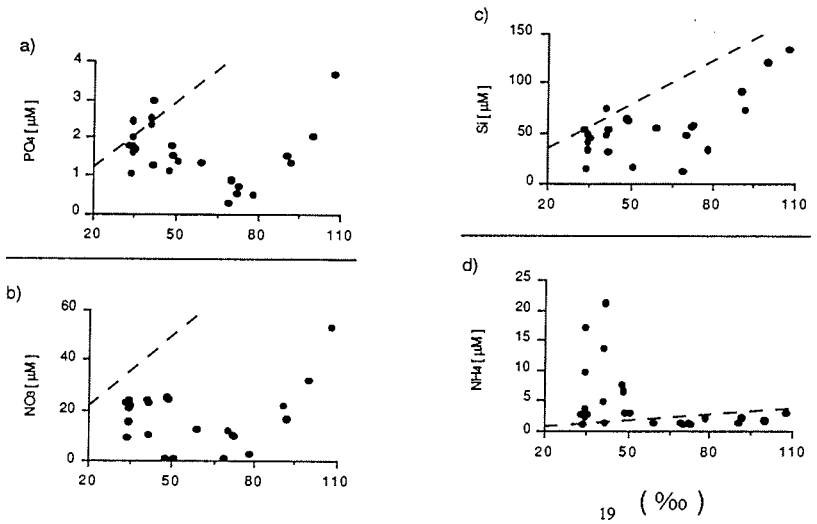

Fig. 10: Concentrations of phosphate (a), nitrate (b), silicate (c) and ammonium (d) as a function of salinity of sackhole samples. Dotted lines show the expected concentration when interpolating surface seawater concentrations to the respective brine salinity.

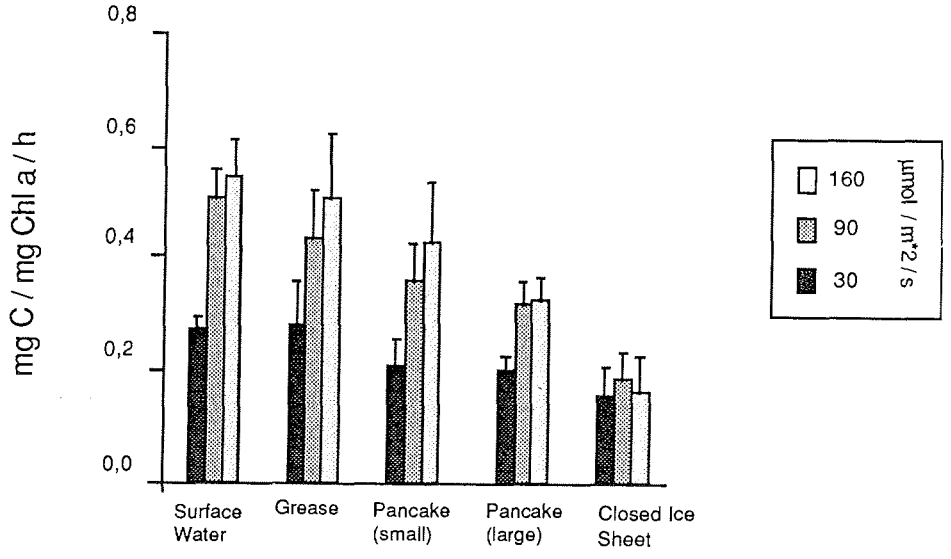

Fig. 11: Chlorophyll a - specific photosynthetic rates of surface water- (n=8), grease ice- (n=6), small pancake ice- (n=4), large pancake ice- (n=6) and closed ice sheet samples (n=4) at three different quantum irradiances. Bars indicate the standard error.

In order to document changes in the photosynthetic performance of incorporated microalgae, samples were grouped according to the different ice types investigated. As can be seen from Figure 11, there was no difference in carbon assimilation rates between open water and grease ice samples. A reduction, however, was observed for samples collected from single pancakes (approx. 0.3 to 1.0 m in diameter) and pancake floes consisting of several units frozen together (> 10 m in diameter). Also, photosynthetic carbon uptake at 160 µmol PAR m^{-2} s^{-1} was only slightly higher or equal to the rate recorded at 90 µmol PAR m^{-2} s^{-1}. Lowest uptake rates were recorded for samples taken from a consolidated, closed pack ice sheet. Also, photosynthesis appeared to be saturated at the lowest light intensity employed. Such variations may be interpreted in terms of a change in light acclimation status of the entrapped microalgal assemblage with increasing ice age. This implies that at least some species of the phytoplankton survive ice incorporation and sustain the capacity to acclimate to changes taking place within the abiotic environment. As sea-ice forms in late austral summer and autumn, a new habitat for plankton organisms is created and at least the microalgal component appears to be growing efficiently in this new stratum. Thus, late season primary production may be profoundly enhanced and the growth period of the phytoplankton significantly prolonged due to the formation of a stabilized ice cover on the sea surface.

3.2.3. REMOTE SENSING, PHYSIOLOGY AND PHOTOADAPTATION OF PHYTOPLANKTON AND ICE ALGAE

D. ROBINSON, C. W. SULLIVAN

The work by our group consisted of three separate yet somewhat related projects. First, Dr. L. Heidt of the National Center for Atmospheric Research and Prof. C.W. Sullivan of the University of Southern California are collaborating to examine the production of volatile brominated compounds by phytoplankton. During the cruise, the atmosphere was periodically sampled by filling evacuated air canisters and corresponding measurements were made of chlorophyll concentration in the adjacent surface water or ice cover. Analysis of the air samples will be completed at the National Center for Atmospheric Research in Boulder, Colorado. In total 48 air samples were taken during the cruise including 10 during the crossing from Cape Town to Antarctica, 13 as the ship travelled through open water and ice in various stages of development, 9 from within core holes in ice of various stages of development, and 16 during the crossing from Antarctica to Cape Town.

A second project was related to satellite remote sensing of ocean color to determine chlorophyll concentrations in the world's oceans. In the Southern Ocean, such determinations are complicated by the presence of ice which may obscure or alter the chlorophyll signature. Our goal with this project was to qualify the reflectance signal of chlorophyll associated with the water and the various ice types. A spectral radiometer on loan from the National Aeronautic and Space Administration (NASA) was used to measure reflectance spectra (400-1100 nm wavelengths) from of the ocean surface. Spectra were to be collected over a range of ice conditions, from 0 to 100% ice coverage. Unfortunately, the low sun angle of the Autumn sun and the incidental crossing of the marginal ice edge zone during periods of low light (late afternoon, night, and early morning) kept reflectance intensities below minimum detection levels.

In a third project, we sought to examine photoadaptation of phytoplankton/ice algae during the ice formation process. Phytoplankton entrained in the vertical mixing cycle of the water column, are exposed to variable and relatively low irradiance. During the initial stages of ice formation, phytoplankton cells are scavenged by frazil ice crystals and are brought rapidly to the surface. Here, as part of the grease ice community, they are exposed to a much higher irradiance than in the water column. As thin pancakes form, the associated phytoplankton are maintained in a relatively high irradiance environment. This set of irradiance conditions, uniquely found during sea ice formation, provided an opportunity to study short-term (less that a generation time) and long-term (greater than a generation time) photoadaptive responses in the natural environment. In particular, we were interested in rapid shifts in the content in xanthophyll cycle pigments (diatoxanthin and diadinoxanthin) and slower changes in the cellular content photosynthetic pigments (chlorophylls a and c, fucoxanthin), and how these changes in pigmentation effect photosynthesis and the quantum yield of photosynthesis.

Algal samples were collected from the water column and a progression of ice-types from grease ice through various stages of pancake ice formation. Ice samples were melted out in sufficient 0.2 mm mesh filtered sea water to maintain salinity above 30 psu. Photosynthesis-irradiance relationships were determined by the small-volume, short-incubation time (photosynthetron) method. Algal cells were filtered onto glass fiber filters (GF/F Whatman) and immediately frozen for later determinations of the absorbance properties of the algae (spectrophotometric analysis) and total cellular pigment content (HPLC).

Preliminary results from photosynthesis-irradiance relationships indicate that changes in photosynthesis have occurred in response to the changing light environment. In particular, the susceptibility to photoinhibition by high irradiance appears to lessen the longer algae are held at the surface. The completion of absorption and pigment analysis

will enable us to determine if these photosynthetic changes are related to changes in pigmentation and the quantum yield of photosynthesis.

3.2.4. COCCOLITHOPHORES FROM ANTARCTIC WATERS.

A. WINTER, M. ELBRÄCHTER

3.2.4.1. Introduction

Coccolithophores have been important components of the marine plankton since the Jurassic. Because of their rapid evolutionary rates and their abundance in marine calcareous sediments they have proved to be useful as stratigraphic markers. Coccolithophores can also be used as paleoceanographic proxies because they are vertically and horizontally stratified in the oceans. It is thought that ocean masses, latitude, nutrients, available light, vitamins and minerals all contribute to their distribution. However, primarily due to lack of data, the exact influence of these parameters is still unknown. Recently coccolithophores have gained international attention because they have been implicated in many global change processes. These include their production of DMSP and halogenated compounds which can change climate patterns. Also because they are extremely abundant at times (especially in temperate latitudes) coccolithophores should play an important role in the global carbonate and carbon cycles.

The purpose of this investigation was to determine the extent and abundance of coccolithophores in Antarctic waters. Only a few other investigations have studied coccolithophores from Antarctica and these have mostly concentrated on the heterotrophic coccolithophores (see 3.2.10). To our knowledge this is the first investigation to study the phototrophic coccolithophores from the water column south of the Antarctic Slope Front and one of the few to systamatically study coccolithophores from Antarctic waters. Also the distribution of coccolithophores near the surface (either by bucket or ship system) were studies on the transect to and from Antarctica.

3.2.4.2. Methods

Water was obtained from the biorosi or bathysonde from at least three different depths and from ice samples (Table 1). Two liters of water were filtered through 14 mm, 0.8 micron type AA millipore filters. The samples were washed with distilled water, air dried and stored for future investigation. This will include abundance studies with the polarizing light and structural studies with a SEM.

3.2.4.3. Preliminary results

Phototrophic coccolithophores of one species were present from a number of open water locations and in a few slush ice station. Positive identification of these coccospheres will have to await detailed study by SEM. To our knowledge this is the first time phototrophic coccolithophores have been observed under the ice and in brown slush ice. It is interesting to note that all the stations where the Antarctic phototrophic coccolithophores were observed were also stations with remnants of warmer summer water in the water column. The finding of a phototrophic coccolithophore with strongly calcified plates may have a special significance for paleoceanographic research of Antarctic waters.

Table 1: Coccolithophore sampling stations. 8T= Ship system; 8W= sea water

Sample	Depths	Date	Longitude	Latitude
1	8T	March 28	E14.45.754	S39.46.754
2	8T	March 29	E13	S40
3	8T	April 1	E5.06.512	S50.30.375
4	8T	April 2	E0.43.618	S52.45.363
5	8T	April 3	W1.21.971	S54.47.072
6	8T	April 4	W2.15.577	S59.17.614
7	8T	April 5	W3.27.047	S64.42.490
8	8T	April 6	W4.17.791	S67.58.964
9	8T	April 7	W4.59.909	S70.08.617
10	ice Bottom	April 8	W7.59.032	S70.30.878
11	ice Bottom	April 9	W8.00.642	S70.30.415
12,13,14	0,13,26	April 11	W7.26.773	S69.57.828
15	brine	April 11	W7.26.773	S69.57.828
16	slush	April 11	W7.26.773	S69.57.828
17	4	April 11	W7.27.007	S70.21.022
18,19,20	10,19,30	April 12	W7.20.72	S69.33.50
21	net tow 0-50	April 12	W7.20.72	S69.33.50
22,23	11,30	April 13	W7.20.0	S68.29.9
24,25,26	23,33,65	April 14	W8	S68.14
27,28,29	0,25,29	April 15	W8.01.9	S69.49.7
30	ice bottom	April 15	W8.01.9	S69.49.7
31,32	10,29	April 16	W8.55.00	S70.21.66
33	sack hole	April 16	W8.53.207	S70.21.064
34,35,36	0,11,23	April 17	W9	S69.46
37	brine	April 17	W9	S69.46
38,39,40	15,29,42	April 18	W9.43.2715	S68.7.962
41,42,43	1,21,31	April 19	W9.45.530	S69.13.968
44,45,46	0,10,20	April 20	W9.44.061	S70.21.281
47,48,49	0,10,20	April 21	W11.00.336	S70.59.250
50,51	10,20	April 22	W11.48.24	S70.59.62
52	ice bottom	April 23	W11.48.24	S70.59.62
53,54,55	0,1,9	April 24	W11.00.11	S69.46.00
56	ice sample	April 24	W11.00.11	S69.46.00
57,58,59	0,10,20	April 25	W11.01.12	S68.40.47
60	pancake ice	April 26	W11.46.621	S67.37.79
61,62,63	0,10,20	April 26	W11.46.621	S67.37.79
64,65,66	10,21,29	April 27	W12.06.28	S67.53.71
70	mixed ice	April 27	W12.06.28	S67.53.71
67,68,69	0,10,20	April 28	W12.06.28	S67.53.71
71,72	0,10	April 29	W12.0.34	S69.53.79
73,74,75	1,10,19	May 1	W11.57.08	S70.18
76	ice	May 1	W11.57.08	S70.18
77,78,79	10,30,50	May 2	W11.59.09	S71.05.09
80,81,82	0,50,19	May 2	W12.01.21	S71.16.67
83,84,85	0,10,20	May 6	W6.7.14	S68.43.95
86	pack ice	May 6	W6.7.14	S68.43.95
87	8T	May 7	W4.55.05	S66.35.42
88	8T	May 7	W2.45.38	S64.40.58
89	8T	May 8	W00.24.64	S62.23.29
90	8W	May 8	W00.24.64	S62.23.29
91	8T	May 8	W00.47.85	S61.10.96
92	8T	May 9	E2.34.85	S59.17.30
93	8T	May 9	E3.20	S58.29
94	8T	May 10	E4.7	S57.37
95	8T	May 11	W0.32.04	S55.38.04
96	8T	May 12	W3.22.91	S54.20.91
97	8T	May 13	E2.50	S51.29
98	8T	May 14	E06.44.35	S49.07.67
99	8T	May 15	E9.13.97	S46.9.13

3.2.5. TAXONOMY AND ECOLOGY OF HETEROTROPHIC ICE-FLAGELLATES.

M. ELBRÄCHTER, M. ZÖLFFEL

3.2.5.1. Introduction

The ice of polar seas harbours a special biocoenosis in which unicellular algae are the primary producers. The biology of the ice algae has been investigated intensively in the past. In contrast, up to now little attention has been paid to the taxonomy and biology of flagellates, in particular the heterotrophic ones, although they may play an important role in the trophodynamic relationships within the ice communities.

The aim of these taxonomic studies is to investigate the diversity of heterotrophic flagellates, with particular emphasis on dinoflagellates and flagellates incertae sedis within the Antarctic sea-ice and water column communities. The choanoflagellates were investigated at the same time and at the same stations (see 3.2.10).

Taxonomy defines the identity of the species. Each species differs from any other not only by morphology but also in physiology, biochemistry and behaviour. Therefore, a taxonomic survey also provides information on the diversity of the ice habitats.

3.2.5.2. Methods

Sea ice samples (grease-, nilas-, pancake-ice of various thickness and consolidated ice) were melted either directly or in normal sea water, respectively in concentrated sea water (salinity approx. 60 psu). In addition, the protists from brine samples, recovered from sack-holes, were investigated. The organisms were observed by various light microscopy methods, including fluorescence microscopy, and others were specially prepared for various staining methods. Some samples were fixed for detailed examination at home for light- and electron-microscopy. Subsamples were cultured with organic material added to some cultures to enhance bacterial growth as food source for the heterotrophic flagellates.

In order to address the question of whether the organisms in the ice are equally present in the water column, water samples and samples taken by the "Mikronetz" (20 µm mesh size) were investigated by the same methods.

3.2.5.3. Preliminary results

DINOFLAGELLATES.

In grease-, nilas-, and thin pancake-ice, large numbers of a small heterotrophic *Gymnodinium* species, rarely seen in the water, dominated the dinoflagellate assemblage. Phototrophic species such as *Gymnodinium baccatum*-like forms were rare. In older pancake and columnar ice various heterotrophic and phototrophic species of *Amphidinum, Gymnodinium, Gyrodinium,* and *Katodinium* were common; most of them are rarely found in the water column. Several thecate heterotrophic dinoflagellate species, rarely seen in the water column, were also present. In "brown ice" (e.g. station 107b) several species occurred that were not found elsewere in the ice. These include two species of *Prorocentrum* (phototrophic), of which only *P. antarcticum* has been found (but rarely) in the water column. *Polykrikos-sp. nov.*was common in the ice during ANT V/3 (November/December 1986) but only a few specimens were encountered during the present cruise. Large, obligate heterotrophic euglenids of the genera *Anisonema, Astasia, Hyalophacus* and *Ploetia* were also found exclusively in "brown ice" samples. Many species of the genus *Protoperidinium* were found in the water column, but not in the ice. Totally, more than 70 dinoflagellate taxa were distinguished during the present study. Living cells of the phototrophic silicoflagellates *Dictyocha fibula* and *D. speculum* were found only in the water column, but not in any ice sample.

During the present investigation, we focussed on trophodynamic relationships. One prominent discovery was that many specimens of various species of *Protoperidinium* and of the "*Diplopsalis*" group do not feed by "pallium-feeding" as has been assumed for

these organisms, but they (also?) feed by uptake of particulate matter into the cell body itself. Various particles including intact chloroplasts of other algae and a cnidocysts of an unknown cnidaria were found inside these thecate dinoflagellates. In one case, a *Protoperidinium* was observed feeding on a tintinnid by myzocytosis. We speculate that in the Antarctic the presumably more primitive food uptake mechanism of phagotrophy has been remained, whereas "pallium-feeding" is a further evolved feeding strategy.

The unarmoured dinoflagellate *Nematodinium sp. nov.* which is abundant in the ice and in the water column, is a voracious feeder despite its possession of chloroplasts. This mixotrophic species ingests various prymnesiophytes, thecate and athecate dinoflagellates, pennate and centric (e.g. *Asterophalus*) diatoms. In one case it was observed ingesting the ciliate *Spiroprorodon garrisoni*, itself a voracious feeder on other dinoflagellates, prymnesiophytes and diatoms. It is likely that mixotrophy is a common nutritional strategy for several organisms living in the ice. Several dinoflagellates having the same morphology either are devoid of chlorophyll, as demonstrated by epifluorescence microscopy, or they are observed with ingested food. However, many specimens also contain various numbers of chloroplasts inside their cytoplasm. Electron microscopy will show whether these chloroplasts are genuine dinoflagellate chloroplasts or "cleptoplasts", as known from other dinoflagellates and ciliates. "Cleptoplasts" are chloroplasts from food organisms that are not immediately digested but remain intact for some time (up to several weeks) and which perform photosynthesis inside their "host". In the same samples, several ciliates of the genus *Strombidium* with "cleptoplasts" were abundant.

True heterotrophs, feeding effectively mainly on pennate diatoms of all size classes, are the small *Cryothecomonas* species, flagellates of unknown affinity. These organisms can attack diatoms with a feeding tube inserted apparently through the girdle bands. Up to 7 *Cryothecomonas* flagellates were observed feeding on a single diatom cell. Several other obligate heterotrophic flagellates, which have been assigned to the genus *Protaspis* are phagotrophic and feed on bacteria, various flagellates and diatoms, as do unidentified taxa of amoeba, and many ciliate species.

The ability of various organisms to feed on bacteria should be tested by feeding experiments. Time series experiments should give information on quantitative aspects. Therefore, DAPI-labelled bacteria or microspheres showing fluorescence were added to natural plankton samples enriched by the Mikronetz. Ciliates, in particular the dominant *Strombidium*, *Strobilidium* and the tintinnid *Codonelopsis* apparently are very sensitive to DAPI stain and even two times washed DAPI-stained bacteria killed the ciliates within several hours. Microspheres were rejected. The foraminifer *Neogloboquadrina pachyderma* also rejected microspheres. DAPI-stained bacteria were rejected in the first hours but with long term experiments we showed for the first time that this species can feed on bacteria. Many species of heterotrophic dinoflagellates showed autofluorescence from small particles on the plasmalemma, indistinguishable from DAPI-stained bacteria or microspheres. Thus the feeding experiments planned could not be applied to dinoflagellates in field samples. In cultures, heterotrophic flagellates showed a slow growth, thus there was not enough material to conduct these planned feeding experiments.

In several copepod species endoparasites, apparently the dinoflagellate *Syndinium* were found.

Food items of different taxonomic groups as observed during the present cruise:

AMOEBA	Flagellates, Dinoflagellates, Diatoms
CILIATES	Bacteria, Flagellates, Dinoflagellates, Silicoflagellates, Diatoms, Ciliates, dead organisms
FLAGELLATES	Bacteria, Flagellates, Dinoflagellates, Diatoms, Ciliates, dead organisms
DINOFLAGELLATES	Bacteria, Flagellates, Dinoflagellates, Diatoms, Ciliates, dead organisms, faeces

Examples of special dinoflagellates: Nematodfinium sp. nov. (with chloroplasts) :Prymnesiophytes, Prasinophytes, Dinoflagellates, pennate and centric Diatoms,Ciliates up to 50 µm Protoperidinium ssp : Prymnesiophytes (and otherflagellates), Diatoms, Tintinnids, cnidocysts.

HETEROTROPHIC FLAGELLATES

Among the non-chloroplast bearing flagellates, approximately 150 genera of small heterotrophic flagellates (e.g. apusomonads, cercomonads and protaspids) have been described in the literature, but which cannot be assigned to any of the major flagellate groups (e.g. euglenids, dinoflagellates and heterokonts). The characteristic features of these heterotrophic flagellates are their minute size (average 10 µm) and fast movement. Only rarely they do possess scales (e.g. *Thaumatomastix*) or siliceous elements (e.g. choanoflagellates), and these groups have not been included in this survey.

Altogether about 30 taxa, of which at least 2 are new to science, were identified in Antarctic sea-ice and water column samples.

Grease, fast and platelet ice is dominated by the filter feeding pedinellids belonging to the genera *Actinomonas* and *Pteridomonas*. Enrichment cultures of these samples showed *Amastigomonas mutabilis* to be the most abundant species.
The richest diversity was revealed by raw cultures of older ice (columnar and brown ice). Typical species are the diatom-devouring *Cryothecomonas* species (distinguishable only by TEM), *Cryptaulax marina*, members of the *Protaspis* group, pedinellids and amastigomonads.

Some marine flagellates (e.g. *Massisteria marina*), common in habitats north to the Antarctic convergence, have not been found in Antarcic sea-ice and water samples.
For comparison, enrichments of sea water north of the convergence (from the sea water pipe of FS 'POLARSTERN' and concentrated by 20 µm filtration) were analyzed. They show a species composition known from marine tropical and temperate sites, being dominated by *Bodo designis*, *Rhynchomonas nasuta*, *Cafeteria* species, *Bordnamonas tropicana*, *Massisteria marina* and *Pseudobodo tremulans*.

Other flagellates (e.g. bodonids) occured in lower numbers in raw cultures of Antarctic sea-ice and water than in enrichment cultures of samples from marine temperate sites (e.g. Northern Atlantic), in which these organisms grow fast and reach densities up to 10^6 cells ml^{-1}.
The investigation of the Antarctic "autumn situation" revealed a diversity different from what is known from habitats of the temperate northern hemisphere.
Therefore, a taxonomical survey on the Antarctic heterotrophic flagellates *incertae sedis* in other seasons is urgently needed.

Additional work was carried out on the planktonic protist *Solenicola setigera*, found exclusively on the diatom *Leptocylindrus mediterraneus*. Chloroplast-like bodies in some *Solenicola* cells were detected with fluorescence microscopy. Light microscopy of living and fixed cells could not rule out conclusively wether *Solenicola* is a life stage of *Leptocylindrus* or, more probably, a highly adapted epizoic/parasitic organism. Bulk

fixations were prepared for further TEM work to define the ultrastructural identity of this and other poorly known but abundant organisms.
To study the parasitic dinoflagellate *Syndinium*, the tissue of various copepod species was mounted for ordinary TEM work.

3.2.6. THE DIMETHYLSULFONIOPROPINATE (DMSP) CONTENT OF MICROALGAE IN THE WATER COLUMN AND DIFFERENT ICE STAGES.

E. VAN HANNEN, W. SCHMIDT

The production of organic sulfur gases such as dimethyl- sulphide (DMS), methane thiol (MeSH), dimethyl disulphide (DM-DS), carbonyl sulfide (COS) and carbon disulfide (CS_2) plays an important role in the global sulphur cycle. In the atmosphere reduced sulfur gases undergo chemical and photochemical oxidation, yielding products which contribute to the acidity of precipitation. Sulphur gases in the atmosphere form aerosol particles which can scatter light or form cloud condensation nuclei and in this way increase the reflectivity and radiative balance of the earth. The large amount of sulphur gases released into the atmosphere has a possible role in global temperature regulation.

The production of DMS by algae in the ocean surface water is one of the major sources of sulfur to the atmosphere. Since it is now generally accepted that DMSP is the precursor of DMS, it is important to establish the amount of DMSP wich is produced by marine algae. DMSP in ice-algae may act as an osmolyte and as a cryoprotectant. Various algal classes of phytoplankton produce DMSP. In general the chlorophyll a/c algae (Dinophyceae, Prymnesiophyceae, some species of the Bacillariophyceae and the Chrysophyceae) and the chlorophyll a/b containing Prasinophyceae produce large amounts of DMSP. In most other chlorophyll a/b algae and the crytomonads and Cyanobacteria DMSP concentration is low.

The objectives of this leg (ANT X/3) were to estimate the content of DMSP in the algae of the water column and in the ice during autumn.

On the downward leg form Cape Town to Antarctica surface-water samples were collected from 52° 32.113'S 00° 42.453'E three times a day until packice was reached at. 70° 09.078'S . 04° 58.731'E. Water samples (5 litres per sample) were filtered using GF/C filters and frozen immediately (-80 °C). Half of the samples were used for chlorphyll measurements and the other half taken back to the University of Bremen for DMSP analysis . During the oceanographic grid water samples (5 litres per sample) were taken from the Biorosette (CTD) from every depth and also filtered using GF-C filters (station numbers: 21/348, 355, 361, 369, 373, 392, 400, 410, 418, 426, 441, 454, 474). Filters were stored at -30 °C (after preliminary freezing at -80 °C). During ice stations samples were taken from the different kinds of ice and melted overnight using dialys´s tubes. After melting samples were filtered (GF/C). Brine water samples were filtered directly after measuring salinity. On the way back to Cape Town surface water samples were taken 3 times a day from 66° 33.78'S . 04° 52.80'E till. 49° 07.67'S . 06° 44.39'E for chlorophyll and DMSP measurements.

3.2.7. NITROGEN CYCLING, PHOTOSYNTHESIS - IRRADIANCE RELATIONSHIPS AND CO_2 EXCHANGES.

M. LUCAS, T. A. PROBYN, C. G. ATTWOOD, K. M. DOWER

3.2.7.1. Introduction

Due largely to man's activities since the 18th Century (fossil fuel combustion, agriculture and de-forestation) "greenhouse gas" concentrations are increasing; notably CO_2,

methane and CFC's which together account for about 87% of the increase at present. Atmospheric CO_2 is increasing at an annual average rate of 1.4ppm; about 0.4% per year. The Intergovernmental Panel on Climate Change (IPCC) concludes that for the period 1980-1989 there was a net excess imbalance between anthropogenic CO_2 emmissions and marine and terrestrial biospheric uptake of about 1.6± 1.4 Gt $C.yr^{-1}$. The uncertainty is due largely to a paucity of data for the southern hemisphere and in particular the Southern Ocean.

Recognising this, the International Joint Global Ocean Flux Study (JGOFS) initiated in 1989 and SCAR (1989) concluded that the Southern Ocean may exert a significant impact on global climate change in terms of meridional heat flux and CO_2 exchange. Because of the extreme seasonality of the region, ocean-atmosphere fluxes of heat and CO_2 are likely to exhibit strong seasonal signals regulated both by physical and biological processes in the water column and by seasonal sea-ice cover. These processes are summarised in Figure 12.

Exchanges of CO_2 at the air/sea interface (2) depend primarily upon the relative partial pressure of CO_2 (pCO_2) in the atmosphere and in surface waters. The transfer velocity of CO_2 across this interface depends upon wind strength and wave shape while CO_2 solubility in seawater is temperature dependent; it being increasingly soluble in colder water. The Southern Ocean has therefore been notionally regarded as a possible CO_2 sink although recent data on aqueous pCO_2 to the south of Africa and in the South Pacific point to a mosaic of "source" and "sink" regions. Seasonal sea-ice cover (10) is clearly important in the inhibition of gaseous exchange while the development of sea-ice microbial communities may have important implications for carbon and nitrogen cycling. It is the exchange of CO_2 from surface waters into the deep ocean which is the critical rate-limiting step between atmospheric and oceanic carbon biogeochemical cycles.

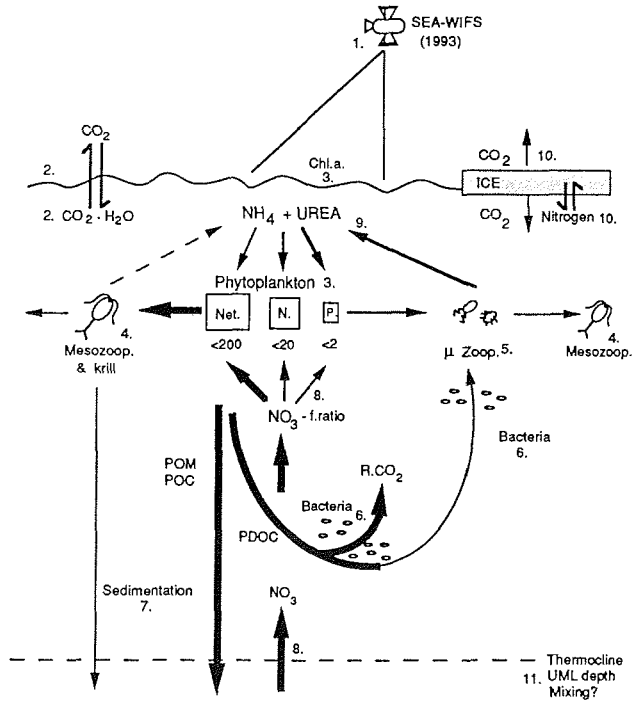

Fig. 12: Conceptual view of carbon cycling processes in the Southern Ocean. The thickness of the arrows represents the relative importance of the carbon flow pathway. The numbers refer to a description of the processes in the text (similarly numbered).

In this respect phytoplankton biomass and photosynthesis (3) provide the basis for transporting fixed carbon into the deep ocean by the processes of direct sedimentation of cells (7) and through particle transformation into rapidly sinking faecal pellets as a result of krill and mesozooplankton grazing (4) on larger (>20 μm) net-phytoplankton cells (3). This is the "biological pump". The rate at which phytoplankton cells and other particles sink is to a large extent size-dependent. This is why it is useful to consider phytoplankton biomass and production on a size basis; splitting them into net-plankton (>20 μm), nano-plankton (2 - 20 μm) and pico-plankton (<2 μm). Small nano- and pico-plankton are not readily consumed by large zooplankton so they enter the micro-zooplankton food chain (5) which is characterised by little sedimentation but considerable regeneration of NH_4 and urea (9) which is preferred and assimilated rapidly by phytoplankton. Phytoplankton cells that do sink through the euphotic zone ultimately become light limited and die, being then partially decomposed by the bacterial/ microzooplankton food chain - the "microbial loop".

A feature of the Southern Ocean generally is that primary production is lower than might be expected on the basis of available nutrients, particularly nitrogen. Explanations for this observation include light limitation, strong grazing pressure by microzooplankton, mesozooplankton and krill and the possibility that micro-nutrients, such as iron, limit algal growth.

Particulate aggregation and sedimentation removes carbon from surface waters, thereby reducing its pCO_2 relative to atmospheric values; so allowing further atmospheric CO_2 to be "drawn down" into the water. Subduction and downwelling of surface water into the deep ocean achieves the same effect. In this instance the oceans are regarded as a "sink" for atmospheric CO_2. Conversely, respiration processes in surface waters, particularly by organisms in the microbial loop, return a large percentage (>50 %) of the photosynthetically fixed carbon to the CO_2 pool in surface waters. This elevates pCO_2 and may reverse the carbon flux sign so that the ocean out-gases CO_2, thus becoming an atmospheric "source" for CO_2. Upwelling of CO_2 rich deep ocean water will also elevate surface water pCO_2 with the same consequence. Physical processes and the size-structure of planktonic communities therefore have a crucial bearing on pCO_2 in surface waters.

Nitrate assimilation relative to total N assimilation by phytoplankton using ^{15}N tracers (8) provides a useful index, the f-ratio, which indicates what proportion of phytoplankton growth is dependent upon NO_3 assimilation - i.e. "new" net production. Under long term equilibrium conditions, the f-ratio provides a measure of export production available to consumers or for sedimentation since NO_3 advection into surface waters must be related to N losses from surface waters. Direct measures of particle flux using sediment traps are complicated by considerable uncertainty in data interpretation. The f-ratio therefore provides a valuable tool for indirectly estimating vertical carbon flux. Furthermore, size-fractionated ^{15}N tracer studies can provide considerable insight into the structure and functioning of planktonic communities which has implications for planktonic trophodynamics and carbon flux.

The processes briefly outlined above are all based on ship-board observations which do not provide a good synoptic scale of events. Remote sensing (1) of ocean colour to provide synoptic estimates of chlorophyll a in surface waters will be critical in the estimation of global oceanic CO_2 fluxes. To this end, researchers are poised to receive images from the sea-viewing, wide-field-of-view sensor (Sea WiFS) to be launched by NASA on the SeaStar mission in August 1993. Sea WiFS will provide improved chlorophyll a concentration estimates with improved corrections for atmospheric aerosols and non-chlorophyll reflecting particles in the water column. There is therefore a need to develop region-specific algorithms for calibrating ocean-colour with surface chlorophyll a and water column production determined by estimating the critical photosynthesis - irradiance (P.I.) curve parameters Pmax and Ik on which the algorithms depend. These observations will assist international climate change programmes (eg. JGOFS) to divide

the world oceans into "bio-optical provinces". This will allow accurate estimates of remotely-sensed surface chlorophyll to be incorporated into measures of water-column photosynthesis so that CO_2 "draw-down" by the "biological pump" can be estimated on regional and global scales.

The oceanography of the Southern Ocean and in particular that of the Weddell Sea and the continental shelf are likely to play a key role in carbon flux. As the "biological pump" elevates deep water DIC concentrations to a point where the pCO_2 of this water exceeds atmospheric pCO_2, outgassing of CO_2 to the atmosphere would occur should this deep water rise to the surface. In this respect the formation of Antarctic Bottom Water (AABW) during sea-ice formation and the erosion of surface "winter-water" by Circumpolar Deep Water (CDW) in summer may reverse the CO_2 flux direction from a regional winter "sink" to a summer "source" scenario unless, in the latter case, phytoplanktonic CO_2 draw-down were to exceed CO_2 outgassing due to the upwelling of high pCO_2 CDW.

3.2.7.2. Objectives

The broad objectives of the South African participants during ANT X/3 were to investigate N and C transformations in the water column and in sea-ice during autumn sea-ice formation when the oceanographic and biotic regimes are rapidly changing. It was anticipated that during autumn there might be strong CO_2 draw-down associated with sea-ice formation and AABW formation. It was also anticipated that with the onset of winter and a marked reduction in day-length, the structure of the planktonic community could change rapidly, especially since the process of ice-formation is thought to incorporate many planktonic organisms into the sea-ice environment. Although the qualitative aspects of sea-ice communities are quite well known, nitrogen transformation processes have not previously been estimated quantitatively.
Specifically our goals were:

To measure size-fractionated ^{15}N NO_3, Urea and NH_4 uptake and $^{15}NH_4$ regeneration rates in the water column and in sea-ice communities.

To determine photosynthesis-irradiance relationships for water-column and sea-ice phytoplankton communities. The aim was to primarily derive water column production and P.I. parameters required for algorithm development, rather than to specifically investigate physiological responses to light.

To measure aqueous pCO_2 throughout the water column adjacent to and over the continental shelf and to measure pCO_2 in surface waters at 30 - 40 nmile intervals along outward and home-bound transects from Cape Town to Neumayer. Additionally, air samples were taken along this transect for $\delta^{13}C$ measurements on the basis that $\delta^{13}CO_2$ depletion would be indicative of CO_2 outgassing by ^{12}C enriched CO_2 originating from deep water particulate decomposition processes.

3.2.7.3. Methods

Study area and sample collection

Water Samples:

Open water and ice-stations were sampled along a series of five oceanographic transects (±250km each) across the Antarctic Slope Front in the vicinity of Kap Norvegia (Fig. 5). The distance between sampling stations was generally 16 nmiles and the transects were approximately 50 nmiles apart. There were three types of CTD and profiling fluorometer sampling stations of interest to us -

"Standard depth" CTD/Bio-Rosy" stations (Depths = 2, 10, 20, 30, 50, 70, 100, 125, 150, 200, 250 and 500m). From these stations (Fig. 5) surface water (2m) was used to

measure size-fractionated (intact, <20μm, <2μm) chlorophyll-*a* and phaeopigment concentrations.

Production CTD/ "Bio-Rosy" stations (Table 2) to 200m depth maximum in which bottles were triggered at 100%, 45%, 20%, 10%, 1.0% and 0.1% light depths based on Secchi Disc depths (typically between 22-32m). Water from each of the light depths was used for whole community ^{15}N uptake (NO_3, Urea and NH_4) experiments. At the surface and chlorophyll maximum, usually at the 10% light depth, 24 litres of water were taken for size-fractionated ^{15}N uptake and $^{15}NH_4$ regeneration experiments. Water samples for P.I. measurements were taken at the 100% and 10% light depths. These samples were also used for size-fractionated chlorophyll-*a* measurements. Daily photosynthetically available radiation (PAR) was determined on deck with a LiCor 1000 4π sensor and Datalogger. Below surface light at 0m, 5m and 10m was recorded for each production station using a Biospherical Instruments submersible 4π sensor (QSP 200) and an on deck reference 4π sensor (QSP 100). For each of the light depths, nutrient analyses for NO_3, NO_2, PO_4, Si and NH_4 were performed on fresh samples using a Technicon TAII auto-analyser. Additionally, urea and NH_4 were measured manually at the 100% and 10% light depths.

Bathysonde CTD/ Rosette stations (no fluorometer). Deployment of this instrument to the bottom (up to 5000m) allowed water samples to be obtained from characteristic water masses (eg. CDW) for pCO_2 estimations through pH and alkalinity measurements.

Ice Samples

For P.I., ^{15}N experiments and pCO_2 measurements, three types of ice-sample were used. These were the ice-platelet layer beneath fast-ice, grease-ice and sackhole-brine (salinity from 36.8 to 67.1 psu) obtained from 4 inch ice-cores drilled into ice of varying types ranging from 20 - 170 cm thick and varying in age from 1-2 months up to 2 years. Ice-stations used and the measurements taken are summarised in Table 3. For the ^{15}N experiments the platelet ice, sackhole brine and grease-ice samples were used immediately without allowing the water/ice-slush mixture to thaw in an effort to preserve *in situ* conditions. However, for P.I. experiments and for measures of size-fractionated chlorophyll-*a*, pH, alkalinity, nutrient analyses and salinity the whole sample (±7.0 litres) was allowed to thaw for approximately 12 h in a darkened fridge at either +1°C or -1.5°C.

CHLOROPHYLL-A

Size-fractionated chlorophyll-*a* and phaeopigment samples were obtained by filtering 1.0 l of seawater onto Whatman 25mm GF/F filters to yield the intact fraction while a further 1.0l was passed through a 20μm mesh plankton screen and then filtered onto 25mm GF/F filters as before to provide the <20μm fraction. A third 1.0 l sample was filtered through a 47mm 2.0 μm pore-size Nuclepore filter. The filtrate was retained for filtration through a 25mm GF/F as before to yield the <2μm fraction. It should be noted however that many of the small organisms <5μm in diameter are sufficiently plastic to squeeze through the 2μm Nuclepore filters, as observed by Dr H. Thomsen. Similarly, some of the diatoms nominally >20μm may pass through a 20μm screen because of their morphological characteristics.

Pigments retained on the GF/F filters were extracted in 10ml 90% Acetone in a darkened fridge overnight after the sample had been ground with glass beads. After centrifugation, the supernatant was transferred into quartz tubes and read on a Turner Designs scaling Fluorometer. Phaeopigments were measured following the addition of 3 drops of 5% 1N HCl.

Table 2: Water column production stations for ^{15}N and P:I: experiments.

Stn.No.	Seicchi Depth (m)	1% Light Depth (m)	Incubation Irradiance ($\mu E.m^{-2}.s^{-1}$)	Max measured PAR* ($\mu E.m^{-2}.s^{-1}$)
354	26	70	169.0	117
361	22	60	148.0	117
369	24	65	147.8	92
377	24	65	143.2	112
389	31	84	137.8	154
391	31	84	134.5	157
398	24	65	134.5	150
410	24	84	124.5	103
418	23	62	120.9	141

* Data kindly supplied by J.Weissenberger

Table 3: Ice stations and measurements.

Station No.	Ice Type	Measurements Chl. sizes	NH_4	Urea	DIC	^{15}N	P.I.
351 AN 99	P	+	+	+		+	
354 AN101	B	+	+	+		+	
354 AN102 A	B				+		+
389 AN106	G	+	+	+		+	
391 AN107 A	G	+	+	+		+	
391 AN107 B	B	+	+	+	+	+	+
400 AN108	G	+	+	+	+	+	+
434 AN114	B	+	+	+		+	
439 AN115	B	+	+	+	+	+	+
448 AN116	G	+	+	+		+	
450 AN117	G	+	+	+	+	+	+
454 AN118 B	G	+	+	+		+	
458 AN119 A	G	+	+	+		+	
458 AN119 B	B	+	+	+	+	+	+
467 AN122	B				+		+
488 AN126	B	+			+		+

P = Platelet; B = Brine; G = Grease-Ice

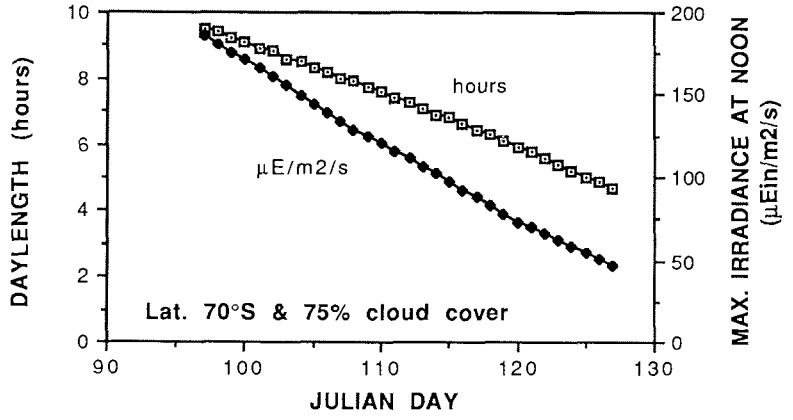

Fig.13: A model of day length and maximum irradiance based on latitude 70 siuth, 75% cloud cover from Sathyendranath et al. 1991.

AMMONIUM AND UREA

Manual analyses of ammonium and urea were determined on fresh samples corresponding with all ^{15}N incubation experiments scaled down to 5ml samples. Standards were prepared at the appropriate salinity of the sample. These manual analyses were not conducted routinely for any other sample.

PHOTOSYNTHESIS-IRRADIANCE RELATIONSHIPS

Nine open water stations were sampled at both the surface and either the 1% or the 10% light depth. Two grease-ice and six brine samples were used for the ice study (Tables 2 & 3).

Photosynthesis-irradiance experiments were carried out using a Photosynthetron and a small volume, short incubation time methodology. Owing to extremely low phytoplankton biomass in the water column (0.09 - 0.33 μgl^{-1}), 2ml water samples were incubated for 5 h with an activity of approx. 14.3 $\mu Ci.ml^{-1}$. One grease ice sample with low biomass (0.37 μgl^{-1}) was treated in the same manner as the water samples while for the second, which had a higher chlorophyll-*a* concentration (1.35μgl^{-1}), 1ml samples were incubated for 3 h with an activity of ~6.25 $\mu Ci.ml^{-1}$. Brine samples (1.02 - 17.17 μgl^{-1}) were incubated for one hour with an activity of ~6.25 $\mu Ci.ml^{-1}$. The light source in the incubator was a Tungsten Halogen 2000 W bulb and additional filters were added to lower irradiances to a suitable range (1 - 600 $\mu E.m^{-2}.s^{-1}$). Irradiance levels in the sample block were measured prior to each experiment using a Biospherical Instruments probe (QSP 200). After incubation 0.4 ml 3M HCl was added to the samples (0.8 ml for the 2ml water samples) and left on a shaker for about 12 h in order to remove inorganic carbonate. Following this 0.3 ml NaOH was added (0.6 ml for 2 ml water samples) and then 10 ml Insta Gel II (Packard) was added to each vial (15 ml for water samples). Time-zero controls were treated in exactly the same way but were acidified immediately after addition of the sample and total activity was determined by adding 20 µl of sample to either 1 ml or 2 ml of sea water to which 20 µl of 3 M NaOH had been added. All vials were then counted in a Packard Tri Carb 1900 TR liquid scintillation analyser. Counts were converted to disintegrations per minute using the external standard ratio.

Photosynthesis-irradiance data were fitted using the equation:

$$P^B(I) = P_s^B\left(1 - e^{-\alpha I/P_s^B}\right) . e^{-\beta I/P_s^B} \qquad \text{----------1}$$

where P^B = photosynthetic rate (mgC(mgChl.*a*)$^{-1}$h^{-1}); P_s^B = light saturated photosynthetic rate (mgC(mgChl.*a*)$^{-1}$h^{-1}) in the absence of photoinhibition; α = the initial slope of the curve (mgC(mgChl.*a*)$^{-1}$h^{-1} (μE m^{-2} s^{-1})$^{-1}$); β = index of photoinhibition (units as α). The maximum photosynthetic rate (P_m^B) is determined from the equation:

$$P_m^B = P_s^B\left[\alpha/(\alpha+\beta)\right] . \left[\beta/(\alpha+\beta)\right]^{\beta/\alpha} \qquad \text{----------2}$$

I_b and I_m are the light intensities where the extrapolated curve intersects the axis and where photosynthesis is maximal, respectively.

$$I_b = P_s^B/\beta \qquad \text{----------3}$$

$$I_m = P_s^B/\alpha \; . \; \ln\left[(\alpha+\beta)/\beta\right] \qquad \text{----------4}$$

The index of photoadaptation (I_k) is derived from:

$$I_k = P_m^B/\alpha \qquad \text{----------5}$$

At a later date the photosynthetic parameter P_m^B, and the derived parameter I_k, will be used together with the biomass profiles obtained from the Bio Rosette, the light attenuation coefficients and the continuous daily PAR measurements to calculate integrated production for the water column.

NITROGEN UTILISATION

Light environment and temperature

During the period of the cruise at the ice-edge (09.04.92 - 05.05.92), measured PAR fell from approximately 3.0 to 0.3 E.m^{-2}.d^{-1}. Air temperatures were variable between approximately -6.0 and -24.0 °C while surface water temperatures varied from -0.92 to -1.89 °C. To control environmental variables all incubations were therefore carried out in a chest-freezer set at -1.5°C but with a controlled light regime approximating to average daily PAR. This was calculated from a light model for 70°S covering the cruise period and assuming 75% average cloud cover. For this, average daylength declined from 9.2 hours (175 μE.m^{-2}.s^{-1} at noon) on 09.04.92 to 5.0 hours (54.8 μE.m^{-2}.s^{-1} at noon) by 05.05.92 (Fig.13). Lights in the incubator were therefore set to provide PAR for the appropriate date. A daily light curve could not be simulated so the incubation bottles received maximal average daily PAR for the daylight period. Incubations normally lasted a total of 6-9 h with day/night cycles of lighting being adjusted for the appropriate daily daylight/ dark proportions for that time of year.

Grease-ice, platelet ice and brine samples were incubated at -1.5°C and at 10% of average daily PAR based on light model averages. In other respects, the light cycle followed that of water column incubations.

Nitrogen uptake measurements

For each of the production station light depths 2 x 1.0 l volumes were supplemented with 0.2 μmol $Na^{15}NO_3$ (99.6 atom%) and 0.1 μmol $CO(^{15}NH_2)_2$ (99.1 atom %)

respectively. For NH_4-N uptake experiments, 2.0 l volumes were spiked with 0.2 µmol $^{15}NH_4Cl$ (99.7 atom%). This sample was split into 2 x 1.0 l volumes; one of which was incubated with the nitrate and urea incubations in 1.0l glass Schott bottles that had been covered with neutral density plastic film to achieve the appropriate shading. The remaining one litre was immediately filtered onto a 25mm GF/F filter which was retained and frozen for later particulate N analysis. The filtrate (900 ml) was retained in a 1.0 l glass Schott bottle to which 500µl $^{15}NH_4Cl$ carrier was added before freezing the sample at -30°C for later isotopic dilution analysis at time zero (Ro). Uptake experiments were terminated by filtration onto pre-ashed (450°C for 6 h) Whatman 47mm GF/F filters which were retained and frozen at -30°C for later analysis of PN and ^{15}N content by interfacing a Carlo Erber CHN analyser with a VG 620 mass spectrometer (Fiedler and Proskch 1975). At the end of the NH_4 uptake experiment, 900 ml filtrate and carrier was retained and frozen as before for isotopic dilution measurements (Rt).

Nitrate and urea uptake rates were calculated as:

$$\rho NO_3 \text{ or } \rho Urea = (PE \times PN) / (Ro \times T) \quad \text{----------6}$$

where PE = percent ^{15}N enrichment of the PON fraction in excess of the natural abundance; PN = particulate N concentration ($\mu mol.l^{-1}$); T = experimental duration (hours) and Ro is the calculated aqueous ^{15}N enrichment at time zero.

Ammonium uptake rates were similarly calculated but corrected for isotopic dilution due to ^{14}N excretion:

$$\rho NH_4 = (PE \times PN) / (R \times T) \quad \text{----------7}$$

where R = exponential average enrichment:

$$R = Ro / kt (1 - e^{-kt}) \quad \text{----------8}$$

and:

$$k = (-\ln Rt / Ro) / T \quad \text{----------9}$$

where Ro and Rt are the measured aqueous ^{15}N enrichments at the beginning and end of an experiment.

A relative preference index (RPI) was calculated for each nutrient assimilated. For example for ammonium —

$$RPI = \frac{\rho NH_4}{\rho \Sigma N} / \frac{[NH_4]}{[\Sigma N]} \quad \text{----------10}$$

where ρNH_4 and $\rho \Sigma N$ are the uptake rates for ammonium and the sum of the rates for the three nitrogen species, and $[NH_4]$ and $[\Sigma N]$ their ambient nutrient concentrations.

Nitrogen assimilation relative to light

On two occassions when the chlorophyll-*a* concentration was sufficiently high (~12μgl^{-1}), 20ml brine samples from stations AN115 and AN119 were incubated in the photosynthetron after supplementing the samples with ^{15}N labelled NO_3, urea and ammonia at the concentrations used previously. The light range covered was 1 to 600$\mu E.m^{-2}s^{-1}$. The incubation period was 2 h. At the end of the experiment all samples (36 for each nutrient) were filtered onto 25mm Whatman GF/F filters for later ^{15}N analyses.

Ammonium regeneration

Aqueous ammonium in the 900ml Ro and Rt samples (frozen) is recovered by diffusion from the thawed samples back at our laboratory in Cape Town. Sufficent MgO is added to increase the pH to >9.0. A 25mm GF/F filter moistened with 50µl 6N H_2SO_4 is

suspended above the sample and the bottle is re-capped. After standing for approx. 2 weeks at room temperature, >50% of the aqueous NH_4 is usually recovered on the filter as NH_4SO_4. The filters are then shaken in 5ml Milli-Q water and a sample is removed for colorimetric ammonium concentration determination.

Ammonium regeneration rates are calculated from the model:

$$r = \frac{\ln(Rt/Ro)}{\ln(St/So)} \cdot \frac{(So - St)}{T} \qquad \text{----------11}$$

where So and St = aqueous ammonium concentrations at the start and end of the experiment. Where ammonium concentrations over the experimental time-course remain unchanged (<0.02μm ol.l^{-1} differential) at <1μmol NH_4^+.l^{-1}, r is calculated as:

$$r = \frac{\ln(Ro/Rt)\,So}{T} \qquad \text{----------12}$$

Size-fractionated experiments
Size-fractionated uptake and NH_4 regeneration experiments were carried out on surface and 10% light level communities at each production station. For each nutrient, 5.0 l of sample was innoculated with ^{15}N label at the same concentration as before. One litre was immediately removed from the NH_4 incubation bottle for aqueous ammonium determinations and isotopic dilution measurements (Ro) as described above. At the end of the incubation period the sample was split into an intact community (1.0 l), a <20μm fraction (2.0 l passed through a 20μm mesh) and a <2μm fraction (2.0 l passed through a 2.0 μm Nuclepore filter). Each separate fraction was then filtered onto 47mm GF/F filters and the particulate ^{15}N enrichment determined as previously. For the NH_4 incubation experiment, 900 ml was collected from the filtrate for aqueous NH_4 measurements (Rt) as outlined before.

TOTAL AQUEOUS CO_2 AND AIR $\Delta^{13}CO_2$
Water samples
Water samples from the Bio-Rosy, Bathysonde and ship-board sea-water supply for underway surface samples (±10m depth) were all treated similarly.

Replicate samples were collected in 350 ml plastic bottles with air-tight caps for pH and alkalinity titrations. Water for nutrient analyses were collected simultaneously. The sealed sample was then allowed to stand to equilibrate to room temperature (20°C) to which the pH meter (Radiometer PHM 84) was calibrated. The pH and temperature of each sample was then recorded.

Alkalinity titrations followed the potentiometric method using a Metrohm 655 Dosimat autoburette. Exactly 50 ml of the sample was pipetted into the autoburette chamber and H^+ ions (0.1M HCl) were titrated against CO_3^- and HCO_3^- over the pH range 3.5 - 2.0 to produce a linear plot of the Gran function (y axis) against the volume of HCl added. From this the HCl volume equivalent at y = 0 can be calculated:

$$V.equiv = intercept / slope \qquad \text{----------13}$$

The alkalinity, pH and temperature values allow aqueous ρCO_2 to be calculated.

Air samples
Air samples for $\delta^{13}CO_2$ analysis were collected from the ship's crows-nest by mechanically sucking air through 500 ml bottles which were then sealed for later analysis using mass spectrometry at the University of Cape Town.

3.2.7.4. Preliminary Results

CHLOROPHYLL-A AND PHAEOPIGMENTS

Size-fractionated chlorophyll-a in surface waters

The data for the size-fractionated pigment analyses of surface waters for the five transect of the oceanographic grid appear in Table 4 and are summarised in Figure 14 (a-e). Plots of total chlorophyll-*a* for surface waters and corresponding surface NH_4 concentrations (G.Dieckmann - Autoanalyser data) are given in Figure 15 (a-e). Representative plots of vertical size-fractionated chlorophyll-*a* profiles are presented in Figure 16 (a-c) and Figure 17. An illustration of relative phaeopigment concentrations (surface water only) for a single transect (stations 21/410 - 21/428) is given in Figure 18.

Size-fractionated Chlorophyll-a in ice-samples

Data for size-fractionated pigment analyses for all ice-samples appear in Table 5. Examples of the relative concentration of chlorophyll-*a* in grease-ice and in the underlying surface water for each sample are shown in Figure 19.

Table 4: Surface water NH_4 and size fractionated chlorophyll data for all stations.

Stn.No.	Intact	NH_4^*	<20	<2	>20	2-20
355	0.12	1.67	0.08	0.07	0.04	0.01
357	0.09	1.81	0.07	0.05	0.02	0.02
359	0.15	1.50	0.10	0.06	0.05	0.04
361	0.29	1.51	0.23	0.09	0.06	0.14
363	0.36	1.16	0.25	0.08	0.11	0.17
365	0.23	1.37	0.23	0.05	0.00	0.18
367	0.32	1.21	0.23	0.08	0.09	0.15
369	0.21	1.48	0.11	0.05	0.10	0.06
371	0.27	1.61	0.11	0.05	0.16	0.06
373	0.12	1.74	0.10	0.04	0.02	0.06
377	0.18	1.86	0.17	0.06	0.01	0.11
389	0.15	1.61	0.12	0.06	0.03	0.06
391	0.08	1.98	0.06	0.04	0.02	0.02
392	0.06	2.04	0.07	0.04	0.00	0.03
396	0.27	1.43	0.20	0.08	0.07	0.12
398	0.29	1.40	0.19	0.08	0.10	0.11
400	0.27	1.23	0.17	0.07	0.10	0.10
402	0.21	1.28	0.18	0.06	0.03	0.12
404	0.18	1.54	0.10	0.04	0.08	0.06
406	0.15	1.72	0.09	0.04	0.06	0.05
408	0.16	1.71	0.08	0.03	0.08	0.05
410	0.09	1.64	0.06	0.03	0.03	0.03
412	0.12	1.74	0.08	0.03	0.04	0.05
414	0.20	1.56	0.12	0.04	0.08	0.08
418	0.25	1.03	0.11	0.06	0.14	0.05
420	0.29	1.53	0.14	0.07	0.15	0.07
422	0.26	1.49	0.14	0.07	0.12	0.07
424	0.25	1.42	0.13	0.07	0.12	0.06
425	0.10	1.87	0.06	0.04	0.04	0.02
426	0.09	1.85	0.06	0.04	0.03	0.02
428	0.06	2.20	0.05	0.03	0.01	0.02
432	0.07	2.43	0.06	0.04	0.01	0.01
435	0.17	1.82	0.14	0.07	0.03	0.07
437	0.22	1.34	0.13	0.06	0.09	0.07
439	0.25	1.37	0.14	0.06	0.11	0.08
441	0.27	1.43	0.16	0.06	0.11	0.10

continued next page

Table 4: contn.

443	0.26	1.51	0.13	0.05	0.13	0.08
445	0.13	1.56	0.07	0.03	0.06	0.04
447	0.13	1.77	0.07	0.04	0.06	0.03
448	0.14	1.37	0.06	0.03	0.08	0.03
450	0.09	1.56	0.06	0.03	0.03	0.03
452	0.11	1.38	0.09	0.06	0.02	0.03
454	0.11	1.43	0.07	0.03	0.04	0.04
455	0.12	0.91	0.07	0.04	0.05	0.03
458	0.12	1.17	0.07	0.03	0.05	0.04
461	0.14	0.99	0.07	0.04	0.07	0.03
464	0.14	1.11	0.10	0.05	0.04	0.05
467	0.18	0.60	0.11	0.05	0.07	0.06
470	0.08	0.75	0.07	0.04	0.01	0.03
472	0.08	0.77	0.07	0.04	0.01	0.03
474	0.06	1.24	0.04	0.03	0.02	0.01
475	0.04	1.53	0.04	0.02	0.00	0.02
476	0.04	1.47	0.03	0.01	0.01	0.02

* NH_4 data from Dieckmann "standard depth" Bio-Rosy stations

Table 5: Clorophyll -a for grease ice., underlying surface water and brine.

	n	>20	2-20	<2	Mean Total Chl.*a* ($\mu g.l^{-1}$)
Water column					
South	17	22.6 ± 10.1	29.8 ± 11.6	47.5 ± 9.1	0.098 ± 0.04
Peak	19	36.1 ± 14.2	38.4 ± 14.8	26.9 ± 4.1	0.250 ± 0.05
North	16	40.4 ± 10.2	31.0 ± 7.0	28.6 ± 9.5	0.141 ± 0.04
Grease-Ice	7	44.8 ± 17.2	37.9 ± 14.0	16.6 ± 9.0	0.59 ± 0.42
Underlying water	7	35.8 ± 12.0	32.3 ± 6.7	31.8 ± 10.1	0.13 ± 0.06
Brine (38‰)	3	36.2 ± 4.7	36.6 ± 18.2	36.0 ± 24.8	2.9 ± 2.1
Brine (54‰)	4	55.6 ± 19.4	37.5 ± 16.9	6.8 ± 3.2	14.5 ± 2.3

Table 6: Mean percentages of chlorophyll by size intervals.

Stn. No.	Grease-ice			Surface water			Brine			Salinity
	Intact	<20	<2	Intact	<20	<2	Intact	<20	<2	‰
AN 99							3.61	2.34	0.32	-
AN 101							1.02	0.58	0.27	36.8
AN 106	0.41	0.35	0.10	0.15	0.12	0.06				
AN 107 A	0.35	0.15	0.09	0.08	0.06	0.02				
AN 107 B							17.17	4.19	0.55	41.3
AN 108	0.37	0.25	0.07	0.27	0.17	0.07				
AN 114							5.58	3.71	2.91	44.4
AN 115							13.58	8.58	1.11	63.8
AN 116	0.63	0.21	0.03	0.14	0.06	0.03				
AN 117	1.43	0.60	0.09	0.09	0.06	0.03				
AN 118 B	0.17	0.10	0.04	0.11	0.07	0.03				
AN 119 A	0.77	0.38	0.08	0.12	0.07	0.03				
AN 119 B							12.87	5.85	1.17	59.5
AN 122							1.25	0.84	0.27	-

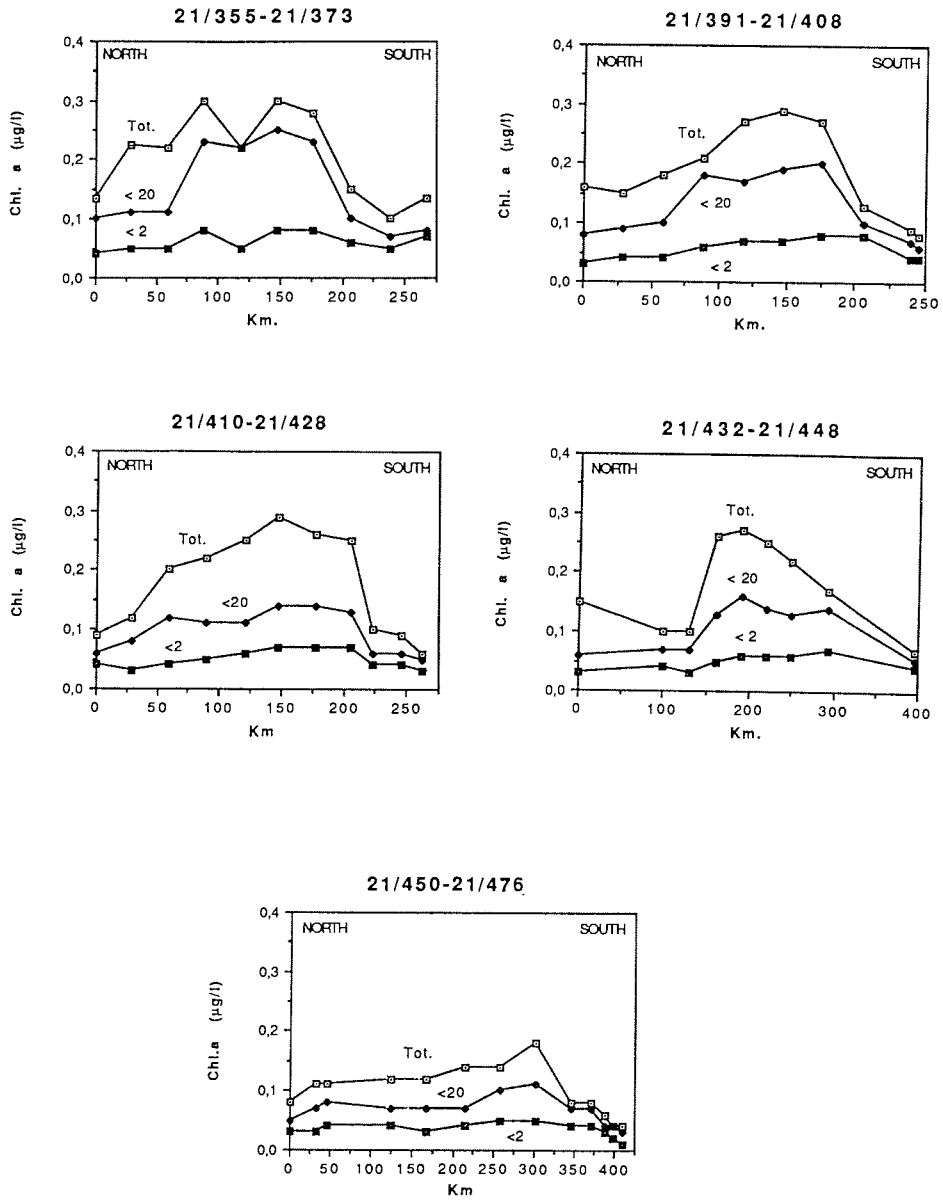

Fig. 14. Size fractionated chlorophyll a measurements in surface water for the indicated transects.

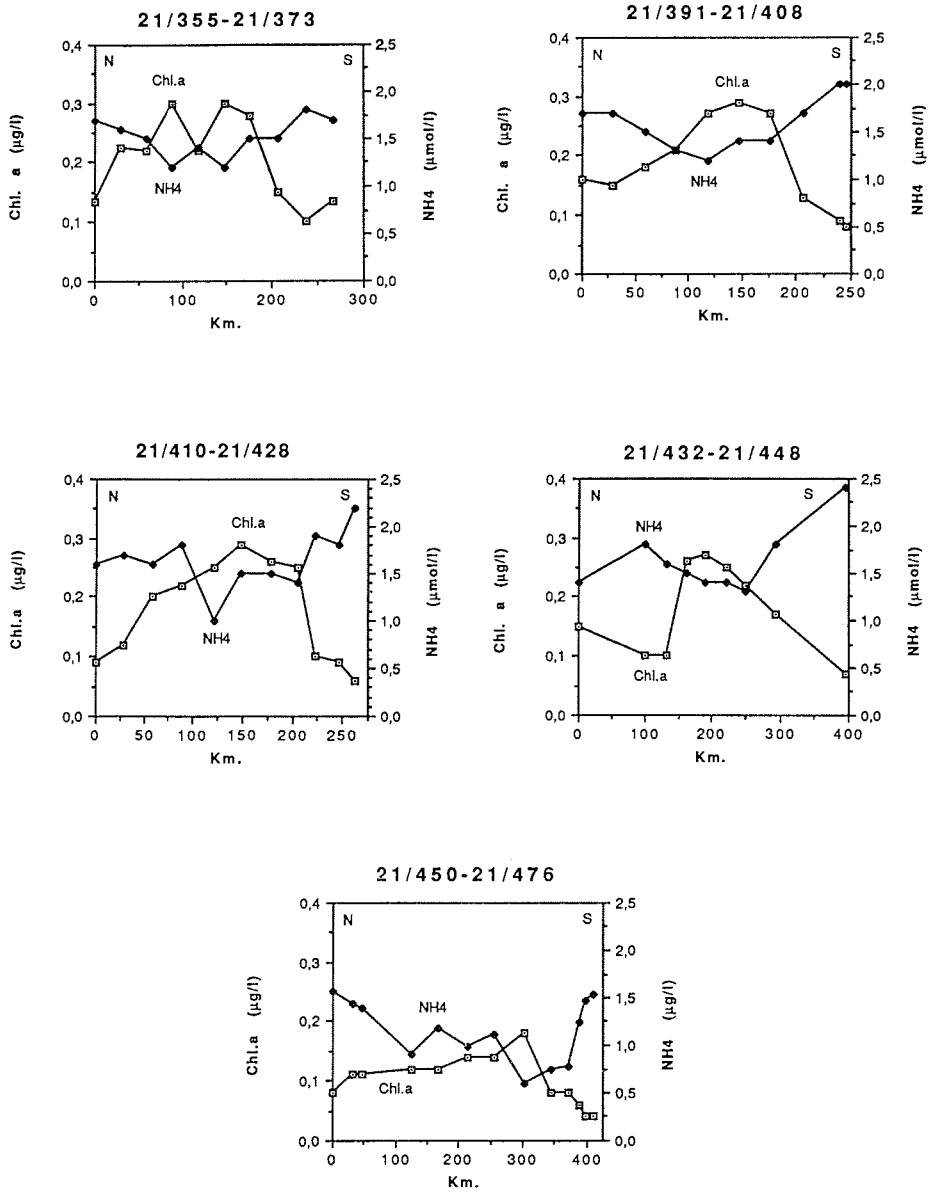

Fig. 15: Total chlorophyll a measurements and corresponding ammonia concentrations in surface waters for the transects indicated.

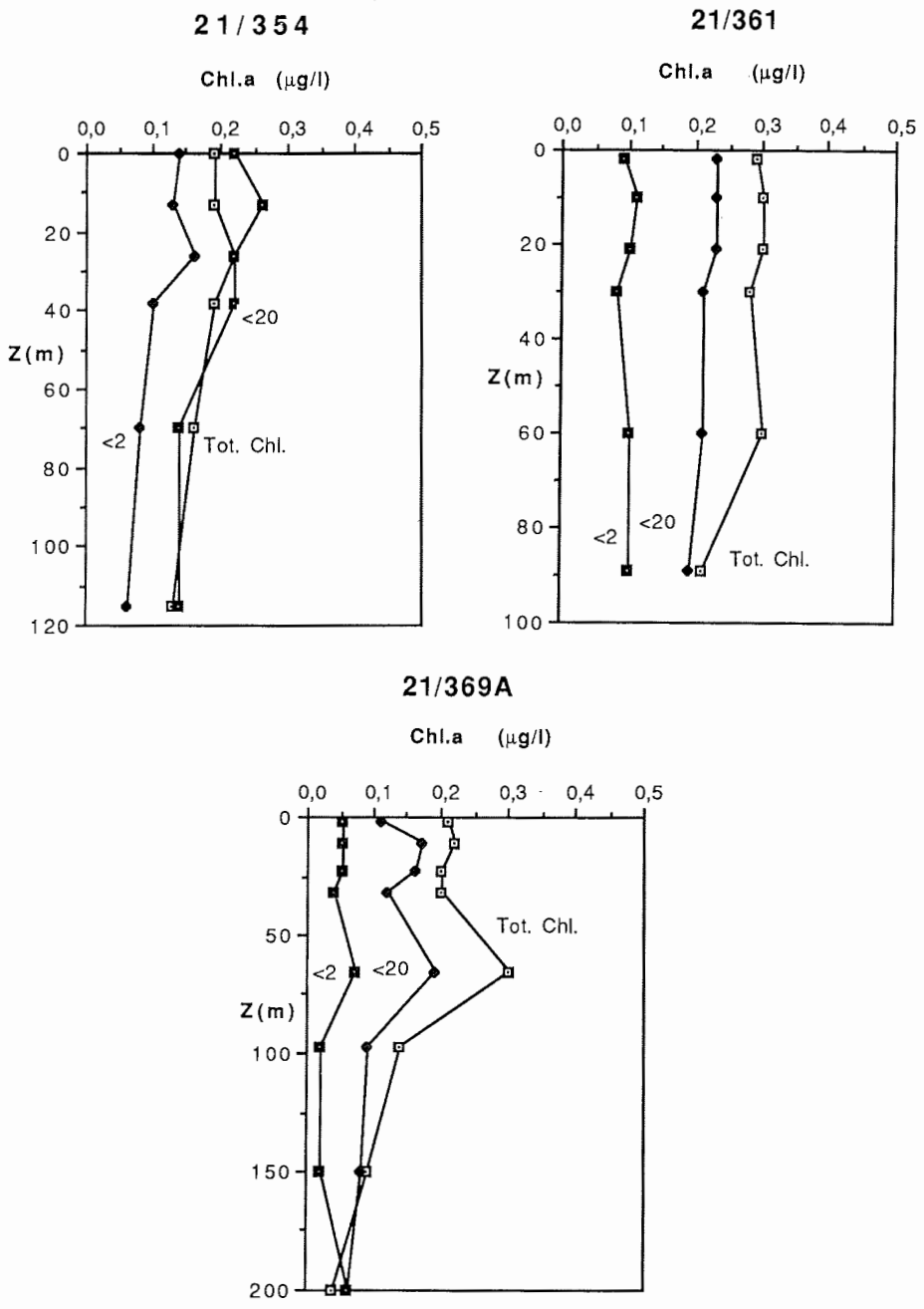

Fig. 16: Selected profiles of size fractionated chlorophyll a at production stations 354 (inshore), 361 (frontal region) and 369 a (offshore).

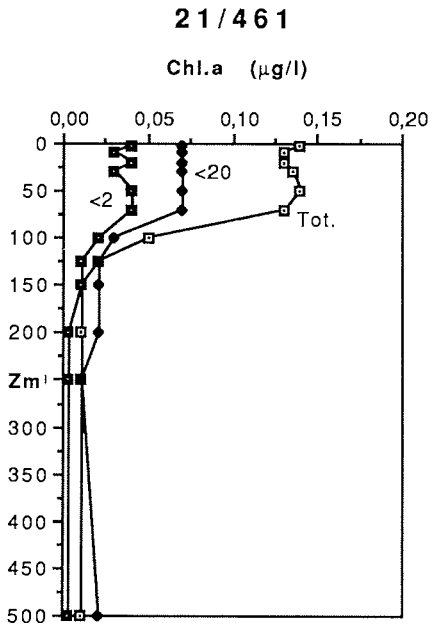

Fig. 17: Size fractionated chlorophyll a profile at Biorosi station 461.

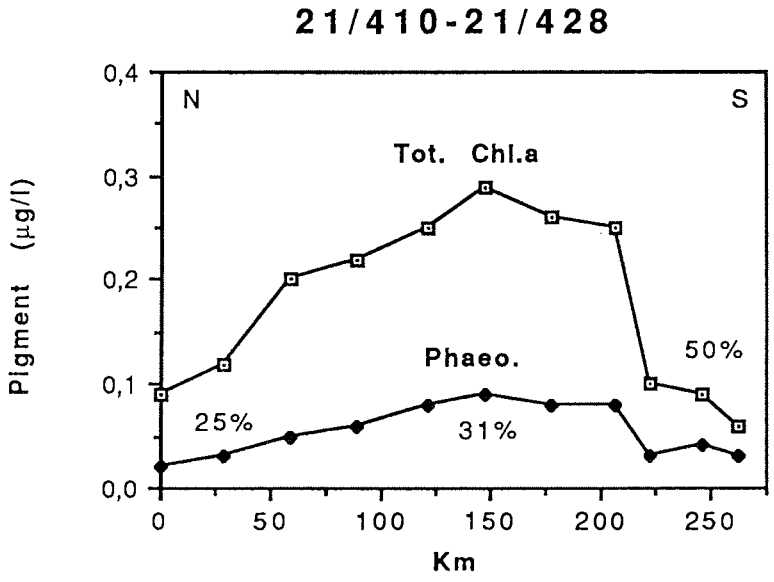

Fig. 18: Example of relative proportions of phaeopigments and total chlorophyll a for a transect (station 410 to 428).

Chlorophyll-a percentages
In an effort to summarise and make relative comparisons between water column and ice-samples, pigment concentrations for the size-fraction intervals >20μm, 2-20μm and <2μm were calculated and expressed as a percentage of the total chlorophyll-*a* value. Transect data were divided nominally into three regions, *viz.* South (Stns. 354-359, 391-394, 425-435, 470-475), Peak (Stns. 361-367, 396-402, 418-424, 437-443, 461-467) and North (Stns. 369-373, 406-414, 445-458). The basis of this was to average all the chlorophyll data corresponding to the chlorophyll maximum (=Peak) and to the north and south of this peak for all the transects in Figure 14 (a-e). Stations to the south, close to the continent, are easily distinguished because of the sharp drop in chlorophyll-*a* concentration while the stations chosen to represent northerly edge of the transect were again lower in chlorophyll than in the maximum chlorophyll-*a* region. These divisions are somewhat arbitrary. While the southerly station grouping probably conforms to an oceanographic regime inshore of the continental slope front, the peak and northerly stations probably cannot be separated on a physical oceanographic basis. For the ice stations, all the grease-ice stations were averaged together while the brine samples were split into high salinity (54 psu mean) and low salinity (38 psu mean) groups on the basis that the higher salinity brine samples probably originated from older ice-floe cores. All these data are summarised in Table 6 which is illustrated in Figure 20.

AMMONIUM AND UREA
Water column ammonium concentrations determined by auto-analyser and by the small volume manual method generally showed good agreement.

For all stations where ^{15}N experiments were performed we have ammonium and urea concentration data. These are shown in Table 7.

PHOTOSYNTHESIS-IRRADIANCE RELATIONSHIPS
Daily irradiance fell from approximately 9.5 $E.m^{-2}.d^{-1}$ at the beginning of the cruise to a low of 0.3 $E.m^{-2}.d^{-1}$ by the time we left the ice (see 3.2.9).

Water samples
For all stations sampled the deep sample (1% or 10% light depths) was above the thermocline and sample temperatures and salinities ranged from -0.92 to -1.89°C and 33.889 to 34.228 psu. Chlorophyll-*a* values for the surface samples ranged from 0.15 to 0.29μgl^{-1} and from 0.08 to 0.32 μgl^{-1} for the deeper samples and at many of the stations a sub-surface chlorophyll-*a* maximum was observed. The two most important P.I. parameters in terms of calculating primary production throughout the water column are P^Bm and Ik. Maximum photosynthetic rate (P^Bm) averaged 0.999±0.495 mgC.mgChl-$a^{-1}.h^{-1}$ at the surface and 0.764±0.332 mgC.mgChl-$a^{-1}.h^{-1}$ at depth while the index of photoadaptation (Ik) ranged from 13 to 41$\mu E.m^{-2}.s^{-1}$ at the surface and from 17-46 $\mu E.m^{-2}.s^{-1}$for the deep samples. A preliminary summary of all the photosynthesis-irradiance parameters can be seen in Table 8, and as an example the P.I. curves of station 418 are given in Figure 21.

Integrated production is still to be estimated using available PAR data, water attenuation coefficients and chlorophyll-*a* concentrations.

Ice samples
Results of the grease-ice and brine photosynthesis-irradiance experiments are incomplete. So far it appears that in most cases photosynthetic capacity (P^Bm) is lower than that found for the water column.

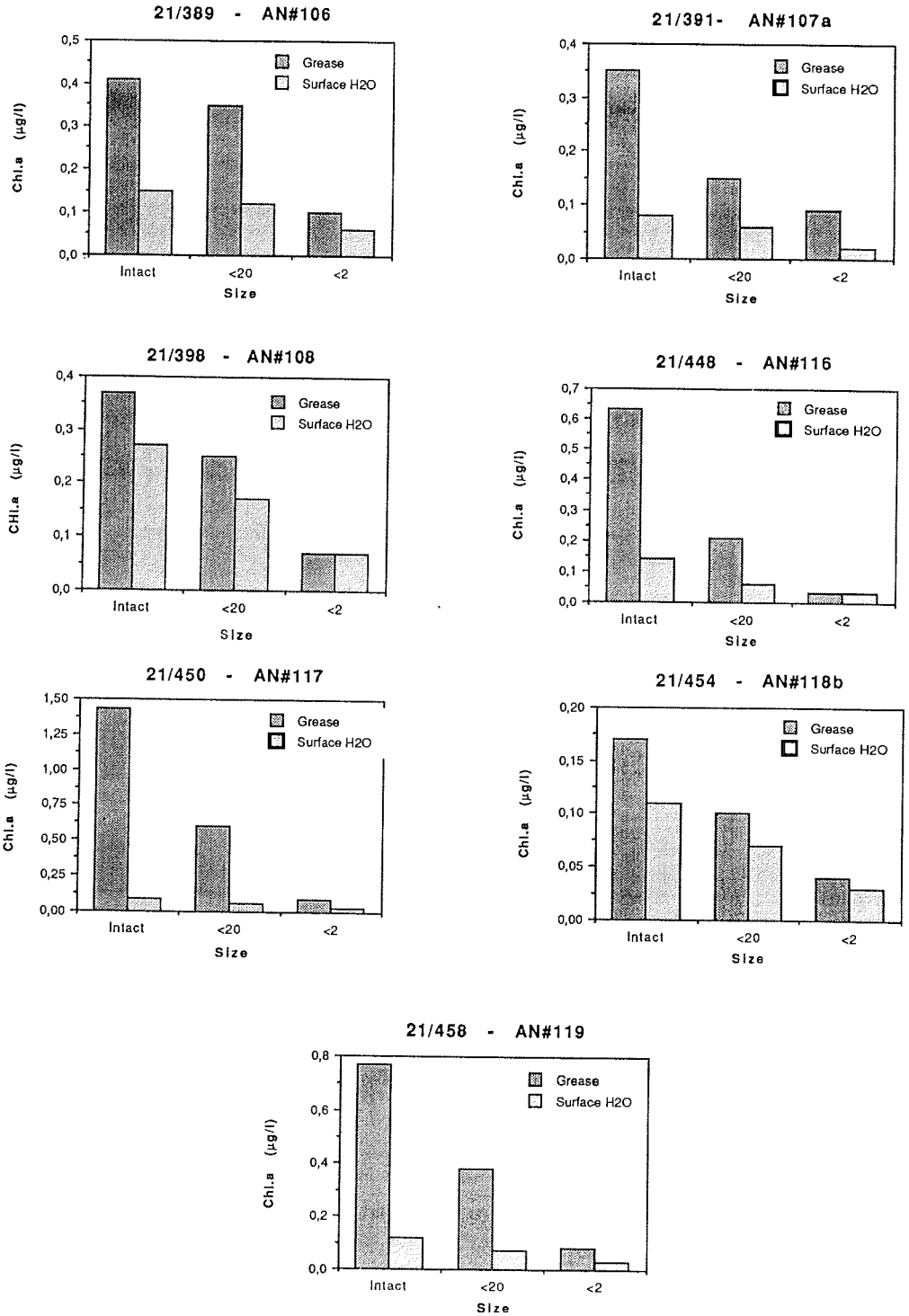

Fig. 19: Size fractionated chlorophyll a from grease ice and surface water for seven ice stations.

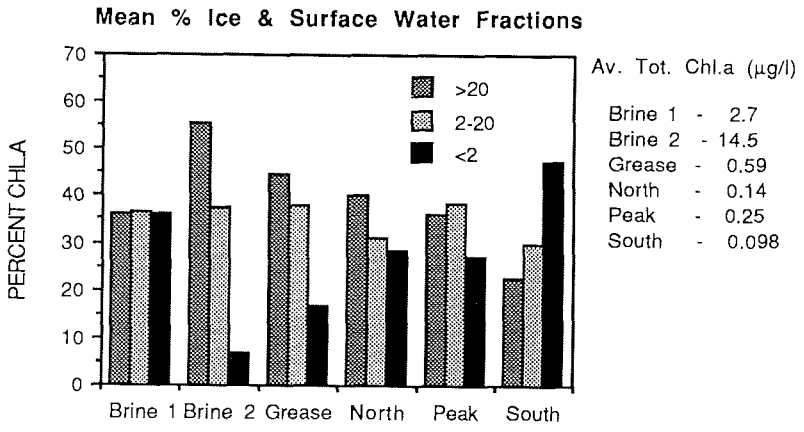

Fig. 20: Relative percentage chlorophyll a for all ice and water stations.

Table 7: Ammonium and urea in water and ice samples (µmol l^{-1})

Station No.	Surface Water		Grease Ice		Brine	
	NH_4	Urea	NH_4	Urea	NH_4	Urea
351 AN 99	2.40+	2.34+	-	-	7.66	3.21
354 AN 101	1.54	0.05	-	-	2.15	0.77
389 AN 106	1.61	0.25	1.93	1.58	-	-
391 AN 107	1.96	0.60	2.09	0.64	4.61	3.00
400 AN 108	1.29	0.28	1.20	0.08	-	-
434 AN 114	-	-	-	-	2.37	3.24
439 AN 115	-	-	-	-	5.18	4.46
448 AN 116	-	-	1.78	3.65	-	-
450 AN 117	-	-	1.84	2.71	-	-
454 AN 118 B	-	-	1.80	1.45	-	-
458 AN 119	-	0.42*	2.09	4.53	1.24	15.16
Platelet AN 99	1.81	3.21	-	-	-	-
Neuston AN 118	2.59	14.15	-	-	-	-

+ Water from immediately beneath the Platelet layer of AN 99
* Immediately beneath the grease-ice sample

Note: Nutrients are from thawed ice samples

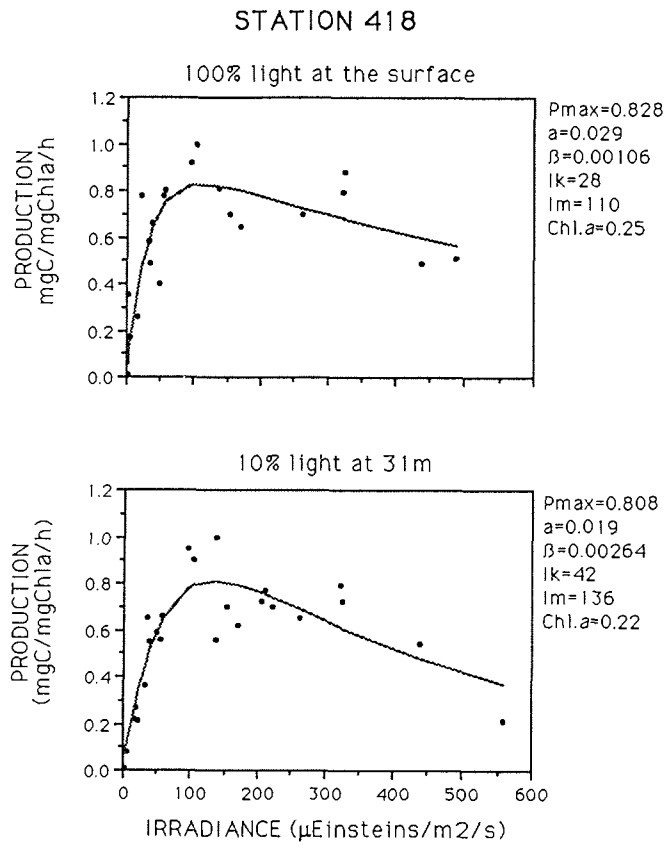

Fig. 21: Two representative P vs I curves for the water column samples at station 418 showing a low Ik , low Pmax and photoinhibition.

Table 8: P vs I parameters for all water column stations for water at the surface and at either the 10 or 1% light depth (= deep).

		MEAN ± S.D.	RANGE
SURFACE	Pmax	0.999 ± 0.495	0.274 - 1.975
	α	0.037 ± 0.019	0.011 - 0.074
	ß	30.8 ± 29.7	4.7 - 85.2
	Ik	28 ± 10	13 - 41
	Is	41 ± 21	15 - 67
	Im	101 ± 22	56 - 129
	Ib	755 ± 528	221 - 1896
DEEP	Pmax	0.764 ± 0.332	0.205 - 1.279
	α	0.025 ± 0.012	0.005 - 0.041
	ß	19.7 ± 12.9	1.9 - 35.9
	Ik	34 ± 10	17 - 46
	Is	47 ± 20	18 - 81
	Im	120 ± 28	79 - 158
	Ib	751 ± 419	384 - 1410

NITROGEN UTILISATION

No data from ANT X/3 are available at this time from our ^{15}N experiments on water or ice samples. Once we have completed our ^{15}N analyses on the mass spectrometer at the University of Cape Town this data will be made available.

TOTAL AQUEOUS CO_2 AND AIR $\Delta^{13}CO_2$

Air $\delta^{13}CO_2$ data will only become available once the samples have been analysed on the mass spectrometer at the University of Cape Town.

Alkalinity and pH measurements in the water column number over 600 covering the oceanographic grid region and the two transects from Cape Town to Antarctica. Preliminary computations of aqueous pCO_2 for the transect from Cape Town to Antarctica have been completed but require further analysis in Cape Town before the data can be presented. Nevertheless the trends are apparent and can be summarised with very approximate value ranges:

STC	NO_3 ($\mu mol.l^{-1}$)	T°C	DIC (kgl^{-1})	pCO_2 (ppm)
39°S	0-1	20/23	1,85-1,95	175-225
45°S	15-20	6/8	2,05-2,15	345-375
60°S	23-26	+1/0	±2.2	275-325
70°S	23-26	+1/-1,8	±2.2	275-325

3.2.7.5. Discussion

Interpretation of the biological data associated with the oceanographic transect grid requires an understanding of the sea-ice and physical water column conditions at the time. There are three features of significant importance

Firstly, at the northern end of the transects (about 100-250 km offshore) there was a strong salinity and temperature gradient at about 100m depth separating a cold (-1.8°C) surface layer (< 34.4 psu) from a warmer (+0.6-0.9°C) and more saline (> 34.6 psu) deep water layer to 1000 m depth. The potential mixing depth here is therefore about 100 m. Further inshore from about 50 km to 100 km offshore the isolines begin to turn downwards slowly. At about 50 km offshore there is a very rapid downward inflection of both salinity and temperature isolines indicative of a strong westerly current flow. The -1.5°C isotherm and 34.4 psu. isohaline descend to approximately 500-600, at the shelf edge. Potential mixing is therefore to the bottom over the shelf. This sharp gradient marks the Continental Shelf Front (CSF) which has no surface expression except in terms of chlorophyll-*a* values (see Fig.13).

Secondly, there is some evidence for a wedge of warm Circumpolar Deep Water (±0.9°C) approaching the shelf (to approx.100 km offshore) between 200 and 300 m depth which compresses the thermal gradient above it.

Thirdly, remnant "summer water" at the surface was found to the east of the oceanographic grid seaward of the CSF at the beginning of the cruise. However, by the end of the cruise, the remnant summer water had been eroded away with the development of winter water, particularly to the west of the oceanographic grid. Indeed, by the time we had returned to the east of the grid for our return to Cape Town, no trace of the remnant summer water was apparent with XBT traces. Our cruise therefore covered the transition from autumnal to /winter oceanographic conditions.

At the same time, as is to be expected, PAR and daylength declined dramatically over the period of the cruise (Fig. 14). Nutrient concentrations were all high and greater than that considered to limit algal growth; micro-nutrients such as iron etc. notwithstanding. The time course for sea-ice formation and it's extent on this cruise are not yet clear. Satellite

imagery provided the general impression that ice-growth proceeded from west to east and from south to north. The final transect was characterised by almost total ice-cover of grease, nilas and pancake ice. As it is believed that frazil ice formation scavenges particles from the water column, this process may also impinge on community size-structure development.

Community genus and species composition is also important in explaining size-structure and potential growth patterns. In the water column the diatom *Chaetoceros* sp. (>20 μm) dominated the large celled community and occurred primarily in the middle of the transects, particularly in the easterly lines. Colony forming diatom groups, (Fragilariopsis), which includes *Nitzschia cylindricus* and separately, the diatoms, *Fragilaria* sp. and Phaeocystis-like cells dominated in the 2-20 μm fraction. Prasinophytes and Prymnesiophytes (3-5 μm) were common and may have passed through our 2 μm Nuclepore filters because of their morphological plasticity. Athecate autotrophic dinoflagellates were also present in these small size classes. Ice samples were apparently dominated by diatoms (*Nitzschia*) and Prymnesiophytes.

Community size-structure and biomass data for our transects (Fig. 13 a-e) are likely therefore to have evolved as a function of mixing depth, light intensity, species composition, grazing pressure by mesozooplankton (data from S. Schiel) and sea-ice formation.

Our first impressions are that more light dependent, relatively faster growing and generally larger diatoms account for the higher biomass and larger size-fractions associated with the middle (peak) regions of all the transects. Here the mixing depth was relatively shallow (±100 m) so that the light environment is more suitable for diatom growth. This community may also be representative of the remnant summer water. Reduced NH_4 concentrations associated with these stations may be associated with phytoplanktonic uptake. Over the continental shelf, small cells dominated in a deeply mixed water column in which light limitation favours the generally slower-growing non-diatom species. Alternatively, or perhaps simultaneously, grazing pressure in this region, primarily apon the larger cells (>10 μm) might account for their absence and explain the more elevated NH_4 concentrations characteristic of inshore stations. To the north of the transects, the mixing depth was relatively shallow (±100 m) but the >20 μm fraction in particular was reduced - possibly again due to grazing pressure by mesozooplankton with concomitant elevated NH_4 concentrations again (data from S.Schiel).

Over the time course of the cruise, PAR declined rapidly and particularly to the west, the erosion of summer water was apparent. The effect of this can be seen in the autotrophic community structure and biomass which resulted in generally smaller cells and a lower total biomass.

Little variation is apparent between photosynthetic parameters of surface and deep samples although at the surface production rates are slightly higher and photoinhibition tends to be stronger. On the other hand the index of photoadaptation (Ik) and the irradiance at which photosynthesis is at a maximum (Im) are both lower for the deep samples. There was no difference in parameters between northern and southern stations although the two highest $P^B m$ values were found toward the north of the transects. P.I. parameters are similar to those recorded previously during the austral winter in the Bransfield Strait area. (During that study chlorophyll-*a* values were in the same range and daily PAR averaged 0.795 $E.m^{-2}$.) Ik and Im values for this study are considerably lower than for the Bransfield Strait area indicating a better adaptation to lower light intensities experienced in comparison to the more favourable light regime at the more northerly location.

We can only speculate on our ^{15}N work at the moment. The general dominance of nanoplanktonic autotrophs <20 μm and NH_4 concentrations which generally exceed

1.0 µmol.l^{-1} would classically lead to highest uptake rates being associated with the smaller size classes using reduced nitrogen species because of relatively low nitrogen requirements, a preference for reduced N and probable inhibition of NO_3 assimilation when NH_4 exceeds about 1.0 µmol.l^{-1}. This would lead to lower rather than high f-ratio values with the implication being that little fixed carbon is available to consumers or for export. Further the implication would be that there was probably tight coupling between heterotrophic consumption of the smaller cells by microzooplankton leading to high nitrogen regeneration rates (NH_4 and urea) and coupled autotrophic uptake of these nutrients. Nevertheless, the apparently large consumer community present would seem to indicate that prior to the onset of winter conditions, algal biomass and production was probably considerably higher than at present.

A striking feature of the NH_4 and urea analyses for water column and grease-ice stations was the general enrichment of urea, particularly in grease-ice. The single high value for urea in the neuston layer would suggest that high grease-ice urea concentrations originate from a detritus rich neuston layer. Observations by D. Garrison from neuston and ice samples point to the extremely high carbon:chl-*a* ratios suggesting the accumulation of detritus or a considerable cell die-off during ice formation. Ice samples generally exhibited a marked increase in the larger cell sizes relative to the smaller cells, particularly in older ice (brine) characterised by higher salinities.

Trends in our pCO_2 analyses conform to what we expect. At the STC where NO_3 concentrations are extremely low and the water temperature is high, DIC and pCO_2 values are depleted due to the high biological activity characteristic of this region. As we moved southwards, pCO_2 values reached atmospheric equilibrium around 45°S while decreasing temperatures rather than biological activity were responsible for decreasing pCO_2 at higher latitudes. For the autumn/winter period at least, the ocean south of 60°S would appear to be a "sink" for CO_2 in this region.

3.2.7.6. Acknowledgements
Grateful thanks are due to the oceanographic, Bio-Rosy and nutrient analyser teams for providing valuable data.

3.2.8. WATER COLUMN BIOLOGY (PHYTOPLANKTON AND NUTRIENTS).

G. DIECKMANN, Z. WANG, M. STÜRCKEN-RODEWALD, U. KLAUKE, V. KOCH, W. SCHMIDT

3.2.8.1. Introduction

The major goal of the plankton investigations was to establish the distribution, standing stock and physiological state of phytoplankton during autumn at the onset of sea ice formation. It was envisaged, that we would encounter a late summer phytoplankton bloom as had been observed previously in late March during cruises to the Weddell Sea. The source of high algal concentrations in sea ice shortly after the onset of its formation in autumn is attributed to the mechanical incorporation of phytoplankton into the ice in areas where concentrations of phytoplankton are high.

The aim was to study the effect of different sea ice formation processes i.e. the chemical and physical features of the watercolumn at the stage where rapid sea ice formation takes place. In order to obtain a temporal and spatial coverage of the phytoplankton and nutrient distribution at the Antarctic slope front and in the area of sea ice formation we carried out a study in the area south of 67°30'S up to the Antarctic continent and between 6°W an 12°W (Fig.22).

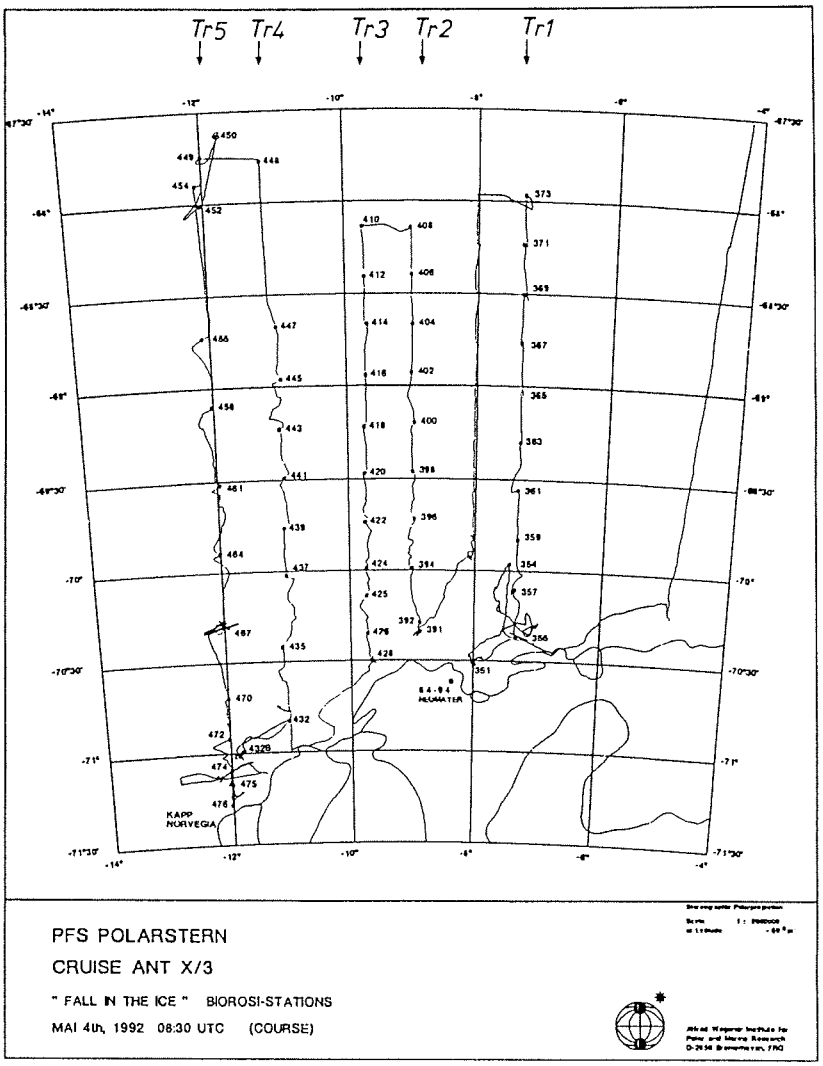

Fig. 22. Map of the cruise track showing transects 1 to 5

3.2.8.2. Methods

A series of five oceanographic transects were carried out. Fig. 22. Samples were obtained using the BIOROSI (see Krause et al.) at specific stations and to a maximum depth of 500m. Parameters recorded continuously by the BIOROSI were: Fluorescence, MIE backscattering, temperature and salinity. The BIOROSI was equipped with twelve 15liter Niskin Bottles, a CTD and Fluorometer. The bottles were usually tripped at following standard depths: 500; 250; 200; 150; 125; 100; 70; 50; 30; 20; 10; 0 meters. Samples for nutrient determinations, chlorophyll *a*, particulate organic carbon/nitrogen, CO_2/Alkalinity, O_2, size fractionated chlorophyll *a* and species composition were taken from the bottles at each station and treated as follows:

CHLOROPHYLL A
Samples of 2 liters were filtered through GF/F filters which were then immediately homogenized in 10ml of 90% Acetone, centrifuged and measured using a Turner Design Fluorometer.

PARTICULATE C/N
Samples of 2 liters were filtered through Precombusted GF/C filters which were stored frozen for subsequent analysis in the lab.

NUTRIENTS
Nutrients (NH_4, NO_3, NO_2, PO_4 and SiO_2) were determined immediately after collection using an Technicon Autoanlyzer and standard methods.

SAMPLES FOR SPECIES ENUMERATION
Subsamples of 100-200ml were filled into brown Utermöhl bottles, preserved with 0,5% buffered Formaldehyde, and stored cool for later microscopy in the laboratory.

3.2.8.3. Preliminary results

CHLOROPHYLL A
All five transects essentially yielded a similar pattern of chlorophyll vertical and horizontal distribution . Figs. 23-27. Chlorophyll a concentrations in the area of investigations were generally low. The highest value recorded was 0,4-μgl^{-1}. Below the picnocline in the northern portions of the transects the conceentrations were below 0,1-μgl^{-1}. Near the coastal zone and in the coastal current the concentrations were also in this range but well mixed down to the bottom. Such concentrations in this area reflect early winter conditions.

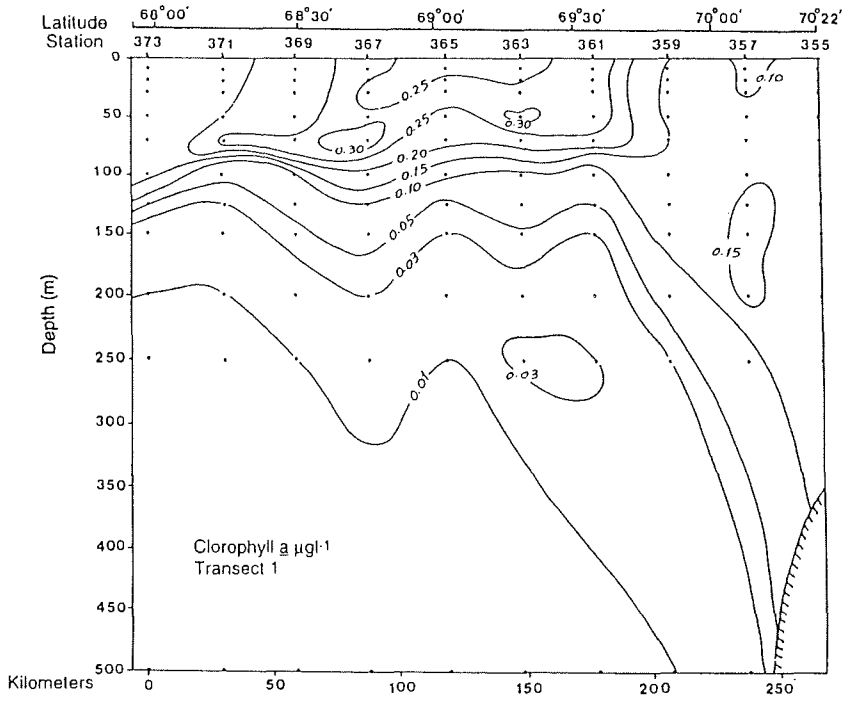

Fig. 23 Chlorophyll a distribution along Transect 1

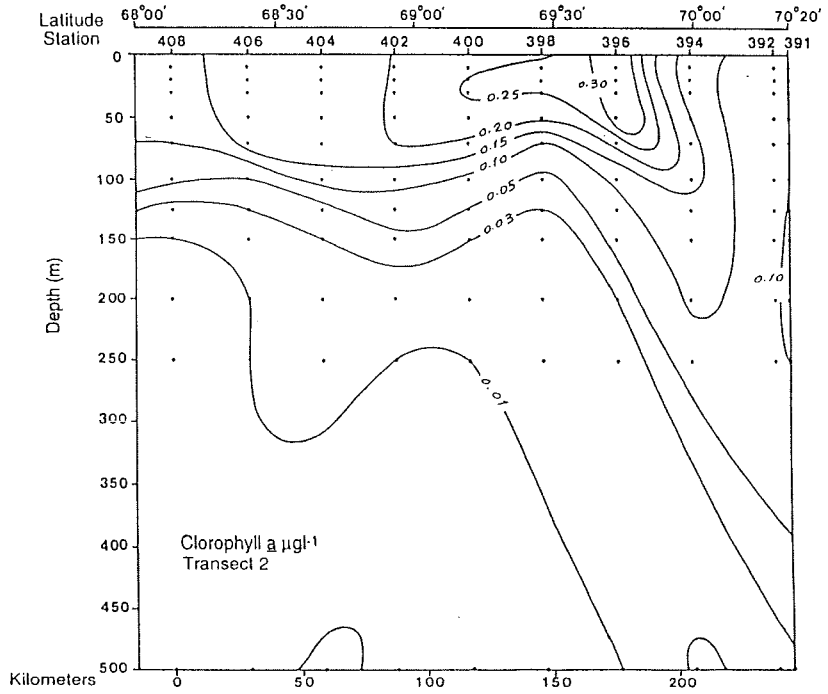

Fig. 24 Chlorophyll a distribution along Transect 2

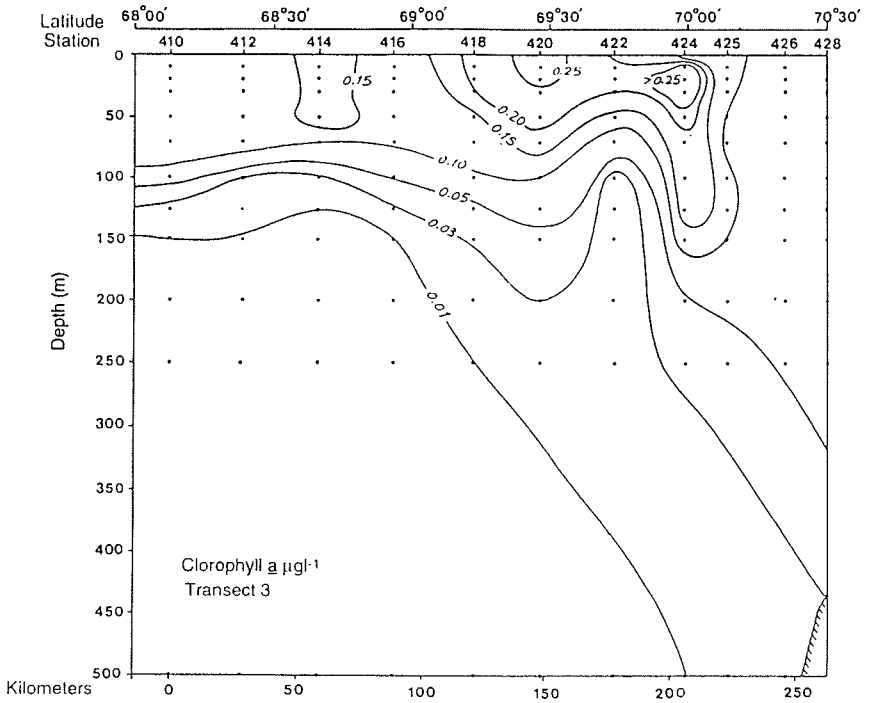

Fig. 25 Chlorophyll a distribution along Transect 3

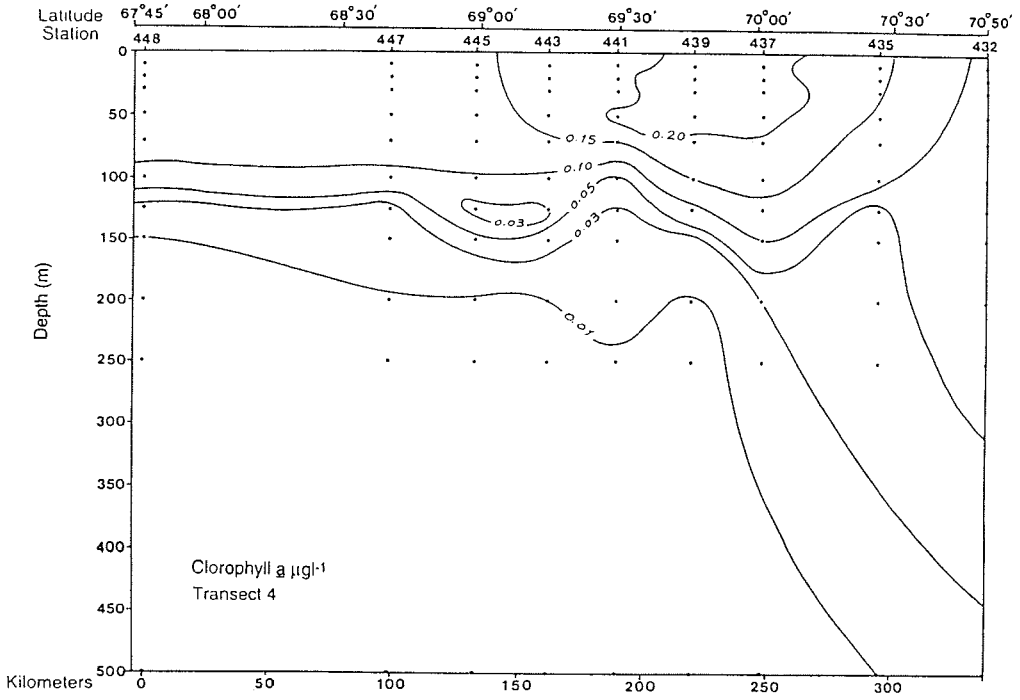

Fig. 26 Chlorophyll a distribution along Transect 4

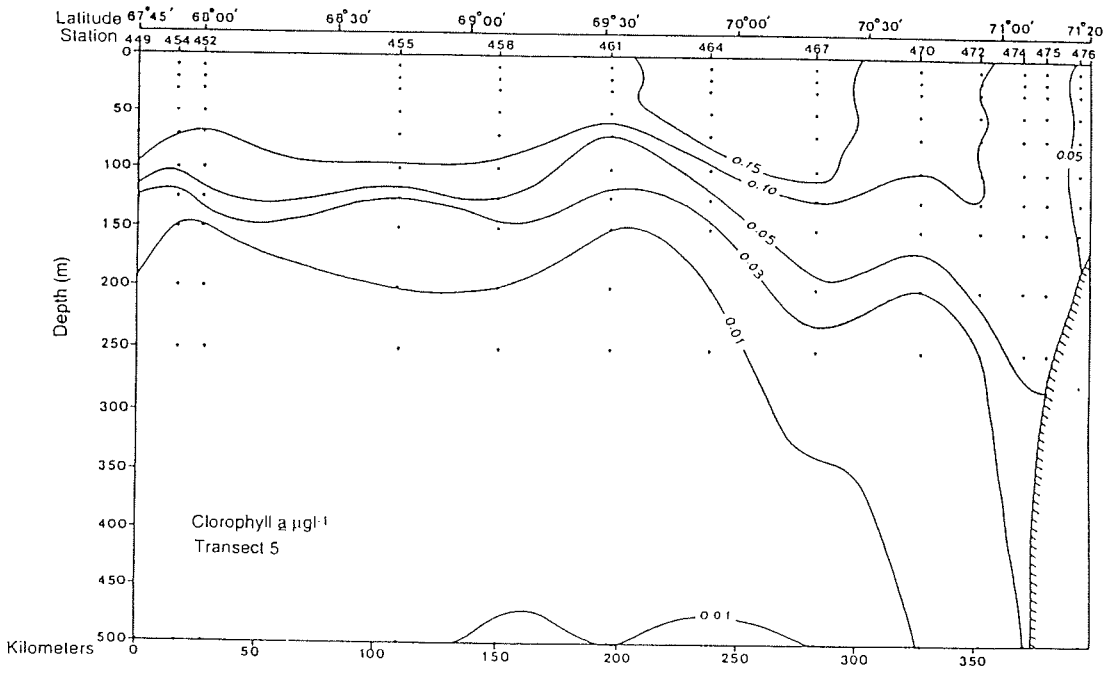

Fig. 27 Chlorophyll a distribution along Transect 5

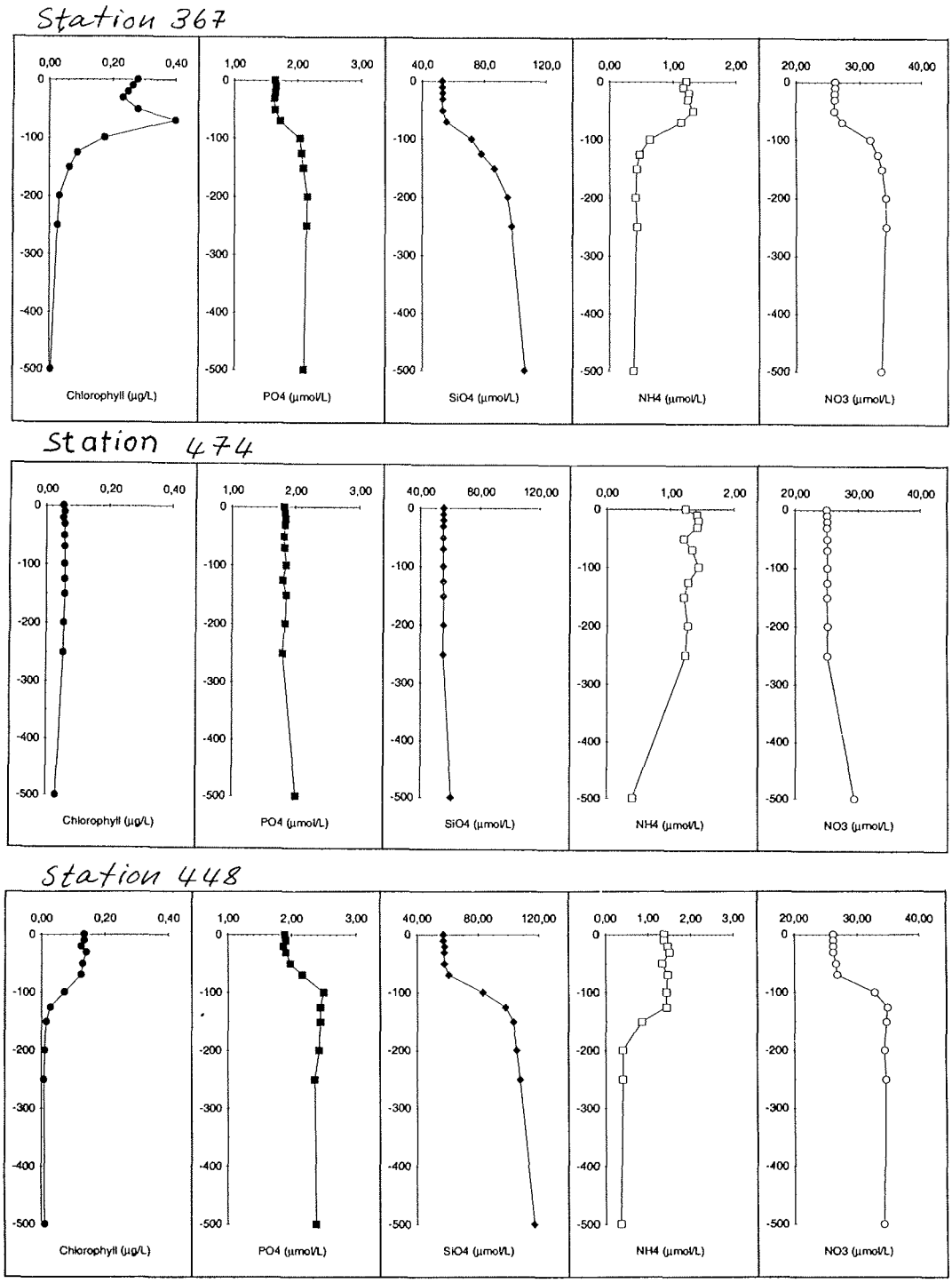

Figs. 28-30 show typical profiles of chlorophyll a and Nutrients on stations 367, 448 and 474. Chapter 3.2.7 provides more details about the transects.

NUTRIENTS

The distribution of nutrients NO_3, PO_4 and SiO_2 and NH_4 are shown for Transect 1 only since all transects were similar with the exception of minor vertical and horizontal differences (Figs. 31-34). Nutrient concentrations also reflect post bloom concentrations, typical of the late Summer early Autumn situation in coastal region of the Weddell Sea. Nutrient concentrations ranged between 25 and 34 µmol l^{-1} for Nitrate, 1,65 and 2,15 µmol l^{-1} for Phosphate, 55 and 105 µmol l^{-1} for Silicate and 0,3 and 1,8 µmol l^{-1} for Ammonia. Lowest concentrations were usually associated with highest chlorophyll levels, whereas high Ammonia levels indicated Zooplankton activity on the one hand and lower concentrations reflected possible depletion by Phytoplankton and correspondingly lower Zooplankton activity. A more thorough discussion of the different transects is provided in Chapter 3.2.7

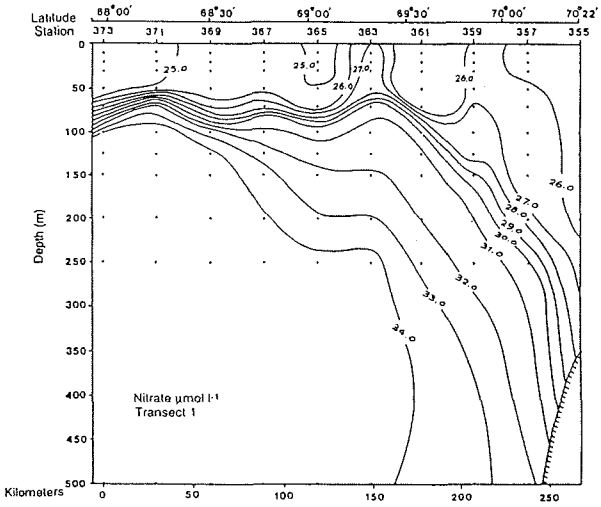

Fig. 31 Nitrate distribution along Transect 1

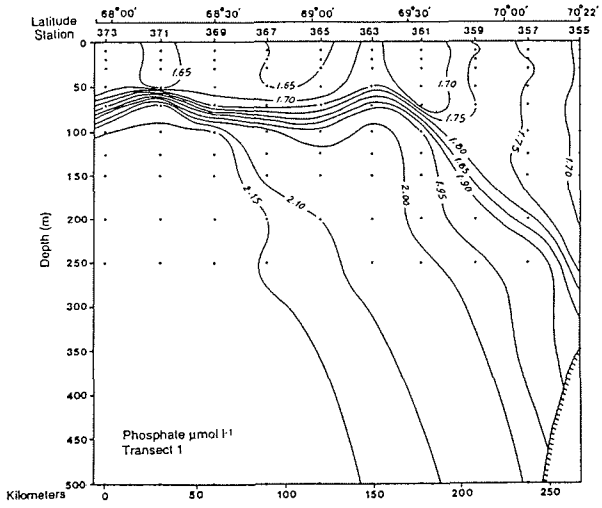

Fig. 32 Phosphate distribution along Transect 1

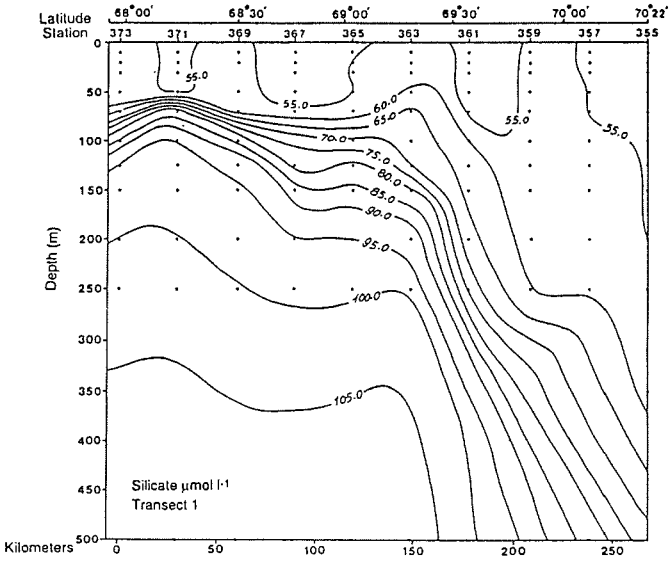

Fig. 33 Silicate distribution along Transect 1

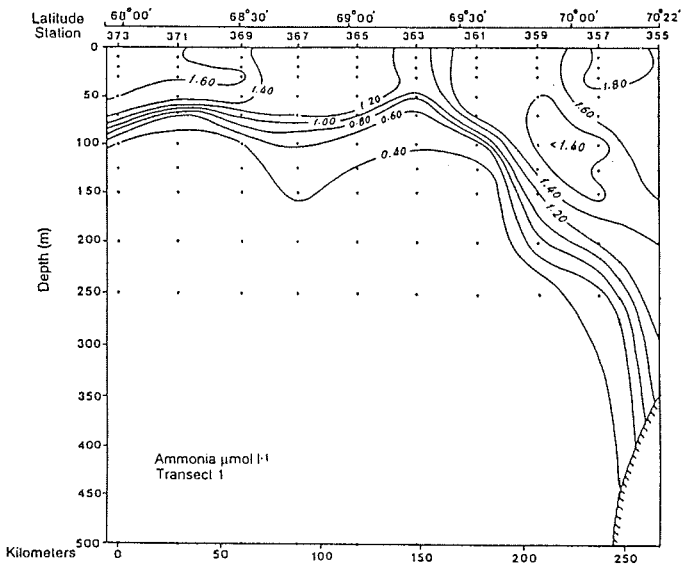

Fig. 34 Ammonia distribution along Transect 1

3.2.9. SEA-ICE BIOLOGICAL INVESTIGATIONS.

R. GRADINGER, J. WEISSENBERGER, K. BEYER

The main aim of our investigation was to study the physical and biological changes and succession patterns occurring during sea ice formation in the Antarctic fall.

Ice samples were obtained from 28 sites using several different sampling devices. Grease ice was collected from a Zodiac or with a specially developed sampler resembling three Niskin bottles. Smaller pancakes and porridge ice was collected with an ice basket, while thicker pancakes or ice floes were sampled using 3" or 4" ice augers. At each location ice temperature, ice and snow thickness and the freeboard of the ice floe were measured as well as the irradiation within and below the ice.

3.2.9.1. Ice texture, chemical and physical properties

For textural and physico-chemical analysis several replicate samples were obtained from each station. Using a centrifuge technique, the brine was extracted from the sectioned ice cores. The centrifuged ice sections were used for textural analysis and subsequently melted. Salinity, chlorophyll a and nutrients (PO_4, NO_2, NO_3, NH_4, SiO_4) were determined both in melted core sections as well as in the brine.

Figure 35 shows the ice thickness and results of the textural analysis for each location. Using the measured values of bulk salinities, ice thicknesses and the ambient air temperatures, the approximate age of each ice sample was estimated. The three ice cores with lengths of more than 1 m were probably formed during the last winter period and had survived the summer melt. Most other cores were not older than 50 days, ice cores with lengths below 20 cm had a maximum age of 5 days.

As an example of the principle differences between older ice floes and newly formed sea-ice, the chlorophyll and salinity distributions of the cores AN10310002 and AN103114 are shown in Figures 36 and 37. Younger ice floes were characterised by a C-shaped salinity distribution and chlorophyll a maxima at the bottom of the cores. The salinity in the upper parts of older sea ice was reduced due to gravity drainage of brine. Internal chlorophyll *a* maxima such as the one we observed in core AN10310002 at a depth of 110 cm are typically found only in ice older than a year.

The nutrient concentrations in the brine of sea ice were considerably different to the values in the water column (Fig. 38, ice core AN103122). There appeared to be a close relationship between silicate and brine salinity. However, different trends were observed for phosphate and nitrate. Ammonium concentrations were significantly higher in the newly formed sea ice than the values estimated from the water column data. A likely cause is the high biological activity derived in this core.

3.2.9.2. Analysis of the community structure

For the quantitative analysis of the community structure of the sea ice biota, ice samples were melted in large volumes of 0.2µm filtered sea water. The abundances of bacteria, diatoms, auto- and heterotrophic flagellates were determined by epifluorescence microscopy. For the determination of abundances of ice meiofauna, the organisms were concentrated using a 10µm gauze and live counted under a dissecting microscope. Sea water samples from the surface (at each ice station) as well as from 10 respectively 70 m depth (during the last hydrographical transect: stations 455 to 476) were analysed by epifluorescence microscopy for later comparison with the results obtained from sea ice samples.

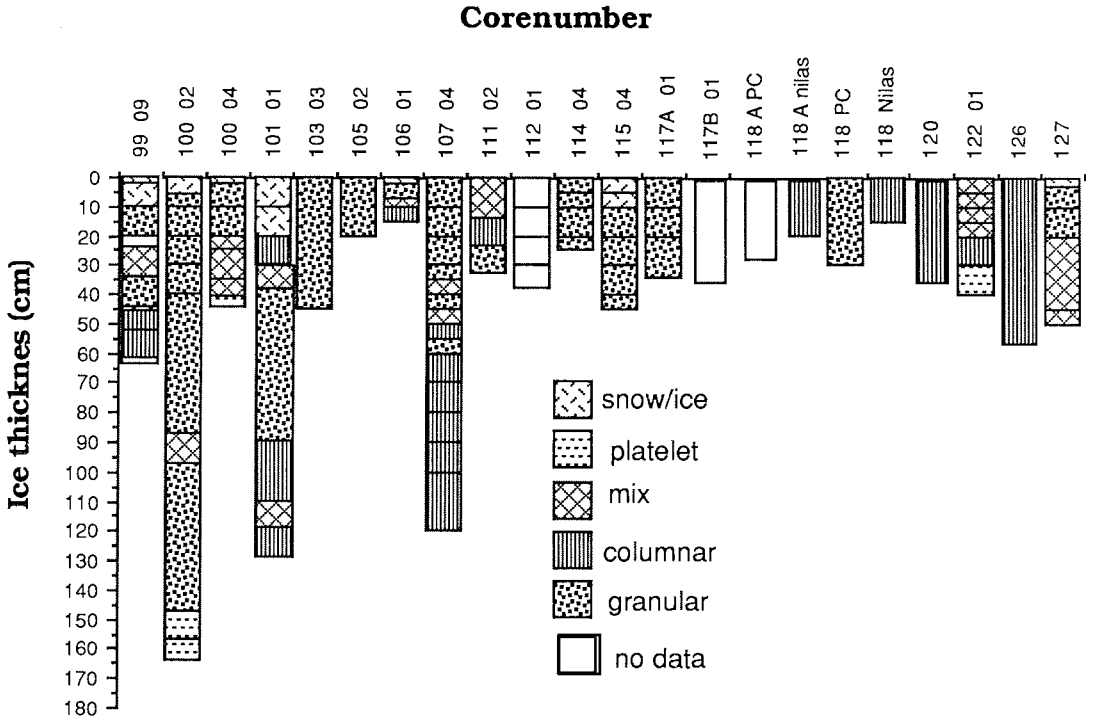

Fig. 35 Thickness and textural composition of the sea ice at all sampling locations

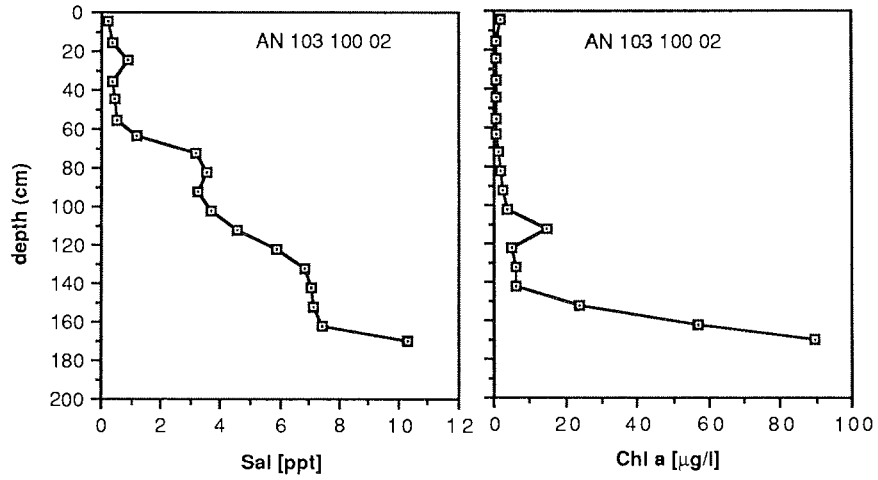

Fig.36 Chlorophyll and salinity distribution in a second year ice floe.

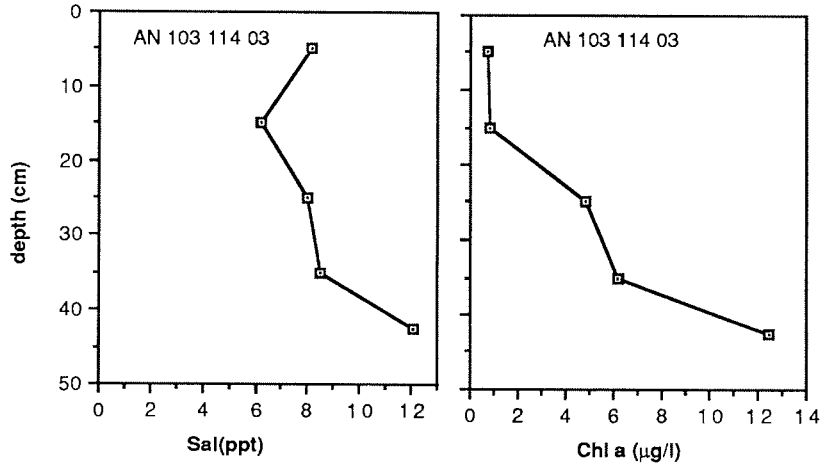

Fig. 37 Chorophyll *a* and salinity distribution in newly formed sea ice.

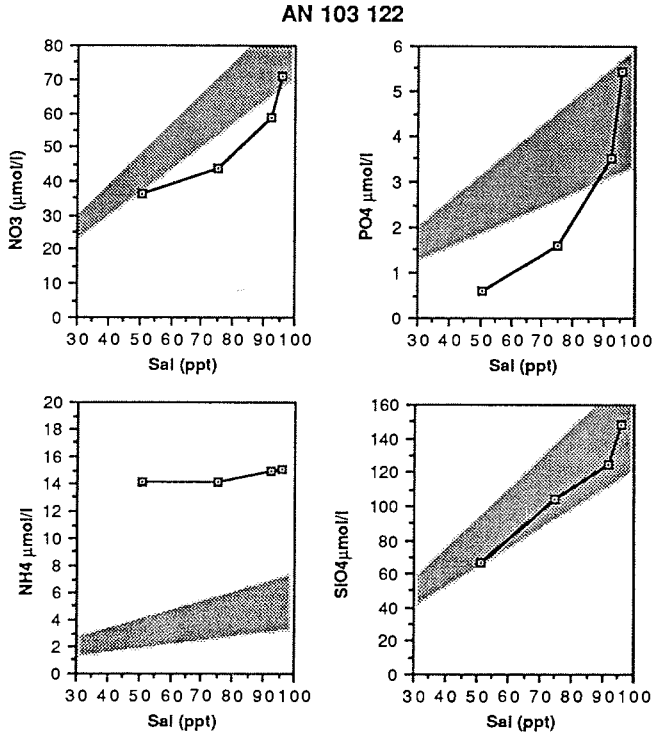

Fig.38 Nutrient concentrations in the brine of core AN103122 in relation to salinity. The shaded areas indicate concentrations which could be expected by concentrating nutrients in the water column to brine salinities.

3.2.9.3. Results from the hydrographical transect

The main primary producers (Fig. 39) in terms of abundance were autotrophic pico- and nanoflagellates (100-440 cells ml^{-1}), followed by pennate diatoms (0-42 cells ml^{-1}). No distinct vertical distribution patterns were observed; the abundances in the samples from 10 m and 70 m were similar at each station. Looking for horizontal differences between the stations, a decrease of the abundances was found between the stations 21/467 and 21/470. Thus, the northern part of the transect (st. 455-467) had higher concentrations of primary producers than the southern part. The same holds true for the occurrence of bacteria (Fig. 40). Their abundances ranged in the northern part of this transect between $4.0x10^5$ to $6.5x10^5$ ml^{-1}, while lower values ($1.2x10^5$-$4.7x10^5$ ml^{-1}).were observed south of station 470. No clear regional differences were observed in the occurrence of heterotrophic flagellates (Fig.40, 100-600 cells ml^{-1}). The biologically characterized division of the transect into a northern and a southern part becomes even more obvious when the ratios between auto- and heterotrophic flagellates as well as between bacteria and heterotrophic flagellates are considered (Fig. 41). At most stations more heterotrophic than autotrophic flagellates were observed, with ratios above 0.4 only found in the northern parts. The ratios between bacteria and heterotrophic flagellates in the northern part was above 1000, while south of station 470 only ratios below 900 were found (with one exception). The abundances and ratios we observed were similar to own findings in Arctic seas during the autumn/winter transition, leading to the final conclusion, that the plankton community, we were dealing with, had reached its last summer/autumn bloom before our cruise leg and was changing during the time of our expedition to a typical winter community.

3.2.9.4. Results from the sea ice investigations

The main aim of our investigation was to study the changes of the community structure of organisms inhabiting different stages of the newly forming sea ice. In the following part we will show examples for the transition steps sea watergrease ice and grease /-nilas ice. Comparing the abundances obtained in the water column with abundances found in newly formed grease ice (Fig. 42), we observed organism enrichments for several organism groups: bacteria were enriched by a factor of 3, diatoms by a factor of 12. On the other hand, no enrichment was observed for both auto- and heterotrophic flagellates. A comparison between abundances in grease ice and nilas ice (Fig. 43) revealed lower abundances of bacteria in the nilas ice than in the grease ice. As a summary of our preliminary results dealing with new ice formation we observed selective differences between the inclusion rates of different organism groups into grease ice. Bacteria and pennate diatoms were selectively enriched, while no enrichment was found for flagellates.

As an example for the results from second year ice, the vertical distribution of organisms in the ice core AN103107B are given in Figure 44. The abundances ranged from $8.0x10^5$ to $19.0x10^6$ bacteria ml^{-1}, showing a distinct internal maximum at a depth of 41 cm. This internal maximum was.found also for the other organism groups with pennate diatoms as the main primary producers.

In contrast to former investigations in the Weddell Sea the pancake cycle was not the dominant ice forming process. The unusually calm weather conditions during our cruise had resulted in the coverage of large parts of our investigation area with a relatively flat and undeformed layer of new ice. The succession patterns from a water column community to an ice community will be highly influenced by changes in the physical environmental conditions inside the brine channels. A further combined analysis of all available data on the sea ice physics, chemistry and biology is needed to develop new scenarios of sea ice formation, organism incorporation and succession patterns under conditions we found during our cruise

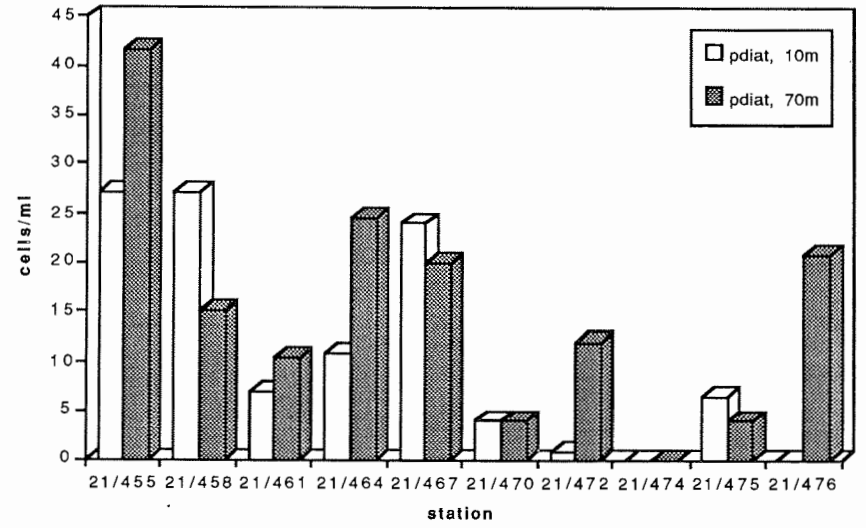

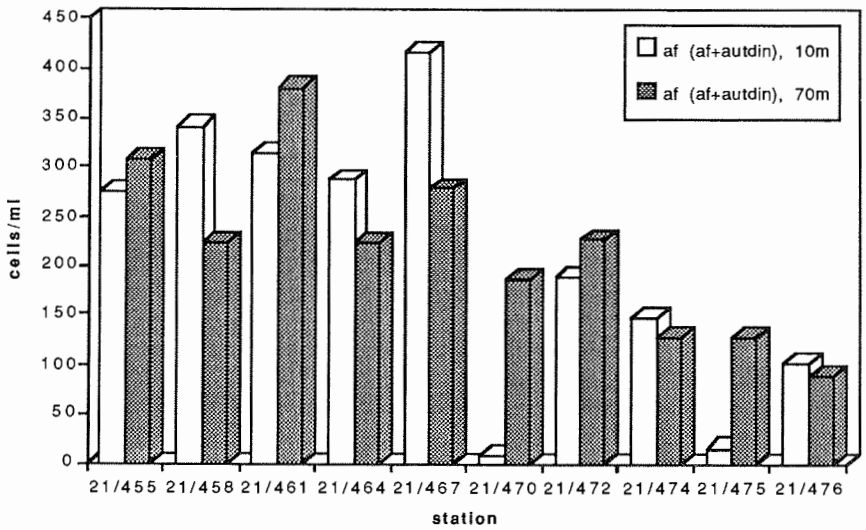

Fig. 39: Abundances of pennate diatoms (pdiat) and autotrophic flagellates (af; autdin=autotrophic dinoflagellates) along transect 4.

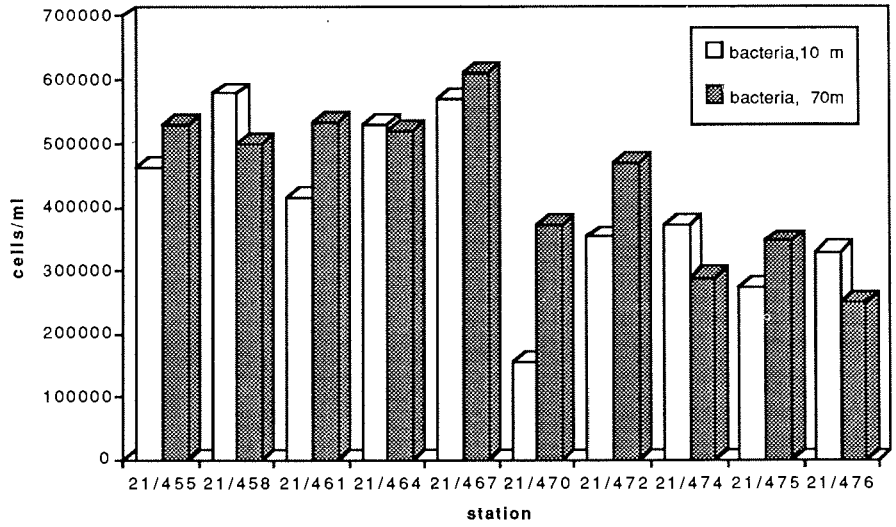

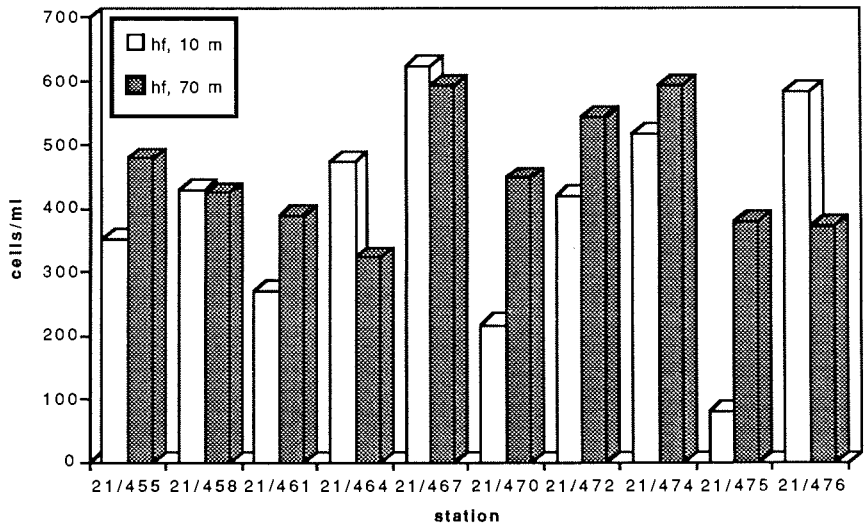

Fig. 40: Abundances of bacteria and heterotrophic flagellates (hf; hetdin=heterotrophic dinoflagellates) along transect 4

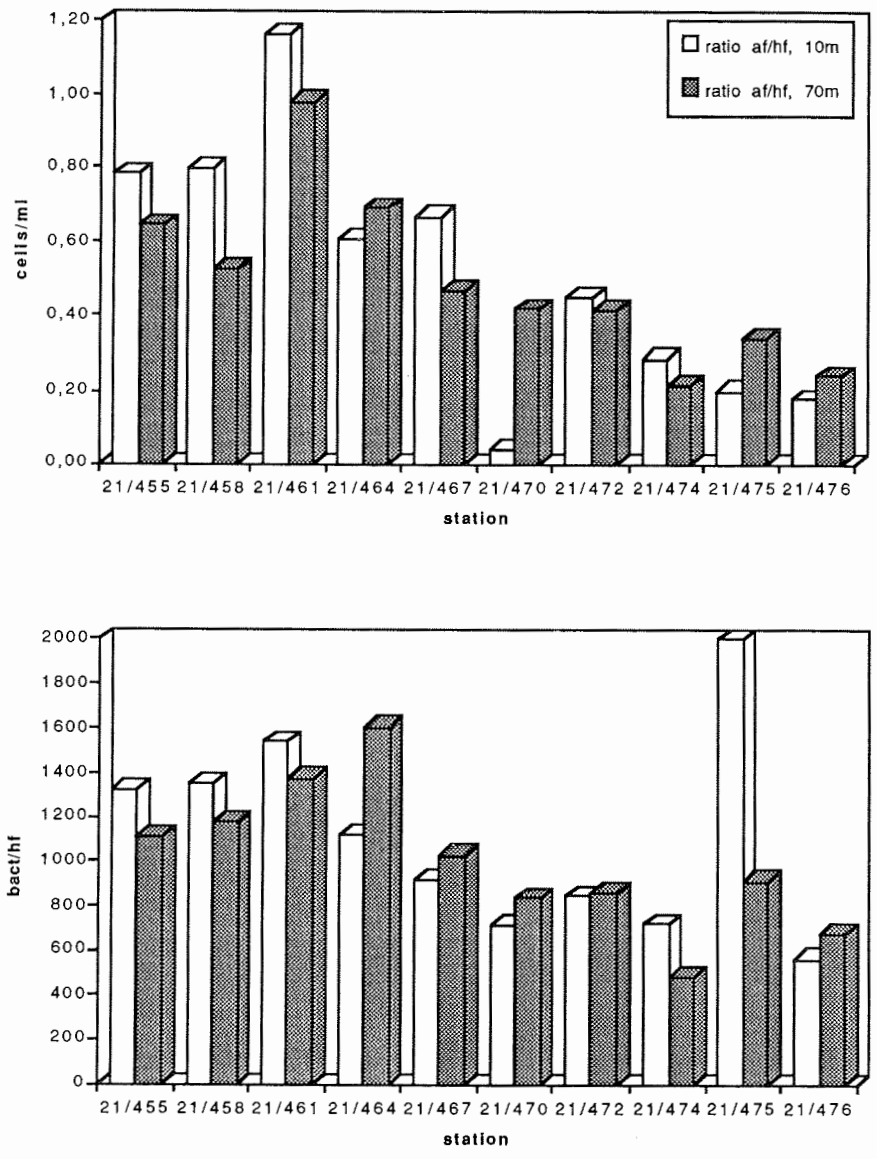

Fig. 41: Ratios of autotrophic *vs.* heterotrophic flagellates (ratio af/hf) and bacteria vs. heterotrophic flagellates (ratio bact/hf) along transect 4.

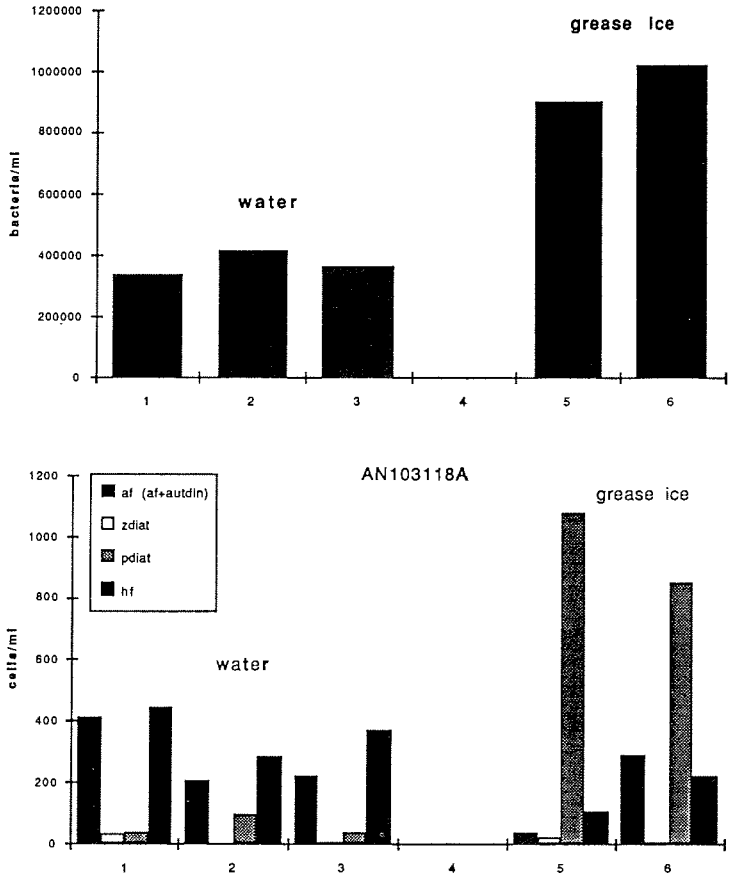

Fig. 42: Comparison of organism concentrations found in the water column (3 parallel samples) and in grease ice (2 parallel samples) at station AN103118A. af=autotrophic flagellates, zdiat= centric diatoms, pdiat=pennate diatoms, hf=heterotrophic flagellates.

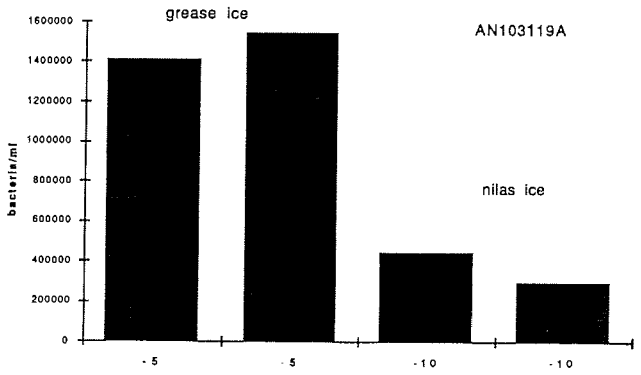

Fig. 43: Comparison of bacterial concentrations found in grease ice and nilas ice at station AN103118A.

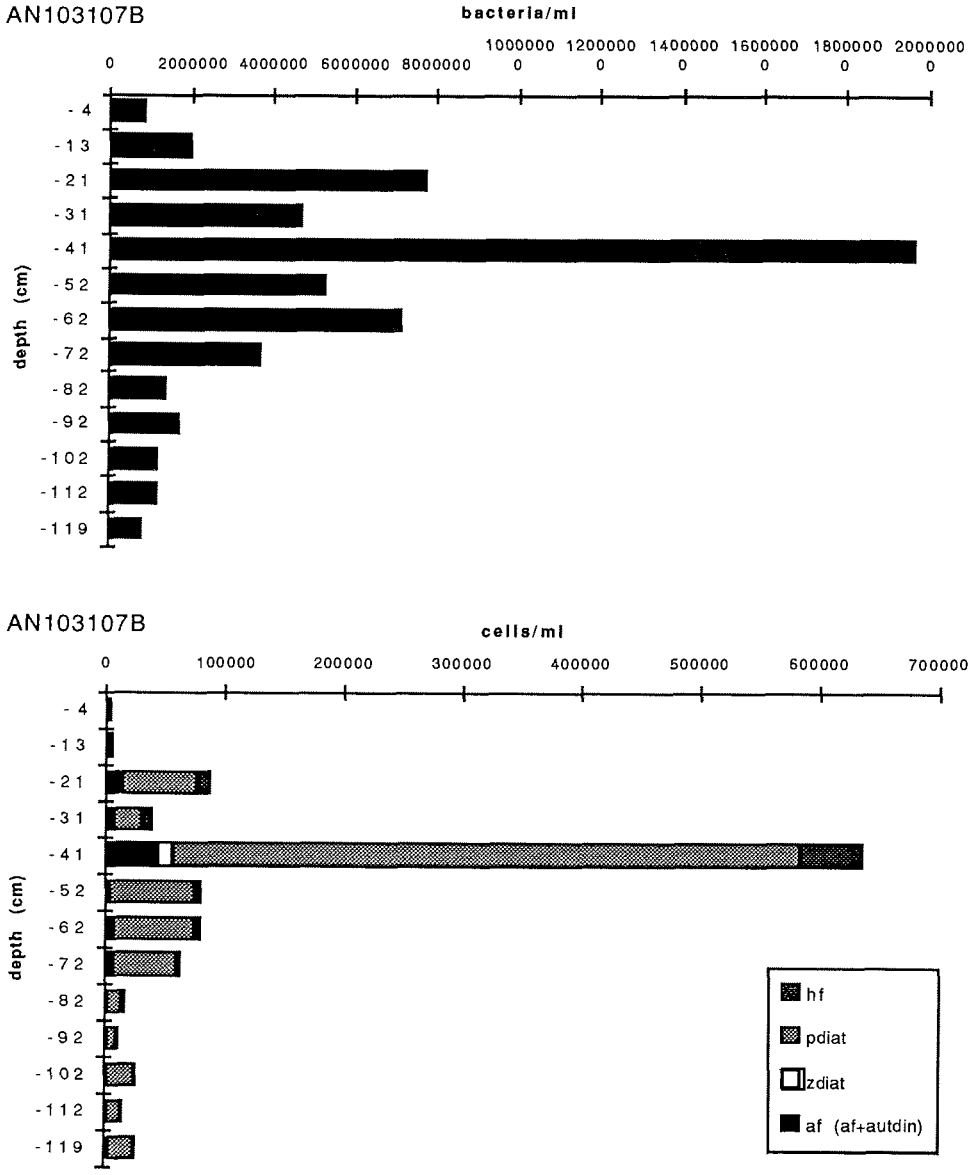

Fig. 44: Vertical distribution of organisms in the ice core AN103107B. af=autotrophic flagellates, zdiat= centric diatoms, pdiat=pennate diatoms, hf=heterotrophic flagellates.

3.2.10. ECOLOGY AND BIOLOGY OF ICE BIOTA

D.GARRISON, H. A. THOMSEN

3.2.10.1. Introduction

Seasonal drifting pack ice covers vast regions of the Southern Ocean. The biota in pack ice are found throughout the ice floes, and this has been attributed to the harvesting and concentration of organisms from the water during frazil ice formation. The frequent formation of frazil ice and the harvesting and concentration of organisms in newly-forming ice is one of the fundamental differences between the pack ice and the land-fast ice habitats; this process is not well understood. During the autumn to winter transition, light levels and atmospheric temperatures decrease, and a considerable amount of seasonal sea ice forms. Organisms incorporated into ice floes during this season will be subjected to low temperatures, high *in situ* salinities and low light.

Our ice biota studies ocused on three areas: 1) composition of the ice assemblage and comparisons with phytoplank-tonic assemblages, 2) survival of organisms incorporated in newly-formed sea ice, and 3) systematic studies of some of the previously neglected or more unusual flagellate species in ice and water.

3.2.10.2. Materials and Methods

Samples were collected from newly-forming ice through older ice floes > 1 meter in thickness. All ice samples were melted into large volumes of filtered seawater at 1°C to prevent loss of organisms as the result of osmotic shock. Aliquots (100 ml) were preserved with Lugol's iodine solution for later examination and counting with an inverted microscope. Smaller volumes (10-25 ml) were concentrated on 0.8 µm Nuclepore filters for examination by fluorescence microscopy. Similar samples, but with larger volumes concentrated on filters, were collected from at least three depths in the water column (usually 2, 20 and 50 meters) at several stations to allow a comparison between ice and water column assemblages. Preliminary examination of some filters were made aboard ship, but most of the samples (over 90 samples from ice and water) will be analyzed later in our laboratories.

Bulk measurements of particulate carbon and nitrogen (POC and PON) and ATP (22 samples) were made on selected ice samples that were also sampled for community composition (these compliment measurements made by the AWI ice biology group). These parameters will also be analysed after the cruise.

Viability of organisms from ice were examined using the fluorescent vital stain Fluorescein Diacetate (FDA) and the mortal stain Ethidium Monoazide (EMA) and by autoradiography. To examine the effect of low temperature and high salinity on survival and activity of ice-associated organisms, ice samples melted in high salinity brine were incubated in a deckboard incubator at near ambient conditions (i.e., -8 to -12 °C). Melted ice samples (200 ml) were inoculated with approximately 50 µCi of ^{14}C in the evening. Samples were allowed to come to ambient temperature overnight in the deckboard incubator, incubated a full light-day and then allowed to melt and were processed during the following dark period. Freezing in the deckboard incubators was prevented by addition of salt to the water in which the samples were incubated (final salinity approximately 250 psu), but individual samples suspended in the incubator froze during the night acclimation period. Incubator temperatures were usually slightly warmer than air temperatures. Samples were incubated for standard dark-light productivity, a replicate sample and a killed control were processed for autoradiography and a sample with no isotope added was incubated to examine with fluorescence stains following the incubation. Samples for autoradiography were preserved with Karnovsky's solution and will be examined later to validate the results of examination using fluorescenct stains. Parallel incubations were performed in a incubator at -1.5 °C and at light levels of 40-50 µE m^{-2} sec^{-1}. Ice samples collected from natural populations and those exposed to low temperature during the experiments were examined with fluorescent vital stains by

concentrating samples (200-500 ml) with either a centrifuge or by using a 2.0 µm Nuclepore filter, incubating the sample with the stain and then examining individual cells for activity with a fluorescence microscope.

Samples collected for single cell and community structure analysis (ca. 60) were examined live onboard the ship. Organisms were documented by video and flashphotographs. Cultures of flagellates and cysts from brown ice samples were established during the initial phase of the cruise. In addition, whole mounts of cells were prepared for both light microscopy (LM) (ca. 100) and transmission and scanning electron microscopy (TEM/ SEM) (ca. 400). Small droplets of nanoplankton material concentrated by centrifugation were placed on either coverslips or grids. The cells were fixed in the vapours of a 1-2% OsO_4 solution for approximately 30 sec. A thorough washing in redistilled water preceded the storage of these preparations. The coverslips were mounted upside down on slides using four small droplets of nailpolish. Material for thin-sectioning (11 samples) was fixed and embedded according to standard protocols. The initial fixation was in a 2% glutaraldehyde solution buffered by cacodylate (0.1 M) and osmotically adjusted by adding sucrose (0.3 - 0.4 M). An OsO_4 postfixation preceded dehydration and embedding in Spurr's low viscosity resin.

Loricate choanoflagellates were examined aboard ship in the light microscope slide preparations described above. Relative abundance among 25 species at 40 ice and water stations was determined from cell counts. At least 200 cells were counted from each preparation. A similarity matrix was constructed among the stations using Percent Similarity Index (PSI). The similarity among ice and water stations was analysed using cluster analysis and multidimensional scaling. In addition to the intact cells, empty loricas were counted as an estimate of mortality (this includes cells damaged during sample processing as well as natural mortality).

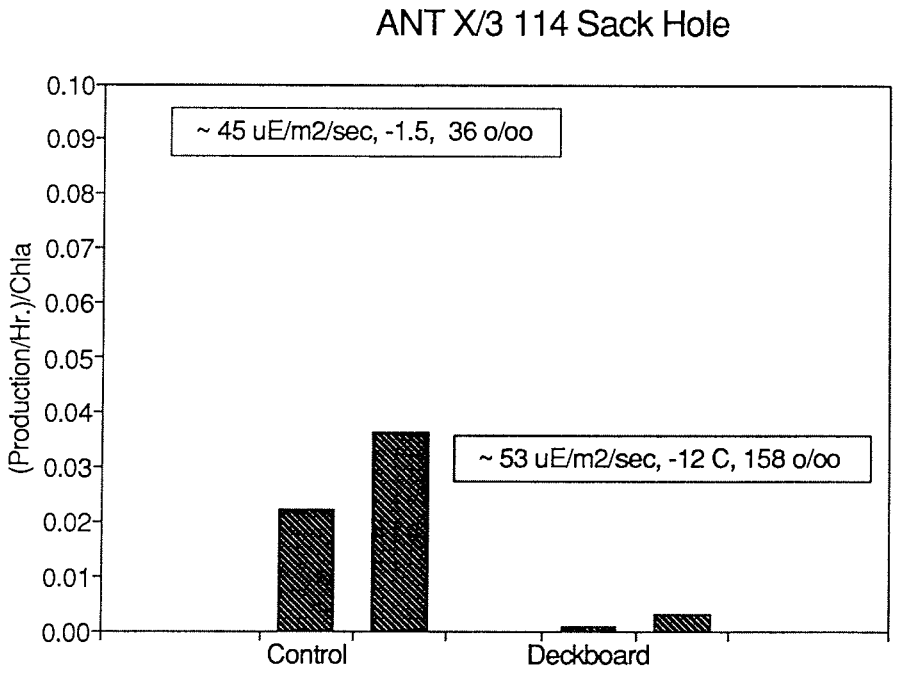

Fig. 45: Results of ^{14}C uptake experiments on ice samples incubated at -1.5°C (Control) and at simulated in situ temperature and salinities (indicated on the figure).

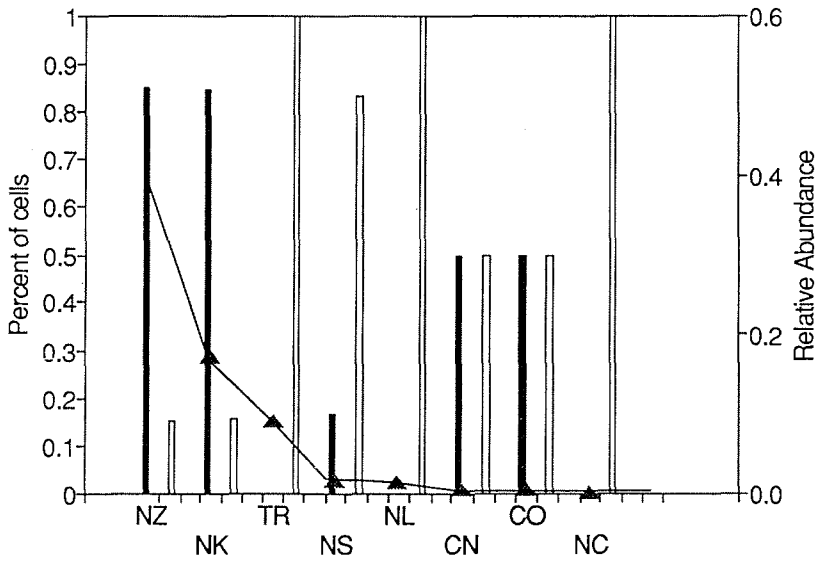

Fig. 46: Results of FDA activity incubation on natural populations from sea ice (AN103103). Cells showing activity (filled bars). Cells not showing FDA activity (open bars). (NZ) *Nitzschia* spp., of the *Fragilariopsis* group, (NK) *N. kerguelensis*, (TR) *Tropodoneis* sp., (NS) *N. subcurvata*, (NL) *N. lecointei*, (CN) *Chaetoceros negoracile*, (CO) *Corethron criophilum*, (NC) *N. closterium*. Relative abundance (filled triangle and line) is indicated on right Y-axis.

3.2.10.3. Preliminary Results

COMMUNITY STUDIES
Bulk chemical measurements of community parameters and detailed population analysis will require extensive examinations after the cruise. Some results for a selected group of heterotrophic flagellates (i.e. loricate choanoflagellates) are presented in the flagellate biology section below.

VIABILITY AND ACTIVITY OF ORGANISMS IN ICE
Preliminary results of the low temperature-high salinity simulated *in situ* production showed significant levels of ^{14}C uptake at temperatures of -12 °C, and at corresponding salinities of 158 psu, although these rates were lower than those measured in parallel experiments at -1.5 °C (Fig. 45). There was considerable variability among experiments on differing ice samples that may reflect the history of the natural populations. Only six experiments were performed during the cruise, and these data may only provide evidence of the feasibility of the experimental approach.

The only fluorescent vital stain that proved useful was FDA. Examination of ice samples incubated with this stain confirmed activity for several *Nitzschia* species of the *Fragilariopsis* group (e.g, *N. cylindrus*, *N. curta*). These species also predominated in the samples that were examined. Other species that are also common in ice (e.g., *Tropidoneis* sp., *N. subcurvata* and *N. lecointei*) showed little FDA activity (Fig.46). In one test where FDA activity was examined before and after low temperature incubations, diatom species showed little change in activity before and after exposure, whereas all of the autotrophic dinoflagellates lost FDA activity after exposure to low temperatures and

high salinities. Other tests suggested that there was little apparent change in FDA activity for diatoms with low temperature exposure, but loss of activity in dinoflagellates was not as apparent. One limitation in using vital or mortal stains (or any other technique that examines single-species by microscopy) for population analysis is that unless a high number of cells can be rapidly concentrated and examined, statistically meaningful information can only be obtained on the dominant species comprising assemblages.

BIOLOGY OF FLAGELLATES

Results of the systematic studies of flagellates largely depend on a subsequent TEM/SEM examination of samples, so the light microscopical results presented here on prymnesiophytes and choanoflagellates only gives an impression of the potential of the material for addressing some of the main objectives of our research.

Prymnesiophyceae (Haptophyceae)

Members of this algal group are frequently encountered in Antarctic water column and ice biota samples. The most prominent example (in terms of biomass and productivity) being flagellates and colonies of *Phaeocystis*.

Heterotrophic coccolithophorids

Until recently it was not considered likely that coccolithophorids were present in polar regions. However, more than 20 species of weakly-mineralized coccolithophorids, which are all morphologically quite distinct from the "classical" coccolithophorid species of the warmer seas, have been consistently found in Arctic and Antarctic water column samples.

Traditionally, all species of Prymnesiophyceae (with one exception, the brackish water coccolithophorid *Balaniger balticus*) have been considered photosynthetic, although several are known to be mixotrophic (e.g. most species of *Chrysochromulina*). Through our examinations of ANT X/3 LM whole mounts using a combination of phasecontrast- and epifluorescense microscopy, it has become evident that all Antarctic coccolithophorids from the genera *Papposphaera*, *Pappomonas*, *Turrisphaera*, *Trigonaspis*, *Wigwamma*, and *Calciarcus* are in fact heterotrophic organism. This new observation extends and emphasizes the functional diversity among members of the Prymnesiophyceae and provides significant new information for phylogenetic interpretation. An electron microscopical examination of sections of some of these species will hopefully indicate whether these polar coccolithophorids are:

1) genuine heterotrophic organisms, and thus likely to be considered more closely related than any other known Prymnesiophyte to the primitive cell, that originally acquired photosynthesis through an endosymbiotic event,

or:

2) whether these organisms have secondarily lost the photosynthetic apparatus (i.e. chloroplast reduced to a leucoplast).

Although some of these atypical coccolithophorid species are also found (in low numbers) at lower latitudes (e.g. Baltic Sea, Thailand coastal waters, Indian Ocean, Sea of Cortez), it is tempting to hypothesise that some connection exists bewteen the heterotrophic nature of these organisms and the fact that they form a significant plankton element only in the marginal regions of coccolithophorid global distribution (i.e. in low temperature and/or low salinity areas).

The heterotrophic coccolithophorids were abundant in the under-ice water samples, and were also found in slush- and grease ice samples. Several cells were found in one particular pancake icecore (AN103107A) and a single live cell of *Wigwamma annulifera* was observed while examining a distinct brown ice community found at the bottom of a 70 cm thick iceblock (AN103113).

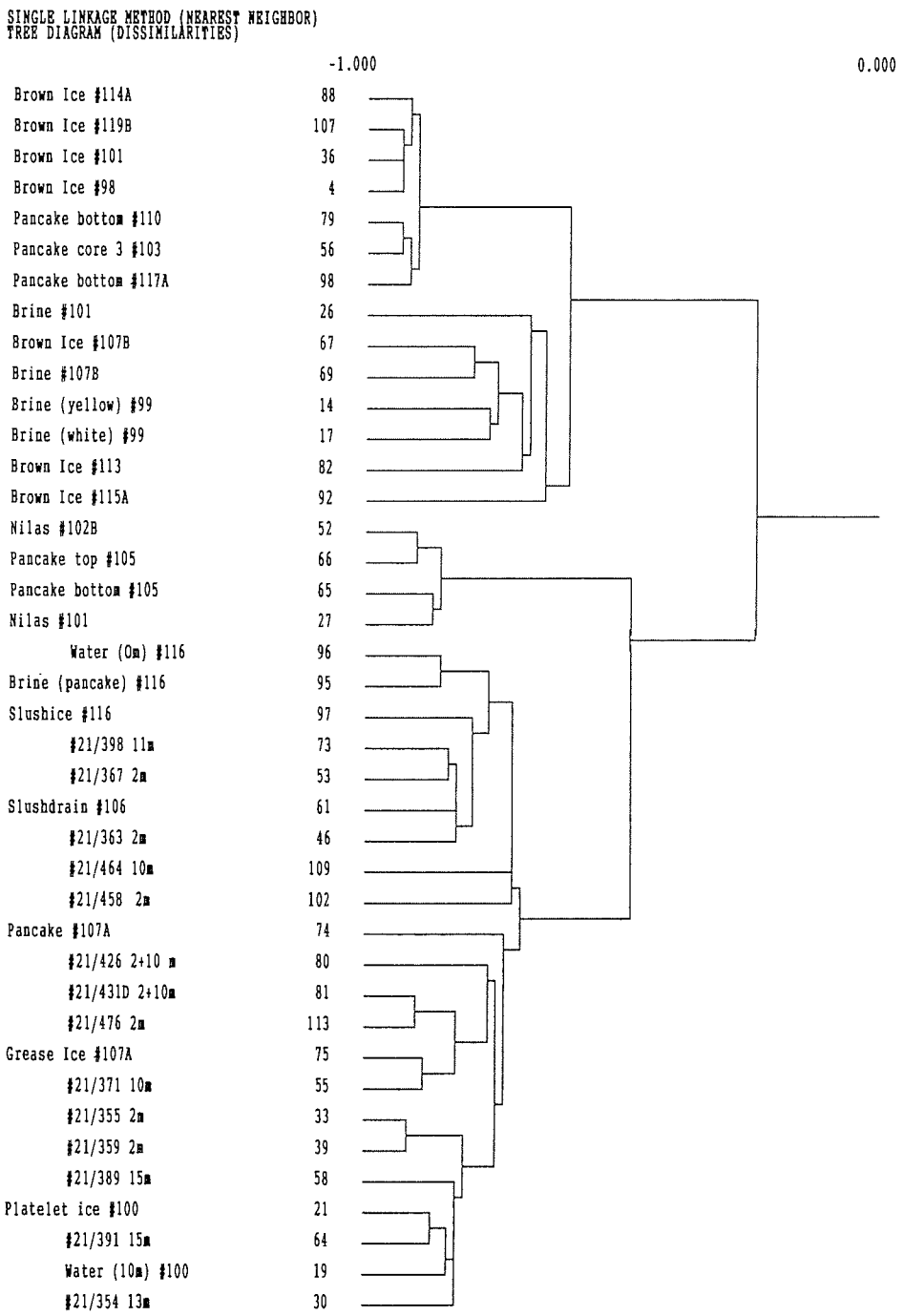

Fig. 47: Results of cluster analysis based on relative abundancies of loricate choanoflagellates.

"Phaeocystis" colonies in the ice

The photosynthetic brown ice assemblage is commonly found to consist of diatoms, dinoflagellates and prymnesiophycean colonies most often identified as *Phaeocystis*. Through our observations of live samples from melted brown ice cores, we have on three occasions observed the release of swarmers from such colonies. Whereas the colonies are indistinguishable, the flagellates that originate from them appear to be different at the generic level. We hope that subsequent TEM examinations of whole mounts and sections will allow a detailed description of both colonies and flagellates.

The formation of swarmers from these "*Phaeocystis*-like" ice biota colonies is most likely triggered by the melting of the ice. We observed in one case that the flagellates released settled after only a few hours on spines and processes of diatoms. This appears to be a most relevant strategy for a primarily ice-associated organism, considering that the large diatoms have a considerable chance of being eventually incorporated into newly formed ice.

It also is important to emphasize that whereas the slow melting of ice cores in large volumes of sterile seawater is obviously needed to recover delicate organisms from ice samples, significant community changes may occur during this process. The transformation of prymnesiophycean colonies into 5-8 µm flagellates obviously creates a vastly different assemblage from that initially in the ice.

During this cruise the only colonies resembling "true" *Phaeocystis* were found in water column samples. Flagellates of what is generally referred to as *Phaeocystis pouchetii* were similarly abundant in water column samples.

Choanoflagellates (Acanthoecidae)

The loricate choanoflagellates are easily recognized in LM whole mounts and we were able to undertake a community structure analysis of these organisms from a multitude of habitats. As shown by the results of cluster analysis (Fig.47), it is evident that the mature choanoflagellate ice-community is significantly different from those of the water column and the early stages of ice formation (i.e. grease, platelet, nilas and thin pancakes). The water column cluster can be further subdivided into four subunits. Three of these (Fig. 47, A-C) are geographically separated within the area sampled, and thus appear to reflect differences in physical and biological parameters. The fourth assemblage, consisting of two nilas and two pancake cores (Fig.47), is clearly differentiated from the other three "water column" clusters and might perhaps be considered intermediate between the two main clusters.

The loricate choanoflagellate ice-assemblage encompasses a range of undescribed organisms (>5) and only two of the water column organisms in these samples reach a relative abundance in excess of 1% (i.e. *Parvicorbicula socialis* = 4.1%; *Diaphanoeca multiannulata* = 1%). *Diaphanoeca multiannulata* is a very large water column species (lorica up to 100 µm long / 15% total rel. abund.) which compared to most other significantly smaller species of choanoflagellates may be more easily trapped during iceformation and thus may tend to be selectively incorporated in the young ice samples. The open water forms of *D. multiannulata* typically possess 4-6 transverse costae. In the ice a somewhat similar form with only 3 transverse costae accounts for 63% of all specimens identified. It seems possible to imagine that this is a special ice morphotype of *D. multiannulata*. The significant reduction in size and the fewer numbers of transverse costae comprising the lorica might be adaptations to life in minute brine channels. Moreover, this reduction of silicious elements may be a response to living in a silicon-depleted habitat.

The frequency of empty loricas occuring in different types of samples have been analyzed (Figs.48 & 49). In water column samples (n=16) the mean value of dead cells is 25% (std. 6.8), as opposed to 40.3% (std. 16.8) in the ice-related samples (n=24). In Figure 49, which shows the same dataset, it is evident that the percentage of dead cells is

particularly high in newly formed ice (nilas, platelet and grease ice), whereas some of the lowest numbers of dead cells were seen in mature and well established brown-ice communities.

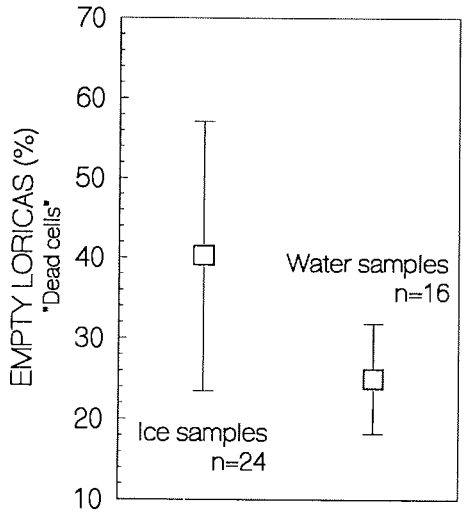

Fig 48: Frequency of empty loricas (= dead cells) in water column samples and ice biota samples.

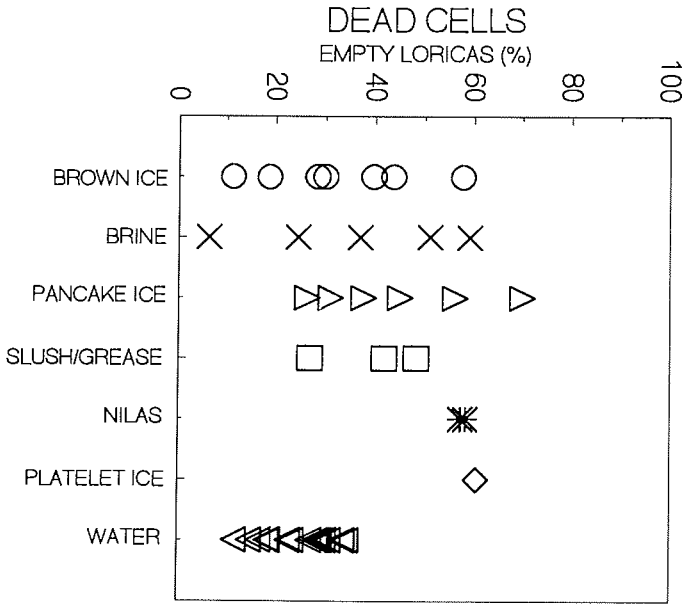

Fig. 49: Frequency of empty loricas in different types of habitats.

3.2.11. ZOOPLANKTON INVESTIGATIONS

S.SCHIEL, W. HAGEN, U. KLAUKE, E. MIZDALSKI, F. PAGES, T. PROBYN, M. STÜRCKEN-RODEWALD, D. THOMAS

3.2.11.1. Objective

LIFE CYCLE STRATEGIES OF MESO- AND MACROZOOPLANKTON WITH EMPHASIS ON CALANOID COPEPODS

Zooplankton, particularly calanoid copepods, has been thoroughly studied in summer and late winter during ANT III/3 and ANT V/3. During ANT X/3 the little known "switching" of zooplankton from the summer to the winter state was investigated. Some herbivorous calanoid copepods are known to stop feeding, descend to greater depths and go into a resting stage (diapause) during autumn, in order to survive the lack of food in winter. Other species seem to stay active in winter and utilise alternative food sources instead of phytoplankton. Few investigations have been published, which have analysed these mechanisms in detail, and none are known from the high Antarctic Weddell Sea. We therefore studied these different "adaptive strategies" of selected zooplankton species (meso- and macroplankton) by means of field work as well as experiments.

To characterise the "autumn state" of these species our research focussed on the following issues: vertical distribution, population structure, maturity of gonads, gut content, feeding activity (phytoplankton, ice algae), respiration as well as quality and quantity of accumulated lipids.

In addition, experiments were carried out, which investigated the relationship between abundance and size of food particles and feeding rates during autumn. Preferential grazing on certain size classes of phytoplankton can lead to an alteration of phytoplankton composition. Copepods feed most efficiently on larger particles, thereby changing the cell size spectrum and consequently phytoplankton species composition in preference of smaller species. However, with increasing food abundance, selective feeding becomes less important.

These investigations during a critical transition period aimed to improve our understanding of the different planktonic life cyles, elucidate their dependency on seasonal factors (light, ice), and hence contribute to a differentiated analysis of this high polar ecosystem.

DISTRIBUTION AND SYSTEMATICS OF THE PLANKTONIC CNIDARIANS IN THE EASTERN WEDDELL SEA

Planktonic cnidarians (medusae and siphonophores) are one of the most conspicuous components of the zooplankton communities worldwide but also one of the less studied. They are important secondary consumers and feed heavily on copepods, fish larvae and other gelatinous zooplankters. Generally, most investigations on Antarctic plankton communities have not dealt with planktonic cnidarians, and little is known about their role in the Antarctic food web.

The objectives of this cruise were to:

Collect a high number of medusae and siphonophore species in order to determine the species composition in Antarctic waters.

Study the horizontal and vertical distribution of smaller planktonic cnidarians along two ice edge - open water transects.

3.2.11.2. Work at sea

The Multinet was equipped with five nets (each 100 µm) to sample discrete depth layers from within 1000 m (or bottom) to the surface. The depth ranges were defined according to the temperature profile at the respective station. Samples were taken along the 7° and 12°W transect. The first transect extended from the pack-ice into open water, the second

one was in an area totally covered by sea-ice. The samples from the 7°W transect were analysed on board for copepod and euphausiid as well as cnidarian distribution.
In addition, a Multinet equipped with 64 µm mesh size was used five times down to 500 m in order to study the distribution of Acantharia cysts and Radiolaria. At nine stations a cylindrical net (Fransz.net; 50 µm mesh) was used from 300 m to the surface to collect small plankton organisms. To investigate the boundary layer between sea ice and water a pump system was employed through ice core holes. The net samples were preserved in 4% buffered formalin or in 25% alcohol (64 µm Multinet samples).

For feeding, respiration and excretion experiments the Bongo net (335 µm) was employed at six production stations down to 200 m to collect live specimens. The following large copepod species were used for experimentation, *Calanus propinquus, Calanoides acutus, Rhincalanus gigas* and *Metridia gerlachei* as well as the small species *Stephos longipes*. Feeding experiments were carried out with natural phytoplankton suspensions from the rosette samples from about 30 m depth, with melted ice cores and with melted platelet ice. To obtain information on preferential feeding on different size classes, size-fractionated chlorophyll measurements were carried out. The respective species and size composition will be determined on preserved samples in the laboratory in Bremerhaven. Additional experiments were done with filtered seawater, to which a sea-ice core was added. The behavioural response of the copepods to the presence of algae in the sea ice was observed. Copepod respiration was measured using a Winkler method. The ammonium and urea concentration was determined according to Grasshoff. All experiments were carried out in the dark in a cooled laboratory container at -1 °C. Specimens from the experiments were subsequently frozen at -30 °C for later determination of dry weight and carbon/nitrogen content.

Samples for activity measurements on digestive enzymes, lipid analyses as well as cnidarian species composition were obtained mainly using a Bongo net (335 µm), Rectangular Midwater Trawl (RMT 1+8; 325 and 4500 µm) and Benthopelagic Trawl. The hauling depths for these nets were usually 500 or 1000 m (see station lists). In the cooling container the organisms were identified as far as possible, measured, sexed and sorted according to developmental stage. The samples were subsequently frozen at -80 °C. A total of about 400 samples of the following taxa (number of species) were collected: Copepods (11), euphausiids (3), amphipods (5), decapods (1), cnidarians (3), mollusks (4), polychaetes (1), chaetognaths (1), fishes (3). The determination of total lipid content, lipid class and fatty acid/alcohol composition will be carried out mainly using chromatographic techniques at the Institut für Polarökologie in Kiel,.

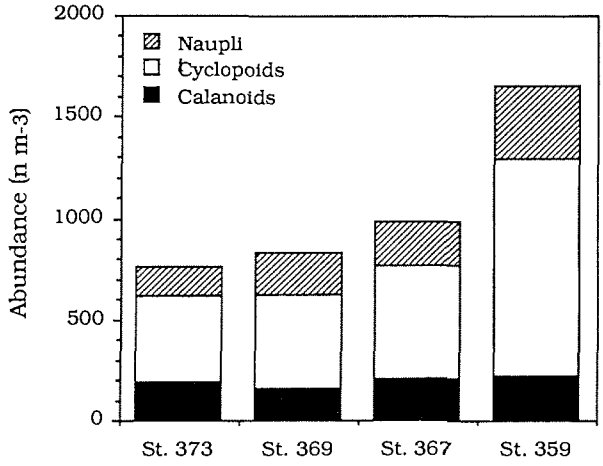

Fig. 50: Abundance of total copepod population (calanoids, cyclopoids and nauplii) in the upper 1000 m.

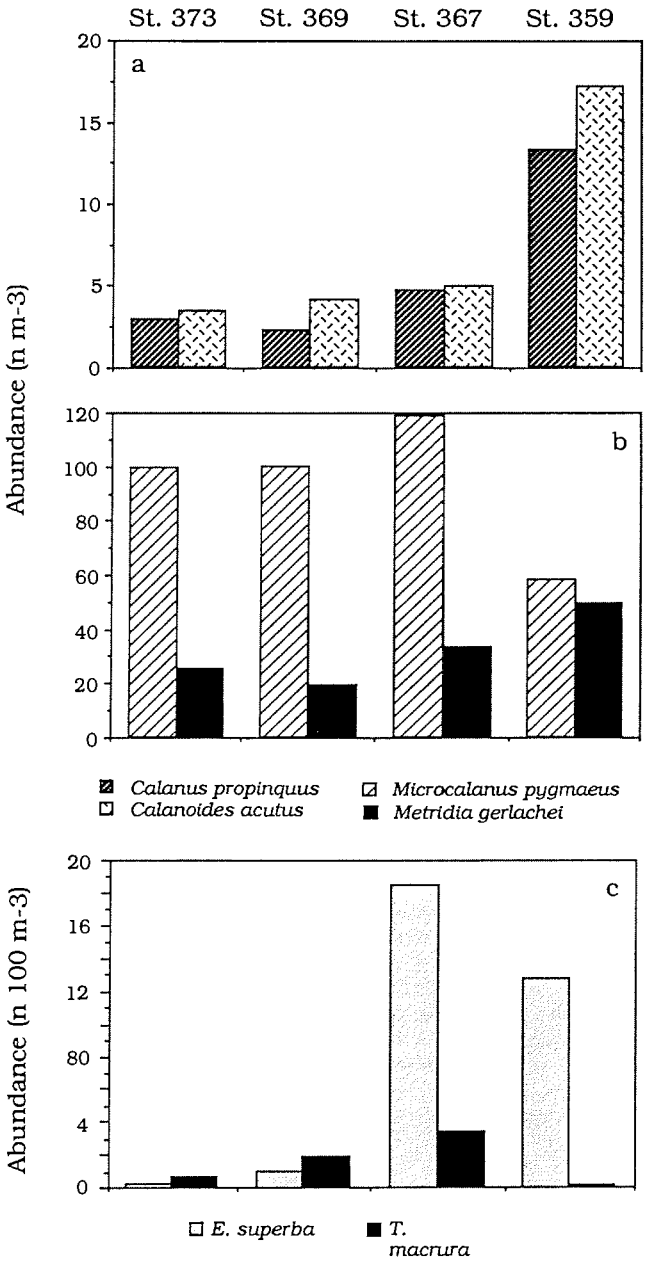

Fig. 51: Abundance of total populations of *Calanoidea acutus* and *Calanus propinquus* (a), *Metridia gerlachei* and *Microcalanus pygmaeus* (b), *Euphausia superba* and *Thysanoessa macrura* (c) in the upper 1000 m.

3.2.11.3. Preliminary results

PRELIMINARY RESULTS ON LIFE CYCLE STRATEGIES

Along the 7°W transect copepods occurred in higher numbers at the southernmost station (St.359) and the abundance decreased in offshore direction (Fig. 50). This feature was more pronounced in nauplii and cyclopoids than in calanoids.

The distribution pattern of four dominant calanoid copepod and two euphausiid species will be discussed in more detail in the following. The abundance of the large copepods, *Calanoides acutus*, *Calanus propinquus* and *Metridia gerlachei*, decreased with increasing distance to the ice shelf (Fig. 51 a,b). In contrast, the smallest species, *Microcalanus pygmaeus*, occurred in lower numbers at the southernmost station (St. 359) and with similar numbers at the three remaining stations (Fig. 51 b). Both euphausiid species showed highest densities at St. 367. *Euphausia superba* was most abundant at stations closer to the ice shelf, whereas higher abundances of *Tysanoessa macrura* were found at more offshore ones (Fig. 51 c).

Older copepodite stages (CIV + CV) dominated the *Calanoides acutus* population, while early stages (CI + CII) were absent at all stations except St. 359 (Fig. 52a). *Calanus propinquus* showed a shift from copepodite stage CIII (51%) at St. 359 to CV (43%) at St. 373 (Fig. 52b). At St. 359 the population of *Metridia gerlachei* had a bimodal stage structure: CI specimens (35%) were present as well as CII (21%) and CV (20%). At St. 373 older copepodite stages and adults were practically replaced by juveniles of a new generation (CI-CIII: 90%) (Fig. 52c). The development of these three species was more advanced at the more offshore stations than closer to the ice shelf. The stage frequency of *Microcalanus pygmaeus* was relatively similar at all four stations (Fig. 52d). Calyptopis CI and CII larvae constituted the bulk of the *Euphausia superba* population at St. 367, where the maximum numbers occurred. At the southernmost station (#359), mainly furcilia stages (I, II, IV) were present (Fig. 52 e). The main components of the *T. macrura* population were late furcilia stages (Fig. 52 f).

The vertical distribution differed greatly between species. At St. 359 the major part of the *Calanoides acutus* population was concentrated below 100 m. At St. 367 and 369 an equal part of the population was found in the cold surface layer and in the Warm Deep Water layer (Fig. 53a). At all stations the population consisted of significantly older stages (CIV + CV) in the deeper layer than in the surface layer, where CIV comprised up to 80% of the total population. At all stations the *Calanus propinquus* population was highly concentrated in the uppermost cold water layer (Fig. 53b). The bulk of the *Metridia gerlachei* population was found in the mixed water layers between 100 and 300 m (Sts. 367, 369, 373) and between 400 and 600 m (St. 359) (Fig. 53c). The vertical distribution of *Microcalanus pygmaeus* was similar to that of *M. gerlachei* (Fig. 53d). Both euphausiid species were clearly concentrated in the upper 100 m except *E. superba* at St. 359 (Fig. 53 e,f).

First results of the feeding experiments showed that *Calanoides acutus*, *Calanus propinquus* and *Metridia gerlachei* fed at highest rates on the larger phytoplankton size fraction, however, all developmental stages of *C. acutus* and *C. propinquus* also grazed on particles <2 µm. In contrast, no feeding on particles <2 µm could be observed in the adults and CIV/CV stages of *Metridia gerlachei*.

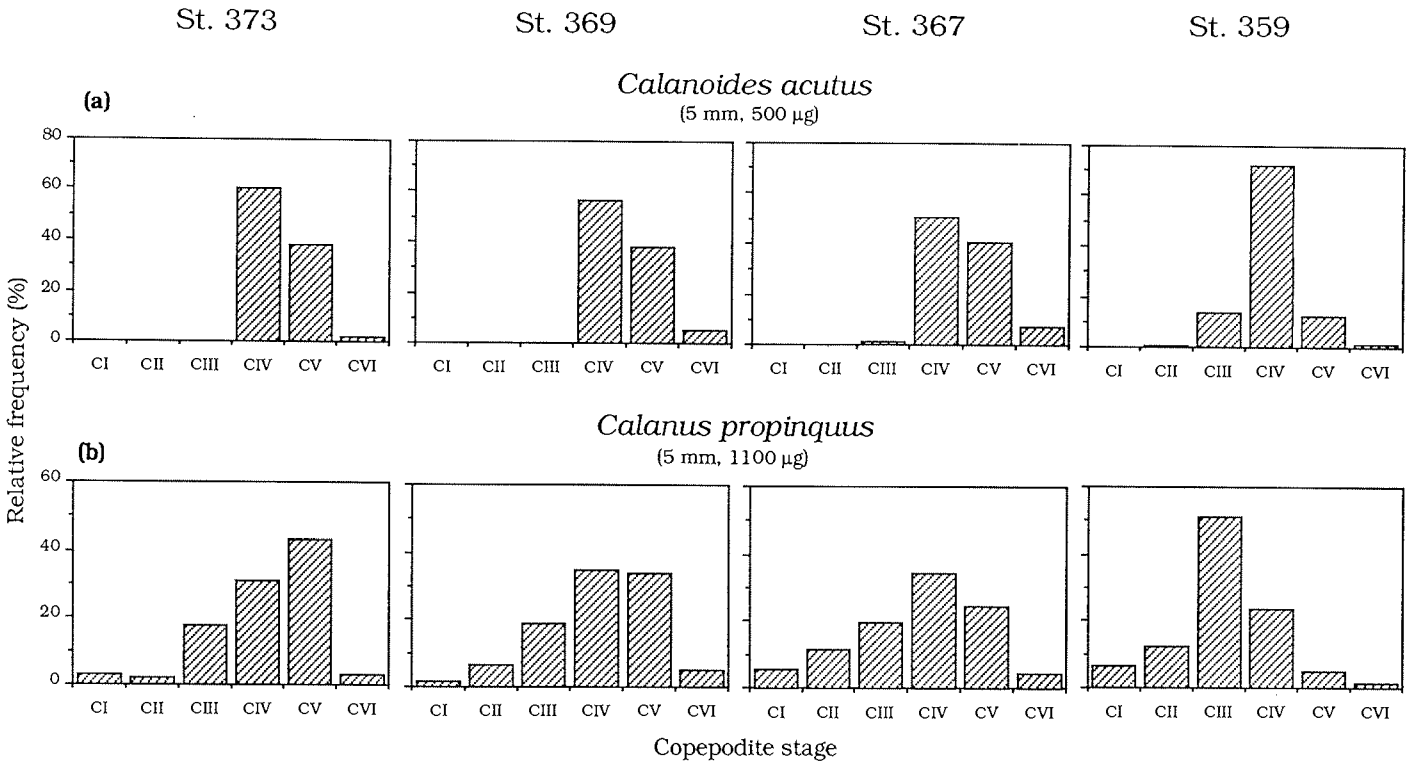

Fig. 52: Percentage frequency distribution of developmental stages of *Calanoides acutus* (a), *Calanus propinquus* (b), *Metridia gerlachei* (c), *Microcalanus pygmaeus* (d), *Euphausia superba* (e) and *Thysanoessa macrura* (f) in the upper 1000 m. Euphausiid developmental stages: CI, CII, CIII = calyptopis I, II, III; FI to F VI = furcilia I to VI; n = total number of individuals identified.

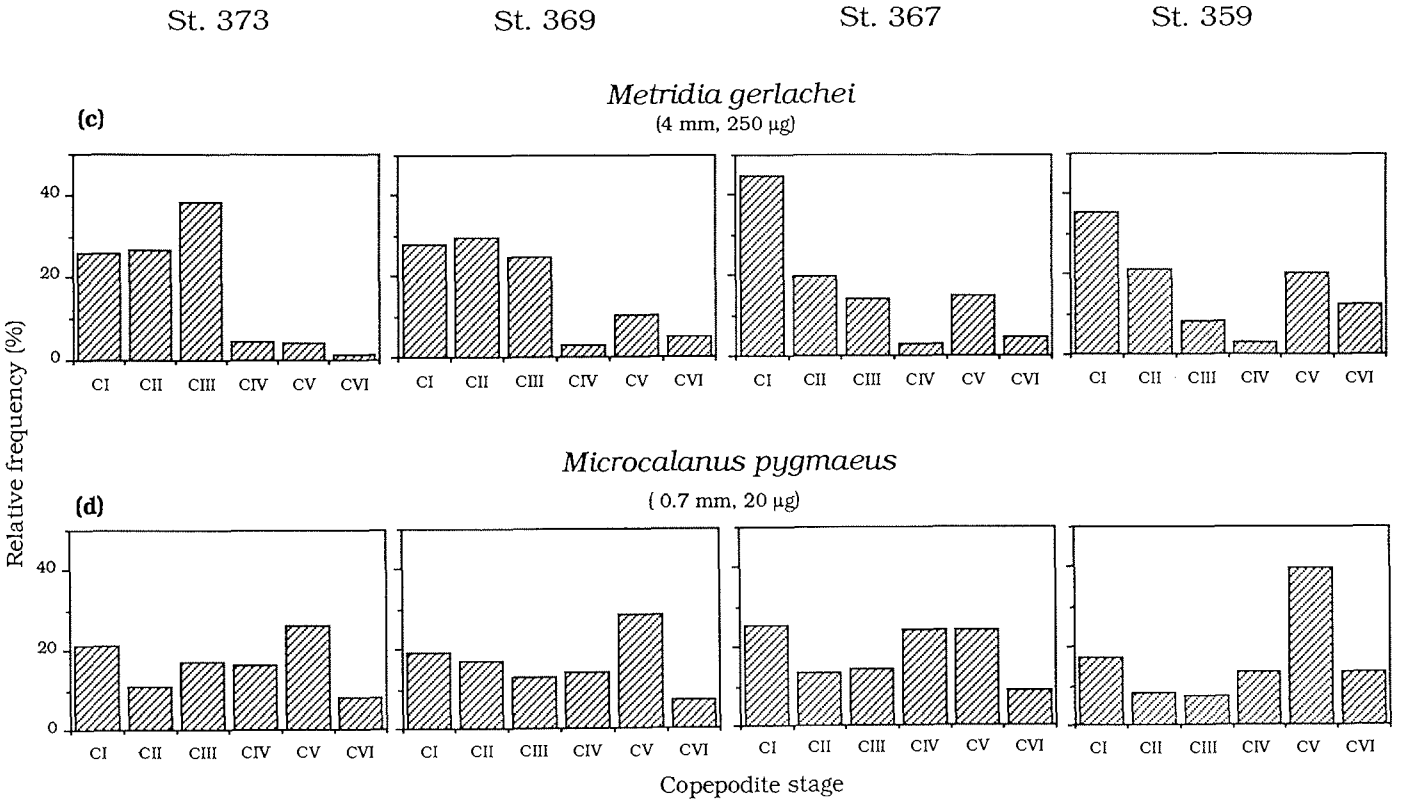
St. 373
St. 369
St. 367
St. 359
(c)
Metridia gerlachei
(4 mm, 250 µg)
(d)
Microcalanus pygmaeus
(0.7 mm, 20 µg)
Relative frequency (%)
0
20
40
CI CII CIII CIV CV CVI
Copepodite stage

Fig. 52 contn.

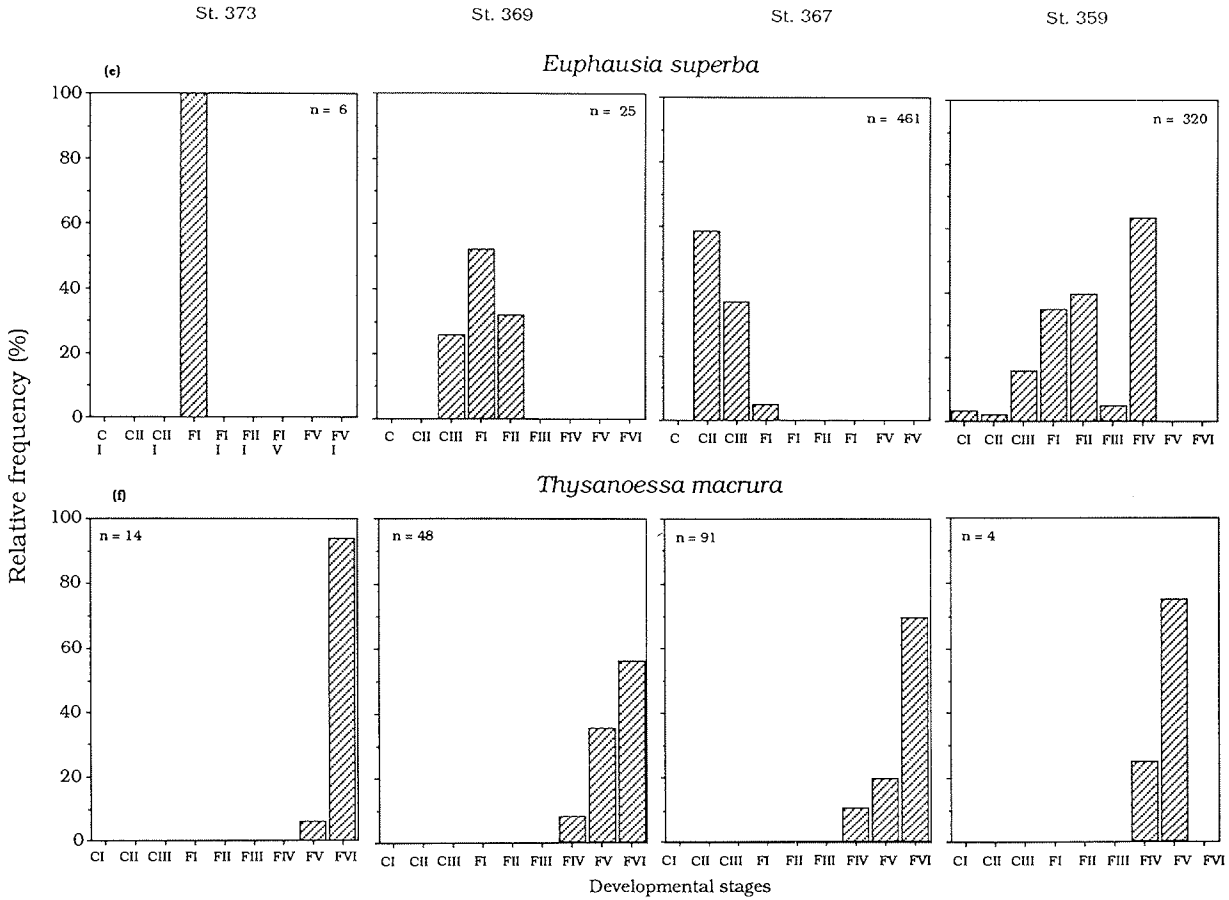
St. 373
St. 369
St. 367
St. 359
(e)
Euphausia superba
(f)
Thysanoessa macrura
Relative frequency (%)
Developmental stages
n = 6
n = 25
n = 461
n = 320
n = 14
n = 48
n = 91
n = 4

Fig. 52 contn.

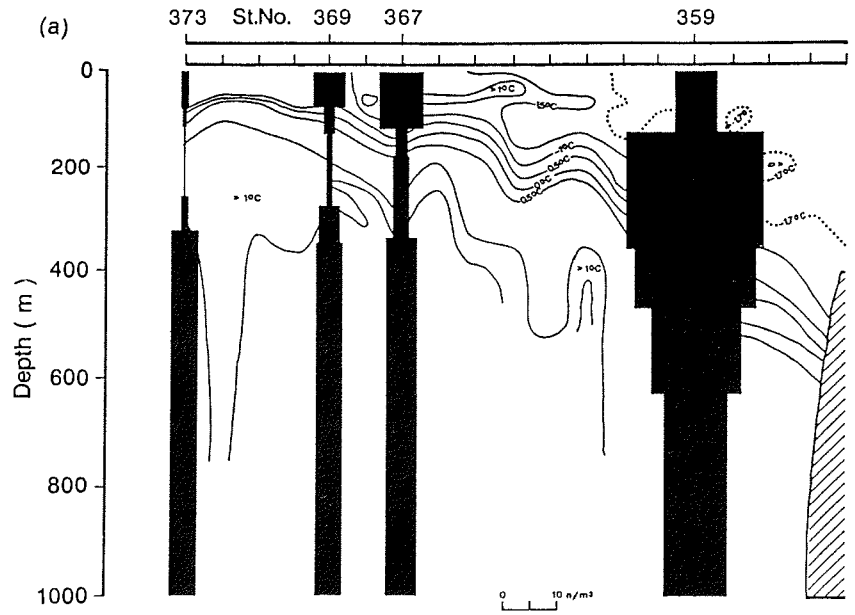

Calanoides acutus

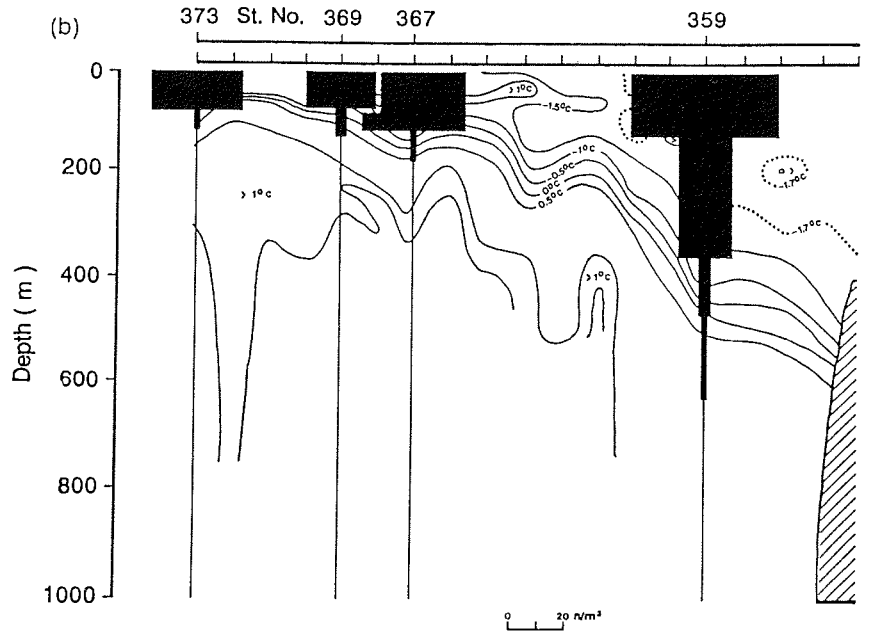

Calanus propinquus

Fig. 53: Vertical distribution of abundance of *Calanoides acutus* (a), *Calanus propinquus* (b), *Metridia gerlachei* (c), *Microcalanus pygmaeus* (d), *Euphausia superba* (e) and *Thysanoessa macrura* (f).

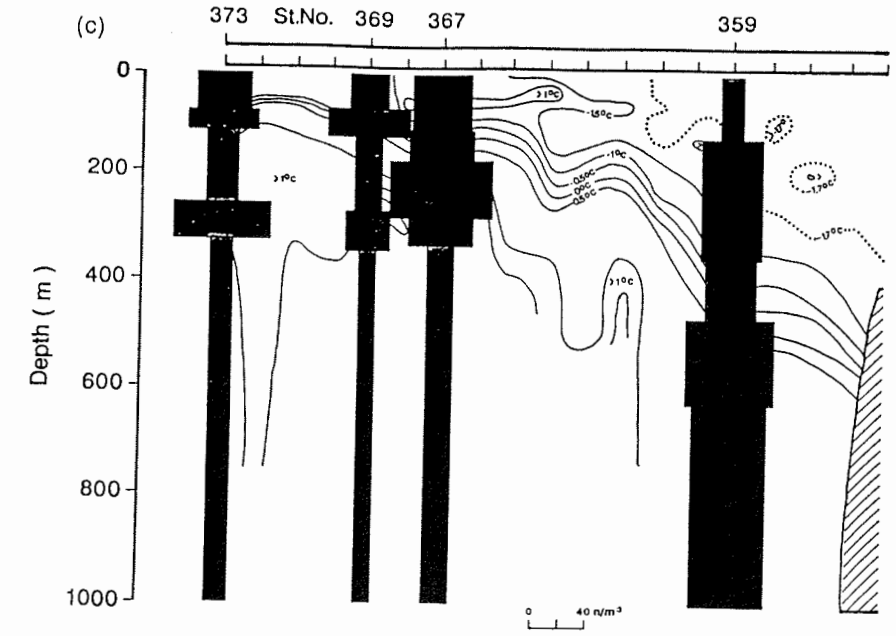

Metridia gerlachei

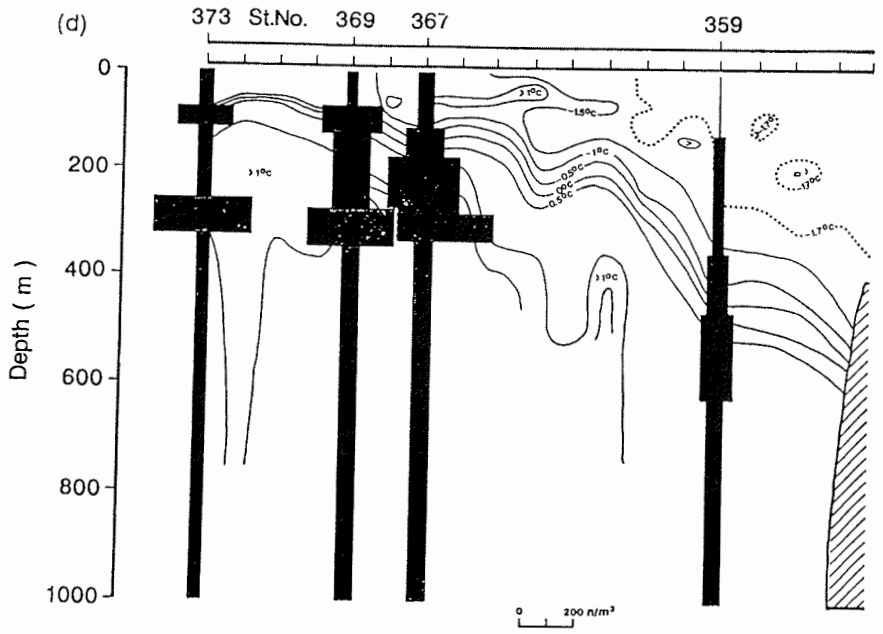

Microcalanus pygmaeus

Fig. 53: contn.

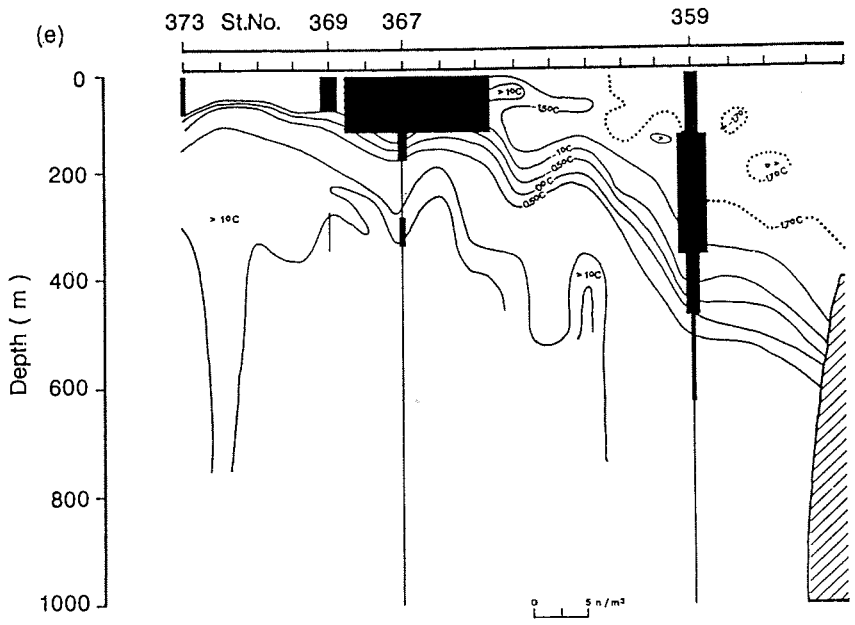

Euphausia superba

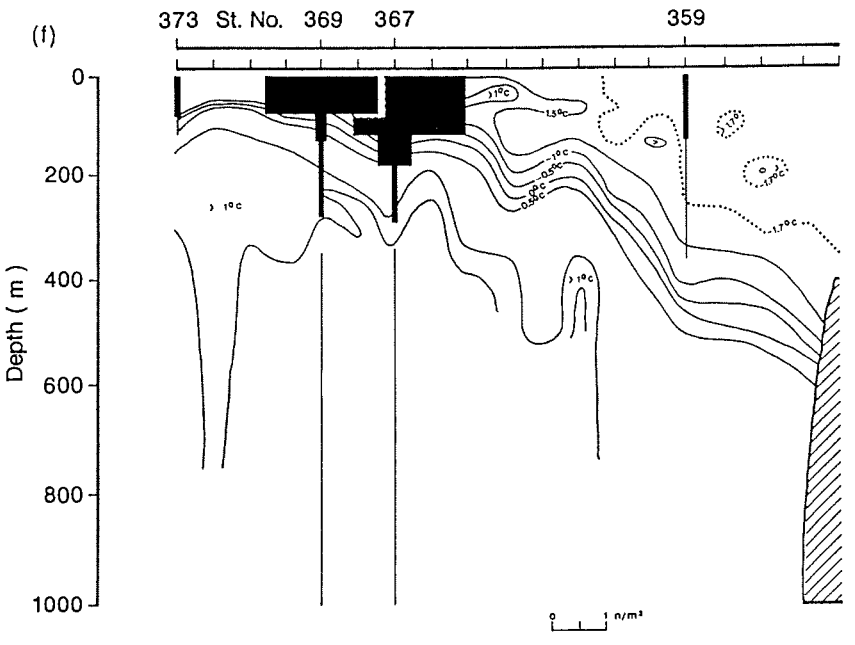

Thysanoessa macrura

Fig. 53: contn

PRELIMINARY RESULTS ON CNIDARIANS

The following fourteen medusae species were identified during the cruise:

Class Hydrozoa
Subclass Anthomedusae
- *Pandea rubra*
- *Zanclonia weldoni*
- *Calycopsis borchgrevinki*

Subclass Leptomedusae
- *Chromatonema rubra*
- *Mitrocomella* sp

Subclass Narcomedusae
- *Pegantha* sp.
- *Solmundella bitentaculata*

SubclassTrachymedusae
- *Haliscera conica*
- *Crossota brunnea*
- *Arctapodema* sp.
- *Pantachogon haeckeli*

Class Scyphomedusae
Order Coronatae
- *Atolla wyvillei*
- *Periphylla periphylla*

Order Semaeostomeae
- *Stygiomedusa gigantea*

Many individuals of several anthomedusan species, young stages of different trachymedusae and a large scyphozoan specimen were not identified to genus level and a further examination will be necessary. Although data on densities are not available yet, the most abundant species were *Calycopsis borchgrevinki*, *Haliscera conica*, *Arctapodema* sp. and *Mitrocomella* sp. Twelve siphonophore species were identified during this cruise:

Class Hydrozoa
Order Siphonophorae
Suborder Physonectae
- *Pyrostephos vanhoeffeni*

Suborder Calycophorae
- *Vogtia serrata*
- *Diphyes antarctica*
- *Dimophyes arctica*
- *Muggiaea bargmannae*
- *Lensia havock*
- *Lensia achilles*
- *Lensia reticulata*
- *Lensia* sp.
- *Heteropyramis maculata*
- *Crystallophyes amygdalina*
- *Sphaeronectes* sp.

Several unidentified eudoxids were also collected. The high number of individuals of *Diphyes antarctica* and *Dimophyes arctica* collected by the RMT is noteworthy. The microscopic examination of the planktonic cnidarians collected by the four Multinet hauls (Sts 359, 367, 369 and 373) made during the first transect provided a general idea of the spatial distribution of these organisms. In the most onshore station (St. 359) which was covered by ice, the medusa *Arctapodema* sp. was the most abundant species and stood

out over the other species. The youngest stages were distributed in the upper 300 m, while the abundance of the old and mature stages increased with depth. No medusae were found in the upper 300 m of the three other stations except for a few individuals of *Solmundella bitentaculata* located in the most offshore station. Only a few individuals belonging to meso- and deep-water cosmopolitan species such as *Atolla wyvillei* were collected in the 300-1000 m depth interval.

The distribution pattern of the siphonophores was different. Colonies of the physonectid *Pyrostephos vanhoeffeni* were located in the upper 100 m of the two most onshore stations while the calycophores *Dimophyes arctica* and *Muggiaea bargmannae* were the most abundant species in the upper 300 m, but the abundance gradually decreased oceanward. Meso-and deep-water cosmopolitan species were collected in waters deeper than 300 m. *Heteropyramis maculata* and *Crystallophyes amygdalina* were the most abundant species in the 300 to 1000 m depth range and no differences in abundance along the transect were observed. Both, sexual (eudoxid) and asexual (polygastric) stages of the most common species were collected but also unidentified eudoxids.

Several species of medusae, siphonophores and ctenophores were kept alive in aquariums for several weeks. This is promising for future experimental investigations on the lifecycle and metabolism of gelatinous Antarctic zooplankton.

3.2.12. PLANKTONIC FORAMINIFERS

D.BERBERICH

Planktonic foraminifera are protozoa, which produce a calcarous shell. Generations of these organisms drop out of the water column and accumulate as sediment on the sea floor. For this reason they are very important for paleoclimatological and paleoceanographic interpretations.

Many studies of the biology of planktonic foraminifers have shown the community structures of this taxoniomic group. Each species prefers a particular biological and abiotic environment for it´s optimal growth.

Neogloboquadrina pachyderma has been found to inhabit the Antarctic sea ice in high numbers. In contrast only a few individuals have been found in the Arctic sea ice. This difference may be due to the different ice form processes between the Arctic and the Antarctic. In the Antarctic the ice is primarily of frazil ice origin whereas in the Arctic mainly columnar ice is found. It has been suggested that ice of frazil ice origin may provide a more suitable habitat for foraminifera.

Recent studies have been made to investigate the incorporation of *Neogloboquadrina pachyderma* into ice and the influence of the latter ice transformation processes on their abundance. Enrichment in the ice may reach levels 60 times that of the underlying water column. These studies have also shown that in ice with high algal biomass, numbers of foraminifers also increase.

But these observations leave still many open questions:

- How do changes in physical, chemical and biological parameters within ice effect the morphology and reproduction of these organisms ?
- Under which hydrographical conditions does the incorporation take place ?
- Is this foraminifer forced to live in the ice, or does this habitat favour the existance of the population ?
- Is the ice a habitat in which there is a high concentration of food organisms ?
- How does the life-cycle change during incorporation into ice ?
- Are they protected from predators ?

3.2.12.1. Methods:
During this cruise many ice samples were obtained on transects from the ice edge into the fast ice. From each ice station at least one core was taken in order to count numbers of foraminifers. Later these individuals will be measured in the laboratory. In conjunction with ice core samples at each ice station an Apsteinnet (20 µm, mesh width) was also deployed in order to analyse their distribution in the water column.
Further correlations with ice algal biomass, phytoplankton biomass and abiotic parameters will be investigated later.

3.2.12.2. Results:
First results are from a transect that began on 23. April and ended on 27. April. On this transect young and old stages of ice were observed. In grease ice, the youngest stage, the lowest number of individuals was found. Grease ice was encountered at ice stations 117 B and 116 A. At these stations the ice was formed from grease ice and young unconsolitated pancake ice. In the one day old grease ice 31 to 40 individuals per litre were found (Fig. 54a).

In the following stage of ice, composed of few small pancakes frozen together, 118 individuals per litre were found (Fig. 54b)

In older pancake ice the results showed that in the lower parts of the ice an enrichment of foraminiferes occurred. Especially in this type of ice an increase in specimense with increasing age was found.

At an ice station with thicker pancake ice from 27. April of an age of 1 to 2 weeks, the lower part of the pancake was inhabited by 259 individuals per liter (Fig. 55a). In a 3 to 4 week old pancake, over 638 individuals per liter were observed (Fig. 55b). The dates from 24. April confirmed previous results that with increasing age the numbers of individuals also increased. In the lower parts of an 4 weeks old pancake, 684 individuals per liter were found (Fig. 55c). Also in the upper parts of this floe more individuals were encountered in comparison to younger ice.

The oldest ice floe on the transect which was over 50 cm thick and a few weeks old, contained 1003 individuals per liter (Fig. 55d). Also the upper parts of the ice high numbers of individuals occurred. This floe was similar in structure to nilas ice. Harvesting and scavengering therefore can be excluded. Such high numbers of individuals is very surprising.

On this transect the lowest number of individuals per litre occurred in young ice. With increasing age the number of specimens also increased.

First correlations with the temperature profile within an one year old pancake ice core showed that in the upper parts with low temperatures of -4°C to -5°C, living individuals were found and with only a few dead ones (Fig. 56). However, in lower parts (120-130 cm) of the floe, with temperature nearly that of the water column, highest numbers of individuals occurred.

The comparison between the water column and ice showed a high enrichment in the ice. In the water column foraminifers had concentrations of only 0,03 to 0,04 individuals per liter in contrast to the high numbers of specimens in the ice.

3.2.12.3. Conclusion:
The high numbers of foraminifers in older ice can be explained by the advanced ice formation processes. Foraminifers will be incorporated into ice through harvesting and scavenging of ice crystals which are formed in the water column and ascend to the surface. Here ice crystals accumulate forming new ice or are incorporated into the existanting ice cover.

If the foraminifers prefer to live in the ice they may gather near the surface during ice formation so that they may be enclosed into the ice. On the other hand, the high numbers found in nilas ice which forms during calm weather conditions, indicates that the enrichment results from other events. For instance, specimens may actively migrate from the water column into the ice. Yet, this assumption can not explain the high numbers in the ice compared to the water column.

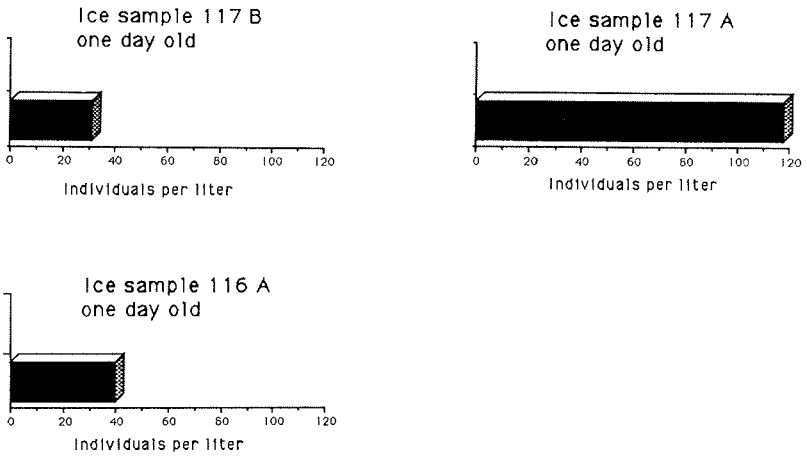

Fig. 54: Numbers of individuals in selected ice samples. a) Grease ice from 26.04. 92: b) "Puzzle ice" from 26.04.92: C) Grease ice from 25.04. 92

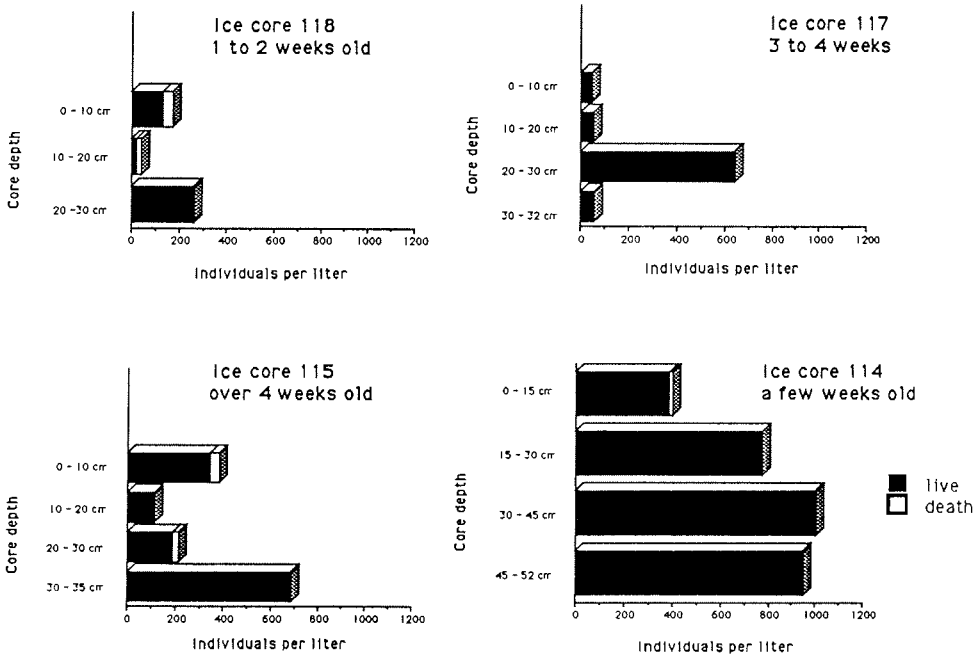

Fig. 55: Numbers of individuals in some ice floes. a) Pancake from 27.04. 92: b) Pancake from 26.04.92: C) Pancake from 24.04. 92: d) Nilas ice from 23.4.92

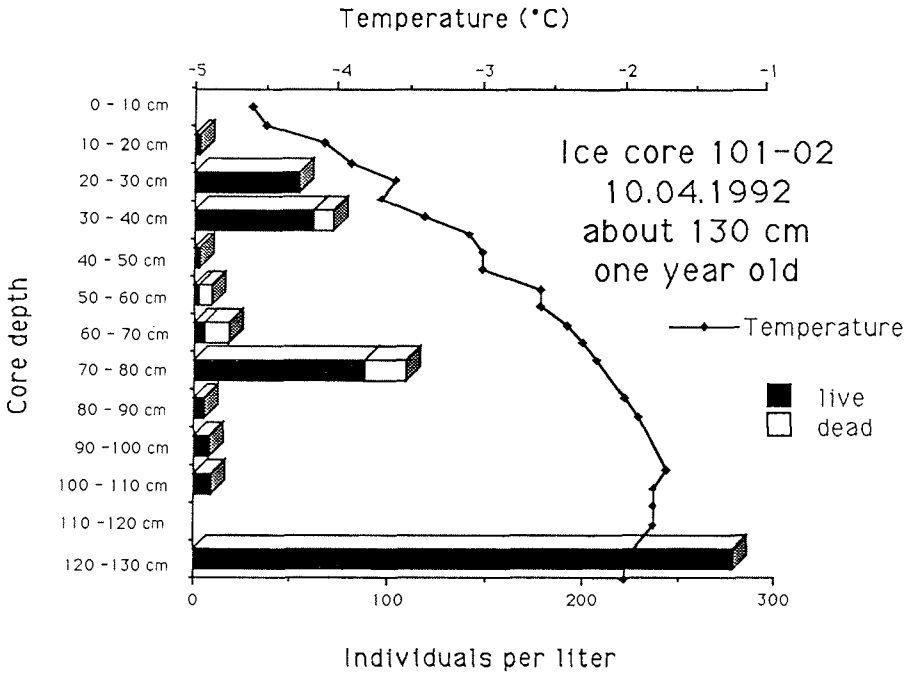

Fig. 56: Number of individuals in a single ice floe.

3.2.13. OBSERVATIONS ON THE CILIATE COMMUNITY OF THE ANTARCTIC SEA ICE AND PLANKTON (CILIOPHORA, PROTOZOA)

N.WILBERT, W. PETZ, W. SONG

Only in the last few years has the biota of the Antarctic sea ice been the aim of intensive study. Ciliates, however, have never been investigated in detail. During this cruise the ciliate community was studied taxonomically and ecologically in various types of sea ice and in the plankton of the eastern Weddell Sea.

3.2.13.1. Material and Methods

Ciliates were investigated qualitatively and quantitatively in melted samples of various types of ice. Planktonic ciliates, which were only studied qualitatively, were collected with an Apstein net from about 0-20 m depth. The living organisms were observed under a precooled microscope.

Protargol silver impregnation and silver nitrate staining (Chatton- Lwoff technique) were used to reveal infraciliary structures. Permanent slide mounts were obtained of all investigated species. Fixation for scanning electron microscopy followed standard protocols.

To clarify special taxonomic questions cultures of some species were established.

Active ciliate abundances were determined using a direct counting method. From each sample eight subsamples á 0.25 ml were examined.

3.2.13.2. Results

TAXONOMY

About 70 ciliate taxa were identified and examined in detail in vivo. About 40 taxa were recorded for the first time from Antarctic sea ice or plankton. Very likely, several of these are new to science. About 35 species occurred exclusively in the sea ice, whereas about 15 oligotrich taxa, i.e. mainly tintinnids and strobilidiids, were only found in plankton samples. In addition, three endocommensal species were examined from dredged sea urchins.

The type specimens of the new species will be deposited in the Collection of Microscope Slides housed in the Oberösterreichische Landesmuseum, Linz, Austria.

ECOLOGY

In newly formed ice, such as grease ice or slush ice, very low abundances of active ciliates occurred. Usually, individual numbers were below 1000 per litre of melted ice. Slightly older pancake ice was more densely populated. For instance, in a 30 cm thick pancake we found about 500 active specimens per litre in the top layer (0- 10 cm core depth), about 5 000 l^{-1} between 10-20 cm and about 8 000 l^{-1} in the lower layer (20-30 cm depth). The upper part (e.g. 0-30 cm) of larger, thicker and therefore, older ice floes was, however, nearly devoid of active ciliates. They were found in higher abundance only in the deeper layers (e.g. 30-50 cm). The maximum number of active ciliates (up to 57 000 individuals l^{-1} melted ice) occurred always within the brown layer. These results clearly indicate that ciliates play an important role in the ice community.

Brine (sea ice pore water) from sack-holes was also investigated. Compared to melted ice cores considerably less active ciliates (about 9 800 individuals l^{-1}) were found.

The species composition of ciliates was distinctly different in the ice and in the plankton (see also above). In the water column tintinnid and strobilidiid species prevailed. In the ice, however, tintinnids were entirely absent and strobilidiids were only rarely found. This habitat is dominated by strombidiid, euplotid and spiroprorodontid species.

3.3. Biology of deeper waters and benthos

3.3.1. DEEP SEA MICROBIOLOGY

E. HELMKE

The microbiological deep sea studies were focused on questions of occurrence, distribution and role of pressure adapted bacteria as well as on the fate of bacteria which are transported from the cold surface water to greater depth. Furthermore barophilic bacteria will be isolated for taxonomical, phylogenetical and physiological studies. The Weddell Sea is an especially suited area for such deep sea studies since the Antarctic bottom water which influences vast parts of the world´s deep sea area is formed here and the constancy of cold temperatures over the entire water column facilitates studies on the connection of cold temperature and high pressure adaptation.

Twelve different sediment and associated water samples were taken in the depth range of 500 to 5000 m by means of the minicorer and were analysed for the concentration of reproductive heterotrophic bacteria with the MPN-method (most probable number) under different pressure and temperature conditions. Subsequent cultivation steps will be carried out in the home laboratory in Bremerhaven and will provide evidence about barotolerance and potential activity status of different bacterial components of deep-sea populations. Water samples from different water depths taken with the rosette sampler were processed correspondingly

Additional experiments with surface water and sea ice samples were directed to the barotolerance and baroresistance of the cold adapted shallow water bacterial communities. Parallel to these cultural approaches sediment and water samples were prepared for total count and biomass determination.

In order to get an idea about the secondary productivity and bacterial turnover in the deep sea environment a selected part of the samples were employed for activity measurements with radioactive labelled substrates under simulated *in situ* conditions.

Further information about the distribution of barophiles is expected by means of biomarkers. The bacterial biomass necessary for such studies was gained by filtering greater volumes of water with *in situ* -pumps which were exposed to different water depths. The filters will be analysed for the specific biomarkers of barophiles in collaboration with the chemical section of the AWI.

Due to relatively slow growth of cold and pressure adapted bacteria the cultural approaches could not be evaluated on board. Subculturing and isolation work, as well as total count and biomass determinations will also be performed in Bremerhaven. However, preliminary results are available from some activity measurements which indicate that pressure adapted bacteria occur regularly in the Weddell Sea in depth beyond 4000m. It became obvious that barophiles are at least functionally dominant in bottom near deep-sea habitats.
Due to a failure of a mooring system the degradation studies and barotolerance experiments related to the bacterial flora enriched on substrates exposed in different water depth could not be accomplished. However, the studies were continued by the deployment of new chitinous material at two new mooring systems.

3.3.2. MACROFAUNA INVESTIGATIONS

D. GERDES

3.3.2.1. Objectives

The leg ANT X/3 had two major objectives of work: The first was to continue the inventory of the Weddell Sea benthos, this time with special emphasis to organisms living in water depths > 1000 m. Secondly the colour PTR camera newly attached to the multibox corer with its recording unit and the control line from board "Polarstern" to the camera and the recording unit had to be tested. Participating in the AGT and BPT catches several benthic species had to be selected for further studies later in the lab.

3.3.2.2. Technical objectives

The multibox corer (MUC) in combination with the UW-video-system was used for the second time in the Weddell Sea. In contrast to the first operation, the videosystem was modified by an additional colour PTR camera, an UW recording unit and additional UW lamps all attached to the MUC. The ships 10 km long koaxial cable acts as a bidirectional connection between board unit and underwater components, enabling the control of different functions of the UW-recorder and the PTR camera as well as the vice versa transport of b/w video signals to the board unit. This system provides high quality coloured videos via the UW-recording unit and online on board the ship b/w control videos from both attached cameras.

3.3.2.3. Work at sea and preliminary results

AGT stations and 2 BPT stations provided material of different shrimp species (mainly *Notocrangon antarcticus* and *Nematocarcinus longirostris*) and a collection of various polychaete species for reproduction and taxonomical studies later in the lab.
MUC and the video system were used on 10 stations in water depths between 250 and 5000 m. Due to technical problems only 4 sediment cores were obtained. From the video system, however, we obtained approx. 2.5 h coloured and 4 h b/w videos. Preliminary

investigations of these show that the deeper parts of the Weddell Sea shelf are inhabited by a poorly developed fauna. This holds especially true for the epifauna, which on the shelf is rich in biomass and diversity. Only seldom single specimens of sea stars, brittle stars or holuthurians are to be seen. The endofauna (probably polychaetes or sipuncolids) seems to be more important here than on the shelf, as indicated by quite regularily occurring holes in the sediment surface and faecal strings in the vicinity.

3.3.3. FISHERIES BIOLOGY AND STRUCTURE AND FUNCTION OF FISH HAEMOGLOBIN

G. DI PRISCO, M. TAMBURRINI, A. KUNZMANN

3.3.3.1. Catches

Fish were caught with the Agassiz Trawl (AGT) and Benthopelagic Trawl (BPT) at seven locations (Fig.57) in the eastern Weddell Sea between 4°W and 13°W. Depths varied between 300 and 850 m on the shelf, only one offshore station (STN 389) had a catch depth of 1000 m at a bottom depth of 1500 m. On station 429 the Agassiztrawl was damaged and only three fish specimens were caught.

In total 605 specimens with a total weight of 30 kg were caught. The onshore BPT haul (STN 479) yielded by far most of the specimens (n=407, Fig. 58). Close to 75% (n=442) of all specimens caught belong to the family Nototheniidae (Fig.59), where mainly three species account for 90% of these (*Trematomus lönnbergi*, n=153; *T. lepidorhinus*, n= 140; *Pleuragramma antarcticum*, n=108). The second most abundant family is Channichthyidae (13%), where the species *Chionodraco myersi* accounts for 42% of the family total. With the exception of the high number of *T. lönnbergi* specimens this is in good agreement with earlier abundances recorded by Ekau (1988).

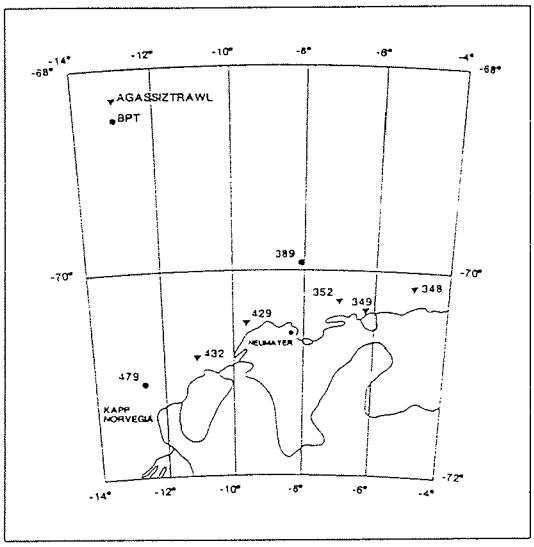

Fig. 57: Positions of fisheries stations during Ant X/3 (March-May 1992) in the eastern Weddell Sea. Given is the three digit station number (STN), which can be referred to in the station list in the annex of this cruise report.

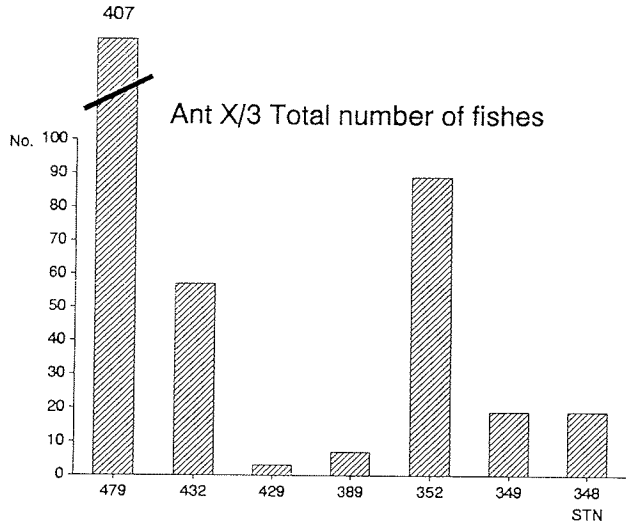

Fig. 58: Total number of fishes caught during Ant X/3 and their distribution at the seven stations. STN = station number, STN 479 yielded a total of 407 fishes.

A comparison on the species level yields a different picture. Nototheniids and artedidraconids each contribute about 25% to the total number of species (n=37), whereas other families contribute about 14 % each (Fig. 60).

3.3.3.2. Tissue and blood sampling

From about 250 specimens samples of liver, heart and muscle were taken and from some selected specimens also samples of spleen, kidneys and gonads. After weighing, these were frozen at -80°C for investigations on tissue metabolism, enzyme cold adaptation and lipid pathways (in cooperation with H.D. Jankowsky & H. Wodtke). The kidneys and gonads were fixed in 4% formalin and will be forwarded to A.L. DeVries for studies on the kidney glomerulization and to K.-H. Kock for studies on reproduction.

From all 605 specimens total length (TL), standard length (SL) and fresh weight (FW) were measured. From some also sex and maturity stage were determined and otoliths will be taken for ageing and growth studies. All these data will enter a database established at the Institute for Polar Ecology, Kiel for studies on the fish community of the Weddell Sea. Specimens of all species were frozen at -30°C for two theses about a community comparison between the Weddell and Lazarev Sea (C. Zimmermann) and studies on antifreeze glycoproteins (A. Wöhrmann).

About 100 blood samples were drawn with heparinized syringes from the caudal vein of 18 different species. These include fourteen species which were investigated for the first time (Table 9, one notothenid, six artedidraconids, one bathydraconid, three zoarcids and three mesopelagic myctophids). Also included are four species, where work on frozen blood samples has been done before. The fresh material from this cruise allowed us to complete also studies on intact red blood cells and purified haemoglobins and to investigate the effect of temperature on the oxygen binding of three notothenids and one bathydraconid (Table 9, lower part).

3.3.3.3. Haematology

Haematological measurements were carried out immediately and comprised haematocrit (Hct), number of red blood cells (RBC) and haemoglobin concentration [Hb]. After centrifugation and separation of cells and plasma, cells were washed with 1.7% saline, centrifuged again and a fraction was stored for functional studies on the intact red blood

cells. The rest of the sample was haemolyzed with 1 mM Tris at pH 8.0 for studies on the haemolysate or for the purification of haemoglobins.

Haematological results of the new species confirmed the hypothesis that the number of red blood cells, the haemoglobin concentration and the number of haemoglobin components (see below) decreases as evolution proceeds. When average values on family level are compared we find a decrease in the order Nototheniidae > Artedidraconidae > Bathydraconidae > Channichthyidae. This is the same order as in a phylogenetic tree based on morphological investigations (Fig. 61).

Two exceptions from the common pattern (see below) are the number of haemoglobin components in *Pleuragramma antarcticum* and *Dolloidraco longedorsalis* (Table 9). *P. antarcticum* is also exceptional as far as the mode of life is concerned. This species has a circumantarctic distribution, is the most abundant and only holopelagic species, undertakes spawning migrations and has low energy requirements. It may well be that this species has conserved three different haemoglobins due to varying environmental conditions during its complex life cycle.

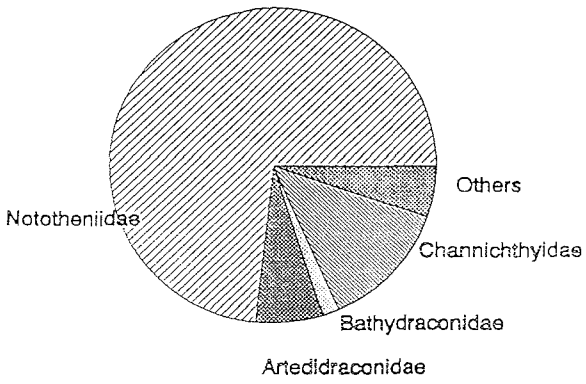

Fig. 59: Abundance of fish families (by specimen number). 'Others' refers to myctophids and zoarcids.

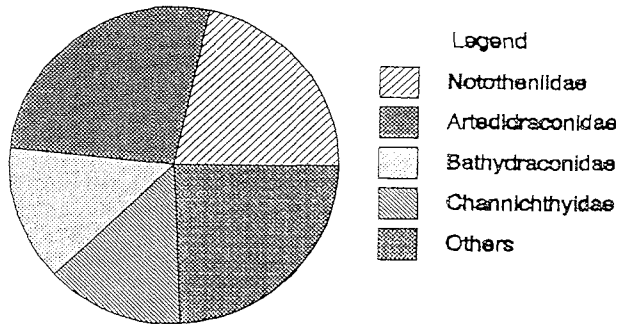

Fig. 60: Abundance of fish families (by number of species). 'Others' refers to myctophids and zoarcids.

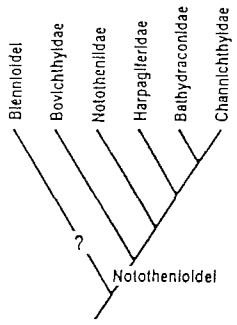

Fig. 61: Phylogenetic tree of endemic Antarctic fish families according to morphological investigations by Iwami (1985).

3.3.3.4. Haemoglobin purification and characterisation

After centrifugation to remove the stromas, electrophoretic analysis on cellulose acetate was carried out on each haemolysate. Table 9 reports the number of haemoglobin components for each species. In general, the electrophoretic patterns were in line with the previous findings, i.e. either a single or a major component (Hb 1, accounting for at least 90% of the total). A single haemoglobin was found in Artedidraconidae. In Bathydraconidae Hb 2 was found in *Racovitzia glacialis*, similar to another bathydraconid, *Cygnodraco mawsoni*. Nototheniidae, except *Aethotaxis mitopteryx*, were found to have Hb 1 and Hb 2; the haemolysate of *Pleuragramma antarcticum* gave two major bands.

Juveniles of several yet unidentified species confirmed that a higher multiplicity is present in the first life stage, also including a much higher level of Hb 2. The surprisingly high number of components of the bathydraconid *D. longedorsalis* may well reflect this observation.

When more than one haemoglobin was present, purification was achieved by ion-exchange chromatography on a column of DE 52 (1 x 20 cm). Elution was carried out at different concentrations of Tris-HCl buffer pH 7.6; the absorbance at 540 nm was monitored, and Figure 62 shows two representative elution patterns. After dialysis of the pooled fractions, the peaks were adsorbed on a small DE 52 column and concentrated by elution with 100 mM Tris- HCl pH 7.1.

The functional characterisation involved the study of the oxygen-binding properties. These were performed on the intact erythrocytes, on the haemolysates (previously "stripped" by running through a column of a mixed-bed resin, in order to remove endogenous organic phosphates, which have a regulatory effect on the oxygen binding), and on some or all of the purified haemoglobins. This study included the investigation of: a) the oxygen saturation capacity at 2°C as a function of pH, in the presence and absence of ATP (Root effect); b) the regulation of the oxygen affinity by pH and ATP in equilibrium experiments (Bohr effect); c) the effect of temperature in the range 2-10°C on the affinity. The results are summarised in Table 9.

Figures 63 and 64 show representative plots of Bohr and Root effects.

Bohr and Root effects were found in all haemoglobins of the myctophid and nototheniid species (except *A. mitopteryx*, displaying very weak effects). In artedidraconids, pH had little or no regulatory effect, except in the presence of ATP; addition of this effector to erythrocytes proved that ATP was never in the cells at saturating concentrations. In comparison with the other notothenioids, the oxygen affinity of the bathydraconid *Racovitzia glacialis* was found to be exceptionally high,.

Ion-exchange chromatography showed that the less anodal electrophoretic band of *P. antarcticum* comprised two haemoglobin components. Thus this species has at least three components, all with pH-regulated oxygen binding, as shown by the presence of the Bohr and Root effects. ATP modulates the Bohr effect of Hb 1 and Hb 2, while it has only a limited regulatory effect on the position of the Bohr curve of Hb 3.

The study of the temperature effect on oxygen binding revealed that the haemoglobins under investigation follow a general trend which is shown by most haemoglobins. In fact, higher exothermic values of heat of oxygenation were obtained at pH 8.0, whereas at pH 7.0 lower values were recorded, due to the endothermic contribution of the ionization of oxygen-linked acid groups. ATP has been shown to regulate this effect.

The three haemoglobins of *P. antarcticum* showed a fine regulation of oxygen affinity by temperature. In fact, different values of heat of oxygenation were obtained for each component in the pH range 7.0-8.0, both in the absence and presence of ATP.

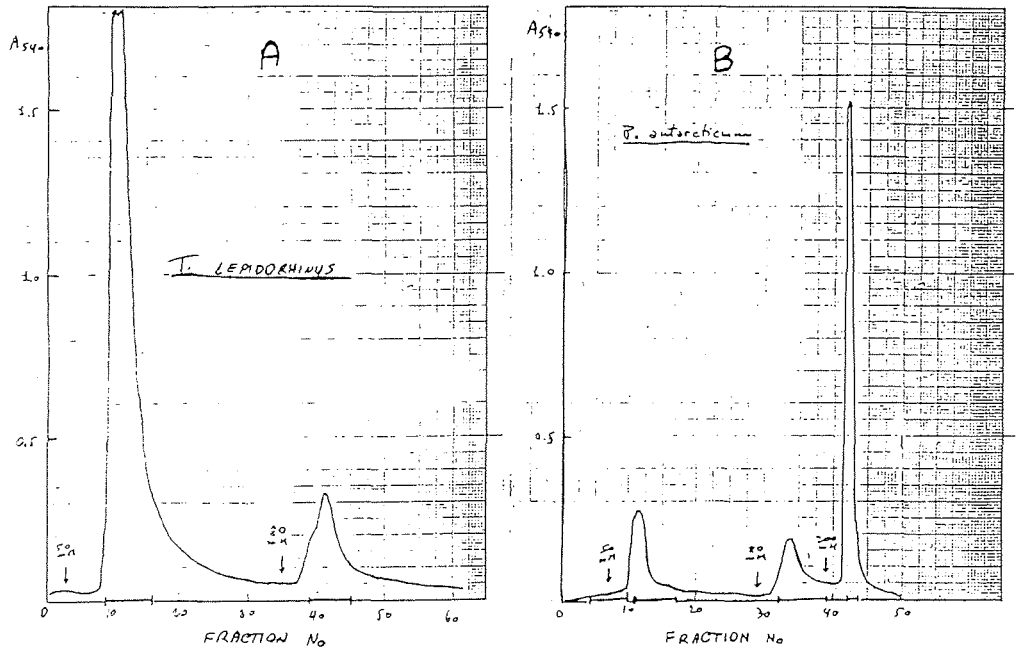

Fig. 62: Ion-exchange chromatography of the hemolysate of *T. lepidorhinus* (panel A) and of *P. antarcticum* (panel B). Experimental conditions: see text.

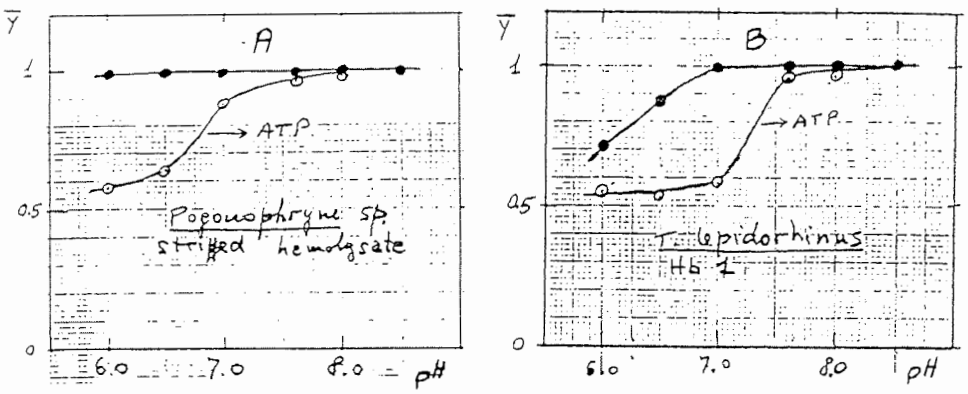

Fig. 63: Oxygen-saturation curves of the stripped hemolysate of *Pogonophryne sp* (panel A), and of the purified Hb 1 of *T. lepidorhinus* (panel B), in the absence (closed circles) and presence (open circles) of 3 mM ATP.

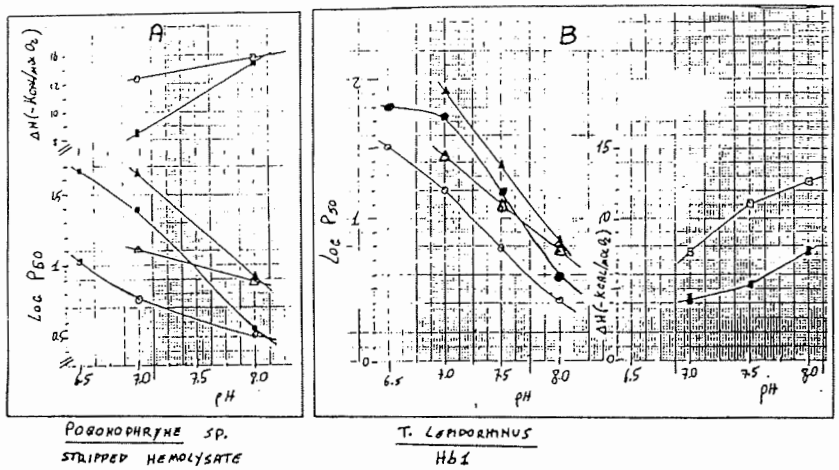

Fig. 64: Oxygen-binding curves and heats of oxygenation of the stripped hemolysate of *Pogonophryne sp* (panel A) and of the purified Hb 1 of *T. lepidorhinus* (panel B). The experiments were performed at 2°C (circles) and at 10°C (triangles), in the absence (open symbols) and presence (closed symbols) of 3 mM ATP and 0.1 M NaCl.

All purified haemoglobins and, in some cases, the haemolysates, have been converted to the stable CN-met derivatives, which will be retrograded at 0°C. These will be used at IBPE in Naples for sequence studies, as well as for additional functional studies and separation attempts.

The results obtained during Ant X/3 extend and, in certain instances, complete the knowledge on the structure and function of Antarctic fish haemoglobin that our groups have gathered in the past years. One of the aims of these investigations is to seek a relationship between the physiological and biochemical adaptation of the oxygen transport system and the lifestyle of fish species, related to their ecology and distribution.

Table 9 Summary of some of the results on haemoglobins of 18 species investigated during Ant X/3. Hb (CAE) = haemoglobin components investigated by Cellulose Acetate Electrophoresis. The question mark denotes species whose identification will be confirmed by taxonomists. n.d. = not determined: it is referred to species with insufficient starting material.

Species	Hb (CAE)	Root	Bohr
Pleuragramma antarcticum		Hb1 + Hb2 + Hb3 +	Hb1 + Hb2 + Hb3 +
Artedidraco orianae		(-)	+
Artedidraco shackletoni			
Dolloidraco longedorsalis		(-)	
Pogonophryne mentella ?		(-)	+
Pogonophryne marmorata ?		(-)	+
Pogonophryne barsukovi ?		(-)	+
Akarotaxis nudiceps		+	
Zoarcid 1		+	
Lycenchelys nigripalatum		+	
Zoarcid 3		+	
Gymnoscopelus spec.		+	+
Bathylagus spec.		+	
Electrona spec.		+	+
Aethotaxis mitopteryx		(-)	(+)
Trematomus lepidorhinus		Hb1 +	Hb1 +
Trematomus eulepidotus		Hb1 +	Hb1 +
Racovitzia glacialis		+	+

3.4. Sediment trap moorings and natural radioisotopes in the water column.

W.SCHMIDT, E. VAN HANNEN, R. PHILLIPS, R. PLUGGE, D. GERDES

The sediment traps are located at four positions, Bouvet Island (BO 1: 56° 20,3'S- 03° 22,6'W), the Polar Front PF4: 50° 07,6'S- 05° 52, 0'E). Wedelmeer (KN4: 70° 59,51'S - 11°46,85'E) and AWI400 (57°18'S - 04°07'E). Objectives are to monitor seasonal particle flux from the photic zone to deeper waters during several years. We hope to quantify intra-annual fluctuations of primary productivity and export of particulate matter from the photic layer. This will include determining their setting velocity. The results from these investigations will be compared to other sediment traps presently deployed in the South Atlantic by Sonderforschungsbereich 261.

At the Polar Front and in the Northeastern Weddell Sea the concentration of the cosmogenic isotope Be-10 as well as the Be10/Be-9 ratio will be measured. The objective is to investigate the relationship between Be-10 content and bioproductivity. Results of measurements of the Be-10 fluxto sediments off West Africa indicated that in areas of high bioproductivity the Be-10 flux, as well as the Th-230 flux to the sediments is much higher than the production rate of the isotopes. This is due to scavenging of the isotopes by settling particles. This causes a concentration gradient of the isotopes from the high productivity area to the open ocean. It is thought that if the correlation between productivity, Be-10 content in the water column, and Be-10 flux to the sediments can be determined, than the Be-10 flux can be used as an index for paleoproductivity.
The Be-10 samples will prepared on board the ship, and the Be-10 content will be measured using the Accelerator Mass Spectrometer at the ETH Zürich.

3.5. Weather and meteorological Observations

F.-U. DENTLER, H. SONNABEND

3.5.1. GENERAL REMARKS

The interaction between the cold air flowing out of Antarctica and the relatively warm and moist air masses of the lower latitude ocean areas causes the development of a series of mid-latitude cyclones which are responsible for the low-pressure belt surrounding the Antarctic continent. This pressure pattern is not only seen on mean pressure maps of this region but also in the daily weather charts, showing quasi-stationary pressure patterns.

"Polarstern" performs an important contribution to the world-wide meterological observation network because most of the year it operates in inaccessible regions with only a few observation stations. Since the latest generation of numerical models for weather prediction are global models, observations from all over the world are required especially from data-sparse areas. During ANT X/3 3-hourly routine surface weather-observations were conducted. In addition, twice a day (0600 UTC and 1200 UTC) radiosondes were launched. Both datasets were transmitted via DCP and satellite respectively by radio operator into the GTS (Global Telecommunication System).

3.5.2. PHASE 1: CAPETOWN - NEUMAYER

During the first part of ANT X/3 we travelled through three climatic zones: subtropical high-pressure belt, temperate belt and then reached the Antarctic climatic zone.

Leaving Capetown, air pressure rose up to 1018 hPa as we passed through the subtropical high southwest of Cape of Good Hope. Afterwards pressure fell in several steps to a value of 961 hPa in a gale center near Bouvet Island (Fig. 65). Between 45 and 55 South we crossed the Polarfront with its wavelike disturbances. The front was not well expressed at this time in the area we travelled through. The atmospheric center of activity in the South Atlantic was the above mentioned gale center at Bouvet Island. Five degrees further to the South windspeeds decreased and turned to southeasterly directions.

Air temperature (at mean sea level) showed a more or less steady decrease from Lat 35° to the 55°S, and from here remained nearly constant at freezing level to 67°S. Further it steeply dropped down to less than -23°C after we passed through the ice-edge.

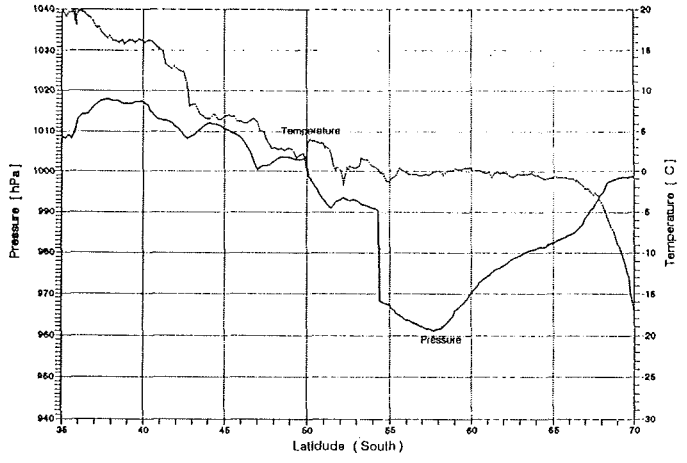

Fig. 65: Air Pressure and air temperature cross section between Lat 35°S and 70°S.

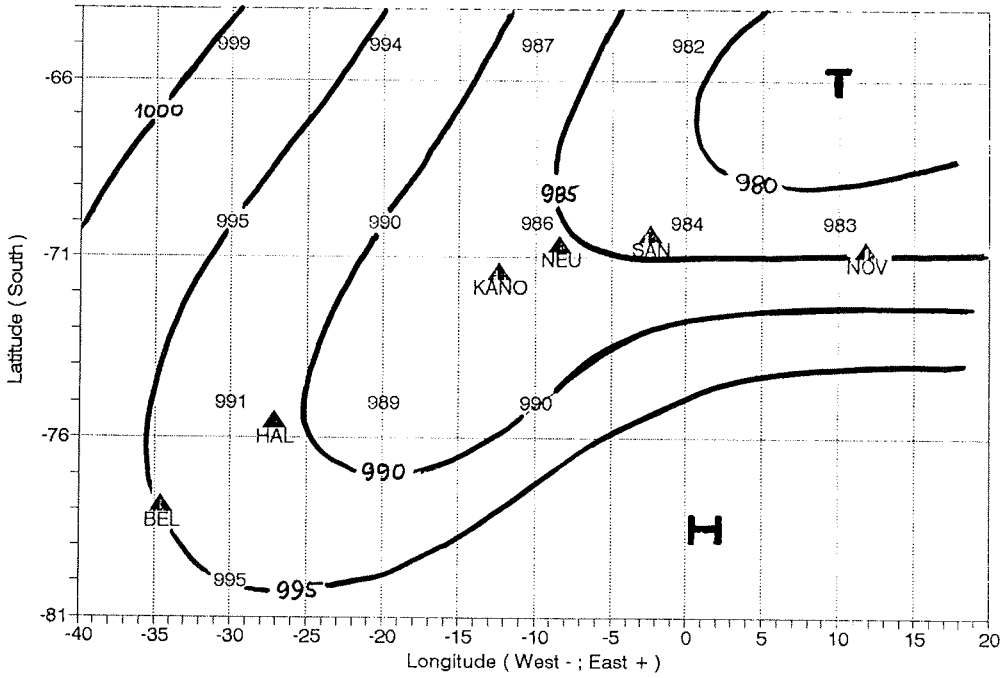

Fig. 66: Atmospheric pressure (MSL) measured between 6.4.92 and 26.4.92

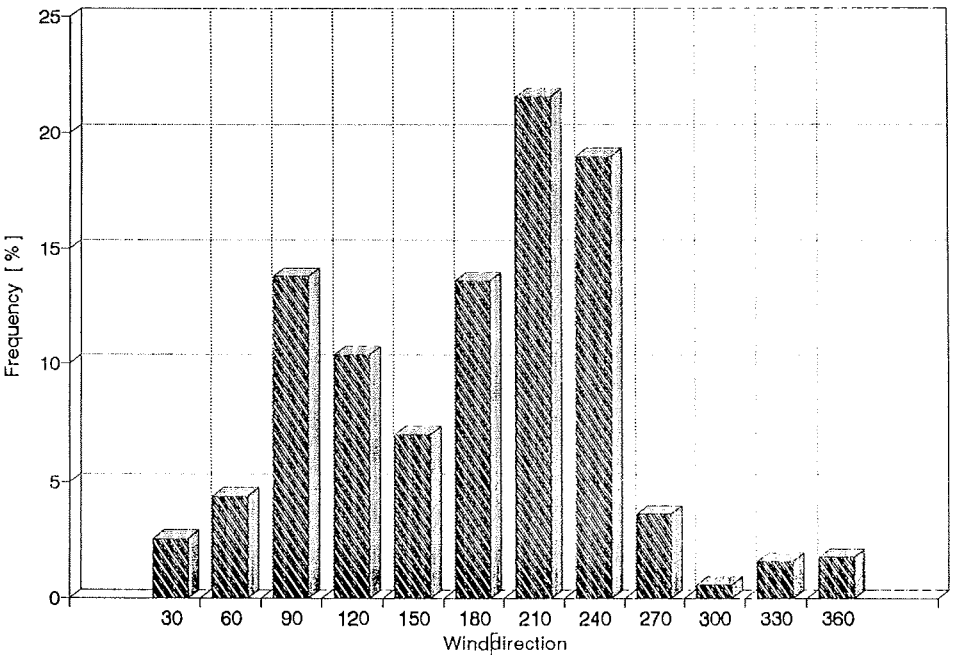

Fig. 67: Histogram of wind direction (sectors) during the period 6.4.92 to 26.4.92.

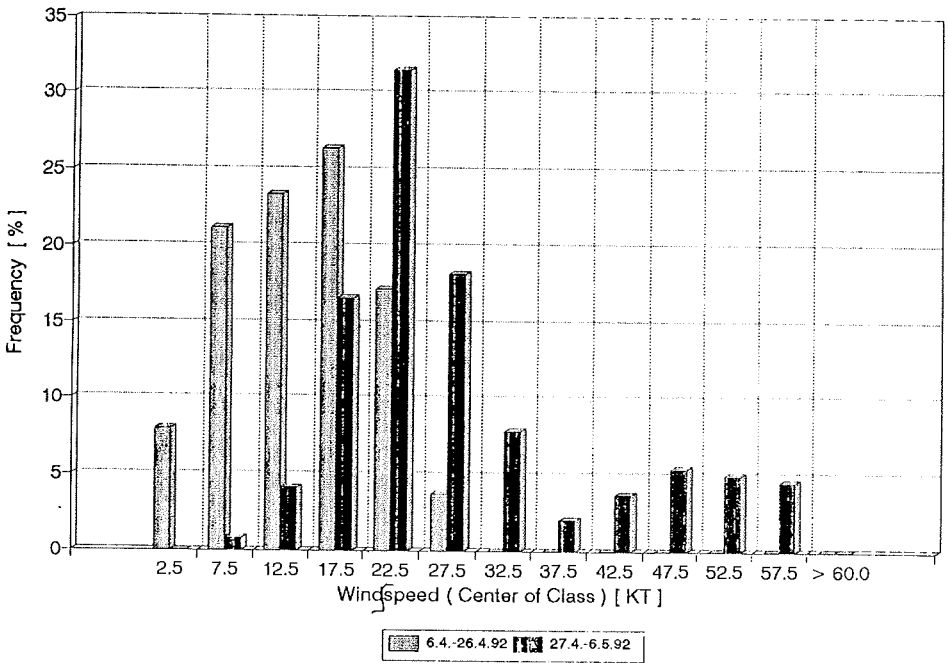

Fig. 68: Histogram of wind spead during the period 6.4.92 to 6.5.92

3.5.3. PHASE 2: WEDDELL SEA

During the first three weeks in the Weddell Sea, from 6.April until 26. April the mean air pressure recorded on "Polarstern" was 985 hPa. During this period a low pressure trough was situated along the east coast of the Weddell Sea (Fig. 66). The upper air soundings from "Polarstern" during this time showed the predominance of southerly or southwesterly winds at all heights, caused by a quasi-stationary trough in the middle and upper troposphere over the eastern parts of the Weddell Sea. The intense advection of cold air from the ice-covered Weddell Sea formed cyclonic storms in the area between South Georgia and Bouvet Island. Several of these depressions deepened to less than 960 hPa.

Due to the cold and dry air coming down from the continent, crossing the ice area in this phase, cloudcover over the ice was relatively small. During day-time, when 3-hourly eye-observations were carried out, mean cloud cover was less than 5 octas (4.8 octas). In nearly 35 % of the observations cloud cover was 3/8 or less, including observations near the ice edge, where the cloudiness increased noticably and frequent snow showers occured. The lowest temperature recorded in this time was -24°C on 24.April

The frequency distribution of the wind direction shows prevailing soutwesterly winds during that period (Fig. 67). The most frequent class of windspeed was that between 15 and 20 KT (Fig. 68).

After 26. April the flow-pattern changed. The upper trough over the eastern Weddell Sea moved towards the East and a new one proceeded from the West to the Antarctic Peninsula. Due to the influence of lee-cyclogenesis a low formed at the east side of

Graham Land, started deepening there and then moved towards the East, intensifying its circulation rapidly.

On 30. April severe easterly gales occurred for a period of 36 hours along the Antarctic Coast west of Novolazarevskaya. The highest windspeed (10-minute-mean) recorded during this period was 61 KT.

During this event a new trough was formed along the east coast of the Weddell-Sea. In contrast to the situation before its trough line was situated more off shore (Fig. 69). Accordingly the histogramm of the wind direction looked rather different. Easterly to northeasterly winds predominated (Fig. 70). Compared with the first period the distribution of windspeed-classes is shifted to higher velocities, with a tail above 40 KT, caused by the above mentioned storm event. In this period the most frequent class of wind velocity is that between 20 and 25 KT (Fig. 67). Cloudiness was significantly higher in that period due to the moisture-advection from the East, mean cloud cover was more than 6 octas (6.1 octas).

3.5.4. PHASE 3: NEUMAYER - CAPETOWN

On the way back to Capetown we passed through a large lowcenter at 62° S (Fig. 71), forming the atmosperic center of activity in the Southern Atlantic. Due to the cold air advection on the back of the low, temperature between the ice edge and the 55. parallel was about 3 K lower than on our course to Antarctica (see also Fig.65).

Between 50° and 55°S a new intense gale center formed becomming stationary later on. It maintained the center of activity near 62° S. After that pressure rose to 1008 hPa in a high pressure ridge between two low centers. North of 45° S the polar front was passed through. The thermal front was assossiated with a low pressure zone indicated by the strong pressure fall north of 43° in this cross section. At the discontinuity between moderate polar air and very moist and warm subtropical air masses a stormcenter develloped associated with windspeeds of more than 45 KT during 18 hours on 16. May.

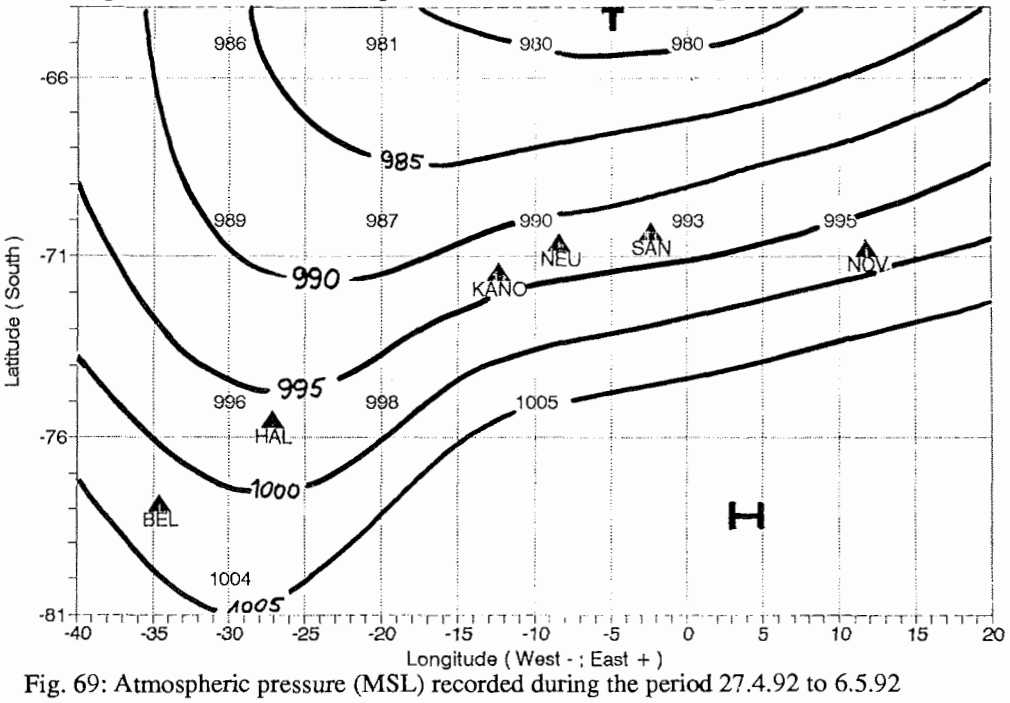

Fig. 69: Atmospheric pressure (MSL) recorded during the period 27.4.92 to 6.5.92

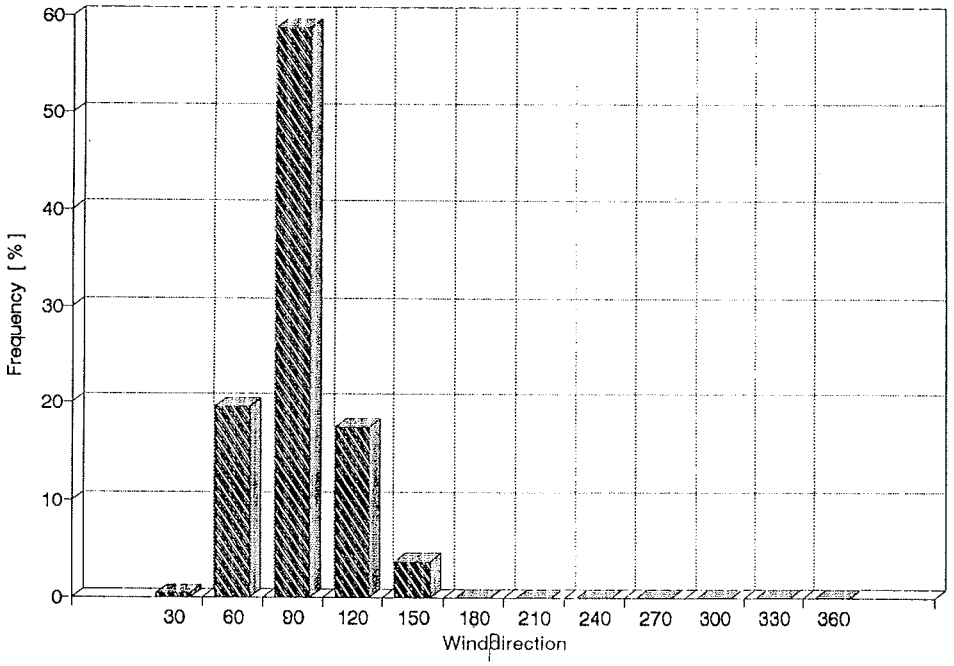

Fig. 70: Histogram of wind direction (sectors) recorded between 27.4. 92 to 6.5.92.

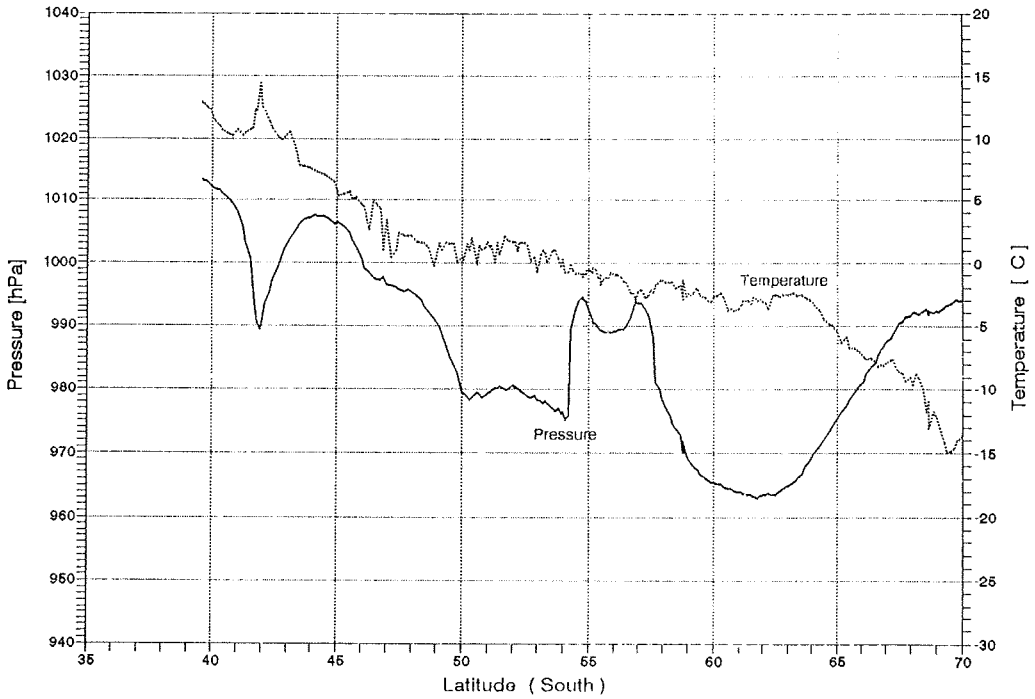

Fig. 71: Air pressure and air temperature. Cross section between Lat 70°S and 35°S.

ANHANG/ APPENDIX

a. Ant X/3 Stations

Gear description:

AGT	Agassiz trawl
APSN	Apstein-net
BS	Bathysonde
BRO	Bio-Rosette
BO	Bongo net
CTD	CTD-Sonde
FN	Franz net
LM	Light meter
MIC	Microcorer
MK	Micro net
MPN	Microplankton net
MUC	Multicorer
MN	Multi net
MS	Multisonde
RMT	Rectangular Mid water trawl
RO	Rosette
SD	Secchi Disc
SF	Sediment trap
XBT	Expendable Bathy thermograph
WS	Niskin sampler
Zodiac	Rubber boat

Stat. No	Date (1992)	Julian day	Time	Latitude	Longitude	Depth (m)	Gear/ Station type
21/228	27.3	87	18.23	34°35,3'S	17°48,3'E	997	Pressure-Recorder
21/229	27.3	87	18.25	34°35,3'S	17°48,2'E	997	XBT
21/230	27.3	87	20.00	34°50,0'S	17°38,2'E	2187	XBT
21/231	27.3	87	22.00	35°09,7'S	17°26,1'E	3210	XBT
21/232	28.3	88	00.14	35°29,9'S	17°10,6'E	3489	XBT
21/233	28.3	88	02.01	35°41,9'S	16°59,3'E	2947	XBT
21/234	28.3	88	02.26	35°43,4'S	16°57,2'E	2839	XBT
21/235	28.3	88	04.15	35°50,1'S	16°52,6'E	7731	XBT
21/236	28.3	88	06.00	35°55,2'S	16°47,2'E	3550	XBT
21/237	28.3	88	09.00	36°06,0'S	16°41,9'E	4339	XBT
21/238	28.3	88	13.13	36°23,8'S	16°32,8'E	4446	XBT
21/239	28.3	88	17.10	36°59,0'S	16°08,9'E	4623	XBT
21/240	28.3	88	19.07	37°18,2'S	15°54,9'E	4686	XBT
21/241	28.3	88	21.07	37°38,6'S	15°40,9'E	4782	XBT
21/242	28.3	88	23.16	38°00,7'S	15°25,1'E	4831	XBT
21/243	29.3	89	01.01	38°19,6'S	15°13,5'E	4779	XBT
21/244	29.3	89	03.10	38°42,4'S	14°53,5'E	4802	XBT
21/245	29.3	89	04.58	39°03,9'S	14°34,9'E	4711	XBT
21/246	29.3	89	07.05	39°29,8'S	14°15,7'E	4806	XBT
21/247	29.3	89	11.09	40°18,2'S	13°46,0'E	4797	XBT
21/248	29.3	89	13.00	40°38,3'S	13°29,8'E	4898	XBT
21/249	29.3	89	15.00	41°00,7'S	13°12,6'E	4544	XBT
21/250	29.3	89	17.00	41°24,7'S	12°55,9'E	2705	XBT
21/251	29.3	89	19.00	41°46,4'S	12°39,5'E	3095	XBT
21/252	29.3	89	21.00	42°08,0'S	12°22,7'E	4533	XBT
21/253	29.3	89	23.00	42°30,1'S	12°05,5'E	4767	XBT
21/254	30.3	90	01.03	42°51,6'S	11°49,5'E	4580	XBT
21/255	30.3	90	02.54	43°09,6'S	11°35,7'E	4475	XBT
21/256	30.3	90	05.00	43°31,8'S	11°19,4'E	4930	XBT
21/256	30.3	90	07.00	43°52,7'S	11°02,2'E	4198	XBT
21/257	30.3	90	09.30	44°22,1'S	10°38,8'E	4677	XBT
21/258	30.3	90	11.11	44°42,5'S	10°23,2'E	4673	XBT
21/259	30.3	90	12.59	45°03,1'S	10°06,5'E	4752	XBT
21/260	30.3	90	15.00	45°27,1'S	09°47,8'E	4558	XBT
21/261	30.3	90	17.00	45°50,6'S	09°28,6'E	4577	XBT
21/262	30.3	90	19.02	46°15,0'S	09°08,8'E	4676	XBT

21/263	30.3	90	21.05	46°40,0'S	08°48,0'E	3841	XBT
21/264	30.3	90	22.10	47°04,5'S	08°28,2'E	3362	XBT
21/265	31.3	91	03.00	47°47,1'S	07°54,0'E	3085	XBT
21/266	31.3	91	05.00	48°08,6'S	07°34,5'E	3657	XBT
21/267	31.3	91	07.00	48°30,6'S	07°16,1'E	2874	XBT
21/268	31.3	91	08.55	48°52,9'S	06°57,2'E	3901	XBT
21/269	31.3	91	10.52	49°14,5'S	06°38,0'E	5415	XBT
21/270	31.3	91	13.00	49°38,1'S	06°17,4'E	3526	XBT
21/271	31.3	91	15.00	50°00,2'S	05°58,4'E	3734	XBT
21/272	31.3	91	15.56	50°07,6'S	05°52,1'E	3790	Hydrophone
"	"	91	16.03			3791	Hydrophone released
"	"	91	16.08			"	2
"	"	91	16.28	50°07,5'S	05°52,1'E	3799	Hydrophone released
"	"	91	16.41	50°07,5'S	05°52,4'E	3790	Engine stop
"	"	91	17.33	50°07,3'S	05°51,5'E	3783	Hydrophone
"	"	91	17.45			"	Signal registered
"		91		50°07,6'S	05°52,2'E	3790	Signal registered
"		91		50°07,7'S	05°52,3'E	3796	Hydrophone
"	1.4	92	06.30	50°07,6'S	05°52,3'E	3796	"
"	"	92	08.10	50°08,7'S	05°53,2'E	3802	Search given up
21/273	"	92	08.42	50°17,6'S	05°36,2'E	3740	XBT
21/274	"	92	09.30	50°28,8'S	05°10,7'E	2800	XBT
21/275	1.4	92	11.00	50°40,5'S	04°45,1'E	3413	XBT
21/276	1.4	92	13.00	50°52,9'S	04°18,1'E	3608	XBT
21/277	1.4	92	15.00	51°04,9'S	03°51,4'E	2949	XBT
21/278	1.4	92	17.00	51°16,8'S	03°25,0'E	3378	XBT
21/279	1.4	92	19.00	51°29,2'S	02°57,8'E	3490	XBT
21/280	1.4	92	21.00	51°42,3'S	02°28,5'E	3230	XBT
21/281	1.4	92	23.00	51°55,3'S	02°01,8'E	2916	XBT
21/282	2.4	93	01.05	52°03,3'S	01°33,4'E	2792	XBT
21/283	2.4	99	03.02	52°20,3'S	01°07,5'E	2747	XBT
21/284	2.4	93	04.03	52°32,0'S	00°42,0'E	2861	XBT
21/285	2.4	93	07.05	52°48,4'S	00°47,9'E	2660	XBT
21/286	2.4	93	09.00	53°10,4'S	01°18,4'E	2592	XBT
21/287	2.4	93	11.00	53°32,0'S	01°52,1'E	2750	XBT
21/288	2.4	93	13.00	53°56,3'S	02°25,0'E	4509	XBT
21/289	2.4	93	15.00	54°07,9'S	02°43,3'E	1621	XBT
21/290	2.4	93	17.05	54°16,8'S	02°56,2'E	1580	XBT
21/291	2.4	93	18.10	54°20,3'S	03°01,1'E	950	XBT
"	2.4	93	19.00	54°20,7'S	03°01,4'E	997	1. Pressure recorder
"	2.4	93	19.24	54°20,7'S	03°01,4'E	994	2. Pressure recorder
21/292	"	93	19.51	54°20,7'S	02°40,4'E	2304	XBT
21/293	"	93	19.54	54°19,5'S	01°54,7'E	5219	XBT
21/294	2.4	93	20.55	54°19,8'S	01°05,7'E	2280	XBT
21/295	2.4	93	22.55	54°21,3'S	01°18,9'W	2250	XBT
21/296	3.4	94	01.02	54°47,2'S	01°21,9'W	1984	XBT
21/297	3.4	94	08.37	55°09,6'S	01°27,7'W		XBT
21/298	3.4	94	10.56	55°26,8'S	01°30,8'W	3559	XBT
21/299	3.4	94	13.00	55°51,8'S	01°35,1'W	3471	XBT
21/300	3.4	94	15.00	56°13,6'S	01°39,1'W	4013	XBT
21/301	3.4	94	17.05	56°34,7'S	01°42,8'W	3440	XBT
21/302	3.4	94	19.06	56°58,5'S	01°48,2'W	3757	XBT
21/303	3.4	94	21.00	57°22,5'S	01°53,7'W	3718	XBT
21/304	3.4	94	23.00	57°44,0'S	01°57,6'W	2400	XBT
21/305	4.4	95	01.00	58°06,8'S	02°01,6'W	4720	XBT
21/306	4.4	95	03.04	58°30,7'S	02°06,2'W	4558	XBT
21/307	4.4	95	05.00	58°54,7'S	02°11,8'W	4987	XBT
21/308	4.4	95	07.04	59°15,4'S	02°15,2'W	5388	XBT
21/309	4.4	95	09.10	59°37,8'S	02°19,8'W	5541	XBT
21/310	4.4	95	11.00	59°56,7'S	02°23,3'W	5365	XBT
21/311	4.4	95	13.00	60°14,2'S	02°27,1'W	4594	XBT
21/312	4.4	95	14.56	60°32,5'S	02°30,8'W	5370	XBT
21/313	4.4	95	17.04	60°54,8'S	02°35,9'W	5249	XBT
21/314	4.4	95	19.00	61°16,4'S	02°39,7'W	4765	XBT
21/315	4.4	95	21.00	61°39,0'S	02°45,1'W	5334	XBT
21/316	4.4	95	22.58	62°02,3'S	02°50,3'W	5330	XBT
21/317	5.4	96	01.00	62°26,3'S	02°55,4'W	5318	XBT
21/318	5.4	96	05.05	62°48,8'S	02°59,0'W	5284	XBT
21/319	5.4	96	05.05	63°12,6'S	03°05,0'W	5246	XBT
21/320	5.4	96	07.00	63°55,9'S	03°16,3'W	5203	XBT

21/321	5.4	96	09.10	64°19,1'S	03°21,4'W	5178	XBT
21/322	5.4	96	13.00	64°44,8'S	03°27,6'W	5093	XBT
21/323	5.4	96	15.00	64°07,9'S	03o33,5'W	5077	XBT
21/324	5.4	96	17.00	65°29,7'S	03°38,1'W	4949	XBT
21/325	5.4	96	19.00	65°47,3'S	03°43,0'W	4892	XBT
21/326	5.4	96	20.57	66°06,5'S	03°48,5'W	4773	XBT
21/327	5.4	96	22.55	66°26,2'S	03°53,1'W	4683	XBT
21/328	6.4	97	01.00	66°44,1'S	03°58,7'W	4686	XBT
21/329	6.4	97	03.25	66°02,4'S	04°03,2'W	4713	XBT
21/330	6.4	97	05.00	67°20,3'S	04°08,3'W	4682	XBT
21/331	6.4	97	07.00	67°37,9'S	04°12,0'W	4570	XBT
21/332	6.4	97	09.00	67°56,3'S	04°16,8'W	4314	XBT
21/333	6.4	97	11.00	68°05,0'S	04°20,5'W	4136	XBT
21/334	6.4	97	13.00	68°10,6'S	04°22,4'W	4063	Arrival on station
"	6.4	97	14.00	68°10,8'S	04°22,8'W	4059	CTD. MIC down
"	6.4	97	14.43	68°11,1'S	04°23,7'W	4050	CTD continued
"	"	97	15.24	68°11,2'S	04°24,6'W	4054	MIC on deck
"	"	97	16.28	68°11,2'S	04°24,7'W	4056	CTD on deck
21/335	"	97	17.34	68°15,0'S	04°24,9'W	3945	XBT
21/336	"	97	17.40	68°24,8'S	04°26,8'W	3602	XBT
21/337	6.4	97	18.07	68°36,5'S	04°30,0'W	3807	XBT
21/338	6.4	97	19.00	68°48,4'S	04°30,8'W	2998	XBT
21/339	6.4	97	20.00	69°00,3'S	04°35,1'W	2725	XBT
21/340	6.4	97	21.00	69°12,3'S	04°39,7'W	2314	XBT
21/341	6.4	97	22.00	69°24,3'S	04°42,6'W	2852	XBT
21/342	6.4	97	23.00	69°33,8'S	04°45,1'W	2562	XBT
21/343	6.4	97	24.00	69°42,9'S	04°48,1'W	2228	XBT
21/344	7.4	98	01.00	69°53,5'S	04°51,1'W	2404	XBT
21/345	7.4	98	02.00	70°00,5'S	04°54,9'W	1873	XBT
21/346	7.4	98	03.15	70°07,5'S	04°56,8'W	875	XBT
21/347	7.4	98	04.05	70°12,5'S	04°57,6'W	318	XBT
21/348	7.4	98	05.05	70°10,4'S	04°57,9'W	368	AGT down
"	7.4	98	06.07	70°09,6'S	04°58,4'w	372	AGT on ground
"	7.4	98	08.14	70°09,2'S	04°58,6'W	380	AGT heave
"	"	98	08.33	70°08,9'S	04°58,9'W	413	AGT on deck
"	"	98	08.53	70°08,5'S	04°58,9'W	476	CTD
"	"	98	09.24	70°08,5'S	04°58,9'W	476	SD down
"	"	98	10.09	70°08,5'S	04°58,9'W	476	SD on deck
"	"	98	10.11	70°08,5'S	04°59,2'W	479	APSN down. 10.27 on deck
"	"	98	10.16	70°08,6'S	04°59,9'W	497	BRO down
"	"	98	10.24	70°08,5'S	05°00,4'W	511	BRO on deck
21/349	"	98	11.11	70°32,1'S	06°19,2'W	246	AGT down
"	"	98	11.55	70°23,5'S	06°18,0'W	232	AGT 700m
"	7.4	98	15.33	70°23,3'S	06°16,9'W	237	AGT heave
"	"	98	15.56	70°23,3'S	06°16,9'W	242	AGT on deck
"	"	98	16.06	70°23,5'S	06°16,8'W	243	Netsounder down for check
"	"	98	16.29	70°23,5'S	06°16,9'W	244	MK down
"	"	98	16.50	70°23,5'S	06°16,0'W	241	MK on deck
"	"	98	17.04	70°23,4'S	06°16,9'W	241	WS down. 17.35 on deck
"	"	98	17.06	70°23,5'S	06°17,4'W	243	Check wireless netsounder
"	"	98	17.25	70°23,9'S	06°18,4'W	253	Ice samples. until 19.47
21/350	"	98	17.40	70°31,1'S	07°59,3'W	247	Begin ice station
"	"	98	19.20	70°30,7'S	08°02,4'W	247	End of ice station
21/351	8.4	99	14.05	70°30,5'S	07°59,3'W	255	BRO down
"	"	99	16.55	70°30,5'S	08°00,5'W	247	BRO on deck
"	9.4	100	08.49	70°30,5'S	08°00,4'W	247	Begin Ice Station
"	"	100	08.49	70°30,4'S	08°01,6'W	247	End ice station
"	"	100	09.00	70°30,3'S	08°01,6'W	247	MUC down
"	"	100	12.00	70°30,3'S	08°01,8'W	247	MUC on deck 13.13
"	"	100	11.20	70°30,4'S	08°01,6W	253	Netsounder down
"	"	100	11.45	70°30,4'S	08°01,6'W	248	" on deck
"	"	100	12.03	70°30,5'S	08°01,2'W	248	Begin ice station (heli)
"	"	100	13.39	70°30,4'S	08°00,4'W	252	Return of helicopter
"	"	100	12.39	70°30,4'S	08°00,4'W	252	BRO down
"	"	100	15.25	70°30,3'S	08°01,6'W	248	BRO on deck
"	"	100	15.12	70°30,3'S	08°00,7'W	247	MK down
"	"	100	15.33	70°30,3'S	08°01,5'W	248	MK on deck
21/352	"	100	15.16	70°18,1'S	07°03,0'W	784	AGT down
"	"	100	15.25	70°17,8'S	07°01,2'W	780	AGT on ground
"	10.4	101	07.09	70°18,8'S	07°00,4'W	623	AGT heave

"	"	101	07.23	70°21,6'S	07°08,7'W	451	AGT on deck
21/353	"	101	08.05	70°12,9'S	07°35,1'W	1026	Ice buoy put down
"	"	101	11.34	70°12,3'S	07°35,4'W	1157	Begin ice station
"	10.4	101	14.43	70°12,3'S	07°25,4'W	1163	MK down
"	"	101	15.15	70°12,1'S	07°35,5'W	1187	BO down
"	"	101	15.19	70°10,4'S	07°35,9'W	1152	BO on deck
"	"	101	15.25	70°09,9'S	07°38,9'W	1129	Begin ice station
"	"	101	16.19	70°06,8'S	07°40,7'W	1135	End ice station
"	"	101	16.55	70°06,7'S	07°40,5'W	1151	Begin ice station
"	"	101	18.23	70°05,5'S	07°40,0'W	1181	Ice scientists aboard
"	"	101	18.38	70°05,3'S	07°37,6'W	1320	Ice samples
"	"	101	18.47	70°05,3'S	07°37,6'W	1320	Ice samples
21/354	"	101	19.10	69°58,2'S	07°28,6'W	2276	MN down
"	"	101	19.46	69°58,0'S	07°27,7'W	2207	MN on deck
"	11.4	102	08.31	69°58,1'S	07°28,0'W	2183	SD
"	"	102	09.25	69°58,0'S	07°27,7'W	2224	RO down
"	"	102	09.11	69°57,9'S	07°27,2'W	2362	RO on deck
"	"	102	09.35	69°58,5'S	07°29,7'W	2417	Begin ice station
"	"	102	09.59	69°57,1'S	07°26,0'W	2447	End ice station
21/355	"	102	10.22	70°22,0'S	07°19,8'W	406	BRO down
"	"	102	12.17	70°22,2'S	07°20,4'W	402	BRO on deck
"	11.4	102	15.55	70°22,1'S	07°20,1'W	406	HN down. 16.12 on deck
"	"	102	16.26	70°22,3'S	07°20,6'W	389	CTD down
"	"	102	16.08	70°22,4'S	07°21,0'W	387	CTD on deck
"	"	102	16.35	70°22,4'S	07°21,0'W	385	Ice sampling until 17.06
21/356	"	102	16.53	70°14,0'S	07°17,2'W	810	XBT
21/357	"	102	17.00	70°06,4'S	07°21,6'W	1548	BRO down
"	11.4	102	18.30	70°06,8'S	07°22,6'W	1475	BRO on deck
"	11.4	102	20.19	70°06,4'S	07°21,6'W	1548	MK down. 20.33 on deck
"	"	102	20.55	70°06,5'S	07°21,9'W	1543	APSN down. 20.36 on deck
"	"	102	20.25	70°06,8'S	07°22,6'W	1466	APSN down. 21.01 on deck
"	"	102	20.32	70°07,0'S	07°23,3'W	1459	CTD down
"	"	102	20.54	70°07,9'S	07°24,8'W	1415	CTD on deck
21/358	"	102	21.12	69°57,8'S	07°20,0'W	1752	XBT
21/359	"	102	22.16	69°49,8'S	07°19,9'W	2416	BRO down
"	12.4	103	00.24	69°49,4'S	07°20,2'W	2426	BRO on deck
21/359	12.4	103	01.46	69°49,8'S	07°19,9'W	2416	APSN down
"	"	103	02.31	69°49,6'S	07°20,0'W	2428	APSN on deck
"	12.4	103	01.47	69°49,3'S	07°20,2'W	2438	CTD and MIC down
"	"	103	02.04	69°49,1'S	07°20,4'W	2421	CTD on ground
"	"	103	02.49	69°48,8'S	07°20,4'W	2404	CTD and MIC on deck
"	"	103	03.30	69°48,9'S	07°20,4'W	2404	FN down
"	"	103	04.30	69°48,6'S	07°20,4'W	2400	FN on deck
"	"	103	04.32	69°48,4'S	07°20,4'W	2767	BO down
"	"	103	04.52	69°48,3'S	07°20,1'W	2308	BO on deck
"	"	103	04.58	69°48,3'S	07°20,0'W	2307	MV down
"	"	103	05.43	69°47,9'S	07°20,0'W	8798	MV on deck
21/360	"	103	05.51	69°40,4'S	07°19,8'W	2631	XBT
21/361	"	103	07.09	69°33,4'S	07°20,7'W	2711	BRO down
"	12.4	103	08.14	69°33,5'S	07°22,0'W	2535	BRO on deck
21/361	12.4	103	09.03	69°33,4'S	07°20,8'W	2735	ASPN down. 09.13 on deck
"	"	103	09.35	69°33,5'S	07°21,2'W	2570	MK down. 09.28 on deeck
"	12.4	103	09.08	69°33,5'S	07°22,6'W	2525	CTD down
"	"	103	09.13	69°33,7'S	07°24,3'W	2399	CTD on deck
"	"	103	09.44	69°33,6'S	07°23,1'W	2464	SD down. 10.00 on deck
"	"	103	10.28	69°33,7'S	07°24,0'W	2414	LM down. 10.21 on deck
"	"	103	09.57	69°33,8'S	07°24,6'W	2376	BRO down
"	"	103	10.15	69°33,9'S	07°25,8'W	2361	BRO on deck
"	"	103	10.39	69°34,0'S	07°26,6'W	2314	Begin ice station
"	"	103	11.00	69°34,0'S	07°27,3'W	2313	Ice scientists aboard
21/362	"	103	11.20	69°26,0'S	07°19,6'W	3455	XBT
21/363	"	103	11.37	69°18,0'S	07°19,1'W	3481	BRO down
"	12.4	103	12.41	69°18,0'S	07°19,2'W	3480	BRO on deck
"	12.4	103	13.43	69°18,0'S	07°19,1'W	3474	APSN down
"	"	103	14.15	69°18,0'S	07°19,2'W	3474	APSN on deck
"	"	103	13.58	69°18,0'S	07°19,2'W	3474	APSN down
"	"	103	14.04	69°18,0'S	07°19,2'W	3508	APSN on deck
"	"	103	14.05	69°18,0'S	07°19,3'W	3478	SD down
"	"	103	14.11	69°18,0'S	07°19,3'W	3478	SD on deck
"	"	103	14.18	69°18,0'S	07°19,3'W	3478	BS down

"	"	103	14.23	69°18,0'S	07°19,0'W	3474	BS on deck
21/364	"	103	14.23	69°10,1'S	07°19,8'W	3249	XBT
21/365	"	103	15.21	69°02,1'S	07°19,6'W	3115	BRO down
"	12.4	103	16.20	69°02,2'S	07°19,8'W	3117	BRO on deck
"	12.4	103	17.24	69°02,1'S	07°19,6'W	3115	MK
"	"	103	17.59	69°02,2'S	07°19,7'W	3115	APSN down
"	"	103	17.27	69°02,2'S	07°19,8'W	3116	APSN on deck
"	"	103	17.51	69°02,1'S	07°20,0'W	3116	BS with MIC down
"	"	103	17.58	69°02,1'S	07°20,4'W	3118	MIC on ground
"	"	103	18.09	69°02,2'S	07°19,7'W	3115	BS with MIC on deck
21/366	"	103	19.27	68°54,0'S	07°19,6'W	3359	XBT
21/367	"	103	20.24	68°45,9'S	07°19,9'W	3205	BRO down
"	12.4	103	21.30	68°45,9'S	07°20,2'W	3207	BRO on deck
"	12.4	103	22.30	68°45,9'S	07°19,9'W	3210	APSN down. 22.56 on deck
"	"	103	23.15	68°45,9'S	07°20,2'W	3207	MK down. 23.15 on deck
"	"	103	22.50	68°45,9'S	07°20,3'W	3211	BS down
"	"	103	23.13	68°46,1'S	07°21,3'W	3261	BS on deck
"	"	103	23.23	68°46,1'S	07°21,1'W	3235	FN down
"	13.4	104	00.13	68°46,1'S	07°20,8'W	3232	FN on deck
21/367	"	104	00.20	68°46,1'S	07°20,8'W	3232	BO down
"	"	104	00.42	68°46,3'S	07°21,0'W	3247	BO on deck
"	13.4	104	00.45	68°46,4'S	07°21,0'W	9192	MN down
"	"	104	01.31	68°47,0'S	07°21,1'W	3266	MN on deck
21/368	"	104	01.40	68°38,0'S	07°19,8'W	2962	XBT
21/369	"	104	03.09	68°30,0'S	07°19,6'W	3372	BRO down
"	13.4	104	04.15	68°30,4'S	07°18,5'W	3284	BRO on deck
"	13.4	104	05.25	68°30,4'S	07°18,1'W	3270	BS down
"	"	104	06.25	68°30,6'S	07°17,2'W	3235	BS on deck
"	"	104	06.34	68°30,7'S	07°17,1'W	3232	FN down
"	"	104	07.19	68°30,9'S	07°16,8'W	3217	FN on deck
"	"	104	07.26	68°31,0'S	07°16,8'W	3215	MN down
"	"	104	07.48	68°31,6'S	07°16,1'W	3156	MN on deck
"	"	104	07.53	68°31,0'S	07°16,8'W	3215	MK down
"	"	104	09.03	68°31,0'S	07°16,6'W	3205	MK on deck
"	"	104	07.55	68°31,6'S	07°16,1'W	3159	LM down. 09.01 on deck
"	"	104	08.05	68°31,7'S	07°16,1'W	3164	APSN down. 09.15 on deck
"	"	104	08.57	68°31,7'S	07°16,1'W	3152	BRO down
"	"	104	09.07	68°31,9'S	07°16,0'W	3131	BRO on deck
"	"	104	09.12	68°31,8'S	07°16,0'W	3146	APSN down. 09.25 on deck
21/370	"	104	09.30	68°22,0'S	07°19,8'W	3961	XBT
21/371	"	104	09.22	68°13,9'S	07°20,1'W	4126	BRO DOWN
"	13.4	104	10.47	68°14,0'S	07°19,3'W	4119	BRO on deck
"	13.4	104	11.54	68°14,0'S	07°19,6'W	4122	MK down
"	"	104	12.38	68°14,0'S	07°19,4'W	4123	MK on deck
"	"	104	12.16	68°14,1'S	07°19,2'W	4118	BS down
"	"	104	12.30	68°14,3'S	07°18,3'W	4122	BS on deck
"	"	104	12.49	68°14,1'S	07°19,2'W	4118	HN down
"	"	104	13.32	68°14,1'S	07°18,9'W	4118	HN on deck
"	"	104	12.49	68°14,1'S	07°18,7'W	4119	APSN down
"	"	104	12.58	68°14,2'S	07°18,6'W	4119	APSN on deck
"	"	104	13.09	68°14,3'S	07°18,3'W	4127	FN down
"	"	104	13.15	68°14,4'S	07°17,8'W	4128	FN on deck
"	"	104	13.37	68°14,5'S	07°17,7'W	4129	MN down
"	"	104	14.00	68°14,7'S	07°17,2'W	4129	MN on deck
21/372	"	104	14.07	68°06,0'S	07°19,7'W	4379	XBT
21/373	"	104	14.30	67°58,0'S	07°19,8'W	4632	BRO down
"	13.4	104	15.42	67°58,0'S	07°19,6'W	4633	BRO on deck
"	13.4	104	16.45	67°58,1'S	07°19,6'W	4685	BS and MIC down
"	"	104	17.21	67°58,6'S	07°19,7'W	4638	MIC on ground
"	"	104	17.33	67°58,4'S	07°17,9'W	4607	BS and MIC on deck
"	"	104	19.00	67°58,6'S	07°19,6'W	4638	APSN down
"	"	104	20.22	67°58,6'S	07°19,7'W	4635	APSN on deck
"	"	104	18.56	67°58,4'S	07°17,5'W	4611	MN down
"	"	104	19.03	67°59,2'S	07°15,7'W	4581	MN on deck
"	"	104	20.36	67°58,5'S	07°17,0'W	4642	MK down. 20.57 on deck
"	"	104	21.55	67°59,6'S	07°15,2'W	4492	RMT down
"	"	104	20.49	68°02,2'S	07°14,3'W	4436	RMT on deck
21/374	"	104	22.20	68°58,0'S	07°41,0'W	4574	XBT
21/375	"	104	23.33	68°58,0'S	08°02,5'W	4573	BS down
"	14.4	105	01.00	67°58,2'S	08°01,6'W	4568	BS on deck

21/376	14.4	105	02.10	68°06,0'S	08°02,0'W	4411	XBT
21/377	"	105	03.43	68°14,1'S	08°01,9'W	4339	BSdown
"	14.4	105	04.47	68°14,1'S	07°59,1'W	4295	BS on deck
"	"	105	06.02	68°14,2'S	07°59,2'W	4291	SD down
"	"	105	09.26	68°14,1'S	07°59,1'W	4295	SD on deck
"	"	105	09.16	68°14,1'S	07°59,1'W	4295	LM down
"	"	105	09.22	68°14,1'S	07°59,0'W	4293	LM on deck
"	"	105	09.22	68°14,1'S	07°59,0'W	4293	BRO down
"	"	105	09.30	68°14,1'S	07°58,9'W	4293	BRO on deck
"	"	105	09.35	68°14,1'S	07°58,8'W	4293	APSN down
"	"	105	09.51	68°14,1'S	07°58,8'W	4293	APSN on deck
"	"	105	09.53	68°14,1'S	07°58,8'W	4293	BO down
"	"	105	09.59	68°14,1'S	07°58,7'W	4289	BO on deck
21/378	"	105	09.57	68°22,0'S	08°02,5'W	4116	XBT
21/379	"	105	10.14	68°30,1'S	08°02,0'W	4033	arrival station
"	14.4	105	11.30	68°30,1'S	08°01,3'W	4033	BS down
"	14.4	105	12.20	68°29,5'S	08°58,6'W	4042	BS on deck
"	"	105	12.37	68°30,0'S	08°00,4'W	4036	APSN down
"	"	105	14.33	68°29,9'S	08°00,2'W	4036	APSN on deck
21/380	"	105	13.14	68°38,0'S	08°02,3'W	3959	XBT
21/381	"	105	13.23	68°46,0'S	08°02,1'W	3906	BS down
"	14.4	105	15.37	68°46,2'S	08°02,0'W	3902	BS on deck
"	14.4	105	16.38	68°46,1'S	08°01,5'W	3905	BS down
"	"	105	17.07	68°46,1'S	08°00,9'W	3906	BS on ground
"	"	105	17.17	68°46,2'S	08°00,0'W		BS on deck
"	"	105	18.07	68°46,1'S	08°01,4'W	3906	APSN down
"	"	105	19.04	68°46,1'S	08°01,3'W	3906	APSN on deck
21/382	"	105	17.32	68°54,0'S	08°01,5'W	3597	XBT
21/383	"	105	17.41	69°02,0'S	08°02,5'W	3567	Begin ice station
"	14.4	105	20.10	69°01,9'S	08°02,6'W	3572	Ice station cont.
"	14.4	105	21.15	69°02,0'S	08°02,4'W	3556	BS down
"	"	105	21.28	69°02,1'S	08°02,3'W	3558	BS on deck
"	"	105	21.42	69°02,0'S	08°02,2'W	3552	APSN down
"	"	105	23.12	69°01,9'S	08°02,1'W	3547	APSN on deck
21/384	"	105	22.06	69°10,0'S	08°02,3'W	3765	XBT
21/385	"	105	22.17	69°18,0'S	08°02,4'W	3242	BS down
"	15.4	106	00.10	69°18,0'S	08°03,3'W	3194	BS on deck
"	15.4	106	01.10	69°18,0'S	08°02,4'W	3242	APSN down
"	"	106	02.28	69°18,0'S	08°02,6'W	3236	APSN on deck
21/386	"	106	01.12	69°25,9'S	08°02,4'W	4463	XBT
21/387	"	106	01.21	69°34,0'S	08°01,9'W	2919	BS down
"	15.4	106	03.28	69°34,1'S	08°03,4'W	3164	BS on deck
"	15.4	106	04.40	69°34,1'S	08°02,5'W	3006	APSN down
"	"	106	06.01	69°34,1'S	08°02,8'W		APSN on deck
21/388	"	106	05.15	69°42,0'S	08°02,3'W	2840	XBT
21/389	"	106	05.25	69°50,2'S	08°02,5'W	1923	BS down
"	15.4	106	07.23	69°50,0'S	08°02,2'W	1832	BS on deck
"	15.4	106	08.39	69°50,0'S	08°02,4'W	1861	SD down. 09.18 on deck
"	"	106	09.22	69°50,0'S	08°02,3'W	1835	MK down. 09.31 on deck
"	"	106	09.13	69°50,0'S	08°02,3'W	1835	APSN down. 09.31 on deck
"	"	106	09.18	69°49,9'S	08°01,7'W	1849	Zodiac outside
"	"	106	09.18	69°50,2'S	08°00,4'W	1758	RMT down
"	"	106	10.15	69°48,5'S	08°04,1'W	1758	RMT on deck
"	"	106	10.43	69°49,3'S	08°01,7'W	1923	Zodiac on deck
21/389	"	106	12.00	69°49,4'S	08°01,6'W	1923	BRO down
"	"	106	12.44	69°49,2'S	08°01,6'W	1924	BRO on deck
"	15.4	106	12.52	69°49,4'S	08°01,6'W	1923	MK down
"	"	106	13.36	69°49,3'S	08°01,5'W	1925	MK on deck
"	"	106	12.52	69°49,1'S	08°01,6'W	1925	Bo down
"	"	106	13.08	69°49,1'S	08°01,5'W	1925	BO on deck
"	"	106	13.54	69°56,0'S	08°05,5'W	2012	SSN down
"	"	106	14.11	69°55,4'S	08°05,7'W	2080	SSN on deck
21/390	"	106	16.10	70°08,1'S	08°30,0'W	2106	XBT
21/391	"	106	19.36	70°22,0'S	08°56,3'W	525	MUC down
"	15.4	106	21.52	70°21,7'S	08°55,4'W	550	MUC on deck
"	16.4	107	09.08	70°21,8'S	08°55,7'W	531	APSN down. 09.48 on deck
"	"	107	09.56	70°21,8'S	08°55,4'W	548	Zodiac on water
"	"	107	09.38	70°21,6'S	08°54,8'W	575	Zodiac on deck
"	"	107	09.50	70°21,6'S	08°54,8'W	573	MK
"	"	107	10.13	70°21,5'S	08°54,5'W	582	BS down

"	"	107	10.10	70°21,2'S	08°53,4'W	686	BS on deck
"	"	107	10.17	70°21,0'S	08°53,2'W	729	BRO down
"	"	107	10.58	70°20,7'S	08°52,4'W	789	BRO on deck
"	"	107	11.12	70°20,6'S	08°52,2'W	808	BO down
"	"	107	11.44	70°20,5'S	08°51,8'W	842	BO on deck
21/392	"	107	11.53	70°18,6'S	08°54,6'W	1076	Begin ice station
"	"	107	12.11	70°18,4'S	08°54,4'W	1101	APSN down
"	16.4	107	13.10	70°18,3'S	08°54,3'W	1115	APSN on deck
"	"	107	13.29	70°18,4'S	08°54,4'W	1101	BS down
"	"	107	13.41	70°17,9'S	08°53,8'W	1191	BS on deck
"	"	107	13.32	70°18,3'S	08°54,3'W	1115	MK down
"	"	107	14.23	70°18,2'S	08°54,1'W	1149	MK on deck
"	"	107	13.42	70°17,5'S	08°53,3'W	1234	End ice station
"	"	107	13.58	70°17,5'S	08°53,3'W	1250	BRO down
"	"	107	14.53	70°17,0'S	08°52,8'W	1319	BRO on deck
21/393	"	107	15.02	70°15,4'S	08°55,0'W	1485	BS. MIC
"	"	107	15.46	70°14,9'S	08°55,0'W	1512	BS. MIC on deck
"	16.4	107	16.17	70°15,0'S	08°54,9'W	1505	MK down
"	"	107	18.05	70°15,0'S	08°55,1'W	1508	MK on deck
"	"	107	17.10	70°15,0'S	08°55,1'W	1508	APSN down
"	"	107	17.29	70°15,0'S	08°55,1'W	1512	APSN on deck
"	"	107	17.41	70°15,0'S	08°55,1'W	1513	BO down
"	"	107	17.55	70°14,8'S	08°55,1'W	1521	BO on deck
21/394	"	107	18.12	69°59,0'S	08°58,8'W	2092	BS. MIC down
"	"	107	18.58	69°59,3'S	09°00,8'W	1986	BS. MIC on deck
"	16.4	107	21.12	69°59,1'S	08°59,4'W	2078	APSN down. 21.39 on deck
"	"	107	22.30	69°59,3'S	09°00,7'W	1945	BRO down
"	"	107	21.20	69°59,4'S	09°01,1'W	2043	BRO on deck
21/395	"	107	22.41	69°51,6'S	09°00,0'W	2457	XBT
21/396	"	107	23.11	69°43,7'S	08°59,1'W	2807	BS down
"	17.4	108	01.15	69°43,5'S	08°59,0'W	2878	BS on deck
"	17.4	108	03.58	69°43,4'S	08°59,0'W	2893	BRO down
"	"	108	04.39	69°43,3'S	08°58,9'W	2967	BRO on deck
"	"	108	04.46	69°43,3'S	08°58,9'W	2987	APSN down. 05.22 on deck
21/397	"	108	05.22	69°34,2'S	08°59,3'W	3427	XBT
21/398	"	108	05.16	69°27,6'S	09°00,6'W	2957	BS down
"	17.4	108	07.07	69°27,3'S	09°00,2'W	2912	BS on deck
21/398	17.4	108	08.31	69°27,3'S	09°00,2'W	2893	APSN. MK down. 09.40 on deck
"	"	108	09.11	69°27,2'S	09°00,2'W	2893	SD. LM down. 09.29 on deck
"	17.4	108	09.23	69°27,1'S	09°00,1'W	2873	LM down. 09.35 on deck
"	"	108	09.24	69°27,1'S	09°00,1'W	2901	BRO down
"	"	108	09.32	69°26,8'S	08°59,8'W	2866	BRO on deck
"	"	108	09.35	69°26,7'S	08°59,8'W	2863	BO down
"	"	108	10.09	69°26,5'S	08°59,7'W	2861	BO on deck
"	"	108	10.14	69°26,4'S	08°59,6'W	2855	BRO down
"	"	108	10.33	69°26,2'S	08°59,5'W	2855	BRO on deck
21/399	"	108	10.43	69°19,6'S	09°00,2'W	3061	XBT
21/400	"	108	10.56	69°12,2'S	08°58,8'W	3563	Zodiac outside
"	17.4	108	12.07	69°12,1'S	08°58,6'W	3582	BS down
"	17.4	108	13.15	69°12,0'S	08°58,5'W	3587	BS on deck
"	"	108	13.45	69°12,0'S	08°58,6'W	3597	Zodiac on deck
"	"	108	14.26	69°11,9'S	08°58,3'W	3619	APSN down
"	"	108	14.21	69°11,8'S	08°58,3'W	3623	APSN on deck
"	"	108	14.32	69°11,8'S	08°58,2'W	3621	MK down
"	"	108	14.42	69°11,8'S	08°58,2'W	3621	MK on deck
"	"	108	14.40	69°11,8'S	08°58,2'W	3621	BRO down
"	"	108	14.50	69°11,8'S	08°58,3'W	3627	BRO on deck
21/401	"	108	14.45	69°03,2'S	08°04,8'W	4134	XBT
21/402	"	108	15.15	68°56,1'S	09°01,2'W	4212	APSN down. 17.51 on deck
"	17.4	108	16.29	68°56,1'S	09°01,1'W	4213	BS down
"	17.4	108	17.42	68°55,9'S	09°00,9'W	4215	BS on deck
"	"	108	18.14	68°55,9'S	09°00,9'W	4215	BRO down
"	"	108	18.53	68°55,9'S	09°00,8'W	4216	BRO on deck
21/403	"	108	19.01	68°47,5'S	08°59,8'W	4010	XBT
21/404	"	108	19.35	68°39,9'S	09°00,5'W	4032	BS down
"	17.4	108	20.43	68°40,1'S	08°59,7'W	4035	BS on deck
"	17.4	108	21.45	68°40,0'S	08°59,4'W	4035	BRO down
"	"	108	22.25	68°40,0'S	08°58,6'W	4033	BRO on deck
21/405	"	108	22.34	68°31,6'S	09°00,6'W	4108	XBT
21/406	"	108	23.07	68°23,9'S	09°00,3'W	3546	BS down

"	18.4	109	00.12	68°23,8'S	09°00,1'W	3624	BS on deck
"	18.4	109	01.12	68°23,9'S	09°00,3'W	3579	APSN down
"	"	109	01.57	68°23,9'S	09°00,3'W	3589	APSN on deck
"	"	109	01.34	68°23,8'S	09°00,1'W	3605	BRO down
"	"	109	01.40	68°23,9'S	09°00,1'W	3667	BRO on deck
21/407	"	109	02.03	68°16,0'S	09°00,0'W	4108	XBT
21/408	"	109	02.35	68°08,0'S	08°59,9'W	4581	APSN down. 04.46 on deck
"	18.4	109	03.38	68°08,0'S	09°00,0'W	4581	MIC. BS down
"	18.4	109	04.38	68°08,7'S	09°01,2'W	4578	MIC. BS on deck
"	"	109	04.39	68°08,7'S	09°01,0'W	4576	BRO down
"	"	109	07.07	68°08,9'S	09°00,8'W	4577	BRO on deck
"	"	109	07,21	68°09,2'S	09°02,7'W	4583	RMT down
"	"	109	08.05	68°10,2'S	09°09,2'W	4597	RMT on deck
21/409	"	109	08.35	68°07,8'S	09°22,8'W	4678	XBT
21/410	"	109	09.51	68°08,0'S	09°43,2'W	4737	SD down. 11.45 on deck
"	18.4	109	10.40	68°08,0'S	09°43,1'W	4737	BRO down
"	18.4	109	11.40	68°08,0'S	09°43,2'W	4737	BRO on deck
"	"	109	11.52	68°08,0'S	09°43,3'W	4737	APSN down
"	"	109	11.52	68°08,0'S	09°43,2'W	4737	APSN on deck
"	"	109	12.18	68°08,0'S	09°43,3'W	4737	BS down
"	"	109	12.27	68°08,2'S	09°44,1'W	4737	BS on deck
"	"	109	12.19	68°08,0'S	09°43,2'W	4737	MK down
"	"	109	15.21	68°08,1'S	09°43,2'W	4554	MK on deck
"	"	109	12.26	68°08,0'S	09°43,2'W	4708	MK down
"	"	109	12.35	68°08,0'S	09°43,2'W	4737	MK on deck
"	"	109	12.38	68°08,2'S	09°44,1'W	4737	BRO down
"	"	109	12.46	68°08,4'S	09°44,1'W	4736	BRO on deck
"	"	109	15.29	68°08,4'S	09°44,1'W	4737	BO down
"	"	109	15.59	68°08,5'S	09°44,1'W	4735	BO on deck
21/411	"	109	16.03	68°16,0'S	09°43,0'W	4632	XBT
21/412	"	109	16.23	68°23,9'S	09°43,1'W	4022	BS down
"	18.4	109	17.20	68°24,3'S	09°'W42,8	3997	BS on deck
"	18.4	109	18.20	68°24,1'S	09°43,0'W	4017	APSN down. 19.20 on deck
"	"	109	20.13	68°24,4'S	09°42,7'W	3996	BRO down
"	"	109	19.10	68°24,3'S	09°42,8'W	3990	BRO on deck
21/413	"	109	20.31	68°32,0'S	09°42,8'W	4255	XBT
21/414	"	109	20.53	68°39,9'S	09°42,3'W	4190	BS down
"	18.4	109	21.51	68°39,8'S	09°41,3'W	4180	BS on deck
"	18.4	109	22.52	68°39,8'S	09°42,1'W	4184	APSN
"	19.4	109	00.47	68°39,8'S	09°41,1'W	4169	BRO down
"	18.4	109	23.39	68°39,9'S	09°40,4'W	4166	BRO on deck
21/415	19.4	110	00.53	68°48,5'S	09°43,0'W	4448	XBT
21/416	"	110	01.37	68°56,2'S	09°42,7'W	4344	BS down
"	"	110	02.39	68°56,6'S	09°42,7'W	4350	BS on deck
"	"	110	03.46	68°56,6'S	09°42,5'W	4349	APSN down. 05.01 on deck
"	"	110	05.57	68°56,7'S	09°42,8'W	4348	BRO down
"	"	110	04.50	68°56,8'S	09°43,0'W	4360	BRO on deck
21/417	"	110	05.53	69°00,0'S	09°43,0'W	4285	XBT
21/418	"	110	06.28	69°12,2'S	09°43,2'W	3899	BS down
"	19.4	110	07.34	69°13,3'S	09°44,7'W	4023	BS on deck
"	19.4	110	08.29	69°12,6'S	09°43,5'W	3939	APSN down. 09.35 on deck
"	"	110	10.48	69°12,7'S	09°43,5'W	3951	Zodiac outside
"	"	110	09.20	69°13,1'S	09°44,1'W	4015	Zodiac on deck
"	"	110	09.25	69°12,7'S	09°43,6'W	3953	MK down. 09.45 on deck
"	"	110	10.25	69°13,3'S	09°44,1'W	4028	BRO down
"	"	110	09.34	69°13,4'S	09°45,1'W	4040	BRO on deck
"	"	110	10.55	69°13,3'S	09°44,9'W	4030	SD down
"	"	110	11.26	69°13,3'S	09°44,9'W	4046	SD on deck
"	"	110	11.03	69°13,9'S	09°45,6'W	3974	BRO down
"	"	110	11.11	69°13,9'S	09°45,5'W	4007	BRO on deck
21/419	"	110	12.09	69°20,0'S	09°43,0'W	4044	XBT
21/420	"	110	12.22	69°28,1'S	09°42,9'W	2872	BS down
"	19.4	110	13.16	69°28,2'S	09°45,0'W	2878	BS on deck
"	19.4	110	14.42	69°28,1'S	09°43,2'W	2877	MK down
"	"	110	16.18	69°28,1'S	09°43,5'W	2971	MK on deck
"	"	110	14.56	69°28,1'S	09°43,5'W	2971	APSN down
"	"	110	15.11	69°28,1'S	09°43,7'W	2869	APSN on deck
"	"	110	15.11	69°28,2'S	09°45,1'W	2879	BRO down
"	"	110	15.23	69°28,2'S	09°45,9'W	2880	BRO on deck
21/421	"	110	16.23	69°36,0'S	09°43,8'W	2298	XBT

21/422	"	110	17.01	69°44,3'S	09°43,2'W	2202	BS down
"	19.4	110	18.30	69°44,2'S	09°44,9'W	2234	BS on deck
"	19.4	110	21.03	69°44,2'S	09°44,3'W	8068	APSN down. 21.43 on deck
21/422	"	110	22.14	69°44,2'S	09°45,5'W	2245	BRO down
"	"	110	21.37	69°44,2'S	09°46,0'W	2306	BRO on deck
21/423	19.4	110	22.35	69°52,0'S	09°43,0'W	2124	XBT
21/424	"	110	23.06	69°59,5'S	09°43,8'W	1780	BS down
"	20.4	111	00.58	69°59,7'S	09°44,2'W	1787	BS on deck
"	20.4	111	02.59	69°59,4'S	09°44,4'W	1787	BRO down
"	"	111	04.05	69°59,2'S	09°44,9'W	1783	BRO on deck
"	"	111	04.11	69°59,4'S	09°44,7'W	1784	APSN down
"	"	111	04.45	69°59,4'S	09°44,7'W	1785	APSN on deck
21/425	"	111	04.37	70°08,1'S	09°42,5'W	1680	BS down
"	"	111	04.43	70°08,5'S	09°44,3'W	1696	BS on deck
"	20.4	111	06.52	70°08,6'S	09°44,5'W	1695	BRO down
"	"	111	08.20	70°09,0'S	09°45,6'W	1655	BRO on deck
"	"	111	08.29	70°08,9'S	09°45,5'W	1676	MK down. 09.14 on deck
"	"	111	09.02	70°09,9'S	09°45,6'W	1637	BO down
"	"	111	08.58	70°09,4'S	09°46,6'W	1740	BO on deck
"	"	111	09.06	70°09,9'S	09°45,6'W	1637	APSN down. 09.24 on deck
"	"	111	09,43	70°09,7'S	09°47,0'W	1806	MUC down
"	"	111	09.07	70°11,0'S	09°48,7'W	1879	MUC on deck
"	"	111	10.09	70°11,5'S	09°50,4'W	1949	Zodiac outside
"	"	111	11.41	70°12,3'S	09°50,4'W	1972	Zodiac on deck
21/426	"	111	12.22	70°20,4'S	09°43,7'W	1619	BS down
"	"	111	13.26	70°20,9'S	09°43,9'W	1609	BS on deck
"	20.4	111	14.58	70°20,4'S	09°43,6'W	1615	MK down
"	"	111	15.54	70°20,5'S	09°43,6'W	1612	MK on deck
"	"	111	15.09	70°20,8'S	09°43,7'W	1609	APSN down
"	"	111	15.19	70°20,9'S	09°43,9'W	1609	APSN on deck
"	"	111	15.42	70°20,9'S	09°43,9'W	1606	BRO down
"	"	111	15.54	70°21,2'S	09°44,2'W	1601	BRO on deck
"	"	111	16.01	70°21,4'S	09°44,4'W	1599	MUC down
"	"	111	16.38	70°22,2'S	09°45,0'W	1577	MUC on deck
21/427	"	111	16.54	70°28,7'S	09°42,0'W	1007	MIC. BS down
"	"	111	18.00	70°28,7'S	09°42,0'W	1006	MIC. BS on deck
"	20.4	111	19.46	70°28,6'S	09°41,9'W	1010	APSN down. 20.30 on deck
"	"	111	20.37	70°28,7'S	09°42,0'W	1011	MUC down
"	"	111	20.09	70°28,6'S	09°42,0'W	1028	MUC on deck
21/428	"	111	20.57	70°30,0'S	09°40,1'W	472	MIC. BS down
"	"	111	21.46	70°30,0'S	09°40,0'W	500	MIC. BS on ground
"	20.4	111	22.35	70°30,0'S	09°40,0'W	466	MIC. BS on deck
"	"	111	22.52	70°30,0'S	09°39,9'W	461	APSN down. 00.03 on deck
"	"	111	23.20	70°29,9'S	09°39,8'W	467	BRO down
"	"	111	23.50	70°30,0'S	09°39,7'W	470	BRO on deck
"	"	111	23.31	70°30,0'S	09°39,8'W	481	APSN
"	20.4	111	23.50	70°30,0'S	09°39,4'W	460	MUC down
"	21.4	112	00.06	70°30,0'S	09°39,8'W	481	MUC on deck
"	"	112	00.19	70°31,1'S	09°36,0'W	368	RMT down
"	"	112	01.18	70°28,8'S	09°39,4'W	825	RMT on deck
21/429	"	112	02.09	70°30,2'S	09°36,2'W	360	AGT down
"	"	112	03.08	70°30,9'S	09°38,7'W	371	RMT on deck
21/430	21.4	112	03.48				Station cancelled
21/431A	"	112	05.14	70°43,2'S	10°20,4'W	297	XBT
21/431B	21.4	112		70°54,3'S	10°18,0'W	225	Begin ice station
"	21.4	112	08.50	70°54,3'S	10°18,1'W	225	End ice station
21/431C	21.4	112	11.05	70°58,0'S	10°44,4'W	426	Ice scientists on mummy chair
21/431D	"	112	12.30	70°59,2'S	11°00,1'W	367	BS down
"	21.4	112	15.33	70°59,2'S	11°00,3'W	370	BS on deck
21/431D	21.4	112	16.11	70°59,3'S	11°00,2'W	369	APSN down. 16.37 on deck
21/432A	"	112	16.41	70°49,5'S	11°00,5'W	499	MIC. BS down
"	21.4	112	16.28	70°49,7'S	11°01,3'W	498	BS. MIC on deck
"	"	112	18.13	70°49,6'S	11°00,9'W	499	APSN down. 18.42 on deck
"	"	112	18.53	70°49,7'S	11°01,4'W	495	BRO down
"	"	112	18.33	70°49,9'S	11°02,1'W	480	BRO on deck
"	"	112	19.02	70°49,7'S	11°02,5'W	505	AGT down
"	"	112	19.45	70°51,3'S	11°64,4'W	444	AGT on deck
21/432B	"	112	20.00	70°59,6'S	11°48,4'W	996	BS down
"	"	112	21.24	70°59,7'S	11°49,1'W	1026	BS on deck
"	22.4	113	07.10	70°59,5'S	11°47,0'W	920	Hydrophone down

"	"	113	07.54	70°59,6'S	11°47,2'W	926	released KN4
"	"	113	09.28	70°59,5'S	11°47,8'W	978	Hydrophone down
"	"	113	09.31	70°59,5'S	11°47,8'W	981	Mooring 550 m
"	"	113	11.00	70°59,8'S	11°48,9'W	1022	Hydrophone down
"	"	113	11.07	70°00,3'S	11°53,9'W	1280	Search given up
"	"	113	11.35	70°00,3'S	11°53,9'W	1280	Ice basket 17.15
21/433	"	113	17.10	70°46,7'S	11°00,0'W	985	BS. MIC down
"	"	113	17.10	70°46,6'S	11°00,5'W	1007	BS. MIC on deck
"	23.4	114	06.08	70°45,9'S	11°01,2'W	1087	RMT down
"	"	114	07.09	70°43,3'S	11°01,9'W	1256	RMT on deck
21/434	"	114	07.41	70°36,5'S	11°04,2'W	1492	Begin ice station
"	"	114	08.59	70°36,2'S	11°06,2'W	1533	End ice station
"	23.4	114	11.00	70°36,2'S	11°06,4'W	1534	BS down
"	"	114	12.19	70°36,0'S	11°08,1'W	1569	BS on deck
"	"	114	12.28	70°36,2'S	11°06,4'W	1534	APSN down
"	"	114	13.25	70°36,1'S	11°16,8'W	1543	APSN on deck
"	"	114	12.28	70°36,1'S	11°06,6'W	1542	MK down
"	"	114	12.42	70°36,1'S	11°07,2'W	1561	MK on deck. APSN down
"	"	114	12.35	70°36,0'S	11°07,9'W	1565	APSN on deck
21/435	"	114	12.56	70°25,9'S	11°05,1'W	2001	Begin ice station
"	"	114	12.15	70°25,6'S	11°05,4'W	2009	End ice station
"	23.4	114	15.43	70°25,6'S	11°05,6'W	2011	MK down
"	"	114	16.53	70°25,6'S	11°05,6'W	2012	MK on deck
"	"	114	17.08	70°25,5'S	11°05,6'W	2012	BS down
"	"	114	17.16	70°25,3'S	11°05,8'W	2020	BS on deck
"	"	114	17.16	70°25,5'S	11°05,6'W	2012	APSN down. 17.43 on deck
"	"	114	18.28	70°25,2'S	11°05,8'W	2022	BRO down
"	"	114	17.18	70°25,1'S	11°05,9'W	2025	BRO on deck
"	"	114	18.36	70°25,1'S	11°05,9'W	2026	BO down
"	"	114	19.12	70°24,7'S	11°05,9'W	1963	BO on deck
21/436	"	114	19.17	70°07,2'S	10°58,1'W	2274	XBT
21/437	"	114	20.45	70°01,6'S	10°59,5'W	2882	BS down
"	23.4	114	23.56	70°01,5'S	10°59,5'W	2883	BS on deck
"	24.4	115	01.04	70°01,6'S	10°59,5'W	2882	APSN down
"	"	115	01.52	70°01,6'S	10°59,5'W	2883	APSN on deck
"	"	115	01.04	70°01,5'S	10°59,5'W	2888	BRO down
"	"	115	01.52	70°01,4'S	10°59,6'W	2887	BRO on deck
"	"	115	02.00	70°01,5'S	10°59,7'W	2888	MUC down
"	"	115	02.35	70°01,6'S	10°59,8'W	2851	MUC on deck
21/438	"	115	02.53	69°53,8'S	11°01,0'W	3059	XBT
21/439	"	115	04.48	69°46,0'S	11°00,1'W	3426	BS down
"	24.4	115	06.10	69°46,0'S	11°00,2'W	3430	BS on deck
"	24.4	115	07.48	69°46,0'S	11°00,2'W	3424	BRO down
"	"	115	08.37	69°46,0'S	11°00,2'W	3420	BRO on deck
"	"	115	08.45	69°45,9'S	11°00,7'W	3435	Begin ice station
"	"	115	09.15	69°45,9'S	11°00,0'W	3434	End ice station
"	"	115	09.36	69°45,9'S	11°00,0'W	3426	APSN down. 10.08 on deck
21/440	"	115	11.09	69°36,6'S	10°57,8'W	4149	XBT
21/441	"	115	09.43	69°29,9'S	10°59,3'W	4098	Begin ice station
"	24.4	115	12.41	69°29,6'S	10°59,0'W	4085	End ice station
"	24.4	115	13.35	69°29,6'S	10°58,7'W	4088	BS down
"	"	115	14.54	69°29,4'S	10°58,4'W	4078	BS on deck
"	"	115	15.12	69°29,6'S	10°58,7'W	4085	MK down
"	"	115	15.55	69°29,5'S	10°58,6'W	4083	APSN down
"	"	115	15.12	69°29,5'S	10°58,5'W	4079	APSN on deck
"	"	115	15.24	69°29,5'S	10°58,4'W	4076	BRO down
"	"	115	15.41	69°29,1'S	10°58,4'W	4073	BRO on deck
21/442	"	115	16.03	69°22,0'S	11°00,5'W	3924	XBT
21/443	"	115	16.39	69°14,1'S	11°01,4'W	4055	BS down
"	"	115	18.20	69°13,7'S	11°01,6'W	4068	BS on deck
"	"	115	19.36	69°14,1'S	11°01,4'W	4053	APSN
"	"	115	20.22	69°13,6'S	11°01,6'W	4071	BRO down
"	"	115	19.38	69°13,4'S	11°01,9'W	4078	BRO on deck
21/444	"	115	20.30	69°06,0'S	11°00,9'W	4158	XBT
21/445	"	115	21.04	68°58,2'S	10°58,9'W	4592	BS down
"	"	115	23.13	68°54,8'S	10°58,3'W	4607	BS on deck
"	25.4	116	01.28	68°58,1'S	10°58,7'W	4596	APSN down
"	"	116	02.16	68°57,9'S	10°58,5'W	4601	APSN on deck
"	"	116	01.39	68°57,7'S	10°58,3'W	4552	BRO down
"	"	116	02.00	68°57,4'S	10°58,0'W	4614	BRO on deck

21/446	"	116	02.22	68°50,0'S	11°00,0'W	4679	XBT
21/447	"	116	03.02	68°41,8'S	11°00,2'W	4597	MIC. BS down
"	25.4	117	04.23	68°40,5'S	11°01,0'W	4533	MIC. BS on deck
"	25.4	117	05.34	68°40,6'S	11°00,9'W	4535	MK down. 08.10 on deck
"	"	117	08.13	68°40,5'S	11°01,0'W	4533	APSN down. 08.24 on deck
"	"	117	08.01	68°40,4'S	11°01,1'W	4533	BRO down
"	"	117	08.12	68°40,4'S	11°01,1'W	4533	BRO on deck
"	"	117	08.24	68°40,2'S	11°01,3'W	4542	BRO on deck
21/448	"	117	08.24	67°47,1'S	11°11,7'W	4761	ICTD down
"	"	117	09.01	67470,1'S	11°11,7'W	4761	ICTD on deck
"	25.4	117	15.27	67°47,0'S	11°11,7'W	4624	ICTD on deck
"	"	117	15.40	67°47,1'S	11°11,5'W	4735	Zodiac outside
"	"	117	15.40	67°47,0'S	11°10,9'W	4810	Zodiac on deck
"	"	117	15.56	67°47,1'S	11°11,5'W	4735	MK down
"	"	117	16.35	67°47,5'S	11°11,3'W	4740	MK on deck
"	"	117	15.55	67°47,1'S	11°11,3'W	4740	Ice sampler outside
"	"	117	16.10	67°47,1'S	11°11,3'W	4740	Ice sampler on deck
"	"	117	16.13	67°46,9'S	11°10,7'W	4677	ICTD down. 16.59 on deck
"	"	117	16.19	67°46,9'S	11°10,6'W	4684	Ice sampler until 17.05
"	"	117	16.50	67°46,7'S	11°10,5'W	4658	BRO down
"	"	117	17.03	67°46,4'S	11°10,5'W	4588	BRO on deck
"	"	117	17.13	67°46,6'S	11°10,7'W	4647	APSN down. 17.32 on deck
"	"	117	17.52	67°46,2'S	11°09,7'W	4395	Ice sampler until 18.41
21/449	"	117	17.22	67°45,1'S	11°59,9'W	4928	BS. MIC down
"	"	117	18.12	67°44,8'S	12°00,3'W	4929	BS. MIC on deck
"	25.4	117	21.15	67°45,0'S	12°00,0'W	4929	APSN down. 21.52 on deck
"	"	117	23.44	67°44,8'S	12°00,3'W	4929	BRO down
"	"	117	21.39	67°44,9'S	12°00,7'W	4929	BRO on deck
21/450	"	117	23.54	67°46,4'S	12°02,9'W	4557	Ice scientists outsode
"	26.4	118	00.32	67°46,5'S	12°03,5'W	4428	End ice station
21/451	26.4	118	08.34	67°37,7'S	11°47,0'W	4796	NS down
"	"	118	09.26	67°37,6'S	11°46,4'W	4497	NS on deck
"	26.4	118	12.00	67°37,5'S	11°45,9'W	4527	MK down
"	"	118	12.09	67°37,5'S	11°46,0'W	4496	MK on deck
"	"	118	12.26	67°37,5'S	11°45,9'W	4524	Zodiac outside
"	"	118	12.33	67°37,6'S	11°46,4'W	4514	Zodiac on deck
"	"	118	12.37	67°37,5'S	11°46,0'W	4496	APSN
"	"	118	12.59	67°37,5'S	11°46,0'W	4520	APSN on deck
"	"	118	12.33	67°37,5'S	11°46,0'W	4496	Ice sampler until 12.36
"	"	118	12.43	67°37,6'S	11°46,2'W	4518	Ice sampler until 12.53
"	"	118	12.35	67°37,7'S	11°46,4'W	4507	Ice sampler until 13.06
"	"	118	12.53	67°37,7'S	11°46,7'W	4448	BRO down
"	"	118	13.05	67°37,8'S	11°46,8'W	4466	BRO on deck
"	"	118	13.26	67°37,8'S	11°46,8'W	4486	MK down
"	"	118	14.02	67°37,8'S	11°46,7'W	4488	MK on deck
"	"	118	13.35	67°36,9'S	11°43,5'W	4555	Ice sampler down
"	"	118	13.43	67°36,9'S	11°43,5'W	4553	Ice sampler on deck
21/452	"	118	14.48	68°00,2'S	12°00,2'W	4919	BS down
"	"	118	14.58	68°00,5'S	12°03,3'W	4919	BS on deck
"	26.4	118	18.13	68°00,2'S	12°00,5'W	4919	APSN down. 18.36 on deck
"	"	118	20.44	68°00,4'S	12°02,1'W	4919	MK down. 20.10 on deck
"	"	118	18.24	68°00,6'S	12°03,2'W	4919	BRO down
"	"	118	20.00	68°00,7'S	12°03,9'W	4918	BRO on deck
"	"	118	20.52	68°00,8'S	12°04,1'W	4918	MN down
"	"	118	21.26	68°01,2'S	12°06,0'W	4918	MN on deck
"	"	118	21.33	68°01,3'S	12°06,2'W	4417	FN down
"	"	118	23.03	68°'01,4S	12°06,6'W	4917	FN on deck
"	"	118	23.15	68°01,6'S	12°07,2'W	4916	MUC down
"	"	118	23.35	68°03,0'S	12°11,2'W	4915	MUC on deck
21/453	"	118	23.57	68°00,1'S	12°04,9'W	4918	Begin ice station
"	27.4	119	03.20	68°00,5'S	12°07,0'W	4918	End ice station
"	27.4	119	09.28	68°00,3'S	12°05,5'W	4910	APSN down. 09.52 on deck
21/454	"	119	10.24	67°53,4'S	12°01,3'W	4922	Zodiak outside
"	"	119	09.42	67°53,6'S	12°02,9'W	4921	Zodiak on deck
"	27.4	119	11.55	67°53,3'S	12°01,4'W	4922	APSN down
"	"	119	12.22	67°53,4'S	12°01,4'W	4922	APSN on deck
"	"	119	11.58	67°53,8'S	12°03,7'W	4921	Ice basket down.
"	"	119	12.07	67°53,9'S	12°05,0'W	4920	Ice sampler down
"	"	119	12.28	67°53,8'S	12°05,1'W	4921	Ice sampler down
"	"	119	13.00	67°53,9'S	12°05,7'W	4920	Ice sampler down

"	"	119	13.09	67°53,7'S	12°06,1'W	4921	BRO down
"	"	119	13.19	67°53,8'S	12°06,9'W	4921	BRO on deck
"	"	119	13.31	67°53,7'S	12°06,1'W	4921	MK down
"	"	119	14.05	67°53,7'S	12°06,3'W	4921	MK on deck
"	"	119	13.31	67°53,7'S	12°06,4'W	4921	APSN down
"	"	119	13.46	67°53,8'S	12°06,7'W	4921	APSN on deck
21/455	"	119	13.53	68°42,7'S	12°01,0'W	4845	MIC. BS down
"	"	119	14.01	68°43,6'S	12°06,5'W	4645	MIC. BS down
"	27.4	119	21.16	68°42,8'S	12°01,2'W	4843	APSN down. 21.38 on deck
"	27.4	119	21.27	68°43,9'S	12°08,1'W	4839	BRO down
"	28.4	120	00.08	68°43,6'S	12°06,8'W	4843	BRO on deck
"	28.4	120	00.16	68°44,1'S	12°08,6'W	4841	MN down
"	"	120	00.52	68°44,6'S	12°10,9'W	4833	MN on deck
"	"	120	01.11	68°44,7'S	12°11,2'W	4834	FN down
"	"	120	02.21	68°44,9'S	12°11,8'W	4829	FN on deck
"	"	120	02.30	68°44,9'S	12°11,9'W	4827	BRO down
"	"	120	02,50	68°45,6'S	12°14,5'W	4801	BRO on deck
21/456	"	120	02.53	68°50,0'S	12°09,1'W	4696	XBT
21/457	"	120	04.33	68°58,0'S	12°00,0'W	4609	XBT
21/458	28.4	120	05.35	69°06,2'S	12°01,9'W	4467	BRO down
"	28.4	120	06.45	69°06,3'S	12°02,6'W	4469	BRO on deck
"	28.4	120	08.10	69°06,2'S	12°02,2'W	4467	MK down. 08.33 on deck
"	"	120	08.45	69°06,3'S	12°02,8'W	4469	BS down
"	"	120	08.24	69°06,9'S	12°06,3'W	4509	BS on deck
"	"	120	08.50	69°06,3'S	12°02,9'W	4469	APSN down. 09.05 on deck
"	"	120	11.28	69°07,0'S	12°06,6'W	4517	BO down
"	"	120	08.55	69°07,3'S	12°08,9'W	4581	BO on deck
"	"	120	11.38	69°07,2'S	12°08,2'W	4557	MK down
"	"	120	13.18	69°07,4'S	12°09,2'W	4577	MK on deck
"	"	120	12.47	69°07,4'S	12°09,1'W	4576	MN down
"	"	120	13.35	69°07,6'S	12°1°,0'W	4887	MN on deck
"	"	120	13.30	69°07,7'S	12°10,0'W	4584	Zodiac outside
"	"	120	14.12	69°07,9'S	12°11,1'W	4599	Zodiac on deck
"	"	120	14.22	69°07,7'S	12°10,3'W	4408	Ice sampler until 14.32
"	"	120	14,58	69°07,7'S	12°10,3'W	4601	Ice sampler until 14.46
"	"	120	14.31	69°07,9'S	12°11,0'W	4600	Ice sampler until 14.56
"	"	120	14.45	69°08,9'S	12°12,5'W	4611	Begin ice station
"	"	120	14.56	69°08,9'S	12°12,5'W	4460	End ice station
21/459	"	120	15.21	69°14,0'S	12°09,4'W	4712	XBT
21/460	"	120	16.56	69°22,0'S	12°02,4'W	4685	XBT
21/461	28.4	120	18.10	69°31,2'S	11°57,6'W	4497	BRO down
"	28.4	120	19.20	69°31,2'S	11°58,4'W	4497	BRO on deck
"	28.4	120	21.40	69°31,1'S	11°57,9'W	4495	APSN. 22.14 on deck
"	"	120	22.18	69°31,2'S	11°58,7'W	4495	BS down
"	"	120	22.02	69°32,3'S	12°02,7'W	4470	BS on deck
"	"	120	22.24	69°32,3'S	12°03,1'W	4467	MN down
"	29.4	121	01.00	69°32,9'S	12°05,9'W	4440	MN on deck
21/462	"	121	01.13	69°37,9'S	11°57,0'W	4274	XBT
21/463	"	121	02.33	69°47,2'S	11°59,6'W	4105	XBT
21/464	29.4	121	04.04	69°53,8'S	11°59,9'W	4205	BRO down
"	29.4	121	06.19	69°53,9'S	12°01,3'W	4226	BRO on deck
"	29.4	121	09.20	69°53,8'S	12°00,6'W	4214	APSN down. 09.46 on deck
"	"	121	09,54	69°54,0'S	12°01,7'W	4221	BS down
"	"	121	09.35	69°54,4'S	12°03,9'W	4178	BS on deck
"	"	121	10.00	69°54,5'S	12°04,8'W	4191	Begin ice station
"	"	121	10.43	69°55,0'S	12°07,3'W	4207	End ice station
21/465	"	121	11.15	70°02,0'S	11°54,9'W	2714	XBT
21/466	"	121	12.08	70°09,4'S	11°59,6'W	2572	XBT
21/467	29.4	121	13.28	70°18,0'S	11°58,0'W	2259	BRO down
21/467	29.4	121	14.16	70°18,2'S	11°59,8'W	2258	BRO on deck
"	1.5	123	06.15	70°18,2'S	11°59,9'W	2259	BS down
"	1.5	123	06.54	70°18,4'S	12°03,8'W	2297	BS on deck
"	"	123	07.00	70°18,4'S	12°03,6'W	2295	MK down. 08.25 on deck
"	"	123	08.23	70°18,5'S	12°03,3'W	2292	MN down
"	"	123	08.15	70°18,2'S	12°05,5'W	2314	MN on deck
"	"	123	08.47	70°18,3'S	12°05,5'W	2299	APSN down. 09.20 on deck
"	"	123	10.04	70°18,5'S	12°06,1'W	2280	Begin ice station
"	"	123	09.10	70°18,8'S	12°08,9'W	2262	End ice station
"	"	123	10.40	70°19,2'S	12°09,9'W	2214	FN down
"	"	123	11.50	70°19,3'S	12°10,9'W	2213	FN on deck

"	"	123	12.02	70°19,3'S	12°19,7'W	2214	BO down
"	"	123	12.23	70°19,3'S	12°12,9'W	2309	BO on deck
"	"	123	12.26	70°19,3'S	12°10,7'W	2214	MK down
"	"	123	12.50	70°19,3'S	12°12,9'W	2309	MK on deck
"	"	123	12.26	70°19,0'S	12°14,2'W	2316	MUK down
"	"	123	13.50	70°19,9'S	12°15,8'W	2421	MUK on deck
21/468	"	123	14.13	70°26,9'S	12°10,4'W	2147	XBT
21/469	"	123	15.44	70°34,0'S	12°04,2'W	1976	XBT
21/470	1.5	123	17.00	70°41,8'S	12°00,0'W	1860	BRO down
"	1.5	123	18.05	70°42,0'S	12°01,1'W	1864	BRO on deck
"	1.5	123	19.30	70°42,0'S	12°01,3'W	1864	BS down
"	"	123	20.23	70°42,2'S	12°02,6'W	1867	BS on deck
"	"	123	20.39	70°42,1'S	12°01,5'W	1865	APSN down. 20.51 on deck
"	"	123	21.34	70°42,3'W	12°03,1'W	1868	MN down
"	"	123	20.44	70°42,5'S	12°04,1'W	1890	MN on deck
21/471	"	123	22.43	70°50,1'S	12°00,0'W	1664	BS down
"	"	123	23.37	70°50,5'S	12°02,1'W	1688	BS on deck
21/472	2.5	124	00.32	70°55,0'S	12°01,0'W	1645	BRO down
"	"	124	01.20	70°55,3'S	12°03,4'W	1590	BRO on deck
"	2.5	124	02.24	70°55,0'S	12°01,0'W	1645	APSN down
"	"	124	03.06	70°55,0'S	12°01,6'W	1647	APSN on deck
"	"	124	02.25	70°55,0'S	12°01,0'W	1645	XBT
"	"	124	02.32	70°55,3'S	12°03,8'W	1603	BS down
"	"	124	02.27	70°55,9'S	12°07,3'W	1721	BS on deck
"	"	124	03.12	70°56,0'S	12°08,1'W	1668	MN down
"	"	124	04.18	70°56,7'S	12°12,5'W	1557	MN on deck
"	"	124	04.31	70°56,7'S	12°13,0'W	1582	FN down
"	"	124	05.54	70°57,0'S	12°14,2'W	1618	FN on deck
"	"	124	06.02	70°57,0'S	12°14,4'W	1620	BO down
"	"	124	06.25	70°57,7'S	12°18,6'W	1578	BO on deck
21/473	"	124	06.28	71°00,2'S	12°03,9'W	1335	BS down
"	"	124	07.50	71°01,2'S	12°09,2'W	1348	BS on deck
"	"	124	09.22	71°00,4'S	12°04,9'W	1229	APSN down. 09.44 on deck
21/474	"	124	10.27	71°05,5'S	12°0°,7'W	1150	BRO down
"	"	124	09.37	71°06,4'S	12°02,9'W	1150	BRO on deck
"	2.5	124	11.30	71°05,5'S	12°00,7'W	1150	APSN down. 11.40 on deck
"	"	124	12.20	71°05,5'S	12°00,7'W	1150	XBT
21/476	"	124	11.30	71°16,7'S	12°00,5'W	184	Ice sampler 14.45 on deck
"	"	124	11.30	71°16,6'S	12°01,0'W	205	BRO down
"	2.5	124	14.44	71°16,8'S	12°01,7'W	203	BRO on deck
"	"	124	14.54	71°16,6'S	12°01,0'W	205	MK down
"	"	124	15.15	71°16,8'S	12°01,7'W	203	MK on deck
21/475	"	124	14.54	71°10,0'S	12°00,2'W	300	APSN down. 16.28 on deck
"	"	124	15.15	71°10,1'S	12°00,6'W	306	BRO down
"	"	124	16.20	71°10,1'S	12°01,3'W	301	BRO on deck
"	"	124	16.25	71°10,1'S	12°01,7'W	303	MIC. BS down
"	"	124	16.47	71°10,1'S	12°02,6'W	307	MIC. BS on deck
"	"	124	16.53	71°10,1'S	12°03,1'W	308	MN down
"	"	124	17.18	71°10,1'S	12°03,7'W	320	MN on deck
"	"	124	17.27	71°10,1'S	12°04,2'W	311	FN down
"	"	124	17.52	71°10,1'S	12°04,7'W	311	FN on deck
21/474	"	124	18.00	71°05,5'S	12°02,0'W	1130	MIC. BS down
"	"	124	18.19	71°06,4'S	12°05,0'W	1071	MIC. BS on deck
"	2.5	124	19.47	71°05,8'S	12°03,0'W	1130	APSN down. 20.15 on deck
"	"	124	20.47	71°06,5'S	12°06,0'W	1030	MN down
"	"	124	20.06	71°07,5'S	12°09,8'W	814	MN on deck
"	"	124	20.59	71°07,2'S	12°10,6'W	866	MUC down
"	"	124	22.13	71°07,4'S	12°13'5'W	760	MUC on deck
21/477	"	124	22.25	71°04,1'S	11°52,3'W	568	MN down
"	"	124	23.33	71°04,1'S	11°54,3'W	761	MN on deck
"	3.5	125	08.02	71°04,5'S	11°53,2'W	559	MN down
"	"	125	08.41	71°04,3'S	11°55,0'W	744	MN on deck
"	"	125	09.10	71°04,5'S	11°53,6'W	621	APSN down. 09.30 on deck
21/478	"	125	09.44	71°02,8'S	11°39,9'W	368	Hydrophone down
"	"	125	09.21	71°02,8'S	11°40,3'W	368	Icesampler
"	3.5	125	10.53	71°02,9'S	11°42,8'W	403	Sediment trap released
"	"	125	10.56	71°03,0'S	11°44,7'W	400	Sediment trap on deck
21/479	"	125	12.45	71°10,2'S	12°13,5'W	347	SSN down
"	"	125	14.15	71°06,7'S	12°58,5'W	730	SSN on deck
21/480	4.5	126	08.57	70°27,8'S	06°39,0'W	435	Begin ice station

"	"	126	13.01	70°27,8'S	06°39,0'W	434	End ice station
21/481	5.5	127	11.30	70°13,3'S	06°00,0'W	1248	XBT
"	"	127	13.00	70°08,8'S	05°59,2'W	1666	BO down
"	5.5	127	17.20	70°08,9'S	06°02,1'W	1496	BO on deck
"	"	127	18.07	70°08,8'S	05°59,3'W	1695	APSN down. 18.25 on deck
"	"	127	19.00	70°08,9'S	06°02,5'W	1442	MN down
"	"	127	18.13	70°09,1'S	06°05,0'W	1512	MN on deck
21/482	"	127	19.07	70°07,9'S	06°06,6'W	1582	XBT
21/483	"	127	19.54	70°01,0'S	06°04,4'W	1872	XBT
21/484	5.5	127	20.20	69°51,0'S	05°58,9'W	2194	XBT
21/485	5.5	127	22.02	69°41,4'S	06°02,2'W	2311	XBT
21/486	6.5	128	00.08	69°23,5'S	06°00,4'W	2222	XBT
21/487	6.5	128	02.05	68°53,6'S	06°00,1'W	2670	XBT
21/488	6.5	128	04.04	68°44,2'S	06°01,4'W	2604	Begin ice station
"	6.5	128	07.40	68°44,3'S	06°04,8'W	2703	End ice station
"	6.5	128	09.25	68°43,9'S	06°07,3'W	2755	BRO down
"	"	128	11.10	68°44,0'S	06°08,4'W	2743	BRO on deck
"	"	128	12.00	68°43,9'S	06°07,3'W	2755	APSN. SD down
"	"	128	12.40	68°43,9'S	06°07,3'W	2755	SD on deck
"	"	128	12.09	68°43,9'S	06°07,7'W	2749	LM down. 12.17 on deck
"	"	128	12.13	68°43,9'S	06°07,7'W	2749	APSN on deck
"	"	128	12.15	68°44,0'S	06°07,8'W	2748	MK down
"	"	128	12.20	68°44,0'S	06°08,1'W	2745	MK on deck
"	"	128	12.22	68°43,9'S	06°07,3'W	2755	XBT
21/489	"	128	12.29	68°37,9'S	06°03,9'W	2786	XBT
21/489	"	128	12.00	68°37,9'S	06°04,0'W	2784	Begin ice station
"	6.5	128	14.00	68°37,9'S	06°05,2'W	2789	End ice station
21/490	6.5	128	14.18	68°23,9'S	05°59,4'W	3978	XBT
21/491	"	128	14.58	68°09,6'S	06°01,7'W	4717	BO down
"	6.5	128	17.12	68°09,4'S	06°03,2'W	4710	BO on deck
"	6.5	128	18.30	68°09,6'S	06°02,0'W	4717	APSN down. 19.01 on deck
"	"	128	19.16	68°09,4'S	06°03,5'W	4709	MN down
"	"	128	18.43	68°09,2'S	06°04,8'W	4708	MN on deck
"	"	128	19.23	68°09,2'S	06°04,5'W	4708	APSN down. 19.52 on deck
"	"	128	19.56	68°09,2'S	06°04,4'W	4708	RMT down
"	"	128	19.37	68°09,4'S	06°02,4'W	4710	RMT on deck
"	"	128	20.12	68°10,2'S	05°57,6'W	4689	RMT on deck
21/492	"	128	20.36	67°58,0'S	05°58,5'W	4725	XBT
	"	128	21.32				
	6.5	128	23.00				
21/493	7.5	129	01.02	67°39,7'S	06°00,0'E	4,780	XBT
21/494	7.5	129	03.00	67°23,3'S	05°52,2'E	4,835	XBT
21/495	7.5	129	05.00	67°09,1'S	05°34,8'E	4,827	XBT
21/496	7.5	129	07.00	66°53,7'S	05°16,5'E	4,818	XBT
21/497	9.5	131	13.28	58°49,4'S	02°59,4'E	4,302	2 pump samples
"	"	131	14.15	58°49,7'S	02°59,4'E	4,435	1 pump samples
"	"	131	14.36	58°49,8'S	02°59,4'E	4,458	16,371,pump on deck
"	"	131	17.29	58°50,9'S	03°01,6'E	4,454	2,pump on deck
"	"	131	13.36	58°49,4'S	02°59,3'E	4,309	MK down
"	"	131	13.52	58°49,6'S	02°59,4'E	4,388	MK on deck
"	"	131	13.54	58°49,6'S	02°59,4'E	4,388	APSN down
"	"	131	14.03	58°49,6'S	02°59,4'E	4,410	APSN on deck
"	"	131	14.21	58°49,7'S	02°59,4'E	4,413	APSN down
"	"	131	15.00	58°49,8'S	02°59,4'E	4,441	APSN on deck
"	"	131	14.29	58°49,8'S	02°59,4'E	4441	MK down
"	"	131	14.49	58°49,8'S	02°59,3'E	4428	MK on deck
21/498	10.5	132	05.16	57°38,3'S	04°02,0'E	?	arrival SF
"	"	132	06.05	57°37,3'S	04°03,9'E	?	releasing SF
"	"	132	09.33	57°36,5'S	04°07.7'E	5779	SF on deck
"	"	132	09.49	57°36,5'S	04°08,6'E	5231	APSN down,10.11 on deck
"	"	132	10.55	57°37,4'S	04°04,7'E	4716	Begin mooring station, SF down
"	"	132	11.20	57°37,3'S	04°04,1'E	4495	1.SF down
"	"	132	12.18	57°37,5'S	04°02,2'E	4437	2.SF down
"	"	132	13.03	57°37,8'S	04°01,0'E	4445	end of mooring station
21/499	12.5	134	06.03	54°20,5'S	03°22,8'E	2770	BRO down
"	"	134	06.42	54°20,6'S	03°22,7'E	2761	BRO on deck
"	"	134	06.08	54°20,4'S	03°22,8'E	2770	APSN down,06.45 on deck
"	"	134	06.35	54°20,7'S	03°22,8'E	2762	arrival SF
"	"	134	08.07	54°20,6'S	03°22,7'E	?	begin of mooring station
"	"	134	08.50	54°20,4'S	03°22,8'E	?	1.SF on deck

"	"	134	10.03	54°21,5'S	03°24,4'E	?	2.SF on deck
"	"	134	11.15	54°22,1'S	03°27,3'E	2888	begin of mooring station
"	"	134	11.34	54°22,0'S	03°26,7'E	2856	1.SF down
"	"	134	13.12	54°20,6'S	03°22,9'E	2780	end of mooring station
21/500	14.5	136	08.05	50°07,4'S	05°52,1'E	3792	begin of mooring station
"	"	136	10.13	50°08,2'S	05°54,9'E	3826	1.SF down
"	"	136	11.34	50°06,2'S	05°05,5'E	3806	2.SF down
"	"	136	11.58	50°06,3'S	05°54,5'E	3804	end of mooring station
21/501	15.5	137	19.03	45°04,5'S	10°05,4'E	4709	XBT
21/502	15.5	137	21.00	44°41,7'S	10°23,6'E	4633	XBT
21/503	15.5	137	23.00	44°17,8'S	10°42,2'E	4638	XBT
21/504	16.5	138	01.07	43°52,5'S	11°03,5'E	4576	XBT
21/505	16.5	138	03.00	43°30,5'S	11°20,3'E	4934	XBT
21/506	16.5	138	05.00	43°06,7'S	11°39,7'E	4667	XBT
21/507	16.5	138	07.03	42°43,4'S	11°56,8'E	4612	XBT
21/508	16.5	138	09.05	42°23,1'S	12°12,8'E	4338	XBT
21/509	16.5	138	21.00	41°07,7'S	12°55,1'E	4538	XBT
21/510	16.5	138	23.00	40°46,1'S	13°12,4'E	4891	XBT
21/511	17.5	139	01.00	40°25,1'S	13°30,3'E	4833	XBT
21/512	17.5	139	03.00	40°03,2'S	13°46,8'E	4821	XBT
21/513	17.5	139	05.00	39°45,9'S	13°59,4'E	4838	XBT
21/514	17.5	139	07.00	39°29,6'S	14°10,6'E	4847	XBT
21/515	17.5	139	09.00	39°12,1'S	14°24,3'E	4777	XBT
21/516	17.5	139	10.56	38°56,1'S	14°38,6'E	4759	XBT
21/517	17.5	139	13.03	38°36,2'S	14°53,6'E	4854	XBT
21/518	17.5	139	15.14	38°20,4'S	15°07,6'E	4763	XBT
21/519	17.5	139	17.00	38°09,1'S	15°18,4'E	4706	XBT
21/520	17.5	139	19.00	37°56,1'S	15°31,0'E	4853	XBT
21/521	17.5	139	21.03	37°42,3'S	15°41,0'E	4735	XBT
21/522	17.5	139	22.55	37°29,4'S	15°48,4'E	4742	XBT
21/523	18.5	140	00.55	37°16,5'S	15°56,4'E	4681	XBT
21/524	18.5	140	03.32	37°01,3'S	16°03,1'E	4655	XBT
21/525	18.5	140	05.03	36°52,1'S	16°10,5'E	4614	XBT
21/526	18.5	140	06.08	36°47,3'S	16°25,8'E	4577	BRO down
	18.5	140	06.50	36°47,1'S	16°16,4'E	4576	BRO on deck
	18.5	140	06.10	36°47,3'S	16°15,8'E	4576	XBT

b. Teilnehmer/Participants

Attwood, Colin	ZUCT
Beese ,Gerhard	Merian
Berberich, Doris	AWI
Beyer, Kerstin	AWI
Brey, Heinz	HSW
Dentler, Frank-Ulrich	SWA
Di Prisco, Guido	CNR
Dieckmann, Gerhard(Scientific Advisor)	AWI
Dower, Katherine	ZUCT
Elbrächter, Malte	BAH
Garrison, Dave	UCSC
Gerdes, Dieter	AWI
Gleitz, Markus	AWI
Gradinger, Rolf	AWI
Großmann, Sönnke	AWI
Günther, Sven	AWI
Hagen, Wilhelm	IPÖ
Helmke, Elisabeth	AWI
Klauke, Ursula	AWI
Koch, Volker	AWI
Krause, Günther (Scientific Advisor)	AWI
Kunzmann, Andreas	IPÖ
Lucas, Mike	ZUCT
Lütjeharms, Johan	OUCT
Maul, Andreas	AWI

Mizdalski, Elke	AWI
Ohm, Klaus	AWI
Pagés, Francesc	CSIC
Petz, Wolfgang	ZIU
Phillips, Richard	UCT
Plugge, Rainer	AWI
Probyn, Trevor	OUCT
Rigg, Gordon	OUCT
Robinson, Dale	USC
Schiel, Sigrid	AWI
Schmidt, Werner	FGB
Song, Weibo	OUQ
Sonnabend, Hartmut	SWA
Spindler, Michael (Chief scientist)	IPÖ
Stürcken, Marthi	AWI
Tamburrini, Maurizio	CNR
Thomas, David	AWI
Thomsen, Helge	IFS
Valentine, Henry	OUCT
van Hannen, Erik	RUG
Vonnekold, Michael	HSW
Wang, Zipan	SIO
Weissenberger, Jürgen	AWI
Wilbert, Norbert	ZIUB
Winter, Amos	UPR
Zölffel, Michael	IFSB

Austria	1
BRD	35
China	2
Denmark	1
Holland	1
Italy	2
Puerto Rico/USA	1
South Africa	8
Spain	1
USA	3

c. Beteiligte Institutionen/Participating institutions

Austria		
ZIU	Zoologisches Institut der Universität Hellbrunnerstr. 34 A-5020 Salzburg Östereich	1
Denmark		
IFS	Institut for Sporeplanter University of Copenhagen Øster Farimagsgade 2D DK-1353 Copenhagen K Denmark	1
China		
SIO	Second Institute of Oceanography, State Oceanic Administratiobn P.O. BOx 507 Hangzhou Zhejiang 310012 China	1
OUQ	Ocean University Qingdao, College of Fisheries Yüshan Road 5 Qingdao 266003 VR China	1
Federal Republic of Germany		
AWI	Alfred- Wegener-Institut für Polar- und Meeresforschung Postfach 120161 2850 Bremerhaven	20
BAH	Biologische Anstalt Helgoland Wattenmmerstation Sylt 2282 List/Sylt	1
FGB	Fachbereich Geowisenschaften Universität Bremen Postfach 33 04 40 2800 Bremen 33	1
HSW	Helikopter Service Wasserthal GmbH Kärtnerweg 43 2000 Hamburg 65	2
IFSB	Institut für Systematische Botanik Altenstein str. 6 W-1000 Berlin 33	1
IPÖ	Institut für Polarökologie Universität Kiel Wischhofstraße 1-3 2300 Kiel 14	2

MER	Dr. Gerhard Beese Quedlinburger Weg 4 2000 Hamburg 61	1
SWA	Seewetteramt Deutscher Wetterdienst Bernahard-Nocht-Straße 76 200 Hamburg	2
ZIUB	Zoologisches Institut Universitaät Bonn Poppelsdorfer- Schloss 5300 Bonn	1
Italy		
CNR	Consiglio Nazionale delle Ricerche Instituto di Biochimica delle Proteine ed Enzimologia Via Marconi 10 - 80125 Napoli Italy	2
Netherlands		
RUG	Biological Sciences Department of Marine Biology University of Groningen P.O.Box 14 9750 AA Haren Netherlands	1
Rep. of South Africa		
OUCT	Dept. of Oceanography University of Cape Town Private Bag Rondebosch 7700 Rep. of South Africa	5
ZUCT	Dept. of Zoology University of Cape Town Private Bag Rondebosch 7700 Rep. of South Africa	3
Spain		
CSIC	Institut de Ciències del Mar Passeig Nacional S/N 08039 Barcelona Spain	1
USA		
UCSC	Institute of Marine Sciences University of California Santa Cruz Santa Cruz California 95064 USA	1

UPR	University of Puerto Rico P.O. Box 5000 Mayaguez Puerto Rico 00681-5000	1
USC	Hancock Institute for Marine Sciences University of Southern California Los Angeles, CA 90089-0373	1

d. Besatzung/Crew

Kapitän	H. Jonas
I. Offz.	K.D. Gerber
Naut. Offz.	U. Grundmann
Naut. Offz.	M. Rodewald
Arzt	Dr. A. Stecher
Elektriker	G. Schuster
Elektroniker	H. Elvers
"	K. Hoops
"	H. Muhle
"	J. Roschinsky
"	M. Arndt
Funkoffizier	H. Geiger
"	K.H. Wanger
Ltd. Ingenieur	K. Müller
I. Ingenieur	G. Erreth
II. Ingenieur	R. Fengler
"	O. Ziemann
Maschinenwart	G. Jordan
"	M. Lesch
"	U. Husung
"	M. Reitz
"	G. Dufner
"	K. Müller
Bootsmann	R. Zulauf
Zimmermann	K. Marowsky
Matrose	A. Meis Torres
"	J. Soage Curra
"	J. Pousada Martinez
"	F. Garcia Martinez
"	B. Iglesias Bermudez
Koch	E. Kubicka
Kochsmaat	M. Dutsch
"	H. Hüneke
I. Steward	H. Vollmeyer
Steward./Krankenschw.	M. Reitz
Steward(ess)	M. Hoppe
"	K. Helpap
"	J. Hasler
II. Steward	Ch. L. Yu
"	K. Yu
Wäscher	Ch. Chang